R-07-52

Sensitivity analysis and development of calibration methodology for near-surface hydrogeology model of Laxemar

Maria Aneljung, Mona Sassner, Lars-Göran Gustafsson
DHI Sverige AB

November 2007

Svensk Kärnbränslehantering AB
Swedish Nuclear Fuel
and Waste Management Co
Box 250, SE-101 24 Stockholm
Tel +46 8 459 84 00

SKB

ISSN 1402-3091
SKB Rapport R-07-52

Sensitivity analysis and development of calibration methodology for near-surface hydrogeology model of Laxemar

Maria Aneljung, Mona Sassner, Lars-Göran Gustafsson
DHI Sverige AB

November 2007

Summary

The Swedish Nuclear Fuel and Waste Management Company (SKB) is conducting site investigations at two different locations, Forsmark and Laxemar, for localisation of a geological repository for spent nuclear fuel. The results from the investigations at these sites are used in a variety of modelling activities supporting the development of site descriptive models, safety assessments and environmental impact assessments. This report describes modelling where the hydrological modelling system MIKE SHE has been used to describe surface hydrology, near-surface hydrogeology, advective transport mechanisms, and the contact between groundwater and surface water within the SKB site investigation area at Laxemar.

In the MIKE SHE system, surface water flow is described with the one-dimensional modelling tool MIKE 11, which is fully and dynamically integrated with the groundwater flow module in MIKE SHE. In early 2008, a supplementary data set will be available and a process of updating, rebuilding and calibrating the MIKE SHE model based on this data set will start. Before the calibration on the new data begins, it is important to gather as much knowledge as possible on calibration methods, and to identify critical calibration parameters and areas within the model that require special attention.

In this project, the MIKE SHE model described in /Werner et al. 2005, Bosson 2006/ has been further developed. The model area has been extended, and the present model also includes an updated bedrock model and a more detailed description of the surface stream network. The numerical model has been updated and optimized, especially regarding the modelling of evapotranspiration and the unsaturated zone, and the coupling between the surface stream network in MIKE 11 and the overland flow in MIKE SHE. An initial calibration has been made and a base case has been defined and evaluated. In connection with the calibration, the most important changes made in the model were the following:

- The evapotranspiration was reduced.
- The infiltration capacity was reduced.
- The hydraulic conductivities of the Quaternary deposits in the water-saturated part of the subsurface were reduced.

Data from one surface water level monitoring station, four surface water discharge monitoring stations and 43 groundwater level monitoring stations (SSM series boreholes) have been used to evaluate and calibrate the model. The base case simulations showed a reasonable agreement between measured and calculated surface water discharges, but the model generally underestimates the total runoff from the area. The model also overestimates the groundwater levels, and the modelled groundwater level amplitudes are too small in many boreholes.

A number of likely or potential reasons for these deviations can be identified:

- The surface stream network description in the model is incomplete. This implies that too little overland water is drained from the area by the streams, which creates ponded areas in the model that do not exist in reality. These areas are characterized by large evaporation and infiltration, contributing to groundwater recharge and reducing transpiration from the groundwater table, in turn creating high and relatively stable groundwater levels compared to those measured at the site.
- In order to improve the agreement between measured and modelled surface water discharges, the evapotranspiration was reduced in the model; in effect, this implied a reduction of the potential evapotranspiration. This probably caused a larger groundwater recharge and less transpiration during summer, thereby reducing the variations in the modelled groundwater levels. If the MIKE 11 stream network is updated (cf. above), the potential evapotranspiration could be increased again, such that the modelling of groundwater dynamics is improved.

- The bottom boundary condition and the hydraulic conductivity of the bedrock may have a large effect on model-calculated near-surface/surface water flows in Laxemar. A sensitivity analysis shows that lowering the hydraulic head at the bottom boundary (located at 150 metres below sea level) lowers the groundwater levels in the Quaternary deposits, but also implies smaller surface water discharges. Lowering the hydraulic conductivity of the bedrock would increase groundwater flows to Quaternary deposits in groundwater discharge areas, which raises groundwater levels and reduces fluctuation amplitudes. An alternative model approach, using a deeper MIKE SHE model down to less fractured bedrock, may also be interesting to evaluate.

It is recommended that the observations above are further evaluated in connection with the next modelling phase for Laxemar during 2008.

A sensitivity analysis has been made on calibration parameters. The most important results from the sensitivity analysis are the following:

- The hydraulic conductivity in the saturated zone proved to be more important than all of the tested vegetation and unsaturated zone parameters. The second most important parameters were the hydraulic conductivity of the unsaturated zone (K_s) and the specific yield (S_y).
- A lower hydraulic conductivity in the saturated zone increases the peak surface water flows, decreases the base flows, and increases the groundwater head amplitudes and the groundwater head elevations.
- A lower hydraulic conductivity in the unsaturated zone (K_s) increases the surface water flows, and, to some extent, decreases the groundwater head elevations.
- A lower specific yield in the unsaturated zone (S_y) increases the surface water flows (although with a smaller effect than K_s), increases the groundwater head amplitudes, and to some extent, increases the groundwater head elevations.

A method for performing the calibrations of future models is also presented based on the results from the base case simulations and the sensitivity analysis.

Sammanfattning

Svensk Kärnbränslehantering AB (SKB) genomför för närvarande platsundersökningar på två platser, Forsmark och Laxemar, i syfte att lokalisera ett slutförvar för utbränt kärnbränsle. Resultaten från platsundersökningarna används i en mängd modelleringsaktiviteter, vilka i sin tur används för att stödja framtagandet av platsbeskrivande modeller, säkerhetsanalyser och miljökonsekvensbeskrivningar. Denna rapport beskriver modelleringar där det hydrologiska modellsystemet MIKE SHE har använts för att beskriva ythydrologi och ytnära hydrogeologi, advektiva transportmekanismer och kontakten mellan grund- och ytvatten inom SKB:s undersökningsområde i Laxemar.

I MIKE SHE beskrivs ytvattensystemen med hjälp av det endimensionella verktyget MIKE 11, vilket är helt och dynamiskt integrerat med grundvattenmodellen i MIKE SHE. Under år 2008 kommer ett kompletterande dataset att levereras, varefter SKB påbörjar arbetet med att uppdatera och kalibrera den existerande MIKE SHE-modellen. Innan kalibreringsarbetet med nya data påbörjas är det önskvärt att samla så mycket kunskap som möjligt om kalibreringsmetodik, och att definiera kritiska modellparametrar och delområden i modellen som behöver studeras närmare.

I detta projekt har MIKE SHE-modellen beskriven i /Werner et al. 2005, Bosson 2006/ vidareutvecklats. Modellområdet har utökats och modellutvecklingen inkluderar även en uppdaterad berggrundsmodell och en utökad och förtätad beskrivning av ytvattensystemet. Den numeriska modellen har uppdaterats och optimerats, framförallt avseende modelleringen av avdunstning och flöden i markens omättade zon samt kopplingen mellan ytvattensystemet i MIKE11 och ytvattnet i MIKE SHE. En första kalibrering har genomförts och ett ”basfall” har definierats och utvärderats. I samband med kalibreringen genomfördes framförallt följande större förändringar i modellen:

- Avdunstningen minskades.
- Infiltrationskapaciteten minskades.
- Den hydrauliska konduktiviteten i den vattenmättade delen av jordlagren minskades.

Data från en ytvattennivåstation, fyra ytvattenflödesstationer och 43 grundvattenrör (borrhål i SSM-serien) har använts i kalibreringen och utvärderingen av modellen. Basfallsberäkningarna visade på en någorlunda god överensstämmelse mellan beräknade och uppmätta vattennivåer och flöden, men den totala avrinningen från modellområdet underskattades generellt i modellen. Resultaten visade även att grundvattennivåerna generellt överskattades i modellen. Beräknade grundvattennivåvariationer är dessutom i många fall för små.

Ett antal troliga eller möjliga orsaker till dessa avvikelser har konstaterats:

- Ytvattensystemet är inte tillräckligt detaljerat beskrivet i modellen. Detta gör att alltför lite ytvatten transporteras ut via vattendragen. Istället bildas en mängd små vattenansamlingar i modellen i områden där sådana inte återfinns i verkligheten. Från dessa sker avdunstning och infiltration, vilket i sin tur bidrar till en alltför stor modellerad grundvattenbildning och reducerad transpiration från grundvattnet i modellen. Detta medverkar också till förhöjda grundvattennivåer med relativt små variationer.
- Det faktum att den beräknade avrinningen blir för låg har korrigerats genom att avdunstningsprocesserna har reducerats i modellen; denna modifiering motsvarar i princip en reduktion av den potentiella evapotranspirationen. Detta har bidragit till en ökad grundvattenbildning och minskad transpiration under sommaren, som i sin tur reducerat grundvattnets nivåvariationer. Om beskrivningen av ytvattensystemet kompletteras enligt föregående punkt, ges möjlighet att återigen öka avdunstningsaktiviteten så att modellens beskrivning av grundvattendynamiken förbättras.

- Höga grundvattentryck i berget kan ha alltför stor inverkan på det ytnära grundvattnet i modellen, antingen beroende på att ansatta tryck vid bottenranden (belägen 150 m under havsnivån) är för höga eller att konduktiviteten i berget är överskattad. I båda fallen erhålls ett för stort grundvattentillskott till jordlagren inom utströmningsområden, vilket både höjer grundvattennivån och minskar nivåvariationerna. Ytterligare känslighetsfall där trycket vid bottenranden och/eller bergets hydrauliska egenskaper varieras bör undersökas. En alternativ modelleringsmetod, där tryckranden i botten ersätts med en djupare modell ner till tätare berg, skulle också vara intressant att utvärdera.

Det rekommenderas att ovanstående punkter utvärderas ytterligare i samband med nästa modelleringsfas för Laxemar under 2008. En känslighetsanalys av parametrar som är aktuella i ett kalibreringsskede har också genomförts. De viktigaste resultaten från känslighetsanalysen kan sammanfattas enligt följande:

- Den hydrauliska konduktiviteten i den mättade zonen visade sig vara av mycket större betydelse än alla testade parametrar för vegetation och omättad zon. De näst mest betydelsefulla parametrarna var den hydrauliska konduktiviteten i omättad zon (K_s) och vattenavgivningstalet (S_y).
- En lägre hydraulisk konduktivitet i den mättade zonen ökar de högsta flödena i vattendragen, sänker basflödet i vattendragen, och ökar såväl medelnivåer som amplituder hos grundvattenytan.
- En lägre hydraulisk konduktivitet i den omättade zonen (K_s) ökar flödet i vattendragen och minskar, i viss utsträckning, grundvattennivåerna.
- Ett lägre vattenavgivningstal (S_y) ökar ytvattenflödet (dock mindre än K_s), ökar grundvattenytans fluktuationer och ökar, till viss del, grundvattennivåerna.

En metodik för kalibrering av framtida modellversioner har också sammanställts baserat på resultaten från basfallssimuleringarna och känslighetsanalysen.

Contents

1 Introduction

The Swedish Nuclear Fuel and Waste Management Company (SKB) is performing site investigations of potential sites for localisation of a deep geological repository for spent nuclear fuel. The site investigations are performed at two sites: Forsmark in the Östhammar municipality and Laxemar in the Oskarshamn municipality; Laxemar is part of the Laxemar-Simpevarp investigation area. The results from the site investigations are used as a basis for a large number of modelling activities that are performed to support the development of site descriptive models, safety assessments and environmental impact assessments.

This report describes modelling activities carried out as a part of the site descriptive modelling. The hydrological modelling system MIKE SHE has been used to describe surface hydrology, near-surface hydrogeology, i.e. primarily groundwater flow in the Quaternary deposits, advective transport mechanisms, and the contact between groundwater and surface water. The surface water systems are described with the one-dimensional modelling tool MIKE 11, which is fully and dynamically integrated with the MIKE SHE groundwater model.

In the present work, MIKE SHE has been used to describe the surface hydrological and near-surface hydrological conditions within a regional catchment at one of the SKB investigation sites, Laxemar. The model area used in previous modelling studies of Laxemar was c. 18 km^2 /Bosson 2006/. In this project, the model area has been extended towards the west and now covers some 27 km^2. Previous MIKE SHE models have not been calibrated or otherwise compared with site specific measurements, mainly due to lack of measurements and continuous data series.

The present MIKE SHE model of Laxemar is based on the data freeze Laxemar 1.2 (November 1, 2004). After August 31, 2007, data from Laxemar 2.3 data freeze are available, and a process of updating, rebuilding and calibrating the MIKE SHE model based on that data set has already started. Before the calibrations with these new data begin, it is important to gather as much knowledge as possible on calibration methods, and to define critical calibration parameters and areas within the model. These are the main purposes of the project presented here. The work is based on experiences drawn from modelling and calibration of the MIKE SHE model of Forsmark, see /Aneljung and Gustafsson 2007/.

The main purposes of the project presented in this report are to

- make a systematic comparison between model results and site specific data,
- calibrate the model against site specific data and describe a calibration methodology to be used in forthcoming model versions,
- perform a sensitivity analysis on critical parameters.

2 The MIKE SHE modelling tool

The modelling tool used in the analysis is MIKE SHE, developed by DHI (Danish Hydraulic Institute). MIKE SHE is a dynamic and physically based modelling tool that describes the main processes in the land phase of the hydrological cycle. The processes considered in MIKE SHE are illustrated in Figure 2-1.

The precipitation can either be intercepted by leaves or fall to the ground. The water on the ground surface can infiltrate, evaporate or form overland flow. Once the water has infiltrated the soil, it enters the unsaturated zone. In the unsaturated zone, it can either be extracted by roots and leave the system as transpiration, or it can percolate down to the saturated zone. MIKE SHE is fully integrated with a one-dimensional channel-flow code, MIKE 11. The exchange of water between the two modelling tools takes place during the whole simulation, i.e. the two programs run simultaneously.

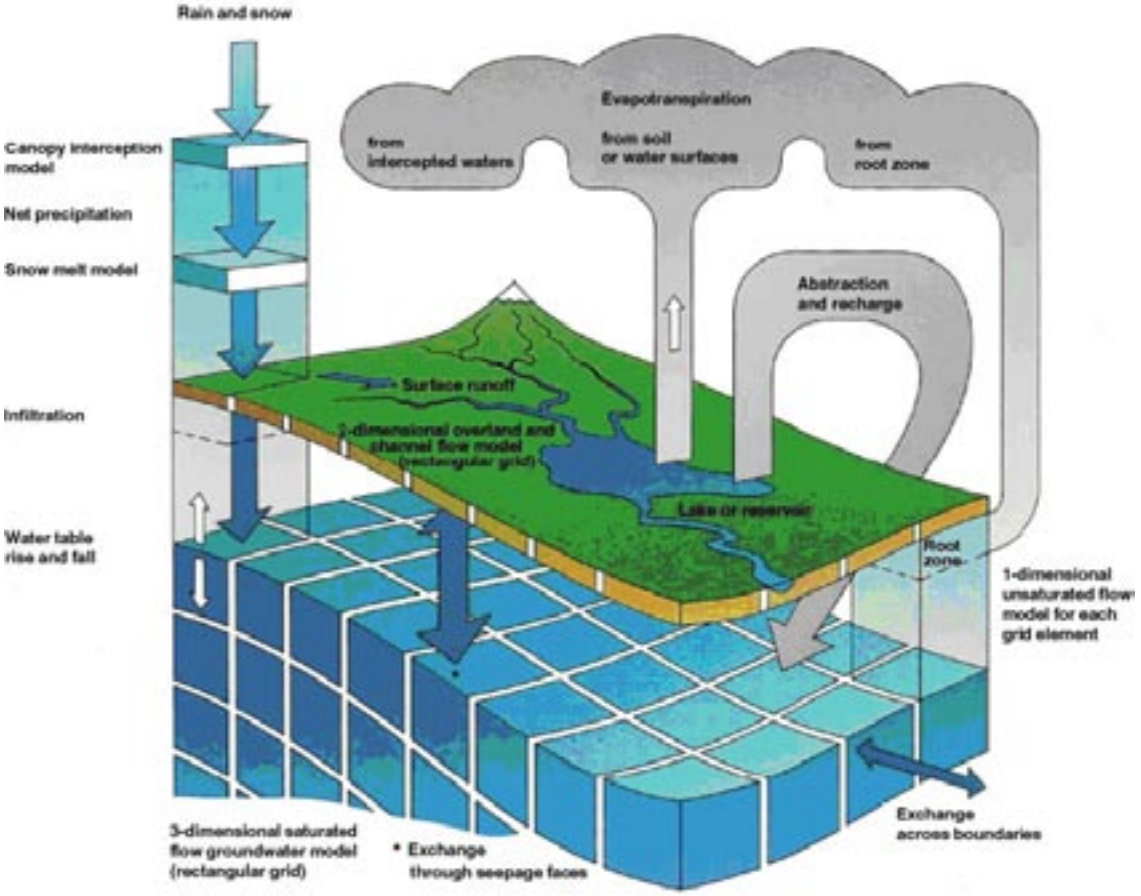

Figure 2-1. *Overview of the model structure and the processes included in MIKE SHE /DHI 2007/.*

MIKE SHE is developed primarily for modelling of groundwater flow in porous media. However, in the present modelling the bedrock is also included. The bedrock is parameterised by use of data from the Laxemar 1.2 groundwater flow model developed using the DarcyTools code /SKB 2004/. In DarcyTools, a discrete fracture network (DFN) model is used as a basis for generating hydrogeological properties for a continuum model /Svensson et al. 2004/. Thus, hydrogeological parameters can be imported directly to the corresponding elements in the MIKE SHE model.

MIKE SHE consists of the following model components:

- Precipitation (rain or snow).
- Evapotranspiration, including canopy interception, which is calculated according to the principles described in /Kristensen and Jensen 1975/.
- Overland flow, which is calculated with a two-dimensional finite difference diffusive wave approximation of the Saint-Venant equations, using the same two-dimensional mesh as the groundwater flow component. Overland flow interacts with streams, the unsaturated zone, and the saturated (groundwater) zone components.
- Channel flow, which is described through the MIKE 11 modelling system for river hydraulics, serving as the river modelling component of MIKE SHE. MIKE 11 is a dynamic, one-dimensional modelling tool for the design, management and operation of river and channel systems. MIKE 11 supports any level of complexity and offers simulation engines that cover the entire range from simple Muskingum routing to the higher order dynamic wave formulation of the Saint-Venant equations.
- Unsaturated water flow, which in MIKE SHE is described as a vertical soil profile model that interacts with both overland flow (through ponding) and groundwater flow; the groundwater table is the lower boundary condition of the unsaturated zone. MIKE SHE offers three different modelling approaches, including a simple two-layer root-zone mass balance approach, a gravity flow model and a full Richards's equation model.
- Saturated (groundwater) flow, which allows simulation of three-dimensional flow in heterogeneous aquifers, with conditions shifting between unconfined and confined conditions. The spatial and temporal variations of the dependent variable (the hydraulic head) are described mathematically by the three-dimensional Darcy equation and solved numerically by an iterative implicit finite difference technique.

For a detailed description of the processes included in MIKE SHE, see /Werner et al. 2005/ and /DHI 2007/.

3 Changes in input data compared to Laxemar 1.2

The input data to the MIKE SHE model include data on topography, land use, geology, hydrogeology and meteorology. Input data used for modelling in this project are mainly based on the input data described in /Werner et al. 2005, Bosson 2006/, such as topography and lake bathymetries, geological layers and lenses, hydraulic properties for the geological units and calculation layers. Data types where input data have been changed from the data set described in /Bosson 2006/ are listed in Sections 3.1 to 3.4.

The present model is based on the MIKE SHE-MIKE 11 model developed for site descriptive model version Laxemar 1.2, with a somewhat extended modelling area as well as an updated bedrock model based on the Laxemar 1.2 rock hydrogeology model, similar to the one in the Laxemar 1.2 "open repository" modelling. These models are described in /Werner et al. 2005/ (the site descriptive model) and /Bosson 2006/ (the "open repository" model).

3.1 Model areas

The model area used in /Bosson 2006/ has been extended towards the west and now covers 27.2 km^2, compared to the previous model area of 18.1 km^2. An additional model area covers the main (inland) catchments on the island of Ävrö, which is located east of the main model area. The model area on Ävrö is 0.8 km^2. The Laxemar and Ävrö model areas are shown in Figure 3-1.

The Ävrö model area was used in a set of test simulations only. No results from these simulations are presented in this report. It should be noted that the island of Ävrö could be of interest for modelling in the future, especially since there are three discharge stations in operation there (not shown below). However, the description of the stream network on the island probably needs to be refined before modelling aiming to reproduce measurement results is performed.

3.2 Meteorology

Data on temperature, precipitation and potential evapotranspiration are used in the MIKE SHE modelling. These data are available for the period from September 9, 2003 to December 31, 2006. The meteorological input data are taken from the meteorological station on the island of Äspö, located slightly north-east of the main model area, see Figure 3-2. The measured precipitation is corrected according to /Alexandersson 2003/, see Figure 3-3. The potential evapotranspiration was calculated with the Penman equation, applied according to /Eriksson 1981/ with data from the local station on Äspö, see Figure 3-4.

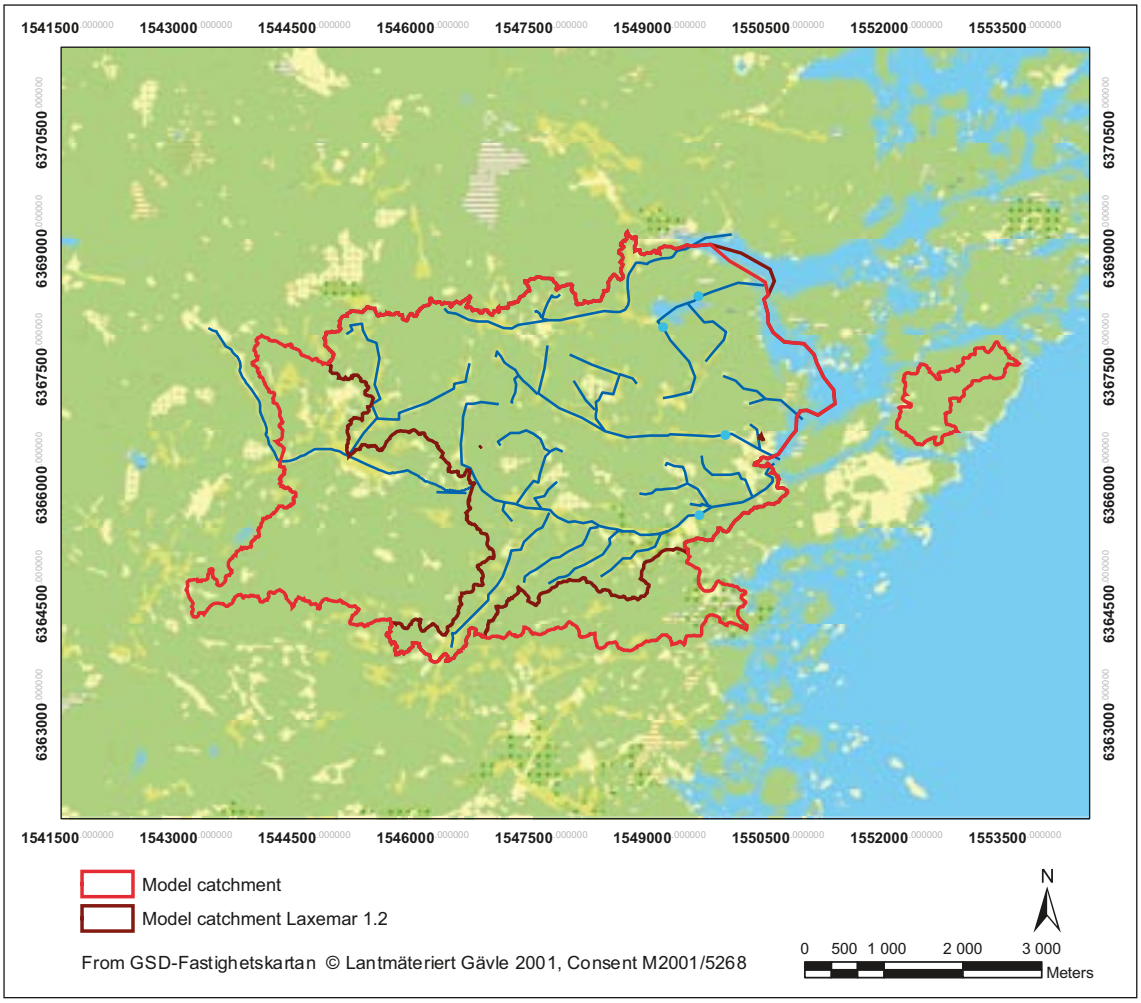

Figure 3-1. *Model areas considered in the present MIKE SHE modelling. The main model area is located in Laxemar on the mainland. Simulations were also carried out for an area on the island of Ävrö, which is located east of the main model area.*

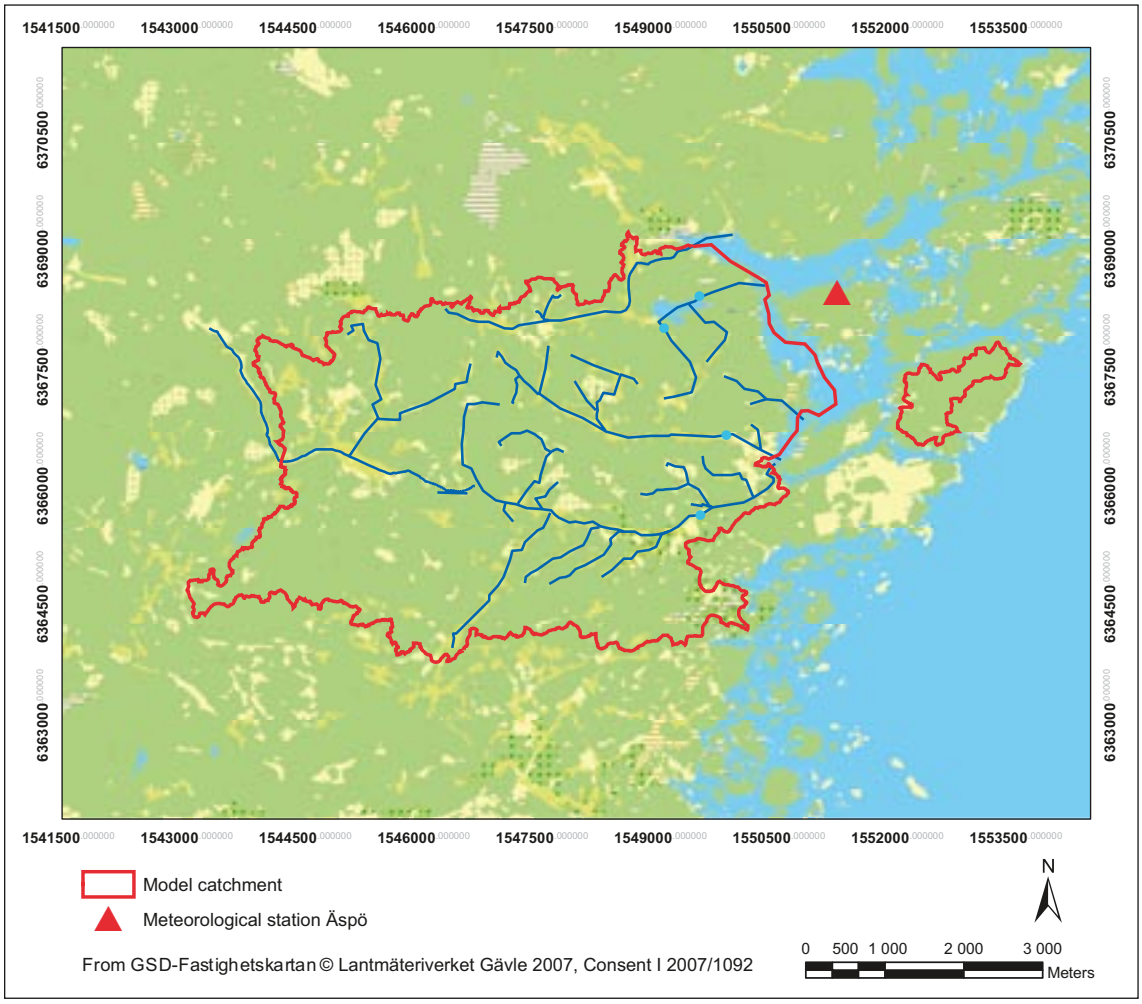

Figure 3-2. *Position of the meteorological station on Äspö.*

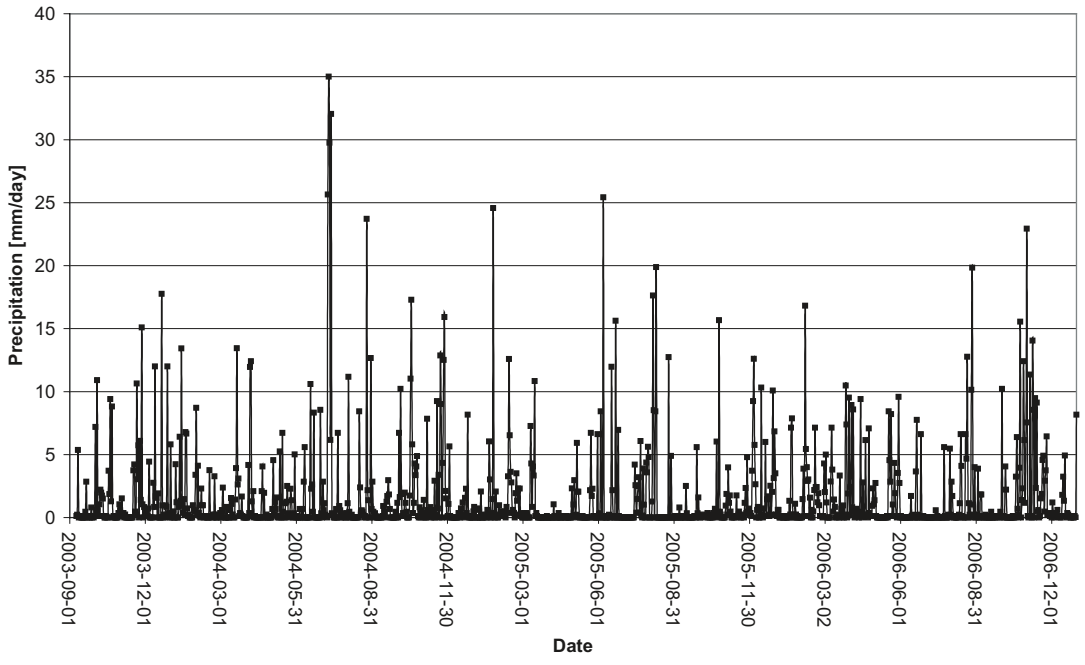

Figure 3-3. *Corrected precipitation time series (daily sums) from the meteorological station on Äspö.*

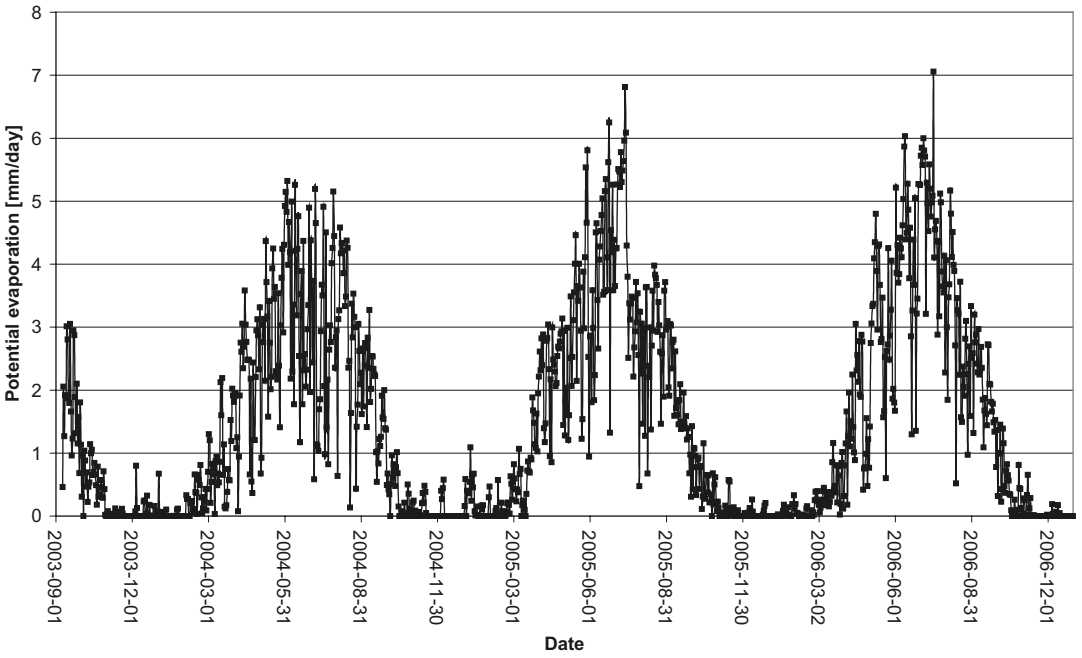

Figure 3-4. *Potential evapotranspiration time series (daily sums) from the meteorological station on Äspö.*

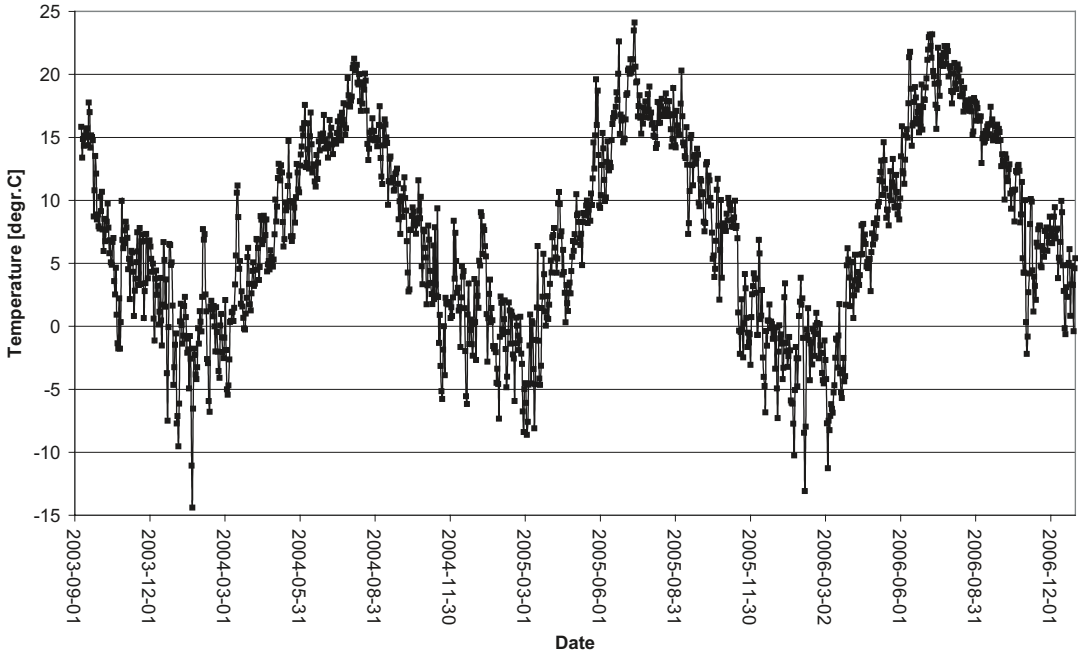

Figure 3-5. *Temperature time series (daily means) from the meteorological station on Äspö.*

The temperature input to MIKE SHE is used in combination with the precipitation to calculate the effect of snow melt and snow cover. The content of the snow storage melts at a rate defined by a degree-day coefficient multiplied with the uncorrected temperature from the meteorological station (Figure 3-5). The degree-day coefficient has been calibrated against measurements of snow cover and is set to 2.82 mm/day/°C (Kent Werner, pers. comm. 2007). During April 2006, an exceptional snow melt event took place when all snow melted during a very short period.

The accumulated corrected precipitation for the simulation period, September 9, 2003, to December 31, 2006, is 1,909 mm, and the accumulated potential evapotranspiration is 1,796 mm. Table 3-1 shows the annual values for the periods January–December 2004, January–December 2005 and January–December 2006. The mean annual precipitation for the whole period is 576 mm and the mean potential evapotranspiration is 578 mm.

3.3 Stream and lake system data

The MIKE 11 stream network described in model version 1.2 /Werner et al. 2005/ has been extended to include more branches according to Figure 3-6. The main reason for extending the stream network in MIKE 11 is to allow for more surface water flow within and from the model. The main changes in the stream network are made within the extended part of the model catchment in association with the water course Laxemarån. The existing stream network has also been extended and updated to include more cross-sections, bank levels and longitudinal profiles.

The Laxemarån water course crosses the model boundary where it has an upstream catchment area of 24.7 km^2. In previous versions of the model, the corresponding boundary condition was set to a constant surface water level, which resulted in a constant baseflow in Laxemarån. This constant water level boundary has been replaced with a time-varying inflow, which was calculated using the MIKE 11 NAM-model.

MIKE 11 NAM is a deterministic, lumped and conceptual rainfall-runoff model, accounting for the water content in up to four different storages. Depending on the requirements, NAM can be prepared in a number of different modes. As default, NAM is prepared with nine parameters representing the surface zone, the root zone and groundwater storages. In addition, NAM provides the following model capabilities:

- Extended description of the groundwater component.
- Two different degree-day approaches for snow melt.
- Irrigation schemes.
- Automatic calibration of the nine most important (default) NAM parameters. Examples of NAM calibration parameters are CQOF (overland flow runoff coefficent), Lmax (maximum water content in the root zone storage) and Umax (maximum water content in the surface storage).

Figure 3-7 show the calculated inflow over the model boundary to Laxemarån from the upstream part of the catchment.

Table 3-1. Annual precipitation and potential evapotranspiration.

Period	Precipitation [mm]	Potential evapotranspiration [mm]
January 2004–December 2004	654	543
January 2005–December 2005	493	601
January 2006–December 2006	582	591

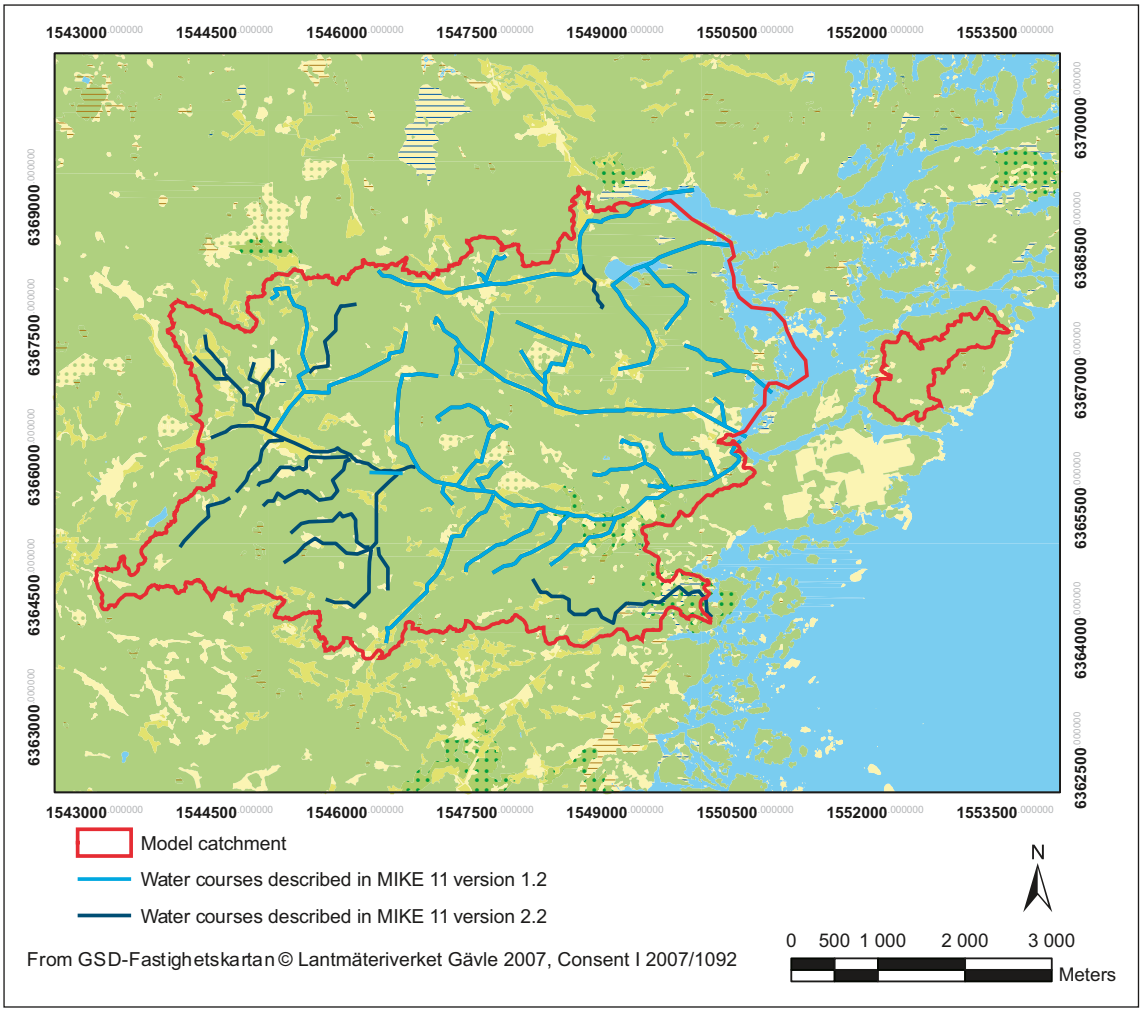

Figure 3-6. *Water courses included in the MIKE 11 stream network model. The light blue lines show the water courses included in the previous version of the model; the dark blue lines show the additional ones in the extended model. Lake Frisksjön is located in the north-eastern part of the main model area.*

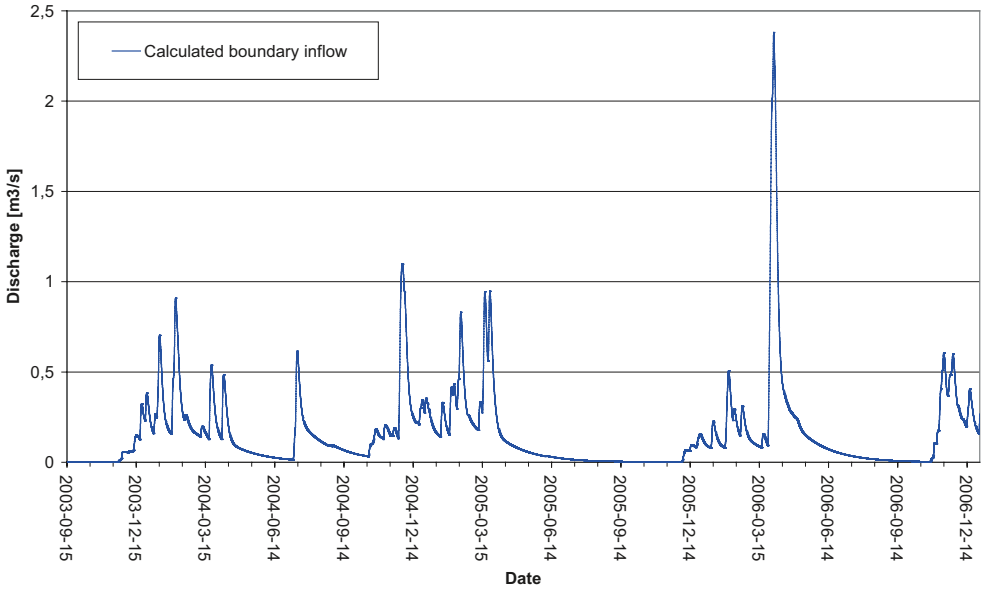

Figur 3-7. *Calculated boundary inflow in the Laxemarån water course.*

3.4 Calibration data

Time series data from one surface water level monitoring station, four surface water discharge monitoring stations and 43 groundwater monitoring wells (SSM-series boreholes in Quaternary deposits) have been used to calibrate and evaluate the model. These observation points are mainly located within the north-eastern part of the main model area, whereas only a few points are located in the western and southern parts.

Figure 3-8 shows the locations of the different surface water monitoring stations used within the model area. PSM000348 includes both lake water level (Lake Frisksjön) and discharge monitoring (of the discharge from the lake); PSM000347, PSM000364 and PSM000365 are all discharge monitoring stations.

Groundwater level measurements in percussion drilled boreholes in the bedrock are in general too disturbed by drilling and other ongoing activities in the area to be useful as calibration data, and have therefore not been used in this project. Figure 3-9 shows locations of the different groundwater monitoring wells from which data are used for the current model calibration. As described above, however, no results of the modelling of the Ävrö area (the smaller model area in Figure 3-9) are presented in this report. Therefore, the groundwater monitoring wells there are not discussed in the following.

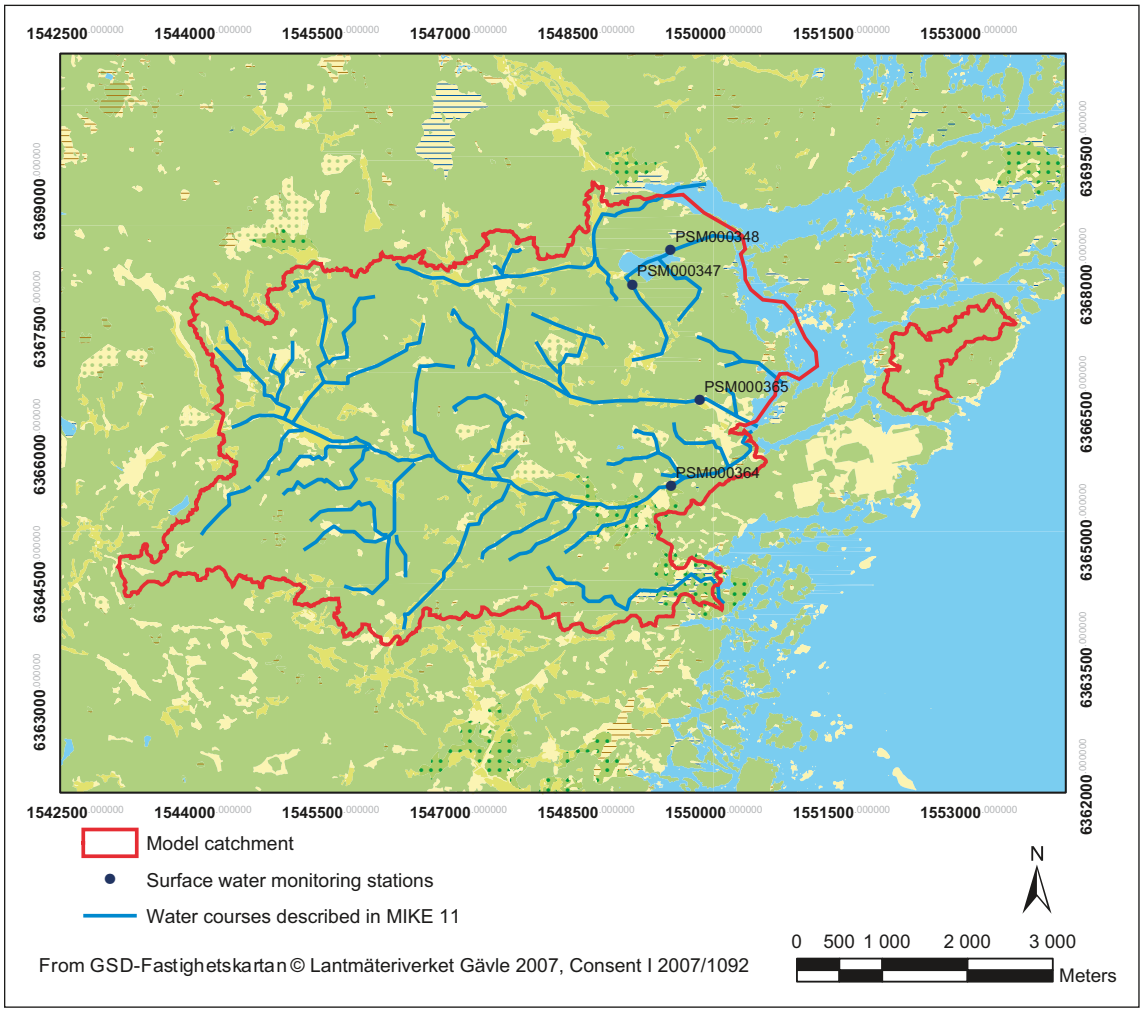

Figure 3-8. *Locations of surface water monitoring stations used for calibration in Laxemar. PSM000348 includes both surface water level (Lake Frisksjön) and discharge monitoring, PSM000347, PSM000364 and PSM000365 are all discharge monitoring stations.*

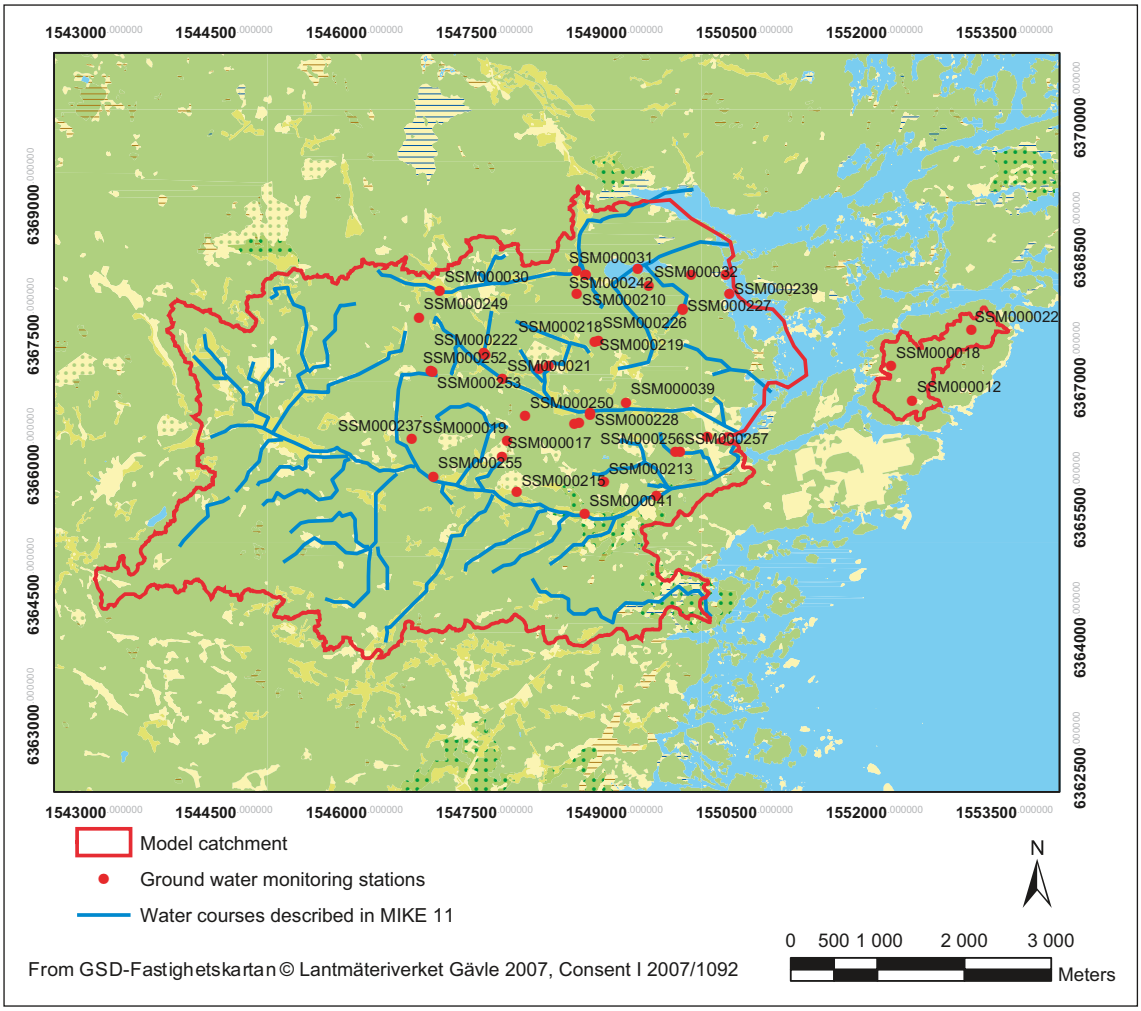

Figure 3-9. *Locations of groundwater monitoring wells used for model calibration.*

4 Model updates and definition of a base case

The modelling performed in this project is based on the MIKE SHE Laxemar 1.2 site descriptive modelling and "open repository" modelling described in /Werner et al. 2005/ and /Bosson 2006/, respectively. The present model area is 27.2 km^2, see Figure 3-1. The horizontal model grid resolution is 30 m; the resolution is the same in the whole model area.

The simulation period is 2003-09-09 to 2006-12-31. Initial conditions for groundwater head elevations and depth of overland water are based on simulated values from a date during 2006 with equivalent conditions as the start date. The results were extracted after multiple runs, when no further changes could be observed, which means they represent so-called semi-stationary conditions.

4.1 Updates of the numerical description

A number of updates have been made to the model in order to improve the numerical solution, the overland solver stability and the model discretisation. Optimization of the time steps and the numerical control parameters for the different model components resulted in the values shown in Table 4-1. In the time step optimisation, there is a trade off between simulation times and numerical stability. The computational control parameters and the time steps for different components are described in /DHI 2007/.

The vertical numerical cell height in the unsaturated zone description was also reduced in order to resolve the high infiltration velocities in some parts of the model. In previous MIKE SHE and MIKE 11 model versions, the communication between the stream network in MIKE 11 and the overland component in MIKE SHE has been a source of numerical instability, which also increases computational times. When updating the numerical description of the model, the so-called "flood code" communication between MIKE 11 and the overland component in MIKE SHE was replaced by the so-called "overbank spilling" option, as described in /Aneljung and Gustafsson 2007/.

Table 4-1. Time steps and computational control parameters used in the model.

Parameter	Value
Initial time step	0.5 h
Maximum allowed OL, UZ, and ET time step	0.5 h
Maximum allowed SZ time step	3 h
MIKE 11 time step	30 s
Maximum number of allowed OL iterations	50
OL iteration stop criteria	1e–5
Water depth threshold for OL	0.001 m
Maximum profile water balance error, UZ/SZ coupling	0.001 m
Maximum number of allowed UZ iterations	50
Iteration stop criteria	0.002
Maximum water balance error in one node (fraction)	0.03
Maximum number of allowed SZ iterations	80
Maximum head change per SZ iteration	0.05 m
Maximum SZ residual error	0.005 m/d
Saturated thickness threshold	0.05 m

In MIKE SHE, the transpiration processes are limited to the uppermost calculation layer of the saturated zone. In order to allow for transpiration processes to be active at a greater depth from the ground surface, the minimum thickness of the uppermost calculation layer was set to two metres. Originally, the calculation layers were defined with respect to a detailed description of lake sediments. An effect of changing the computational layers is that the hydraulic properties of each layer are recalculated as a harmonic mean value with respect to the thickness of each geological unit which is part of the calculation layer. Note that the geological layers and units are not changed in the input data. Computational times were also reduced by reducing the number of computational layers in the bedrock from eight to four layers. Section 6.6 illustrates the effect of reducing the number of calculation layers in the bedrock.

Moreover, in order to ensure that the evapotranspiration processes are correctly modelled in ponded areas, areas with major ponding were selected for unsaturated zone calculation in each grid cell through the so-called partial automatic classification, instead of using the fully automatic classification option.

4.2 Initial calibration

An initial calibration of model parameters and other model input was made in order to define a base case for the area. The initial calibration followed a number of steps, which are described in this section.

Initial simulations showed too little runoff from the overland component to the surface water system, especially during snowmelt events. To correct this, the MIKE 11 model was evaluated and supplemented with more branches and cross-sections in order to allow for more communication between the overland component in MIKE SHE and the stream network in MIKE 11. Initial results showed a small constant baseflow in the water course Laxemarån. The MIKE 11 boundary at Laxemarån (constant water level) was therefore replaced with a calculated discharge from the upstream catchment, as described in Section 3.3 with a resulting inflow across the upstream boundary according to Figure 3-7.

The overland flow Manning number in MIKE SHE was decreased from 10 to 1 $m^{1/3}s^{-1}$, since this is a more realistic number that also provides a more stable numerical solution. Larger values, like 10 $m^{1/3}s^{-1}$ or higher, are appropriate for larger water depths (channel flow) or smoother grass surfaces, which conditions are not consistent with those found in the Laxemar area.

Boreholes located close to the sea are likely affected by the internal boundary condition in the sea, where a fixed head of 0 m.a.s.l. (metres above sea level) was defined in the Laxemar 1.2 model. This resulted in very low amplitudes of the groundwater head variations near the sea. In the uppermost MIKE SHE calculation layer and in MIKE 11, the fixed head boundary condition was therefore replaced by measured time-varying water levels in the sea, calculated as an average from the three stations PSM000369, PSM00370 and PSM00371.

The other boundary conditions were not changed compared to Laxemar 1.2, that is, the bottom boundary condition, as well as the horizontal boundary conditions for the bedrock layers, are fixed head elevations with input from the regional DarcyTools model /Svensson 2006/. The horizontal boundaries of the soil calculation layers are set to a zero flux, i.e. a no-flow boundary, along the land side of the boundary, and a fixed head of 0 m.a.s.l. for the outer sea boundary, except for the uppermost layer where the above-mentioned time varying head boundary is applied.

The crop coefficient (K_c) was changed to a constant value of 0.9 for all vegetation classes, describing a less active vegetation; the original data contained many values above 1. The leaf area index (LAI) and the interception coefficient (C_{int}) were reduced to 50% of the original values for all vegetation. All of these changes resulted in less evapotranspiration and hence more runoff.

The unsaturated zone description in areas with near-surface bedrock was changed to a description closer to organic soils with larger porosity, i.e. rather the thin soil layer on top of the bedrock than the bedrock itself. The motivation for this is that the groundwater depths in these areas most likely are very small, due to the low hydraulic conductivity of the bedrock, and that the important unsaturated zone processes are taking place in the thin soil layers on top of the bedrock.

The unsaturated zone description for gravel was changed to a more sandy soil with lower hydraulic conductivity (K_s was reduced from $1 \cdot 10^{-3}$ m/s to $2 \cdot 10^{-5}$ m/s), mainly due to numerical instability reasons. The conductivities in the unsaturated zone description were reduced; K_s was reduced by a factor of 20 and the Averjanov constant was increased by adding 3 to the original value, in order to increase the surface runoff and reduce the infiltration.

The hydraulic conductivities in Quaternary deposits and near-surface bedrock were reduced in the following way:

- The horizontal conductivities of Quaternary deposit layers Z1, Z2 and Z3 (see /Bosson 2006/) were reduced by a factor 4.
- The vertical hydraulic conductivities of Quaternary deposit layers Z1, Z2 and Z3 were reduced by a factor 20.
- The horizontal and vertical hydraulic conductivities of the two top bedrock layers were reduced by a factor 2.

The simulation times for the base case were totally c. 19 hours. The most time consuming components in the model are the unsaturated flow with just above 7.5 hours, the saturated zone with around 6 hours and the MIKE 11 river network with 3 hours.

4.3 Summary of model updates compared to Laxemar 1.2

The most important updates of the model compared to the previous Laxemar 1.2 “open repository” model, as described in Chapter 3, and Sections 4.1–4.2, are the following:

Updates of the numerical model:

- Optimisation of time steps and computational control parameters.
- The vertical numerical scheme for the unsaturated zone description was refined.
- New model code for the coupling between the stream network in MIKE 11 and the overland component in MIKE SHE.
- Increased layer thickness of the uppermost calculation layer to allow for evapotranspiration at greater depths.
- Reduction of the number of computational layers in the bedrock.
- Updates in the unsaturated zone classification routine (e.g. partial automatic classification); this is done in order to increase the number of points in the computation, especially in cells with ponded water.

Updates and changes of the physical model parameters:

- Updates of meteorological input data.
- Extension of the model area.
- Extension of the bedrock model from DarcyTools in accordance with the extended model area (lower levels, initial potential heads, hydraulic conductivities, storage coefficients and specific yield).
- Updates of the physical description of the stream network and Lake Frisksjön (increased number of water courses, increased number of cross sections, bank levels, and a new type of boundary condition in Laxemarån).
- Reduction of the Manning number in the overland flow component.
- Updates in the unsaturated zone description of the near-surface bedrock.
- Reduction of hydraulic conductivities in Quaternary deposits and near-surface bedrock layers.
- Reduction of K_c, LAI and C_{int} to reduce the evapotranspiration.

5 Base case results

The results from the base case are presented in terms of model-calculated groundwater recharge and discharge areas, as a comparison between measured and calculated head elevations at a number of observation points, and as a total water balance over the land part of the main model area.

5.1 Recharge and discharge areas

The base case model results show that groundwater discharge occurs in and around Lake Frisksjön and the sea. Figure 5-1 and 5-3 show the difference between the calculated groundwater level and the head elevation in calculation layer 7 (located at approximately –100 metres above sea level), indicating regional-scale recharge/discharge areas.

Figures 5-2 and 5-4 show the difference between the calculated groundwater level and the head elevation in calculation layer 5, which is the uppermost bedrock layer. The latter hydraulic gradients hence indicate more local-scale groundwater recharge/discharge areas, in the soil layers. Note that Figures 5-1 and 5-2 show results for winter conditions, whereas Figures 5-3 and 5-4 show results representing summer conditions.

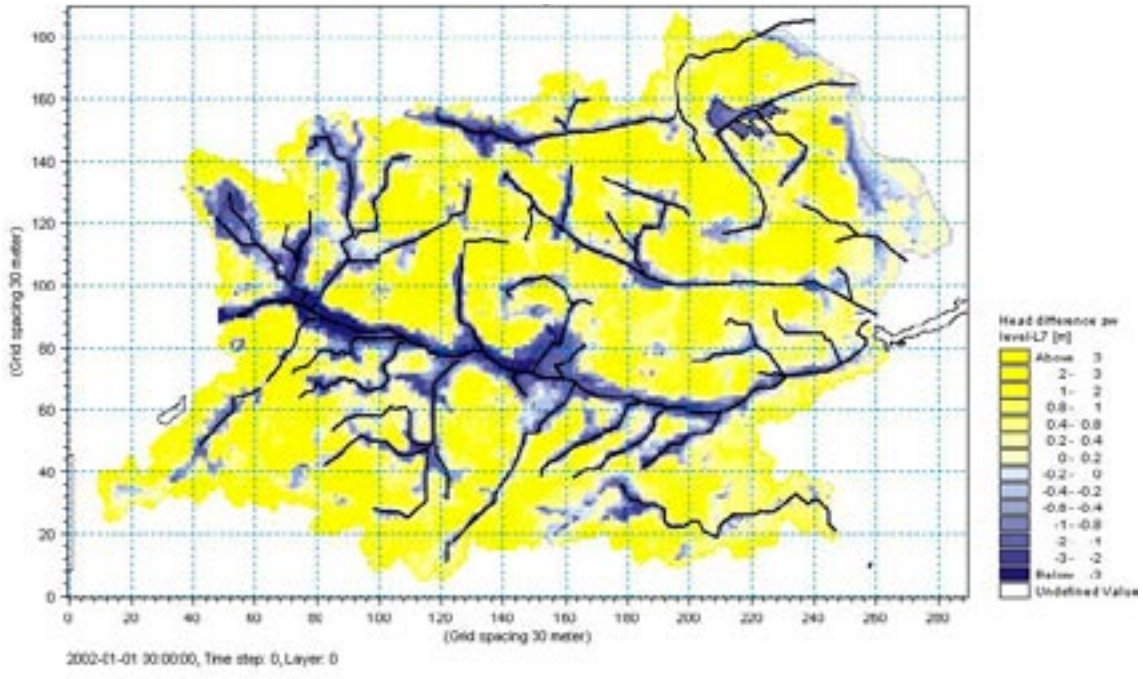

Figure 5-1. *Regional-scale recharge and discharge areas under winter conditions (2005-01-12). Yellow colours show the vertical head differences in recharge areas and the light blue to dark blue the head differences in discharge areas. The mean head difference in the recharge areas is 1.7 m and the corresponding mean head difference in the discharge areas is 1.0 m (note that the legend scale differs from adjacent figures).*

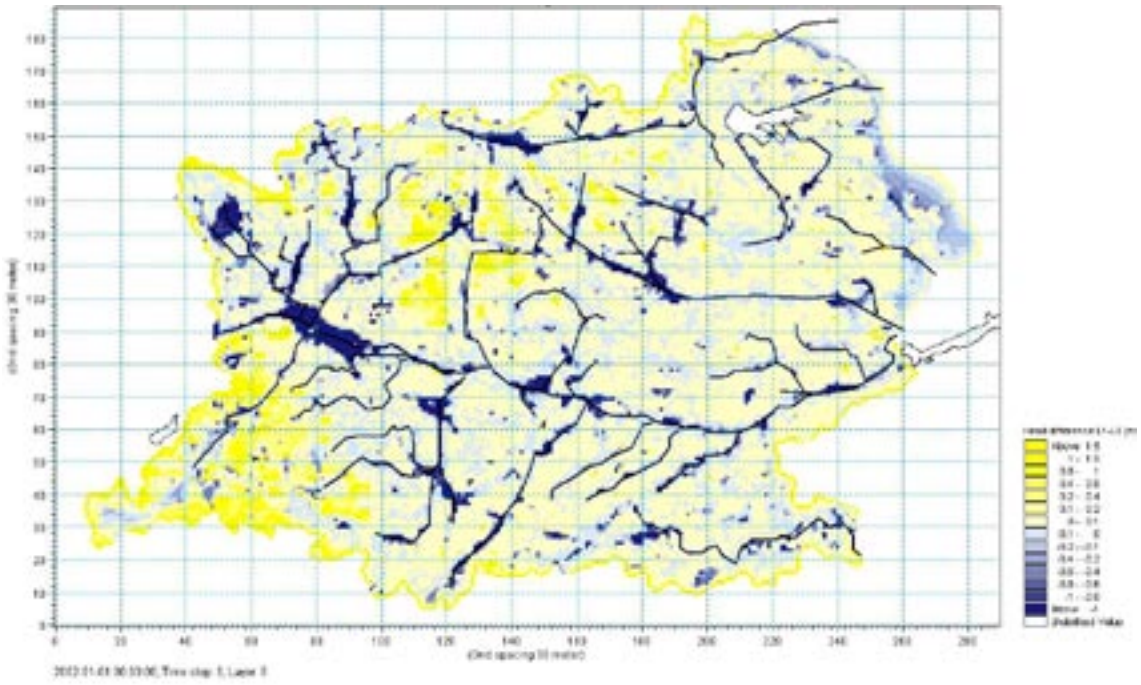

Figure 5-2. *Local recharge and discharge areas under winter conditions (2005-01-12). Yellow colours show the vertical head differences in recharge areas and the light blue to dark blue the head differences in discharge areas. The mean head difference in the recharge areas is 0.32 m and the corresponding mean head difference in the discharge areas is 0.26 m (note that the legend scale differs from adjacent figures).*

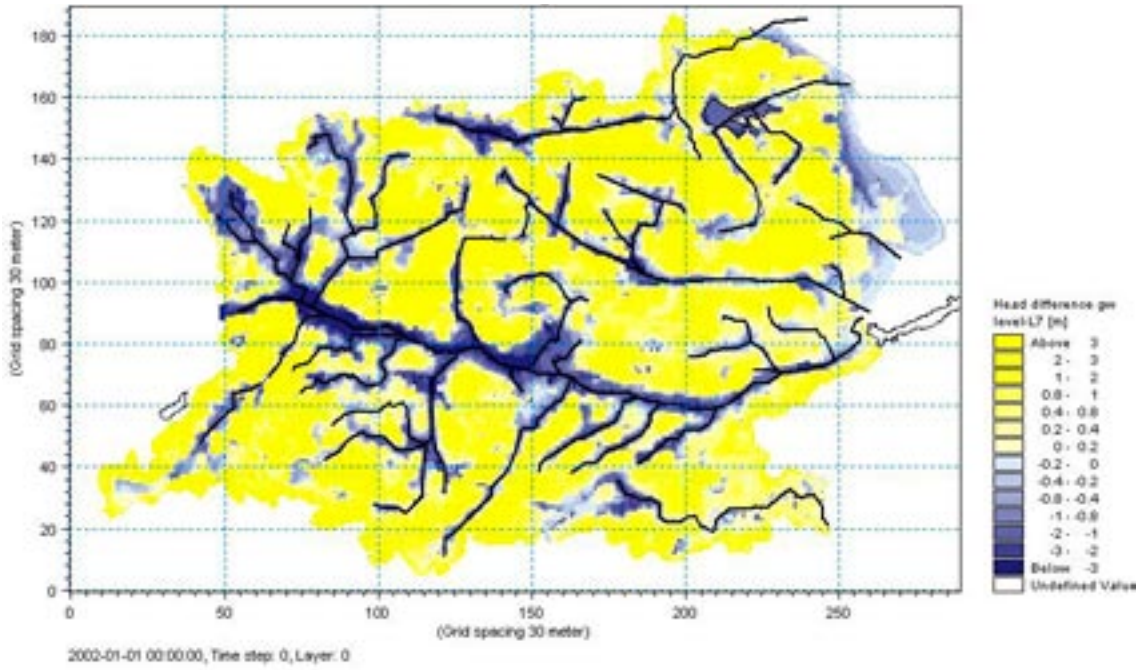

Figure 5-3. *Regional-scale recharge and discharge areas under summer conditions (2005-08-20). Yellow colours show the vertical head differences in recharge areas and the light blue to dark blue the head differences in discharge areas. The mean head difference in the recharge areas is 1.9 m and the corresponding mean head difference in the discharge areas is 1.1 m (note that the legend scale differs from adjacent figures).*

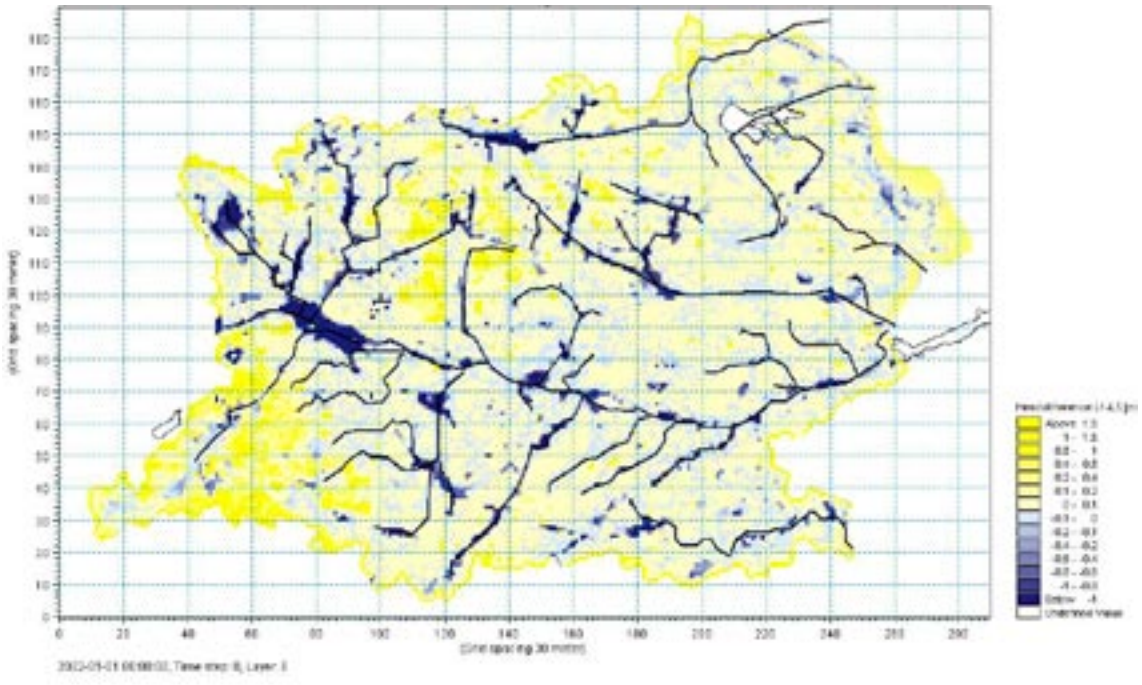

Figure 5-4. *Local recharge and discharge areas under summer conditions (2005-08-20). Yellow colours show the vertical head differences in recharge areas and the light blue to dark blue the head differences in discharge areas. The mean head difference in the recharge areas is 0.30 m and the corresponding mean head difference in the discharge areas is 0.34 m (note that the legend scale differs from adjacent figures).*

During winter, discharge areas are mainly found around Lake Frisksjön and the water courses in the area. Both recharge and discharge head differences are considerably larger when analyzing head differences between the groundwater level and the deeper bedrock layer, compared to the local head differences in the Quaternary deposits. The conditions are very similar during the summer, but with somewhat stronger recharge and discharge areas, i.e. with larger vertical head gradients.

In the sea, the calculated head differences reflect momentary “snap shots” of the differences between the time-varying sea level (daily variations) and groundwater heads below the sea. This is why recharge conditions are indicated in some off-shore areas in some of the figures. These highly transient head differences are probably not representative of the real recharge-discharge conditions below the sea. Note also that the pattern of the gradients is not necessarily equivalent to the vertical flow pattern. The flow is also affected by the distance over which the gradient operates and by the vertical hydraulic conductivities. The direction of the flow will however always be the same as indicated by the gradient.

5.2 Surface water levels and surface water discharge

The hydrological monitoring stations used in the evaluation of the base case are shown in Figure 5-5. Discharge measurements are made in the inlet (PSM000347) and outlet (PSM000348) of Lake Frisksjön, and in the Laxemarån (PSM000364) and Ekerumsbäcken (PSM000365) water courses. PSM000348 is also a surface water level station, where the level of Lake Frisksjön is monitored.

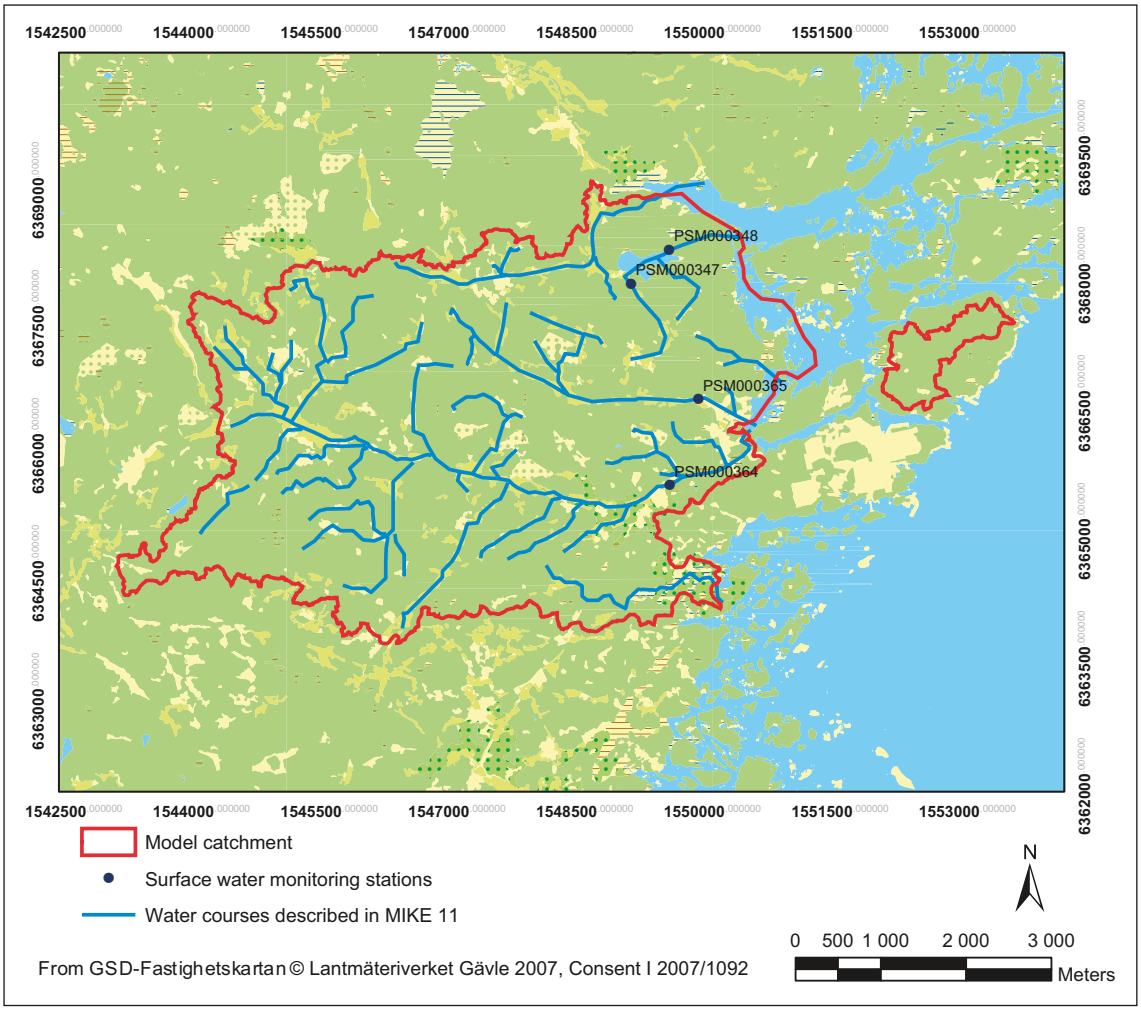

Figure 5-5. *Locations of hydrological monitoring stations used for calibration and evaluation of results of surface water discharge calculations.*

Generally, there is an acceptable agreement between measured and calculated water levels and discharges. Figure 5-6 shows a comparison between measured and calculated water levels in PSM000348 at the outlet of Lake Frisksjön. The model-calculated water levels are somewhat higher than the measured levels during the summers. The measured water levels generally demonstrate slower changes than the simulated water levels.

Figures 5-7 to 5-10 compares measured and calculated discharges at PSM000347 (Figure 5-7; upstream from Lake Frisksjön), PSM000348 (Figure 5-8; at the outlet from Lake Frisksjön), PSM000364 (Figure 5-9; near the outlet of Laxemarån), and PSM000365 (Figure 5-10; near the outlet of Ekerumsbäcken). The model generally calculates quicker changes of the water level compared to the measurements, which means that the model yields too narrow discharge peaks. The exceptional snow melt event in April 2006 is not well described in the model, with far too small peak discharges. The lack of runoff during this event can be explained, at least to a certain extent, by snow melt losses in the model during the previous months, when observed discharges do not indicate any snowmelt or runoff.

This also results in a number of small peaks and a higher base flow during the winter 2005/2006, compared to observed discharges. This pattern is clearly seen at PSM000348, where the total flow volume during the winter/spring period 2005/2006 is correct, but the temporal distribution is not. A reason for this might be a limitation in the model code, where snow melt occurs as soon as the temperature reaches zero degrees or higher. In reality, the snow pack has a storage capacity of melted water, which later on can refreeze. Adjusting the temperature thresh-

old for snow melting in the model could be a way to resolve this problem, and a relevant test to perform in future modelling. However, this was not further investigated in the present project. It should also be noted that the monitoring stations in and near Lake Frisksjön (PSM000347 and PSM000348) have some uncertainties regarding the quality of the measured data.

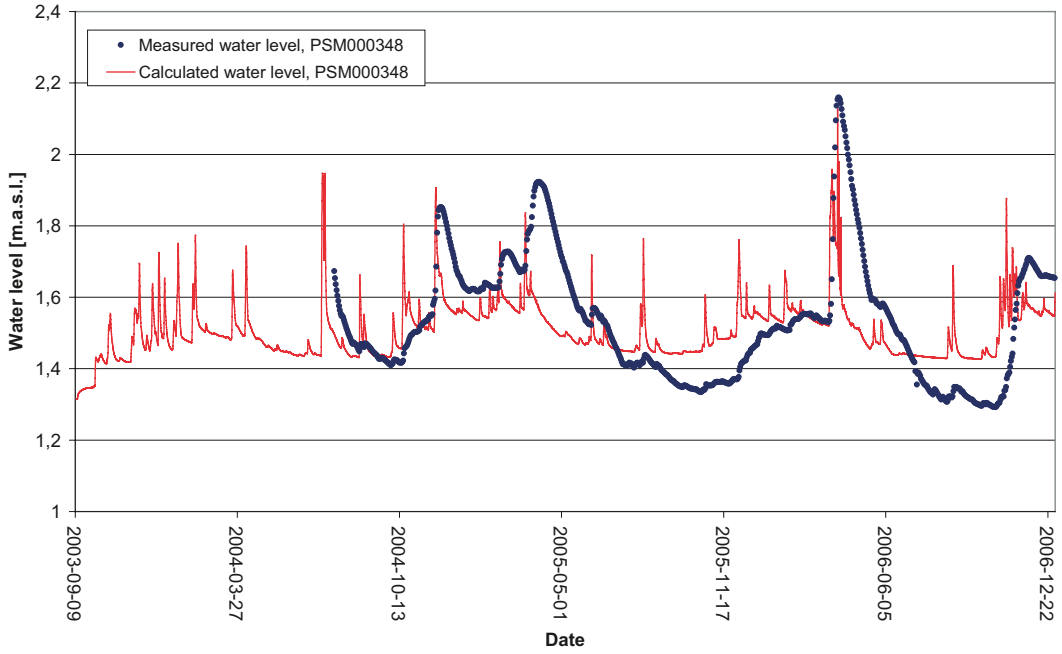

Figure 5-6. *Comparison between measured and calculated water levels in Lake Frisksjön.*

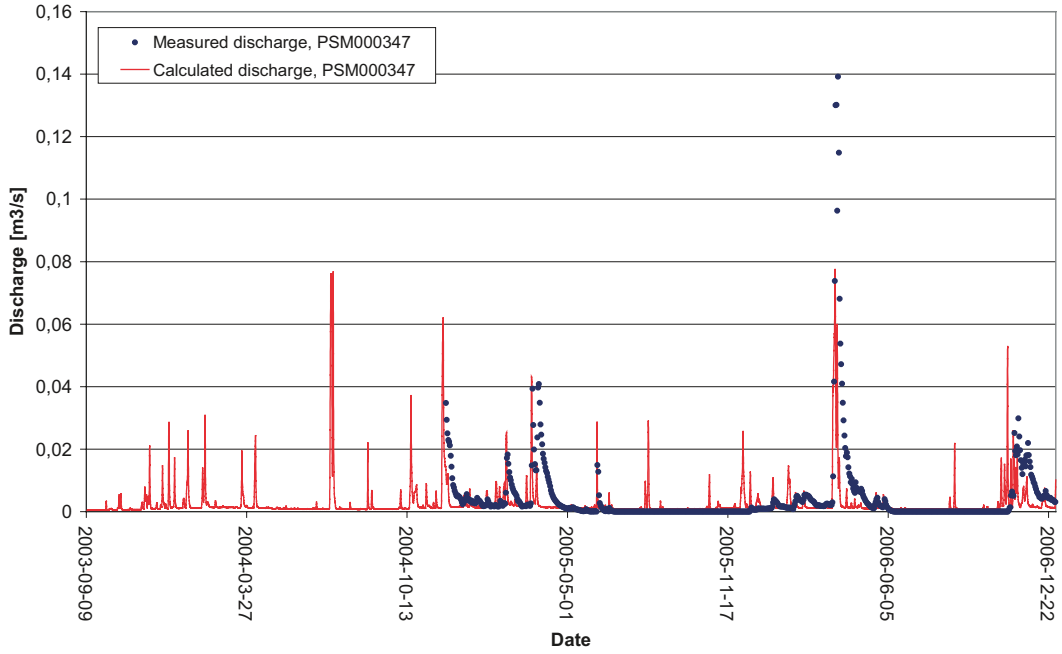

Figure 5-7. *Comparison between measured and calculated discharge at PSM000347 (upstream from Lake Frisksjön).*

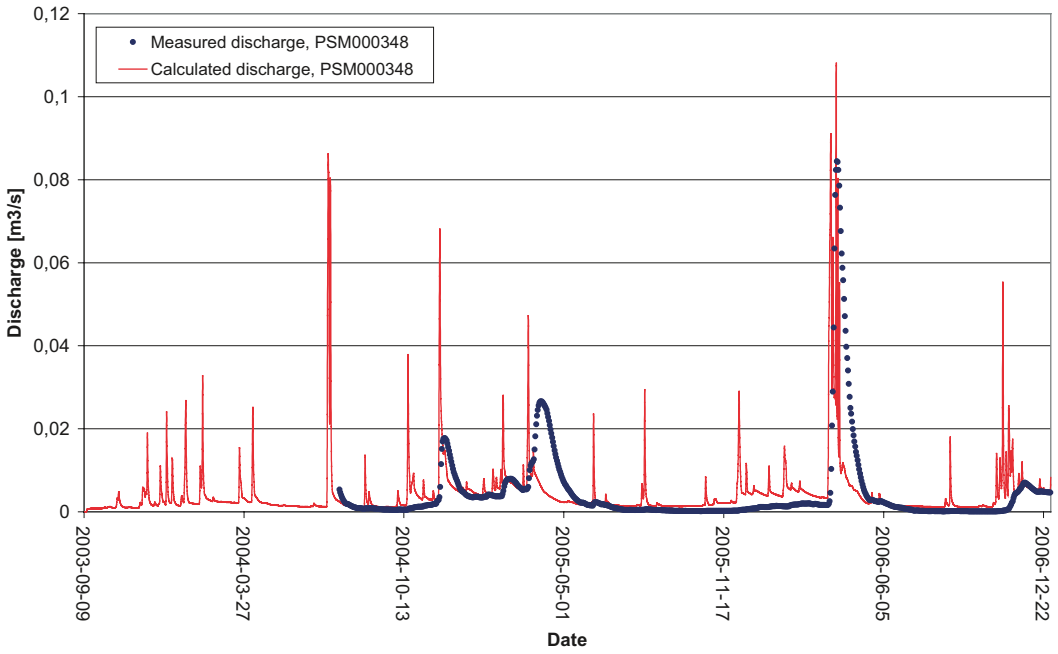

Figure 5-8. *Comparison between measured and calculated discharge at PSM000348 (in the outlet of Lake Frisksjön).*

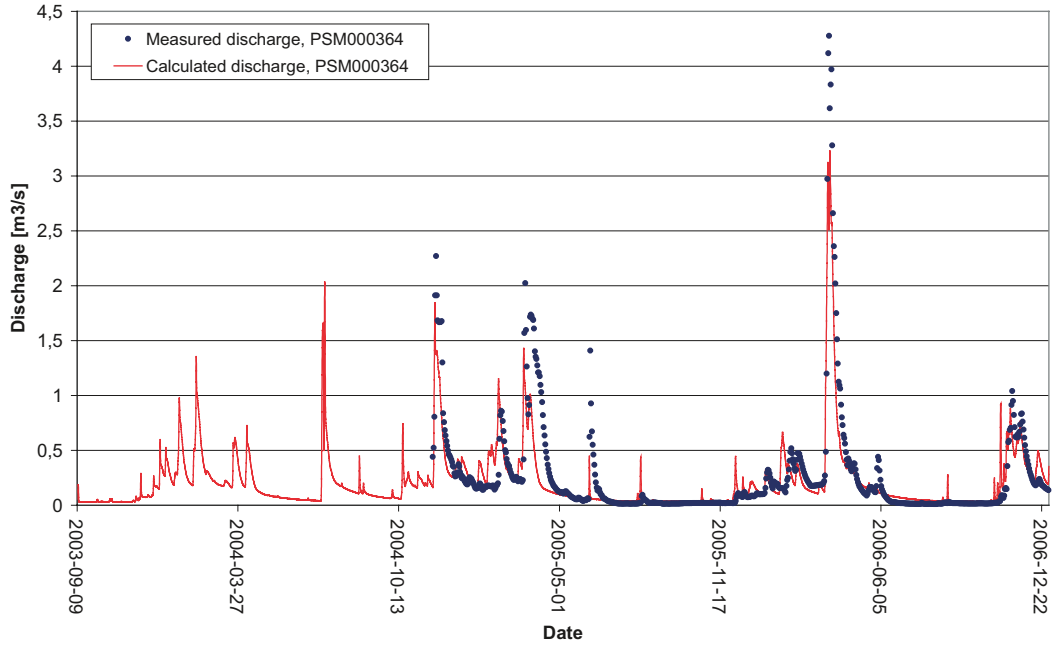

Figure 5-9. *Comparison between measured and calculated discharge at PSM000364 (near the outlet of Laxemarån)*

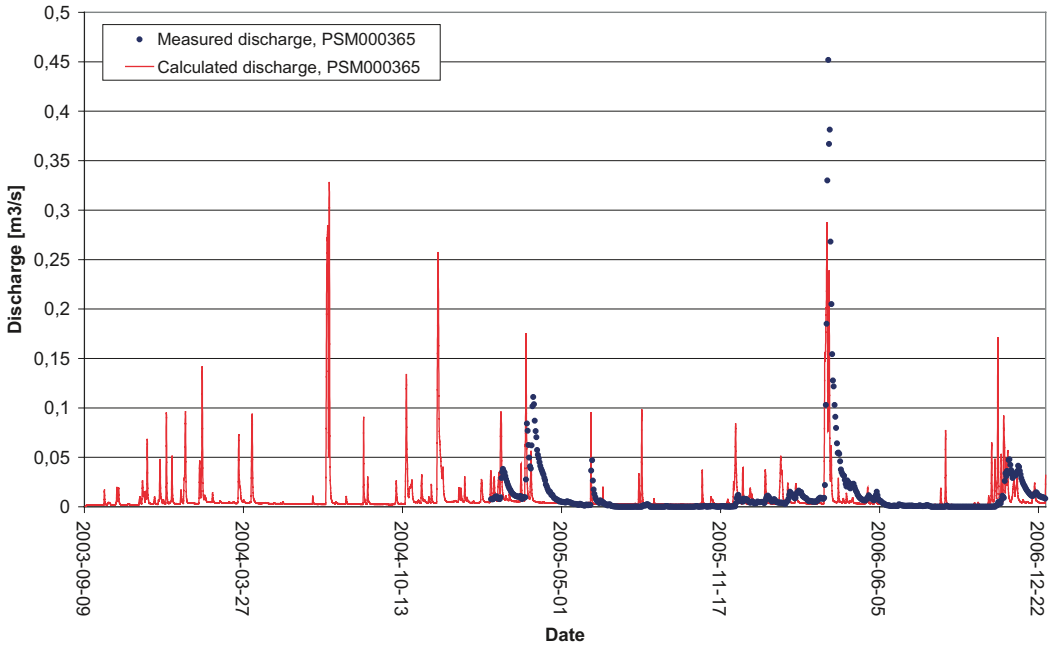

Figure 5-10. *Comparison between measured and calculated discharge at PSM000365 (near the outlet of Ekerumsbäcken).*

Figures 5-11 to 5-14 show the accumulated observed and simulated discharges for the stations PSM000347 (Lake Frisksjön inlet), PSM000348 (Lake Frisksjönoutlet), PSM000364 (in Laxemarån) and PSM000365 (in Ekerumsbäcken). The lack of runoff in connection with larger rain and snow melt events is obvious. On the other hand, the base flow is slightly over-estimated. An increased surface runoff through local streams, combined with reduced infiltration, would change the results in the right direction.

5.3 Groundwater head elevations

The monitoring wells used in the evaluation of the base case are shown in Figure 5-15. The chosen wells have continuous groundwater level data series covering most of the simulation period. It is seen that a majority of the monitoring wells are located in the north-western part of the main model area, whereas the southern and western parts are not represented in the present data set. However, additional groundwater monitoring wells have, to some extent, been installed also in these parts of the model area. The reason for not using them here is that the data time series are too short to be useful. Note that the three monitoring wells on the island of Ävrö have been used in test simulations only, and that no results are presented in this report for these wells.

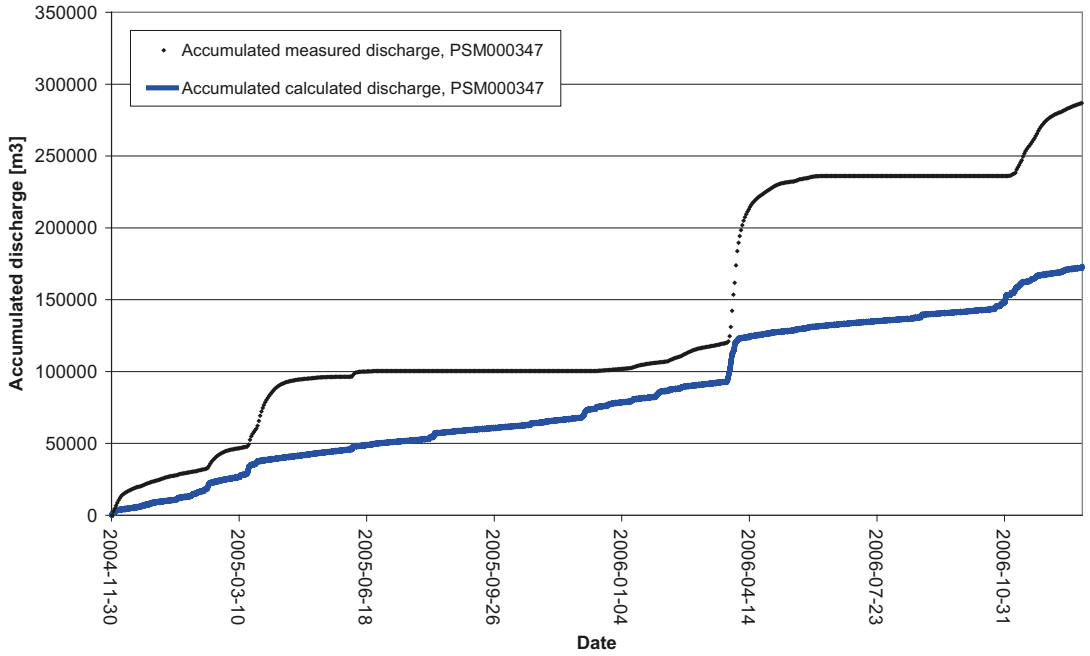

Figure 5-11. *Accumulated measured and calculated discharges [m³] between 2004-12-08 and 2006-12-31 in PSM000347 (upstream from Lake Frisksjön).*

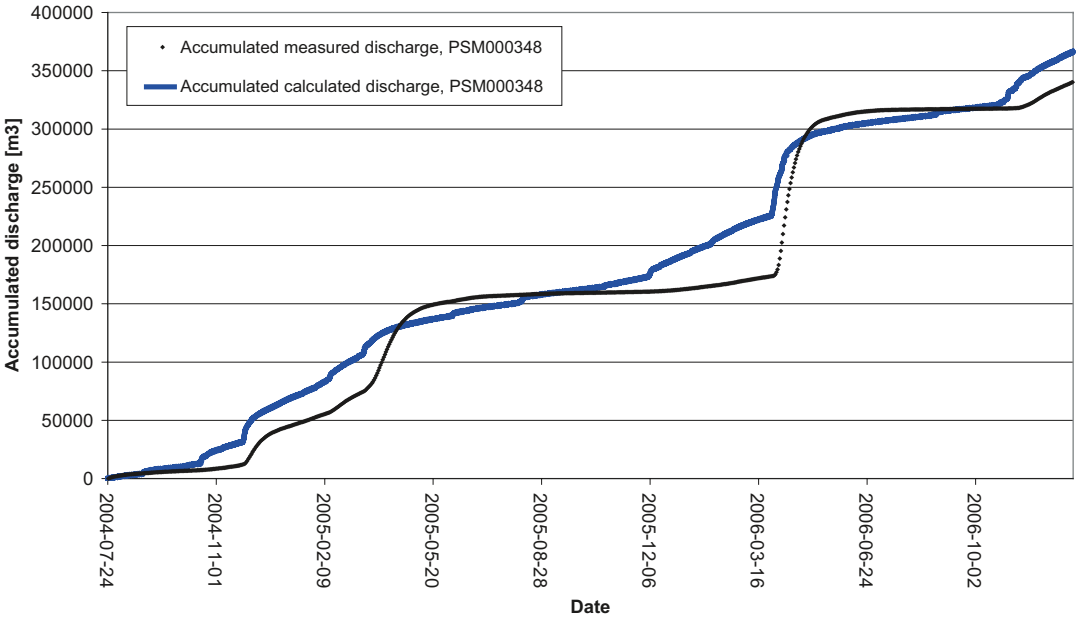

Figure 5-12. *Accumulated measured and calculated discharges [m³] between 2004-12-08 and 2006-12-31 in PSM000348 (in the outlet of Lake Frisksjön).*

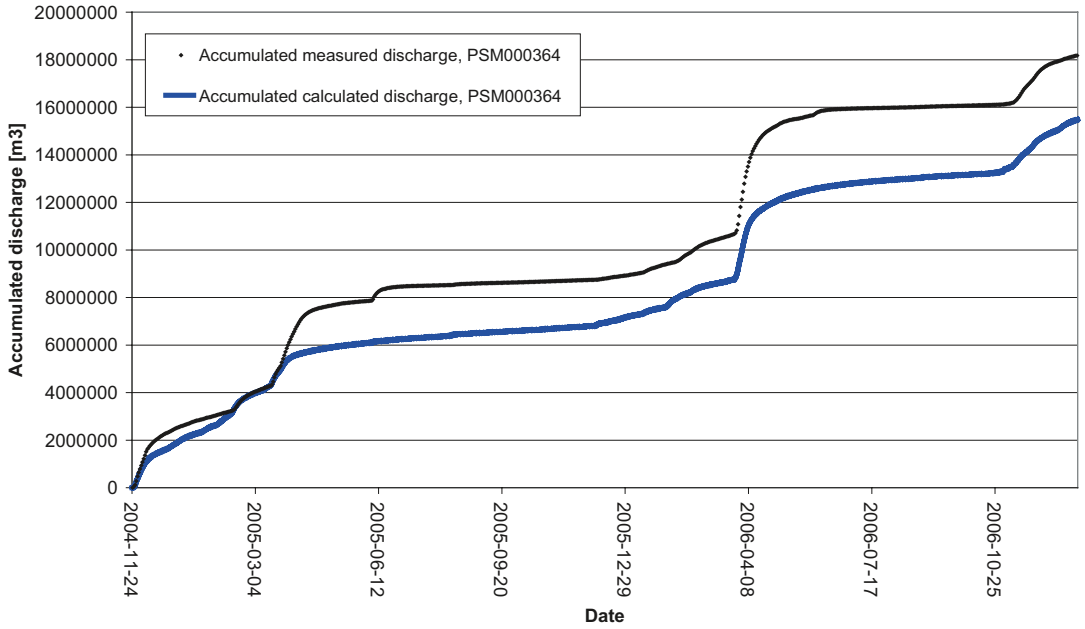

Figure 5-13. *Accumulated measured and calculated discharges [m³] between 2004-12-08 and 2006-12-31 in PSM000364 (in Laxemarån).*

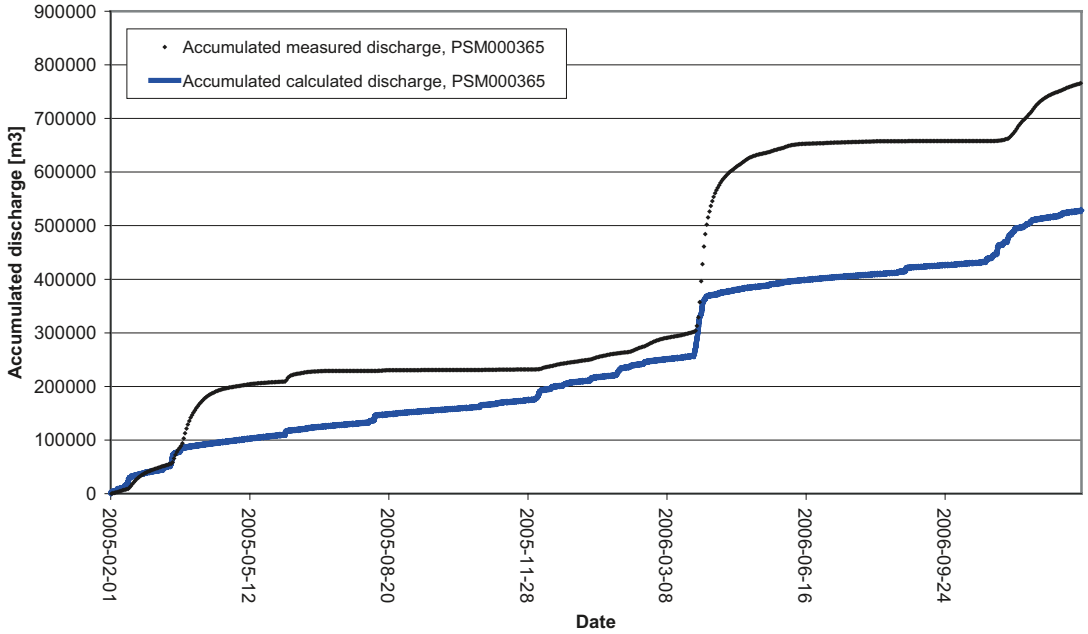

Figure 5-14. *Accumulated measured and calculated discharges [m³] between 2004-04-14 and 2005-07-31 and between 2004-12-08 and 2006-12-31 in PSM000365 (in Ekerumsbäcken).*

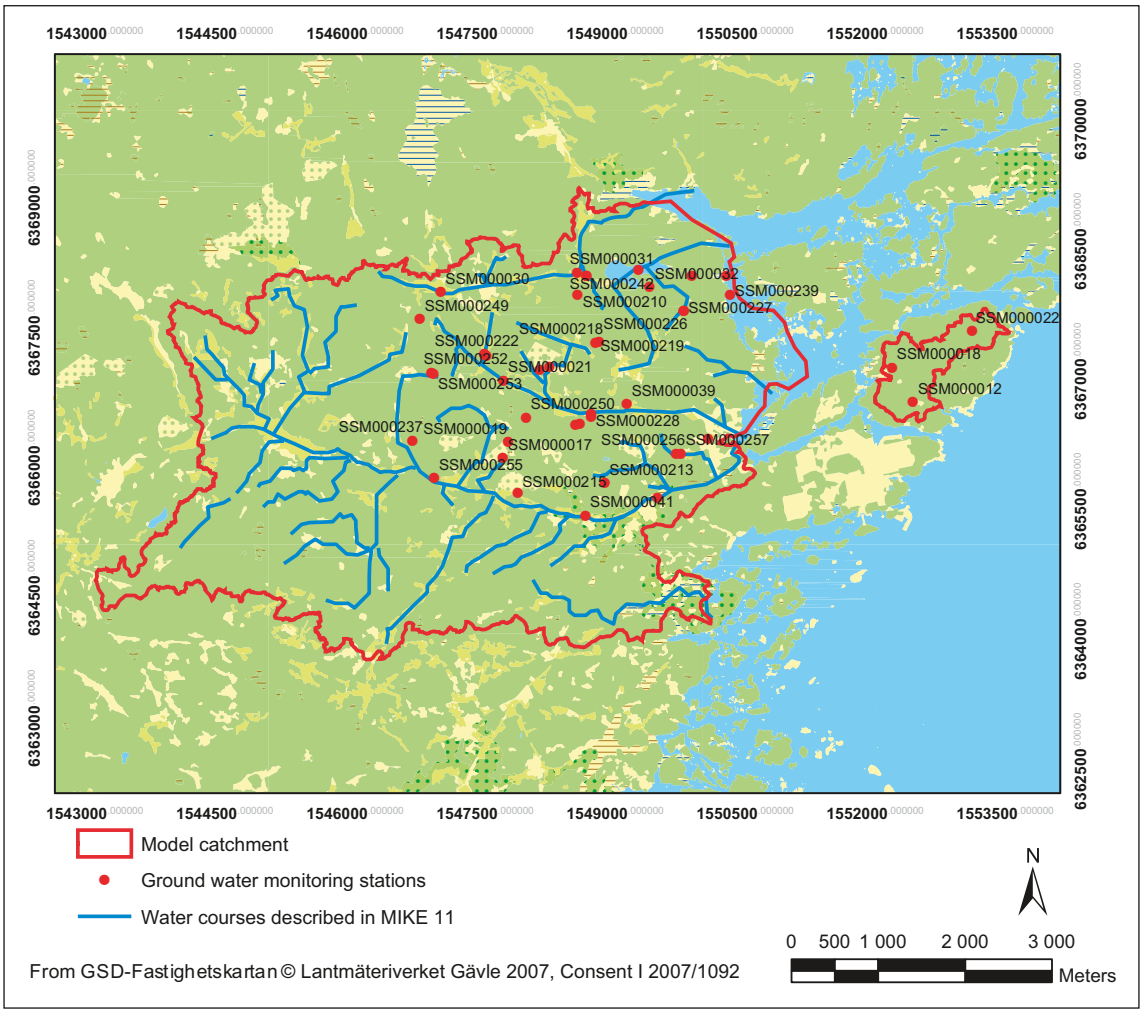

Figure 5-15. *Locations of groundwater monitoring wells used for calibration and evaluation of groundwater head elevations.*

Figures 5-16 to 5-23 show a comparison between measured and calculated groundwater head elevations. Compared to the measurements, the model generally calculates too high head elevations, with too slow reactions and too small amplitudes. However, it should be noted that the scale of the vertical axis is adjusted to the graphs in each plot and therefore the scale differs between plots. This means that a comparison, at first glance, may look more unfavourable than really is the case when analysing mean absolute errors (cf. below) or similar quantitative measures of errors. As described in more detail below, the mean error is less than or equal to one metre in about half of the boreholes. On the other hand, the errors are very large for some boreholes.

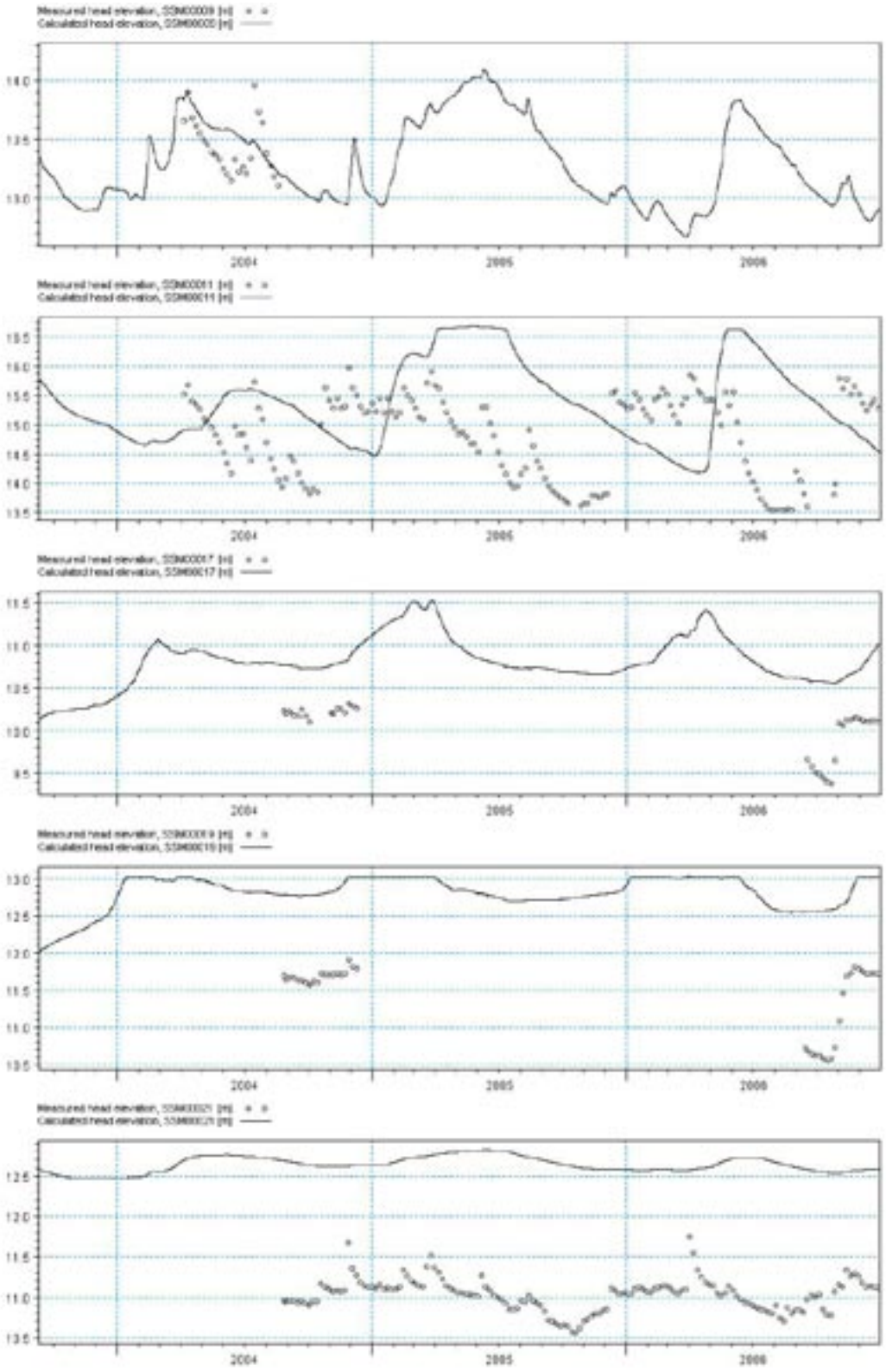

Figure 5-16. *Comparison between measured and calculated groundwater head elevation in SSM000009, SSM000011, SSM000017, SSM000019 and SSM000021.*

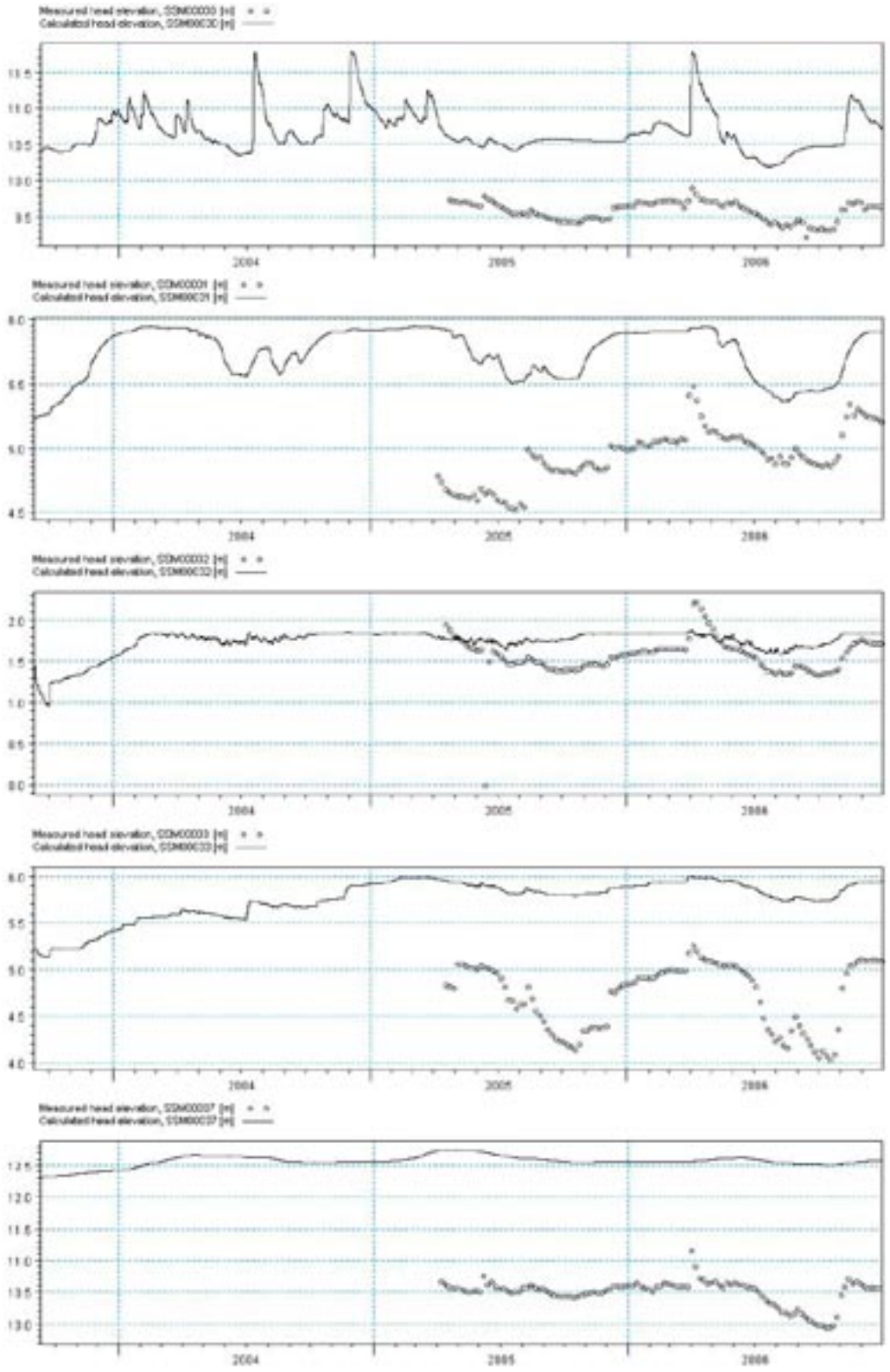

Figure 5-17. *Comparison between measured and calculated groundwater head elevation in SSM000030, SSM000031, SSM000032, SSM00033 and SSM000037.*

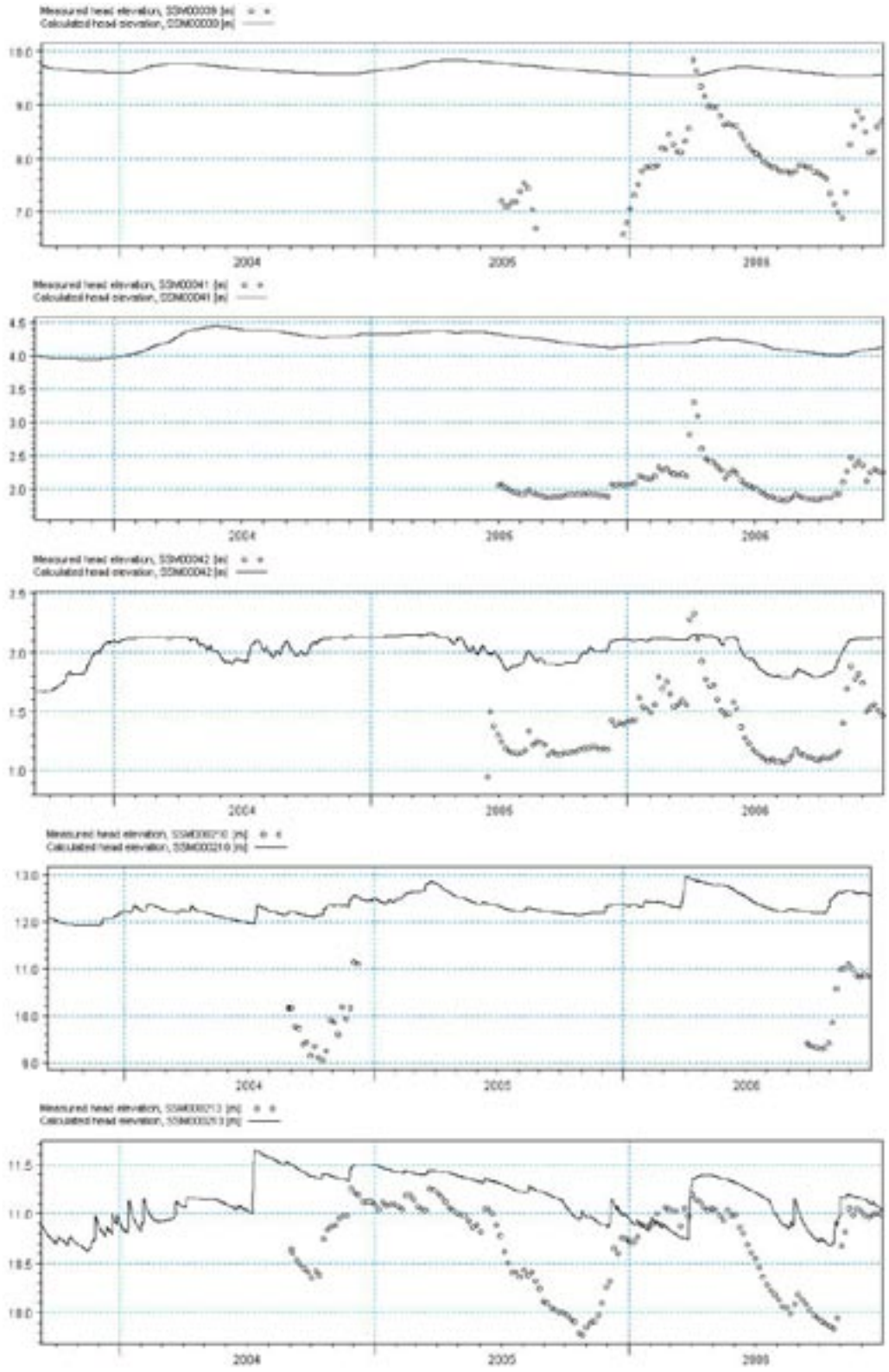

Figure 5-18. *Comparison between measured and calculated groundwater head elevation in SSM000039, SSM000041, SSM000042, SSM000210 and SSM000213.*

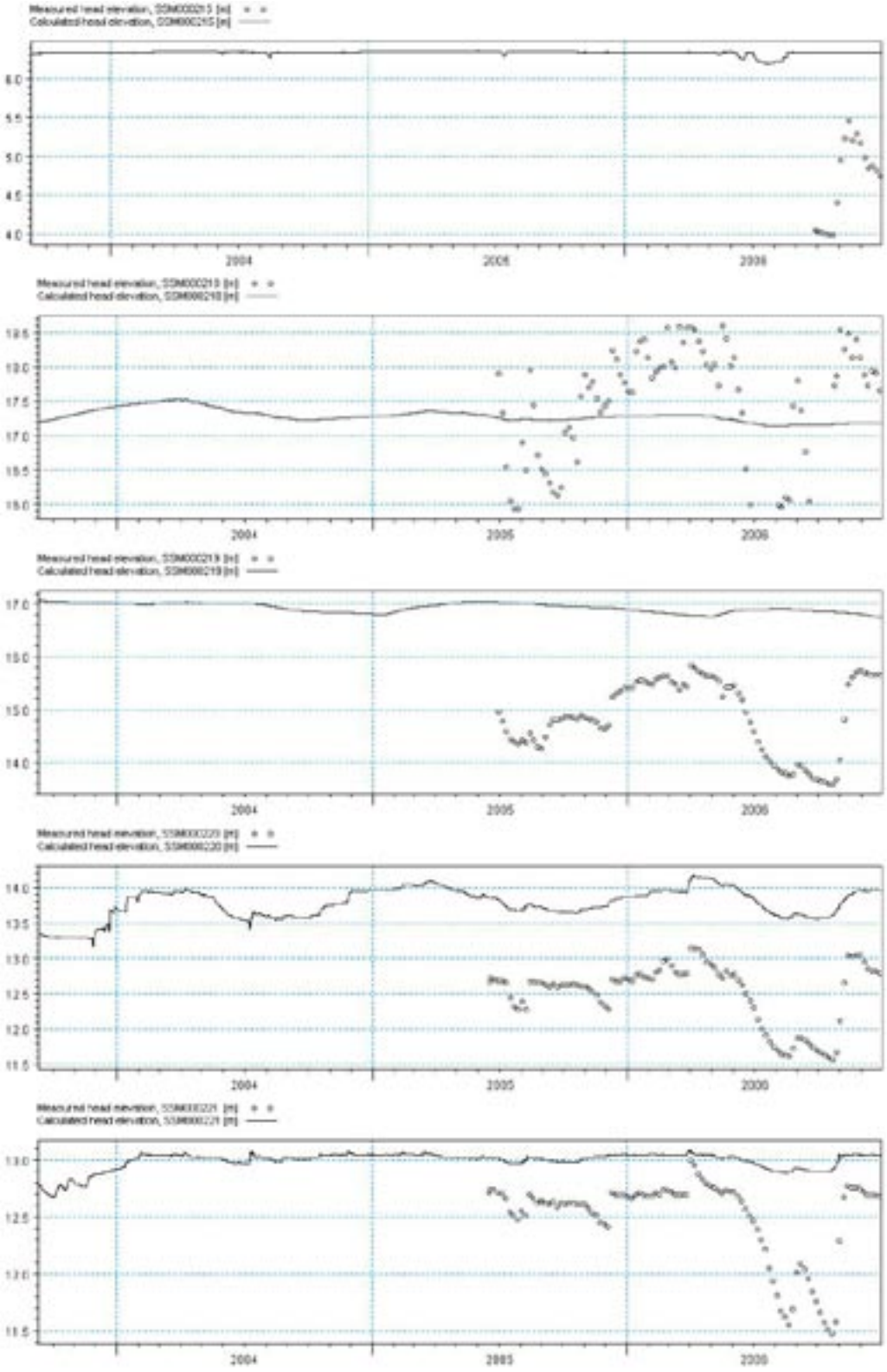

Figure 5-19. *Comparison between measured and calculated groundwater head elevation in SSM000215, SSM000218, SSM000219, SSM000220 and SSM000221.*

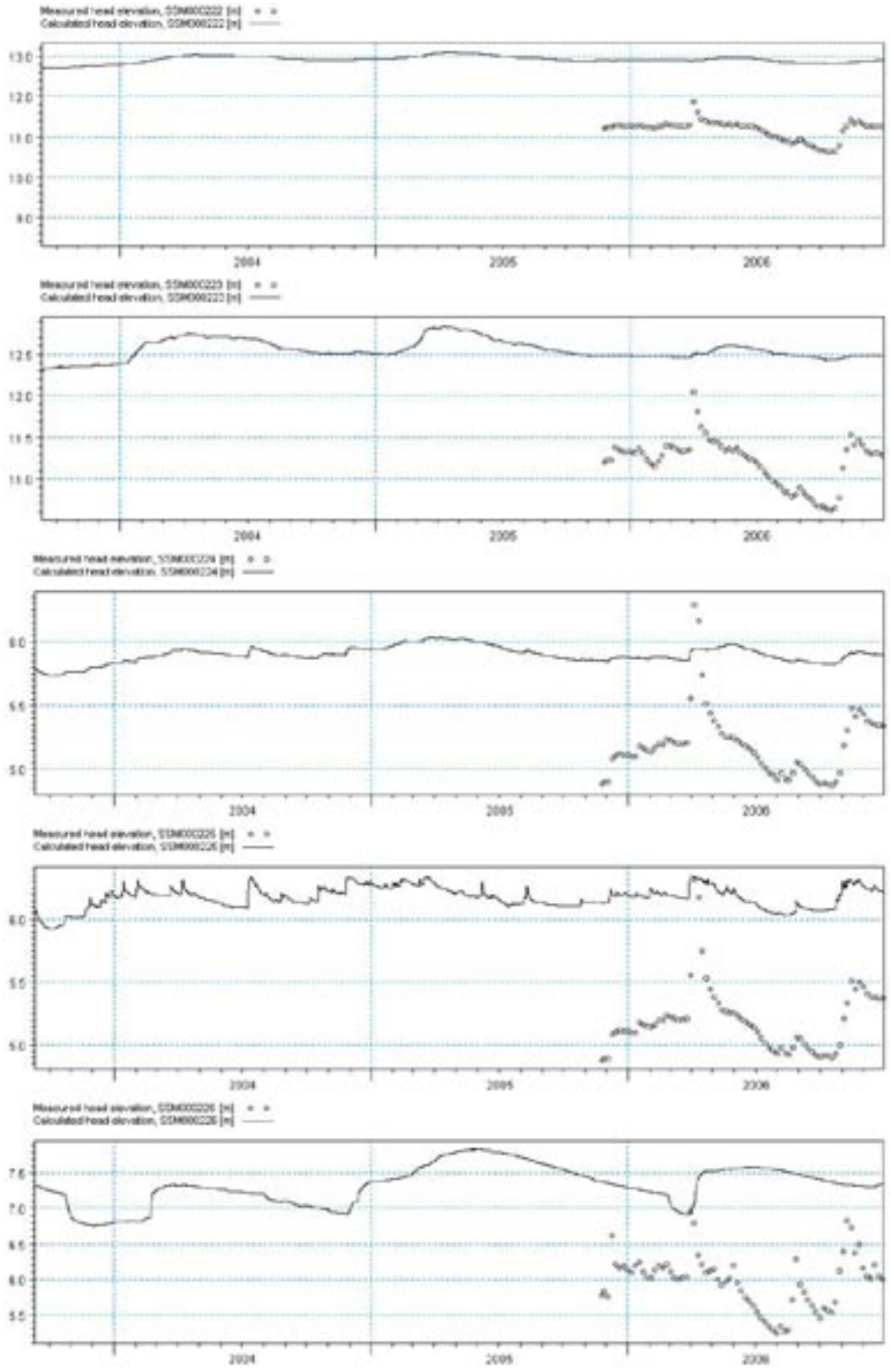

Figure 5-20. *Comparison between measured and calculated groundwater head elevation in SSM000222, SSM000223, SSM000224, SSM000225 and SSM000226.*

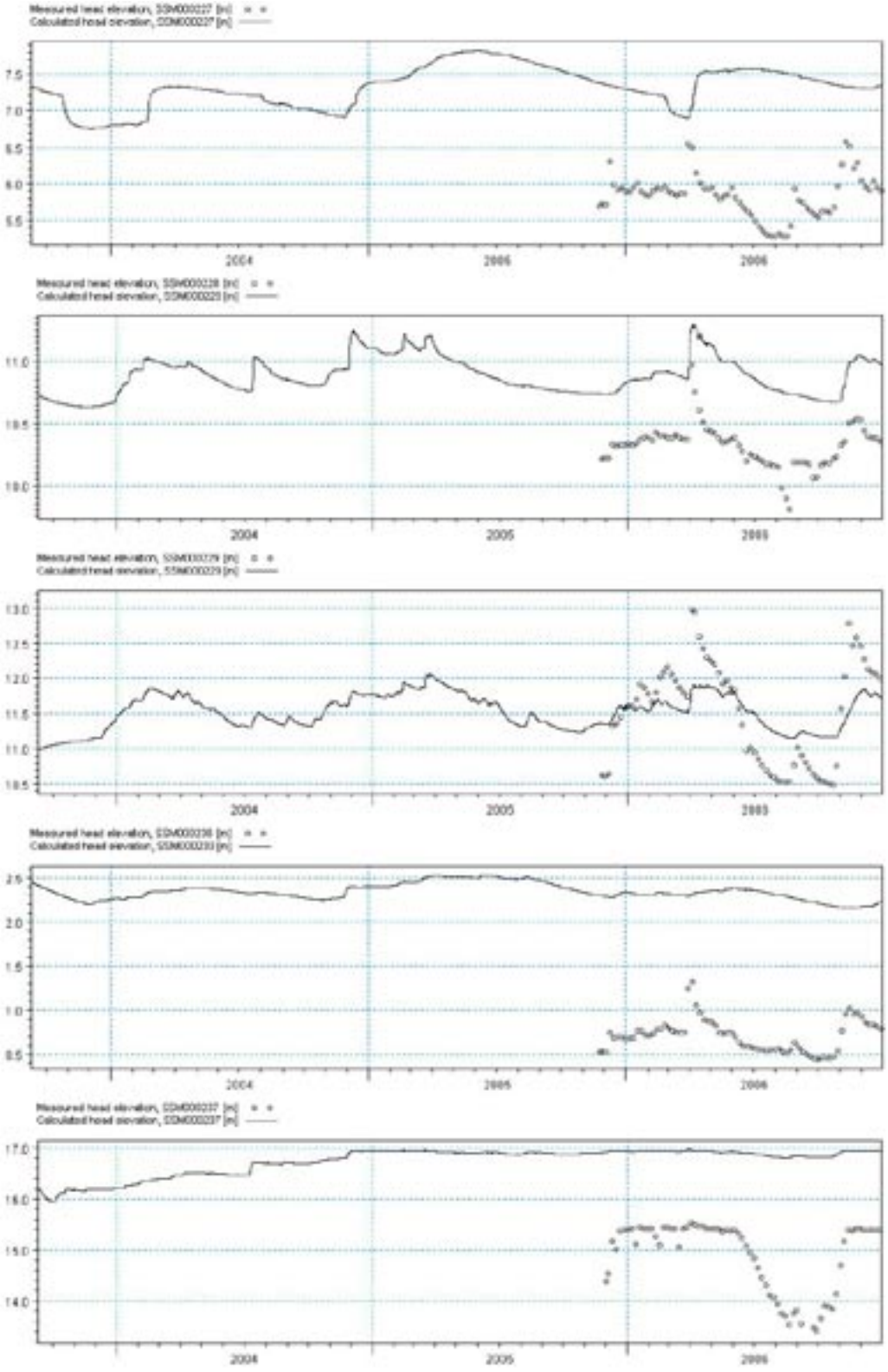

Figure 5-21. *Comparison between measured and calculated groundwater head elevation in SSM000227, SSM000228, SSM000229, SSM000230 and SSM000237.*

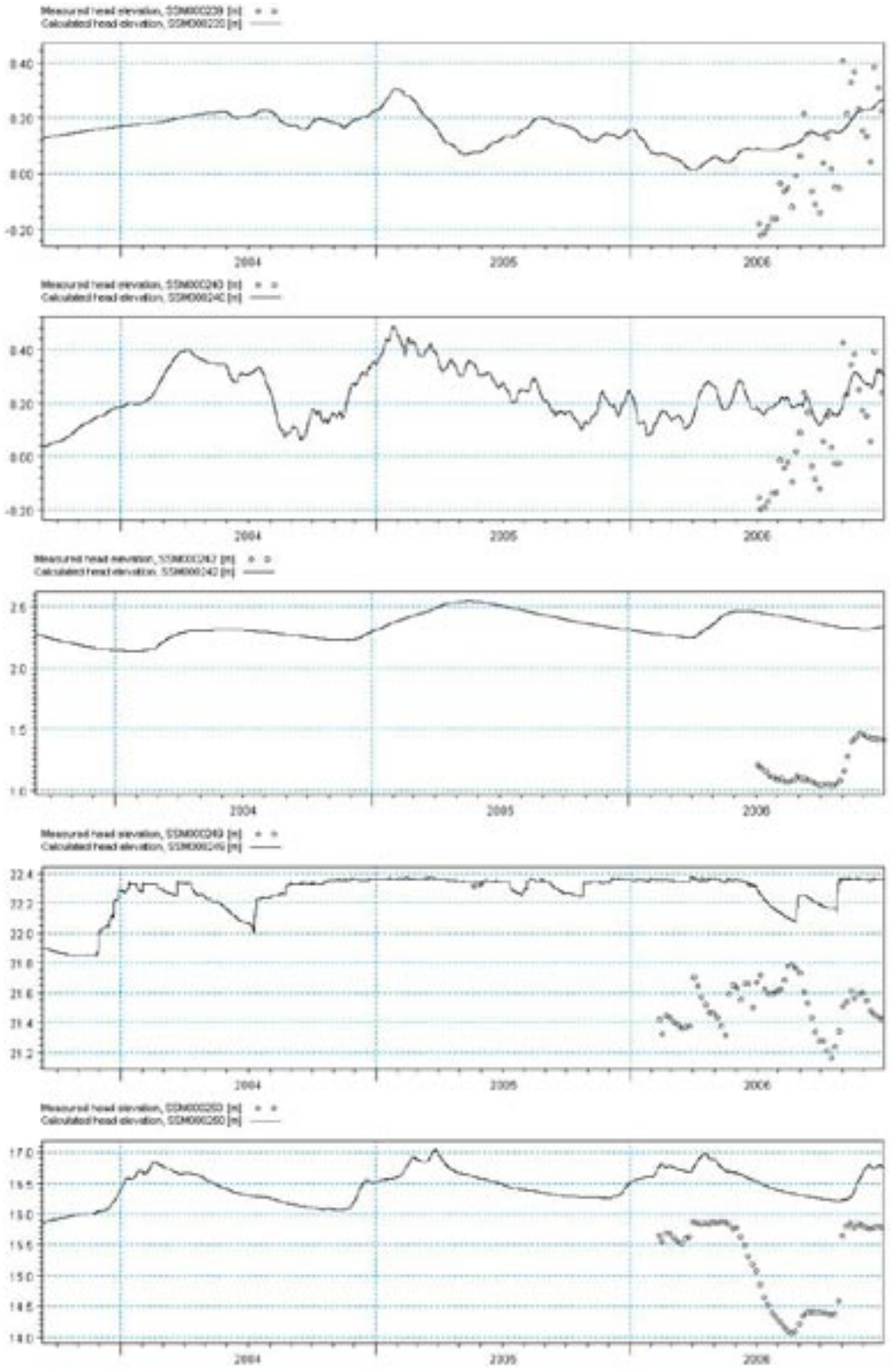

Figure 5-22. *Comparison between measured and calculated groundwater head elevation in SSM000239, SSM000240, SSM000242, SSM000249, and SSM000250.*

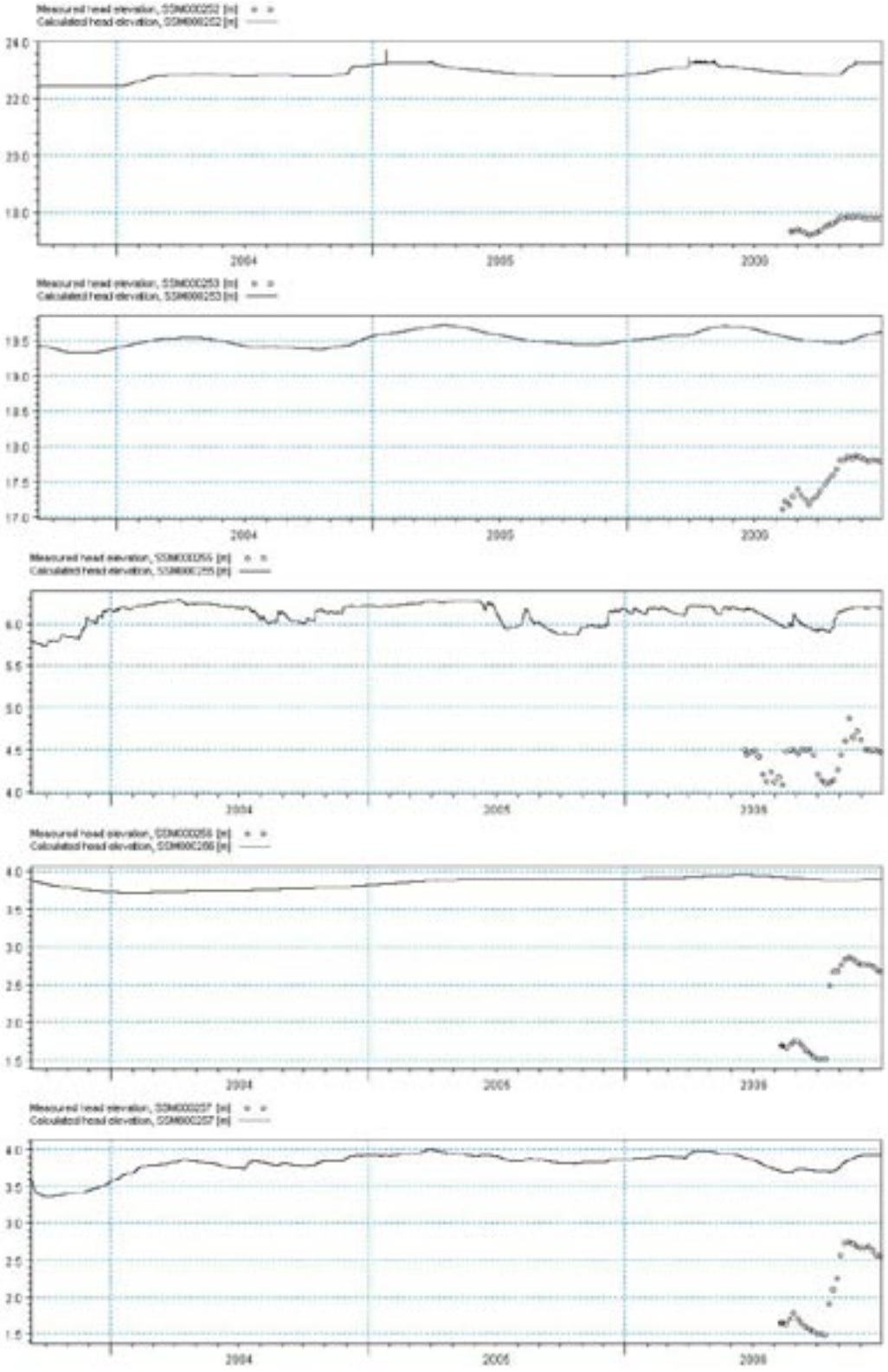

Figure 5-23. *Comparison between measured and calculated groundwater head elevation in SSM000252, SSM000253, SSM000255, SSM000256, and SSM000257.*

Statistical evaluations of the differences between measured and calculated groundwater heads are used extensively in this report. In particular, mean absolute error differences between the measured and calculated heads are presented both for the base case evaluation in this chapter and comparing various sensitivity cases in Chapter 6. The mean absolute error (MAE) is based on the difference between the measured and the calculated value at the same location and time. The error, or residual, for such an observation-calculation pair is

$$E_{i,t} = Obs_{i,t} - Calc_{i,t}$$

where $E_{i,t}$ is the difference between the observed and calculated values at location *i* and time *t*.

The mean absolute error, MAE, at location *i* where *n* observations exist is then

$$MAE_i = \left|\overline{E}_i\right| = \frac{\sum_t \left|E_{i,t}\right|}{n}$$

Table 5-1 shows the mean absolute errors comparing measured and calculated (base case) head elevations and a rough classification of the different deviations from measured groundwater heads that occur in the different monitoring wells in the model area. The rightmost column describes the results of a direct visual inspection; “OK” indicates a good fit, whereas “Alt.” stands for alternating deviations (shifting from positive to negative such that no representative value can be defined).

The average absolute mean error for all the evaluated boreholes is 1.3 m, which is a relatively poor result. There are many possible reasons for this, but the most probable ones are:

- The groundwater recharge is too large. A larger surface runoff, with less ponding on the surface, would decrease the infiltrated amount. A larger transpiration and evaporation from the groundwater zone would also decrease the recharge, but this would also affect the surface stream flow negatively (i.e. reduce it).
- The groundwater flow from the deeper bedrock layers is too large. This may either be due to the applied head boundary condition in the bottom bedrock layer, i.e. too high heads on the bottom boundary, or to local errors in the applied hydraulic conductivities in the bedrock.

Table 5-2 shows a comparison between mean values of measured and calculated head elevations. The table also shows the model ground surface (based on the SKB Digital Elevation Model, DEM, of the area) at each monitoring well location, as well as the observed ground level at the borehole. In some boreholes a relatively large deviation between modelled and observed ground level can be seen, which can be an additional reason for the deviation between modelled and observed groundwater table. Especially in local depressions this can be of great importance for the modelled groundwater table, because the groundwater table is affected by transpiration processes, and transpiration is depth dependent. At sites with larger deviations in ground level, the groundwater depth, rather than absolute level, might be more appropriate to evaluate. This was not done in this project, but should be investigated during the next modelling phase of Laxemar.

At a large number of points, the applied bottom boundary head is higher than both observed and simulated heads. This means that either the boundary head or the applied hydraulic conductivities in the bedrock can be adjusted in order to reach a better agreement between observed and simulated data in the Quaternary deposits. This is further evaluated later in this report.

Table 5-1. Classification of calculated deviations from measured groundwater heads; "OK" indicates small and "Alt." alternating deviations.

Borehole	MAE [m]	Good agreement	Error in absolute head	Too slow variation	Too small amplitude	Too large amplitude	Groundwater level above ground	Comment from visual inspection of head deviations
SSM000009	0.22			x				OK
SSM000011	1.17		x					Alt.
SSM000017	0.71		x					+0.7 m
SSM000019	1.35		x				x	+1.5 m
SSM000021	1.63		x		x			+1.5 m
SSM000030	1.02		x			x		+1 m
SSM000031	0.77		x		x			+0.5 m
SSM000032	0.23	x			x			OK
SSM000033	1.15		x		x			+1 m
SSM000037	2.09		x					+2 m
SSM000039	1.62		x		x			+1.5 m
SSM000041	2.06		x		x			+2 m
SSM000042	0.63		x		x			+0.5 m
SSM000210	2.35		x		x			+2 m
SSM000213	0.54		x		x			+0.5 m
SSM000215	1.63		x		x		x	+2 m
SSM000218	0.77				x			Alt.
SSM000219	2.02		x		x			+2 m
SSM000220	1.31		x					+1 m
SSM000221	0.51		x		x			+0.3 m
SSM000222	1.74		x					+1.7 m
SSM000223	1.29		x		x			+1 m
SSM000224	0.72		x		x			+1 m
SSM000225	0.98		x					+1 m
SSM000226	1.41		x		x			+1 m
SSM000227	1.54		x		x			+1 m
SSM000228	0.56		x					+0.5 m
SSM000229	0.44				x			Alt.
SSM000230	1.58		x		x			+1.5 m
SSM000237	1.97		x		x			+1.8 m
SSM000239	0.14				x			Alt.
SSM000240	0.16				x			Alt.
SSM000242	1.18		x					+1 m
SSM000249	0.78		x					+1 m
SSM000250	1.34		x		x			+1 m
SSM000252	5.42		x					+5 m
SSM000253	1.96		x					+2 m
SSM000255	1.67		x					+1.5 m
SSM000256	1.67		x		x			+2 m
SSM000256	1.68		x		x			+2 m

Table 5-2. Comparison between measured and simulated mean head elevations, ground surface (DEM) and applied bottom boundary head elevation. The bold letters indicate points where applied boundary conditions or conductivities in the bedrock result in difficulties to reach agreement between observed and simulated heads.

Borehole	Ground level, observed [m.a.s.l.]	Ground level, model topography [m.a.s.l.]	Mean head elevation, observed data [m.a.s.l.]	Mean head elevation, calculated data [m.a.s.l.]	Boundary head elevation, Darcy-Tools [m.a.s.l.]
SSM000009	15.32	16.78	13.45	13.28	12.72
SSM000011	16.50	18.64	14.82	15.34	12.71
SSM000017	10.98	**11.54**	**10.02**	**10.81**	**11.32**
SSM000019	13.21	**13.02**	**11.45**	**12.82**	**12.55**
SSM000021	12.63	**13.30**	**11.03**	**12.64**	**12.42**
SSM000030	11.19	**11.82**	**9.58**	**10.73**	**13.25**
SSM000031	6.32	**5.98**	**4.94**	**5.73**	**5.04**
SSM000032	2.81	1.22	1.57	1.75	2.39
SSM000033	5.82	5.22	4.72	5.76	2.36
SSM000037	12.70	**12.85**	**10.49**	**12.57**	**12.86**
SSM000039	11.70	**10.93**	**8.00**	**9.65**	**9.14**
SSM000041	4.15	**3.57**	**2.10**	**4.22**	**5.72**
SSM000042	3.35	**2.08**	**1.37**	**2.02**	**2.90**
SSM000210	11.31	**13.00**	**10.00**	**12.31**	**10.67**
SSM000213	11.85	11.13	10.67	11.18	9.00
SSM000215	6.74	**6.32**	**4.71**	**6.34**	**6.91**
SSM000218	18.93	17.56	17.55	17.29	12.98
SSM000219	16.27	15.89	14.86	16.93	13.16
SSM000220	13.13	14.49	12.50	13.76	12.00
SSM000221	13.17	12.88	12.49	13.00	11.83
SSM000222	12.79	**12.32**	**11.16**	**12.93**	**13.02**
SSM000223	13.69	**13.19**	**11.21**	**12.56**	**12.70**
SSM000224	6.90	6.33	5.19	5.90	5.08
SSM000225	6.94	6.33	5.20	6.20	5.08
SSM000226	6.97	**9.20**	**5.97**	**7.30**	**7.74**
SSM000227	7.28	**9.20**	**5.83**	**7.29**	**7.74**
SSM000228	13.09	**12.29**	**10.32**	**10.87**	**11.56**
SSM000229	13.68	12.54	11.53	11.51	11.59
SSM000230	5.10	**5.02**	**0.71**	**2.33**	**1.48**
SSM000237	15.93	16.19	14.93	16.75	14.31
SSM000239	0.56	**0.01**	**0.06**	**0.16**	**1.45**
SSM000240	0.61	**0.01**	**0.08**	**0.24**	**0.86**
SSM000242	2.11	**–0.84**	**1.19**	**2.33**	**1.52**
SSM000249	22.07	22.38	21.51	22.26	17.32
SSM000250	16.84	17.17	15.21	16.42	13.43
SSM000252	18.39	**18.36**	**17.59**	**22.89**	**18.29**
SSM000253	17.96	**21.15**	**17.56**	**19.50**	**18.26**
SSM000255	5.94	**6.21**	**4.06**	**6.13**	**11.13**
SSM000256	3.60	**3.22**	**2.23**	**3.84**	**3.98**
SSM000257	3.36	**3.30**	**2.11**	**3.80**	**3.77**

5.4 Water balance

Table 5-3 shows the monthly accumulated water balance between 2003-12-09 and 2006-12-23 for the land part of the main model area. A negative value shows an inflow and a positive value an outflow from the model area. Figure 5-24 shows the total accumulated water balance over the same period.

The annual average precipitation over the three-year period is 591 mm/year. The calculated evapotranspiration is 421 mm/year. This means that the average net precipitation is 170 mm/year, of which 103 mm/year is net surface runoff, and the remaining 68 mm/year is net groundwater recharge. Of the net groundwater recharge, 31 mm/year discharges to the stream network, 23 mm/year discharges to the deep rock and the sea and the rest is the groundwater storage change. The storage terms are rather large. A possible explanation for this is the lack of a surface stream network in some areas that can drain overland water from local depressions in the ground surface. Instead, small lakes build up. Another reason is the quite large amount of precipitation during the last two months of the period studied.

Due to the fluctuating internal head boundary in the sea, water can be transferred in both directions across the overland boundary. The exchange across the boundaries of the saturated zone includes both a horizontal component, with a net outflow of 5 mm/year, and the communication with the bottom layer boundary, where the net outflow is 18 mm/year. The calculated evapotranspiration (on average 421 mm/year) is about 73% of the potential evapotranspiration, which during the simulated period on average is 578 mm/year. Moreover, 72% of the precipitation is emitted through evapotranspiration.

Since large parts of the catchment area can be described as wet with both many mires and lakes, as well as with near-surface groundwater, it is likely that the actual evapotranspiration is relatively high in the area. The large amount of water evaporating in the area leads to the relatively small total runoff. Table 5-4 shows a detailed average annual water balance [mm/year] for the different components included in the total water balance previously described.

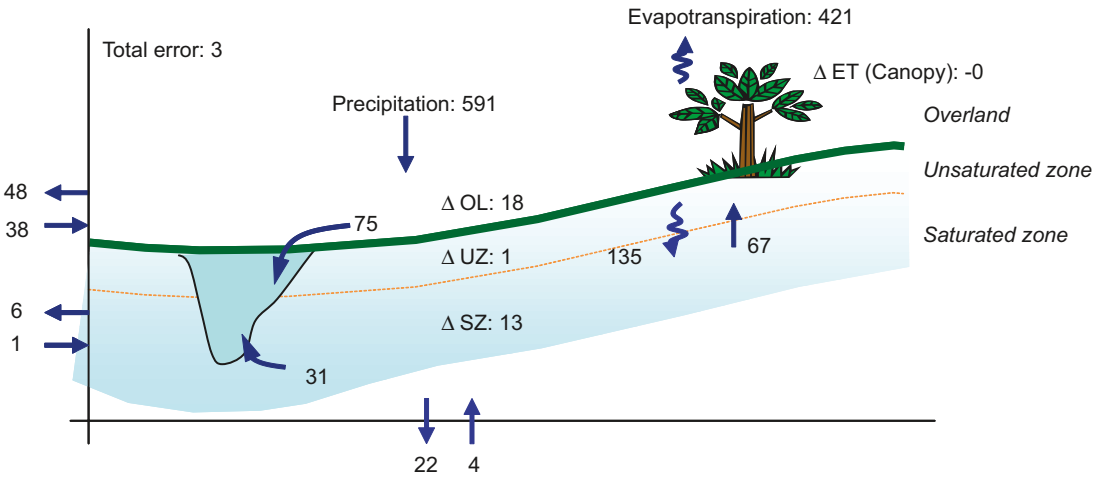

Figure 5-24. *Average annual water balance [mm/year] between 2003-12-19 and 2006-12-23 for the land part of the main model area. The saturated zone boundary in- and outflow also contains the communication with bottom layer boundaries. Due to the fluctuating sea level, water can be exchanged both ways over the overland boundary.*

Table 5-3. Total accumulated water balance for base case in Laxemar between 2003-12-09 and 2006-12-23 [mm].

Date	Precipi-tation	Canopy Storage Change	Evapotrans-piration	Snow storage change	OL Storage Change	OL Boundary Inflow	OL Boundary Outflow	OL to River	SubSurface Storage Change	SubSurface Boundary Inflow	SubSurface Boundary Outflow	Baseflow to River	Baseflow from River	Error
2003-12-09	0.0	0.0	0.0	0.0	0.0	0.0	0.0	0.0	0.0	0.0	0.0	0.0	0.0	0.0
2004-01-08	-66.0	0.1	1.9	6.9	9.5	-0.2	0.7	5.5	38.3	0.5	1.7	2.1	0.0	0.1
2004-02-07	-126.8	0.1	2.9	0.0	21.0	-0.5	1.9	15.4	78.1	0.9	3.5	4.6	0.0	-0.7
2004-03-08	-140.8	-0.5	14.4	0.2	21.7	-0.9	2.6	17.9	72.8	1.3	5.4	7.7	0.0	-1.0
2004-04-07	-201.0	0.1	40.3	0.0	30.1	-1.5	3.7	24.5	86.3	1.6	7.6	10.8	0.0	-0.6
2004-05-07	-220.4	-0.5	96.5	0.0	25.1	-2.2	4.6	26.1	49.2	2.0	10.0	13.9	0.0	0.3
2004-06-06	-249.9	-0.5	177.0	0.0	21.5	-2.9	5.4	26.3	-2.3	2.3	12.3	16.6	0.0	1.3
2004-07-06	-297.0	-0.5	250.2	0.0	20.1	-4.0	6.5	26.5	-30.8	2.6	14.7	19.0	0.0	2.1
2004-08-05	-449.0	-0.5	318.9	0.0	36.5	-9.3	14.6	54.5	0.5	3.0	17.1	21.6	0.0	1.9
2004-09-04	-505.9	-0.5	386.6	0.0	36.3	-9.4	14.9	56.8	-13.4	3.3	19.3	24.0	0.0	5.5
2004-10-04	-526.2	0.1	426.2	0.0	34.3	-14.7	20.2	57.0	-34.9	3.7	21.4	26.2	0.0	5.8
2004-11-03	-599.9	0.1	433.8	0.0	40.4	-16.4	23.4	66.9	6.1	4.1	23.5	28.5	0.0	2.3
2004-12-03	-692.2	0.1	435.5	0.0	50.2	-22.1	31.9	87.9	55.1	4.5	25.5	31.1	0.0	-1.6
2005-01-02	-709.0	0.1	437.1	0.0	48.2	-29.3	40.1	93.7	59.9	4.8	27.6	34.2	0.0	-2.4
2005-02-01	-752.4	0.1	443.0	20.0	49.3	-58.9	70.4	98.0	64.4	5.2	29.8	37.1	0.0	-4.3
2005-03-03	-797.9	0.1	447.7	22.3	50.2	-62.0	75.6	109.5	82.2	5.5	32.4	40.3	0.0	-5.1
2005-04-02	-829.9	-0.5	469.9	0.0	51.2	-62.5	78.5	122.5	93.7	5.8	35.2	43.8	0.0	-3.9
2005-05-02	-835.2	-0.5	518.8	0.0	46.6	-62.5	78.7	122.9	51.9	6.1	38.1	47.2	0.0	-0.1
2005-06-01	-868.4	-0.5	585.6	0.0	43.7	-62.5	78.7	123.2	17.6	6.4	41.1	50.2	0.0	2.2
2005-07-01	-939.9	-0.5	677.8	0.0	43.9	-62.8	79.1	125.5	-10.3	6.7	43.9	52.9	0.0	2.9
2005-07-31	-979.4	0.1	753.0	0.0	39.1	-64.0	80.2	125.5	-45.0	7.0	46.5	55.3	0.0	4.3
2005-08-30	-1057.6	-0.5	816.0	0.0	42.4	-70.6	87.3	129.0	-39.9	7.4	49.0	57.7	-0.1	5.3
2005-09-29	-1067.7	-0.3	851.5	0.0	39.2	-70.7	87.4	129.0	-65.5	7.7	51.3	59.8	-0.1	6.2
2005-10-29	-1094.9	-0.5	864.9	0.0	40.8	-70.7	87.5	130.1	-57.8	8.1	53.5	61.8	-0.1	6.5
2005-11-28	-1117.2	0.1	867.2	5.0	41.9	-72.5	89.5	131.5	-49.9	8.5	55.6	63.8	-0.1	6.4
2005-12-28	-1180.4	0.1	868.1	2.6	48.0	-74.2	92.4	139.8	-4.3	8.9	57.6	66.0	-0.1	6.6
2006-01-27	-1224.0	0.1	868.7	32.7	47.6	-74.8	93.9	142.8	1.6	9.3	59.6	68.3	-0.1	6.9
2006-02-26	-1283.1	0.1	870.7	46.6	49.8	-75.0	95.3	150.6	29.3	9.7	61.5	70.6	-0.1	6.6
2006-03-28	-1335.9	0.1	880.5	66.6	54.8	-75.0	95.9	154.6	37.5	10.1	63.5	73.0	-0.1	5.5
2006-04-27	-1397.1	-0.5	917.8	0.0	55.4	-76.3	103.3	194.4	75.8	10.5	65.5	76.1	-0.1	3.7
2006-05-27	-1437.4	-0.5	983.5	0.0	52.0	-76.3	103.6	195.8	46.5	10.8	67.9	79.1	-0.1	3.4
2006-06-26	-1473.7	0.1	1068.3	0.0	46.8	-76.6	103.9	196.3	-2.3	11.1	70.5	81.8	-0.1	4.1
2006-07-26	-1480.3	-0.5	1144.4	0.0	37.6	-76.6	104.0	196.3	-64.6	11.5	73.0	84.0	-0.1	5.7
2006-08-25	-1528.5	-0.5	1197.3	0.0	35.8	-76.7	104.0	196.6	-69.5	11.9	75.2	85.9	-0.1	7.7
2006-09-24	-1572.5	-0.5	1244.8	0.0	36.9	-79.5	107.0	198.2	-77.9	12.3	77.3	87.8	-0.1	9.2
2006-10-24	-1620.1	0.1	1259.7	0.0	43.2	-80.1	107.8	199.6	-56.6	12.7	79.3	89.6	-0.1	9.6
2006-11-23	-1746.7	0.1	1263.2	0.0	55.3	-99.6	129.6	218.5	26.1	13.1	81.3	91.7	-0.2	6.3
2006-12-23	-1773.6	0.1	1263.8	0.0	54.7	-113.3	144.6	224.7	42.8	13.5	83.2	94.3	-0.2	7.7

Table 5-4. Detailed average annual water balance of the land part of the main model area. Positive values indicate outflows from the model.

Water balance component	Average annual amount [mm/year]
Precipitation	–591.2
Evaporation from canopy and snow	117.0
Canopy throughfall to overland	–474.2
Evaporation from ponded water	14.2
Upward flow from saturated zone to overland	27.0
Downward flow from overland to saturated zone	–35.2
Inflow to overland from boundary of sub-catchment	–37.8
Outflow from overland to boundary of sub-catchment	48.2
Overland outflow to MIKE 11 water courses	74.9
Overland outflow from MIKE 11 water courses	0.0
Infiltration from overland to unsaturated zone	–348.2
Direct evaporation from soil	49.0
Transpiration from the root zone	201.1
Recharge from unsaturated to saturated zone	–99.4
Upward flow from saturated zone to overland	27.0
Downward flow from overland to saturated zone	–35.2
Evapotranspiration directly from saturated zone	40.0
Inflow to saturated zone from sub-catchment	0.9
Saturated zone flow out of the sub-catchment	5.8
MIKE 11 base flow to saturated zone	–0.1
Saturated zone base flow to MIKE 11	31.4
Saturated zone flow to internal head boundaries	22.0
Flow from internal head boundaries	–3.7

6 Sensitivity analysis

Based on the initial calibration described in Chapter 4, a sensitivity study has been performed using the same simulation period (2003-09-10 to 2006-12-31) as in the initial calibration. Table 6-1 summarises the different simulations included in the sensitivity analysis. The parameters investigated in the sensitivity analysis can be divided into different groups. In this chapter, these parameter groups are used as a basis for a detailed description of the sensitivity analysis.

The results were evaluated at the locations of the four hydrological stations and at the locations of eight monitoring wells. The four surface discharge measurement points are the following (see Section 5.2 for the results commented below):

- PSM000347, located upstream of the inlet to Lake Frisksjön in the north-eastern part of the main model area. The comparison of the base case model results and the measured data shows that the model underestimates the discharge.
- PSM000348 is located in the outlet of Lake Frisksjön. The comparison of the base case model results and the measured data shows a fairly good agreement, although the model somewhat overestimates the discharge.
- PSM000364 is located in the water course Laxemarån, approximately 1 km upstream from its outlet. The comparison of the base case model results and the measured data shows a good agreement in terms of the shape of the discharge curve, although the model somewhat underestimates the discharge.
- PSM000365 is located in the water course Ekerumsbäcken in the middle of the main model area. The comparison of the base case model results to the measured data shows that the model underestimates the discharge.

Table 6-1. Simulation cases included in the sensitivity analysis.

Simulation case	Parameter
Sens1	Interception coefficient, C_{int}, increased by a factor of 2.
Sens2	Interception coefficient, C_{int}, reduced by a factor of 2.
Sens3	Root mass distribution parameter, A_{root}, increased by a factor of 2.
Sens4	Root mass distribution parameter, A_{root}, reduced by a factor of 2.
Sens5	Specific yield in the unsaturated zone, Sy, increased by a factor of 1.5.
Sens6	Specific yield in the unsaturated zone, Sy, reduced by a factor of 2.
Sens7	The Averjanov constant “n” for hydraulic conductivity in unsaturated zone increased by a factor of 1.5.
Sens8	The Averjanov constant “n” for hydraulic conductivity in unsaturated zone reduced by a factor of 2.
Sens9	Hydraulic conductivity in the saturated zone in both vertical and horizontal direction, K_v and K_h, increased by a factor of 5 in all soil layers as well as in rock layers *berg3* and *berg7*.
Sens10	Hydraulic conductivity in the saturated zone in both vertical and horizontal direction, K_v and K_h, reduced by a factor of 5 in all soil layers as well as in rock layers *berg3* and *berg7.*
Sens11	Pressure heads from Darcy Tools reduced by 3 metres in all bedrock layers and the internal boundary condition in the bottom rock layer *berg135.*
Sens12	Saturated hydraulic conductivity, K_s, in the unsaturated zone reduced by a factor of 5.
Sens13	Subsurface drainage applied in all areas with ponding water.
Sens14	All calculation layers from the initial model are included.

The eight monitoring wells used to illustrate groundwater head results are the following:

- SSM000032 is located in a local depression close to Lake Frisksjön in the north-eastern part of the catchment. The calculated results from the base case show a smaller amplitude than the measured data.
- SSM000042 is located in a local depression close to Laxemarån. There is a relatively good fit to measurements, although the calculated amplitude is smaller than the measured.
- SSM000213 is located on a slope north of Laxemarån. There is a relatively good fit to the measurements, although the model shows a smaller amplitude and higher head elevation values.
- SSM000225 is located on a slope north of Lake Frisksjön. The calculated head elevation shows a smaller amplitude and higher values than the measurements.
- SSM000228 is located in a local depression in the middle of modelling area. The calculated and measured results show the same variation, although the calculated results show somewhat higher head elevation values.
- SSM000229 is located close to SSM000228. The calculated head elevation amplitude is smaller than the measured.
- SSM000240 is located in the sea in the north-eastern part of the main model area. The calculated head elevation amplitude is smaller than the measured.
- SSM000250 is located on a local height in the middle of the main model area. The calculated results show smaller amplitudes than the measured ones. The calculated head elevation values are also higher than the measured.

Statistical evaluations of the mean absolute error differences between the base case and the sensitivity cases are presented in separate tables for each tested parameter. The mean absolute error (MAE) is based on the difference between the measured and the calculated value at the same location and time; the calculation of MAE is described in Section 5.3.

6.1 Vegetation parameters

The sensitivity of the model to changes in the vegetation parameters was evaluated by changes in the root mass distribution, A_{root}, and in the interception coefficient, C_{int}. Sections 6.1.1 and 6.1.2 describe the vegetation parameters and the simulation results.

6.1.1 Interception coefficient

Interception is defined as the process whereby precipitation is retained on the leaves, branches, and stems of the vegetation. The amount of precipitation intercepted by the vegetation canopy is determined by multiplying the interception capacity, C_{int}, by the leaf area index, LAI. The intercepted water evaporates without adding to the moisture storage in the soil. The coefficient, C_{int}, defines the interception storage capacity of the vegetation and depends on the surface characteristics of the vegetation type. In the sensitivity analysis for Laxemar interception coefficients of twice the initial, sensitivity case Sens1, and half of the initial, Sens2, were evaluated.

Figures 6.1 to 6.4 show the effect of changing the C_{int} parameter on the surface water discharges. The discharges are expressed in terms of accumulated discharge during the period for which discharge measurements have been made. In the figures, the measured discharge is compared to calculated discharges from the base case, Sens1, and Sens2. All figures indicate that the effect of changing the interception coefficient is small with regard to the surface water discharge.

Figures 6-5 to 6-12 show the effect of changing the C_{int} parameter on the groundwater head elevations. Similar to the surface water discharges, the effect of changing the C_{int} parameter is small on groundwater head elevations.

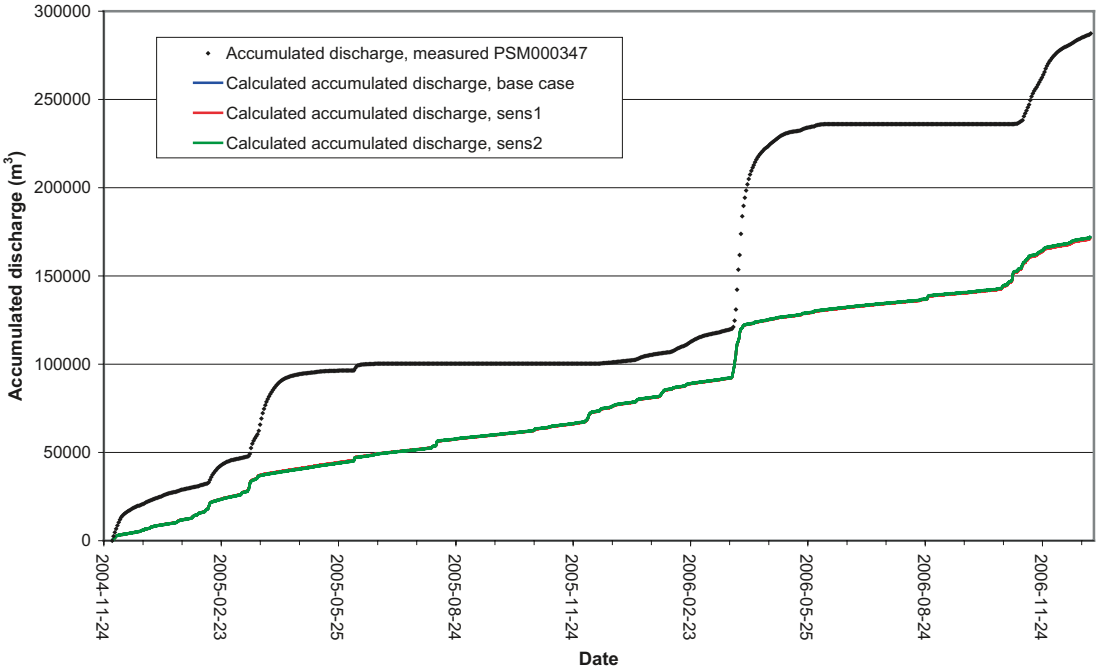

Figure 6-1. *Results for PSM000347 from sensitivity analysis of the interception coefficient (C_{int}).*

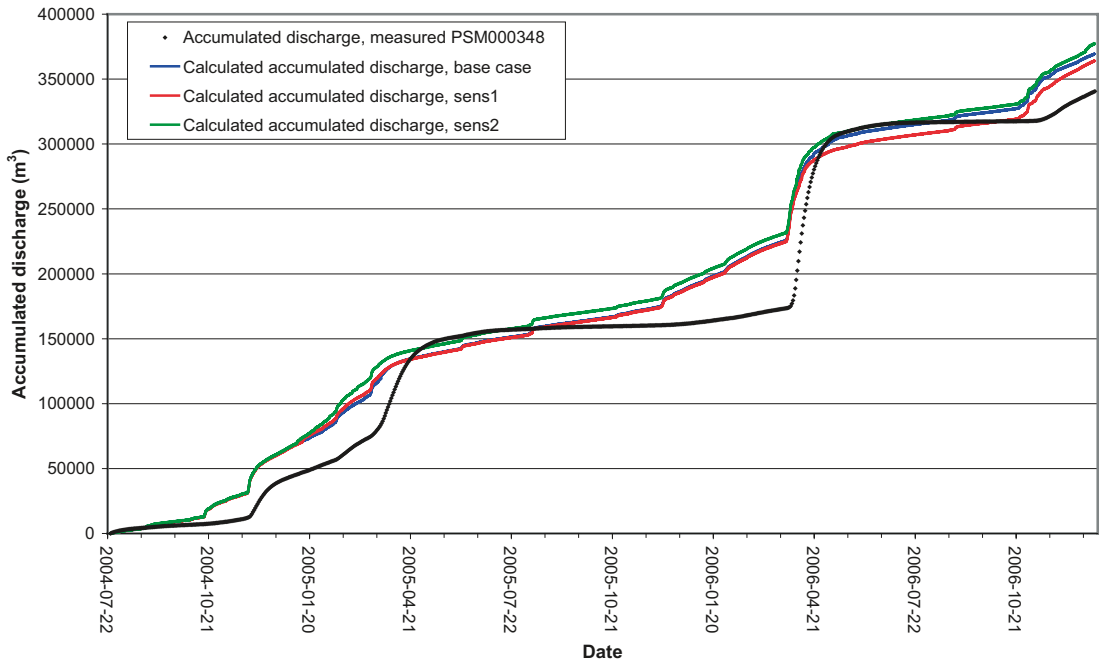

Figure 6-2. *Results for PSM000348 from sensitivity analysis of the interception coefficient (C_{int}).*

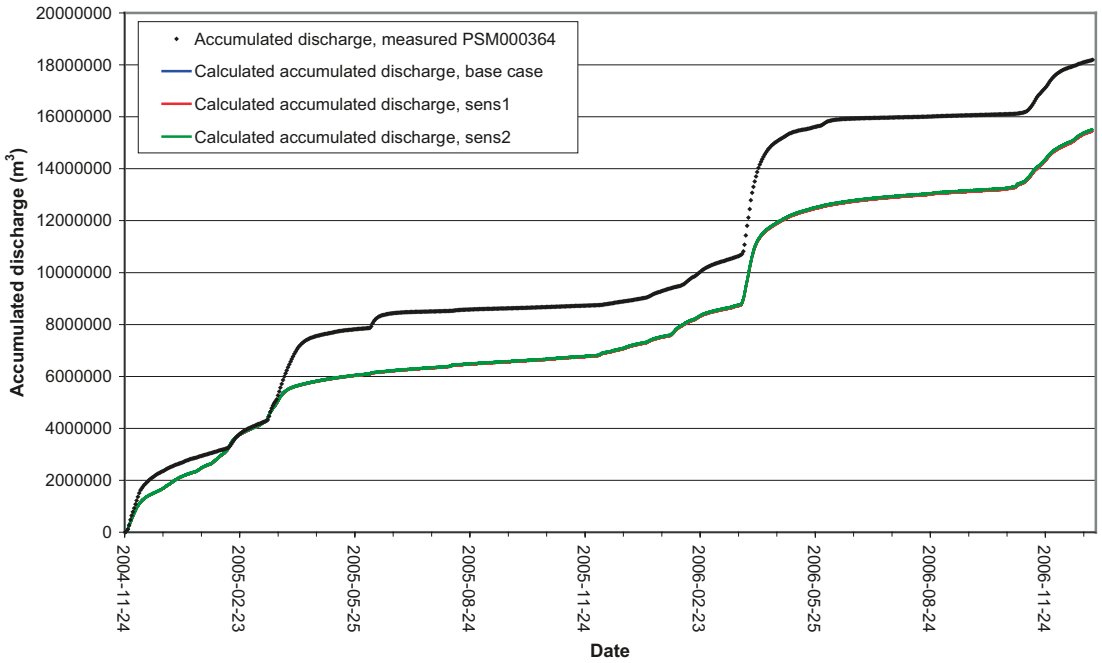

Figure 6-3. *Results for PSM000364 from sensitivity analysis of the interception coefficient (C_{int}).*

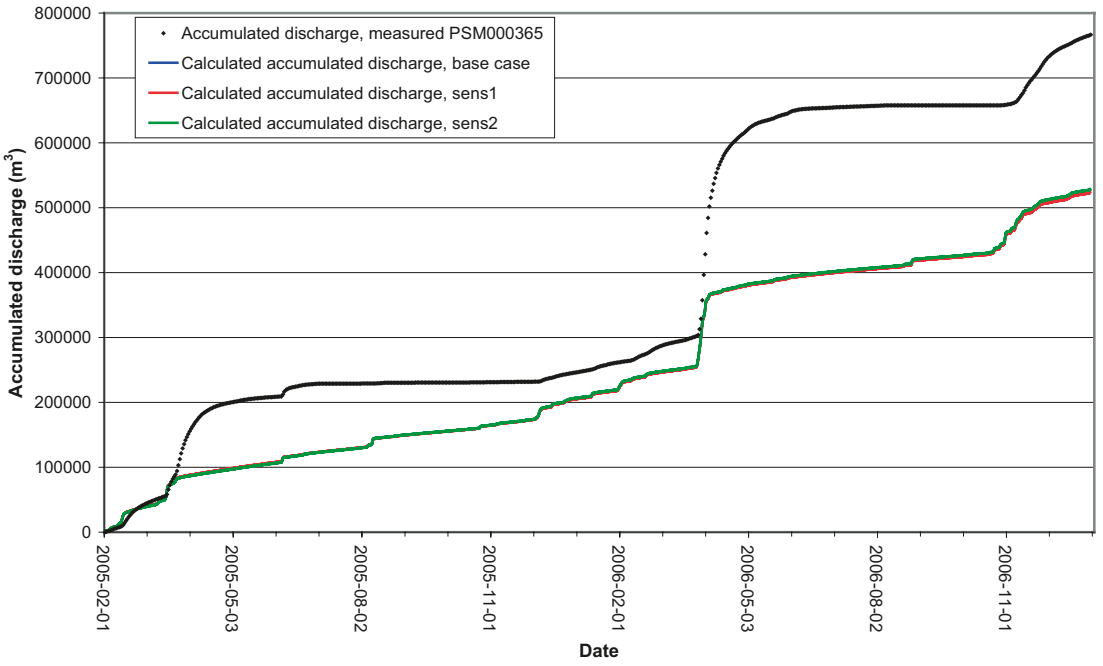

Figure 6-4. *Results for PSM000365 from sensitivity analysis of the interception coefficient (C_{int}).*

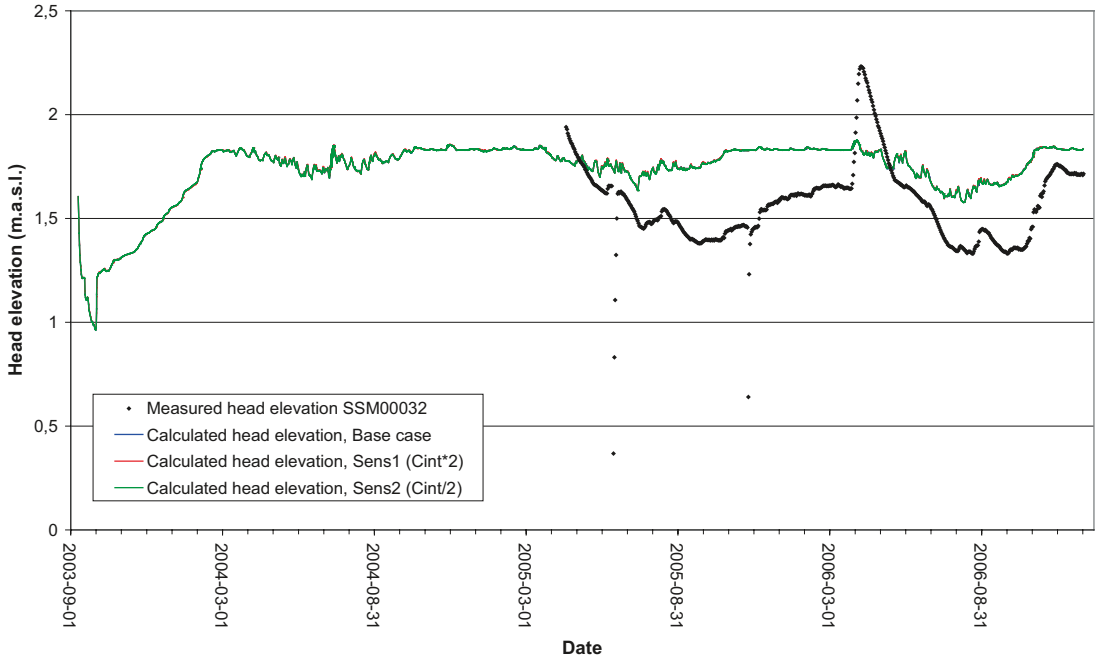

Figure 6-5. *Results for SSM000032 from sensitivity analysis of the interception coefficient (C_{int}).*

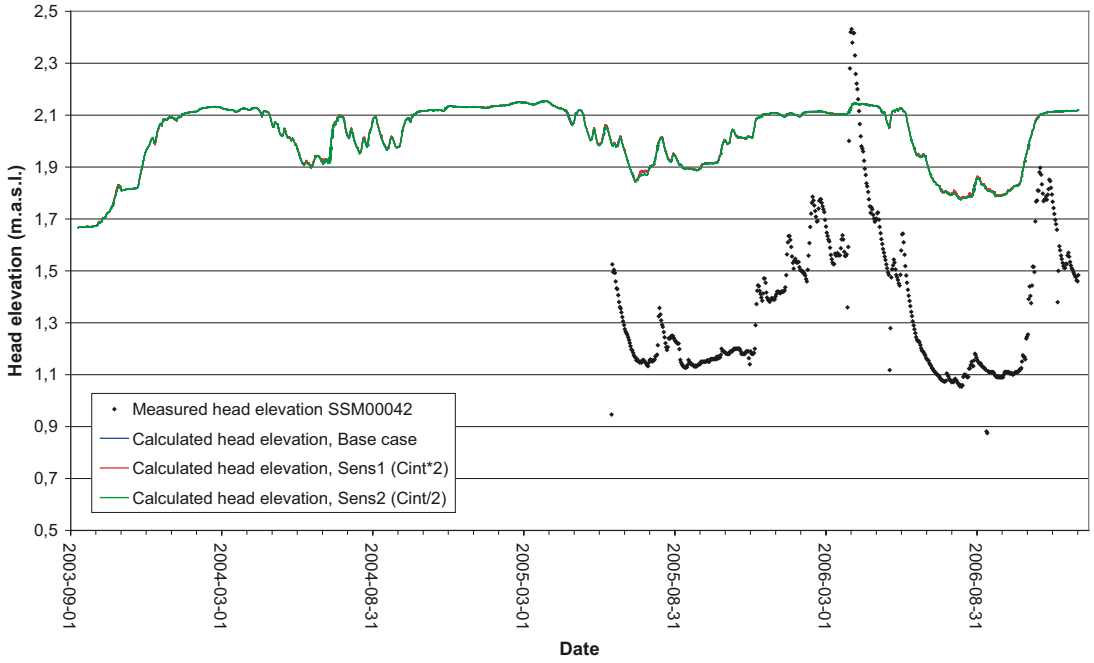

Figure 6-6. *Results for SSM000042 from sensitivity analysis of the interception coefficient (C_{int}).*

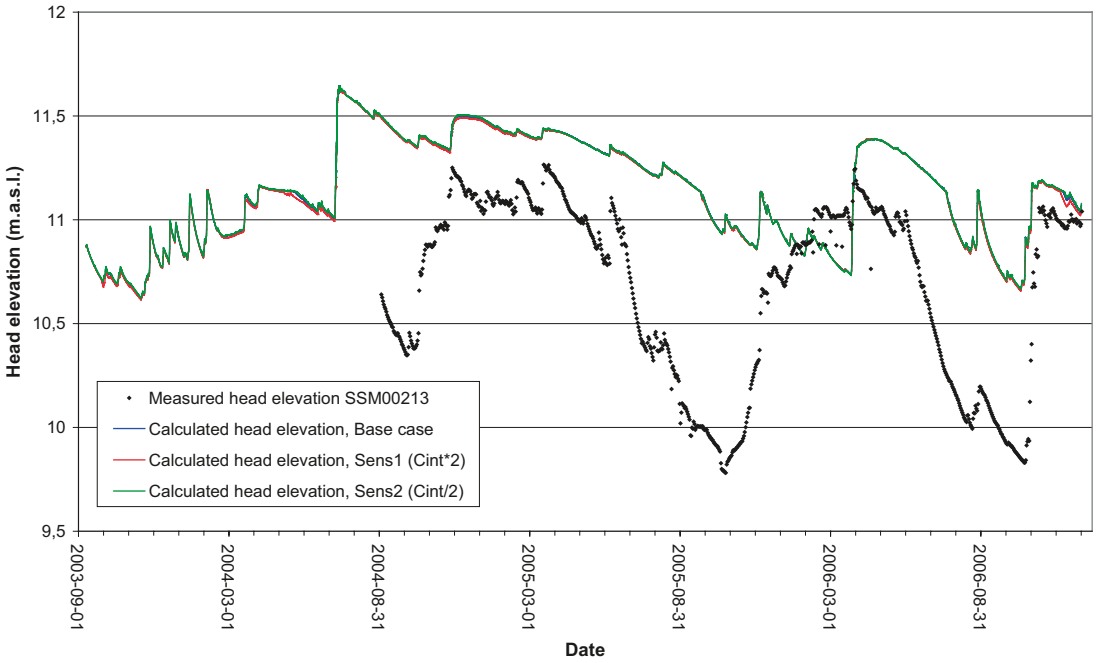

Figure 6-7. *Results for SSM000213 from sensitivity analysis of the interception coefficient (C_{int}).*

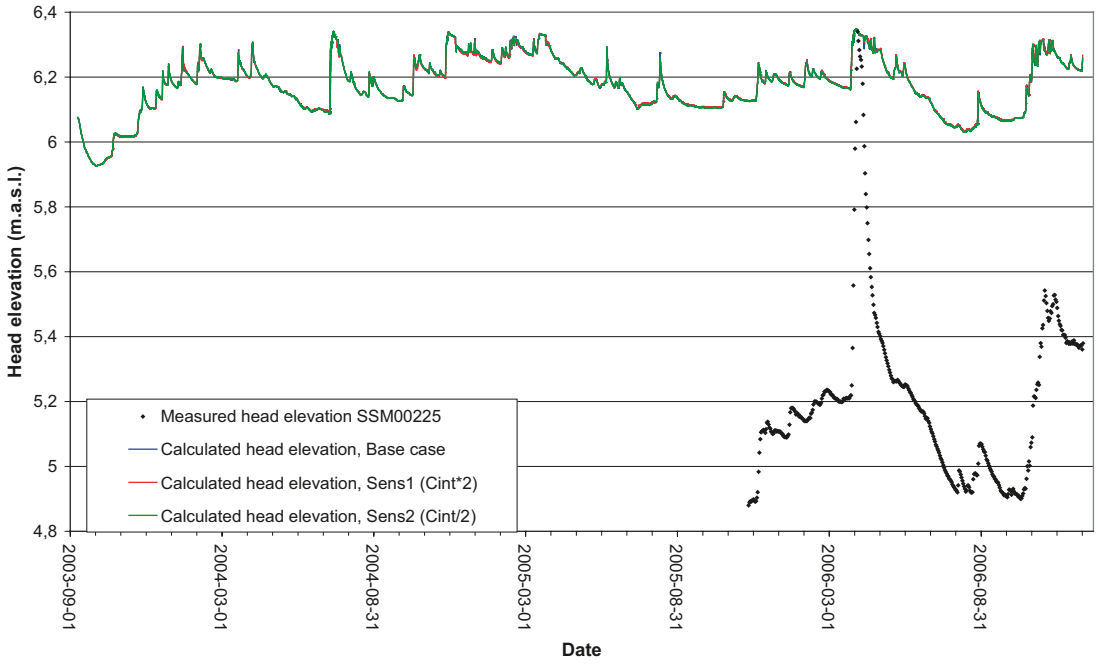

Figure 6-8. *Results for SSM000225 from sensitivity analysis of the interception coefficient (C_{int}).*

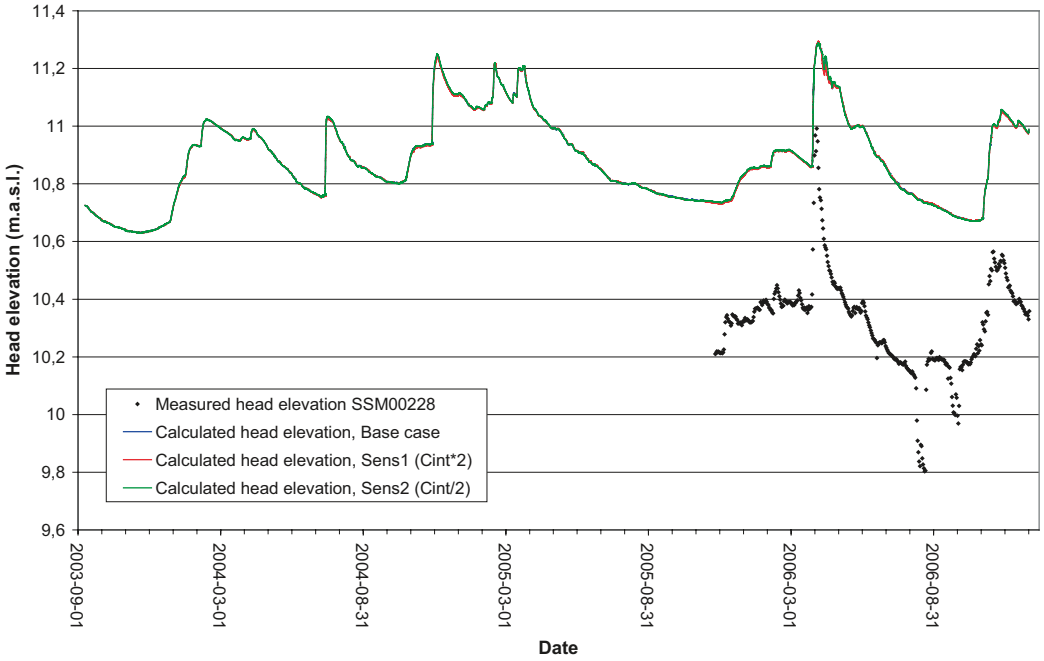

Figure 6-9. *Results for SSM000228 from sensitivity analysis of the interception coefficient (C_{int}).*

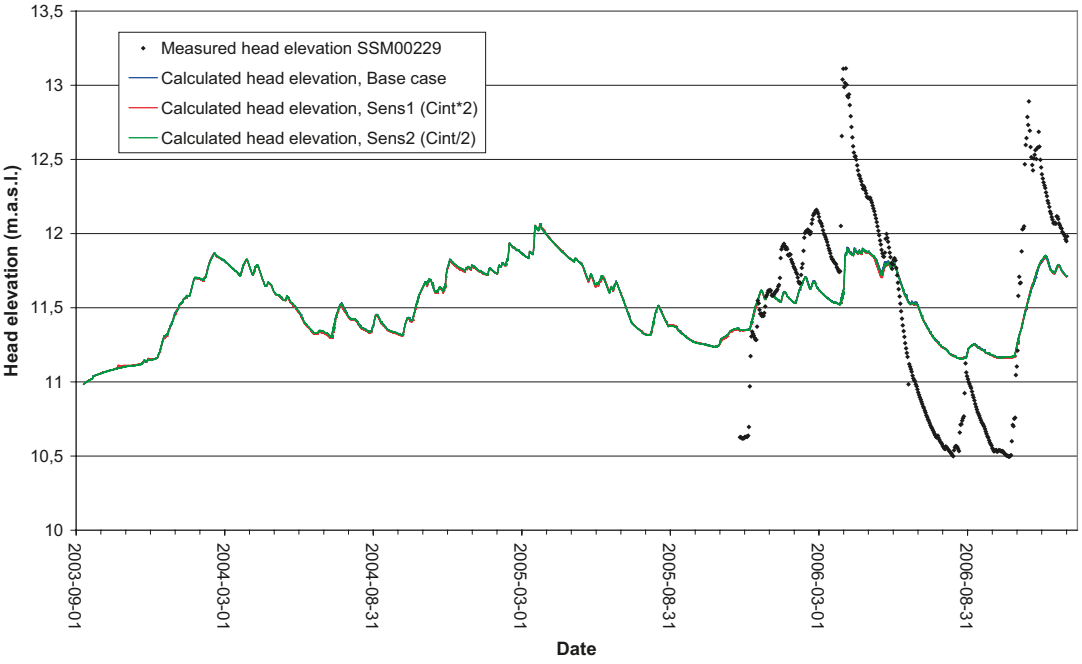

Figure 6-10. *Results for SSM000229 from sensitivity analysis of the interception coefficient (C_{int}).*

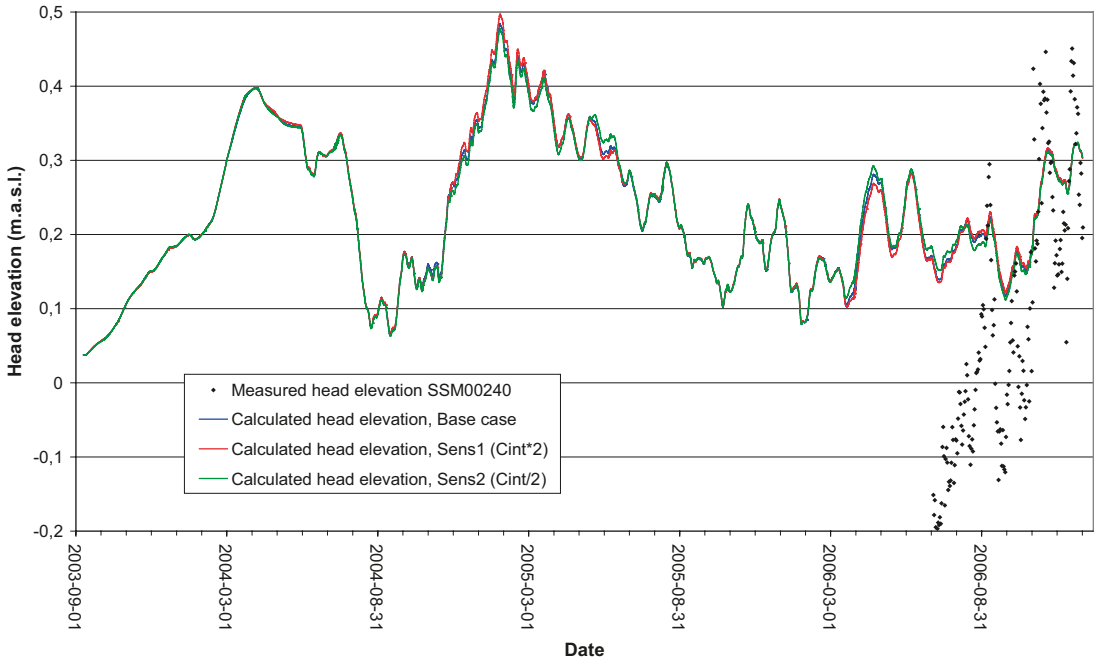

Figure 6-11. *Results for SSM000240 from sensitivity analysis of the interception coefficient (C_{int}).*

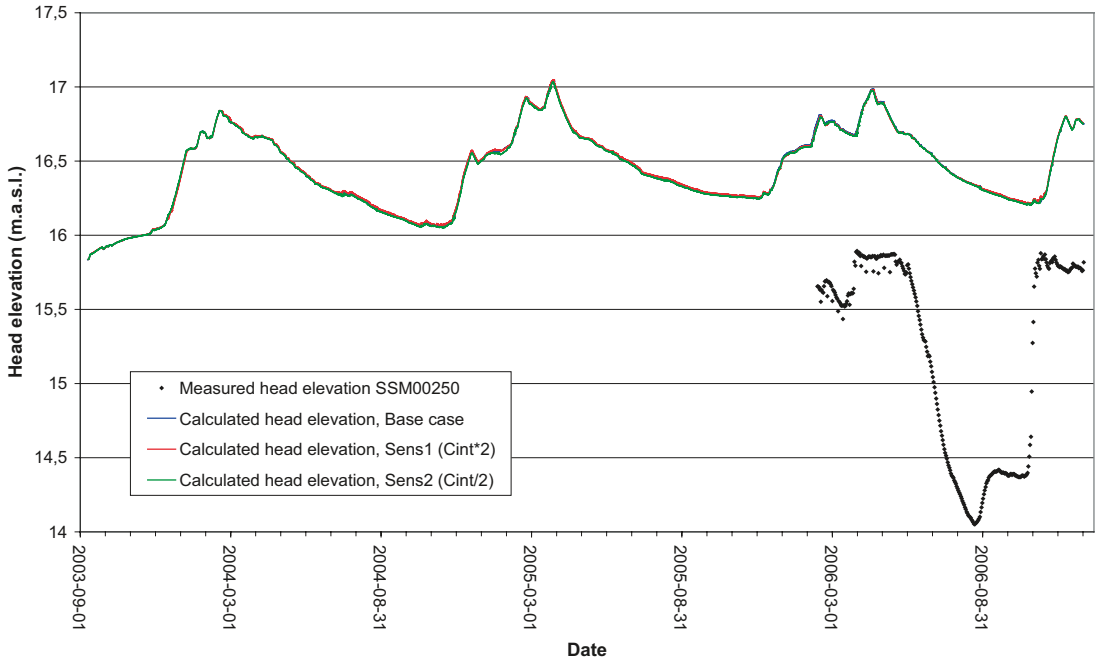

Figure 6-12. *Results for SSM000250 from sensitivity analysis of the interception coefficient (C_{int}).*

Table 6-2 shows a comparison of statistical mean absolute errors, MAE, for each of the groundwater monitoring wells for the base case, Sens1 and Sens2. For most monitoring wells there is no change at all on the mean error. There are very small effects for some of the monitoring wells.

Table 6-2. Comparison of mean absolute errors between the base case, Sens1 and Sens2 ("+" represents an improvement, "o" no change and "–" reduced agreement compared to the base case).

Borehole	Mean Absolute Error, Base case	Mean Absolute Error, Sens1 (C_{int}*2)	Mean Absolute Error, Sens2 (C_{int}/2)	Improved agreement with Sens1	Improved agreement with Sens2
SSM000009	0.21	0.22	0.21	–	o
SSM000011	1.17	1.18	1.17	–	o
SSM000017	0.70	0.71	0.70	–	o
SSM000019	1.35	1.35	1.35	o	o
SSM000021	1.63	1.63	1.62	o	+
SSM000030	1.03	1.03	1.02	o	+
SSM000031	0.77	0.77	0.77	o	o
SSM000032	0.23	0.23	0.23	o	o
SSM000033	1.15	1.15	1.15	o	o
SSM000037	2.09	2.10	2.09	–	o
SSM000039	1.62	1.62	1.62	o	o
SSM000041	2.06	2.07	2.06	–	o
SSM000042	0.63	0.63	0.63	o	o
SSM000210	2.35	2.34	2.35	+	o
SSM000213	0.53	0.53	0.53	o	o
SSM000215	1.63	1.63	1.63	o	o
SSM000218	0.77	0.76	0.77	+	o
SSM000219	2.02	2.03	2.02	–	o
SSM000220	1.31	1.31	1.31	o	o
SSM000221	0.51	0.51	0.51	o	o
SSM000222	1.74	1.74	1.74	o	o
SSM000223	1.29	1.29	1.29	o	o
SSM000224	0.72	0.72	0.71	o	+
SSM000225	0.98	0.98	0.98	o	o
SSM000226	1.41	1.41	1.40	o	+
SSM000227	1.54	1.54	1.53	o	+
SSM000228	0.56	0.56	0.56	o	o
SSM000229	0.44	0.44	0.44	o	o
SSM000230	1.57	1.56	1.56	+	+
SSM000237	1.97	1.97	1.97	o	o
SSM000239	0.14	0.14	0.14	o	o
SSM000240	0.16	0.16	0.16	o	o
SSM000242	1.18	1.18	1.18	o	o
SSM000249	0.76	0.74	0.76	+	o
SSM000250	1.34	1.34	1.34	o	o
SSM000252	5.42	5.42	5.41	o	+
SSM000253	1.96	1.96	1.96	o	o
SSM000255	1.66	1.66	1.66	o	o
SSM000256	1.67	1.67	1.67	o	o
SSM000257	1.68	1.68	1.68	o	o
Mean MAE	1.30	1.30	1.30		

Table 6-3 shows the total water balance for the base case compared to water balances for Sens1 and Sens2. The results show small or no changes in the water balance components. For Sens1, the evapotranspiration is somewhat larger than in the base case, while the flow from overland to river is somewhat smaller. Results from Sens2 show the opposite results.

6.1.2 Root mass distribution

The vertical distribution of the water extraction by transpiration depends on the A_{root} parameter. As A_{root} approaches zero, the root distribution, and hence the transpiration, becomes more uniformly distributed with depth. The sensitivity analysis considered evaluation of a root mass distribution of 0.5, case Sens4, corresponding to a higher root mass density at depth in the soil profile than in the base case (i.e. a more even root distribution over depth). The other A_{root} sensitivity case, Sens3, had a root mass distribution of 2, corresponding to a higher root mass density in the uppermost part of the soil profile than in the base case.

Figures 6-13 to 6-16 show the effects of changing A_{root} on the surface water discharges. The simulations indicate that a higher A_{root} value (Sens3) leads to higher surface water discharges, due to less transpiration from the deeper part of the soil profile, and a smaller A_{root} value (Sens4) leads to smaller discharges, due to larger transpiration from the deeper part of the soil profile. However, the differences are small.

Figures 6-17 to 6-24 show how changes in the A_{root} parameter affect the head elevations in the groundwater monitoring wells. The results show different patterns for different wells. For five of the eight monitoring wells, an increased A_{root} value leads to somewhat increased head elevations. For the remaining three wells, SSM000032, SSM000229 and SSM000240, the effects are small and more difficult to interpret.

Table 6-3. Comparison of total water balances between base case, Sens1 and Sens2.

Parameter	Base case	Sens1	Sens2
Precipitation	–1,774	–1,774	-1,774
Canopy storage change	0	0	0
Evapotranspiration	1,264	1,266	1,264
Overland storage change	55	55	55
Overland boundary inflow	–52	–53	-52
Overland boundary outflow	84	84	83
Overland to river	225	222	226
Subsurface storage change	43	43	42
Subsurface boundary inflow	14	14	14
Subsurface boundary outflow	83	83	83
Baseflow to river	94	94	94
Baseflow from river	0	0	0
Error	7	7	7

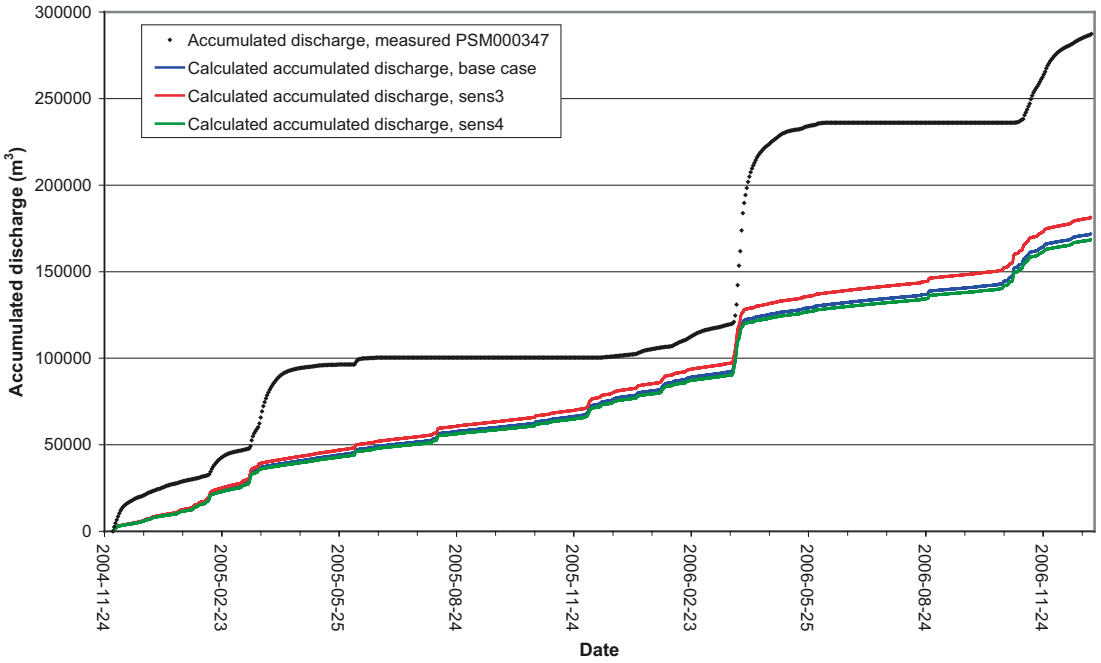

Figure 6-13. *Results for PSM000347 from sensitivity analysis of the root mass distribution parameter* A_{root}.

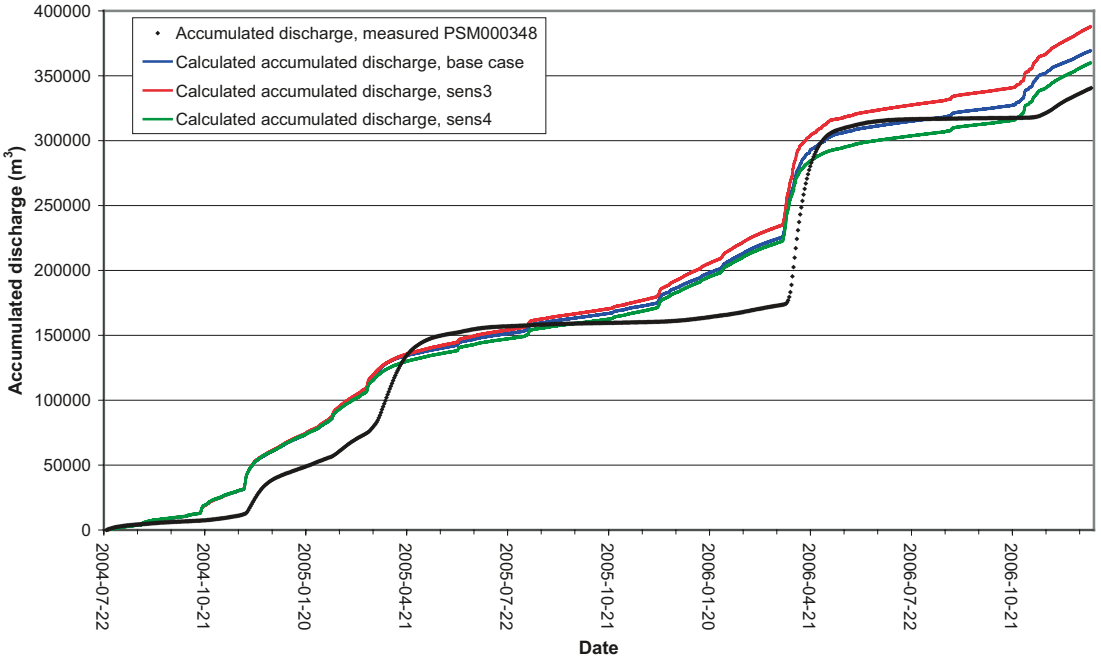

Figure 6-14. *Results for PSM000348 from sensitivity analysis of the root mass distribution parameter* A_{root}.

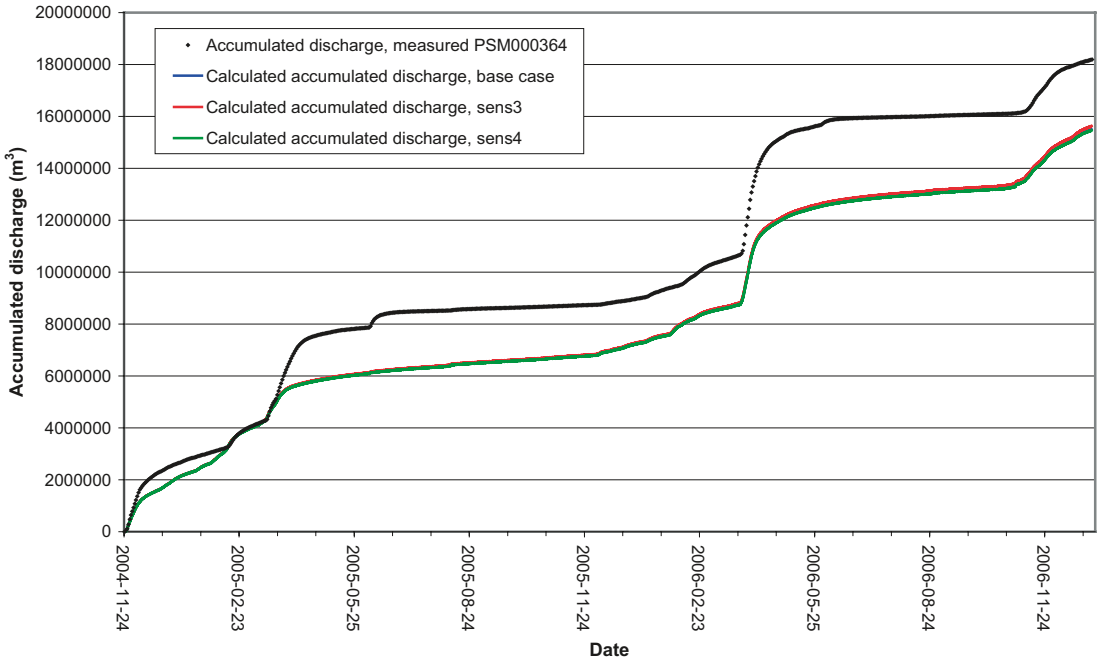

Figure 6-15. *Results for PSM000364 from sensitivity analysis of the root mass distribution parameter* A_{root}.

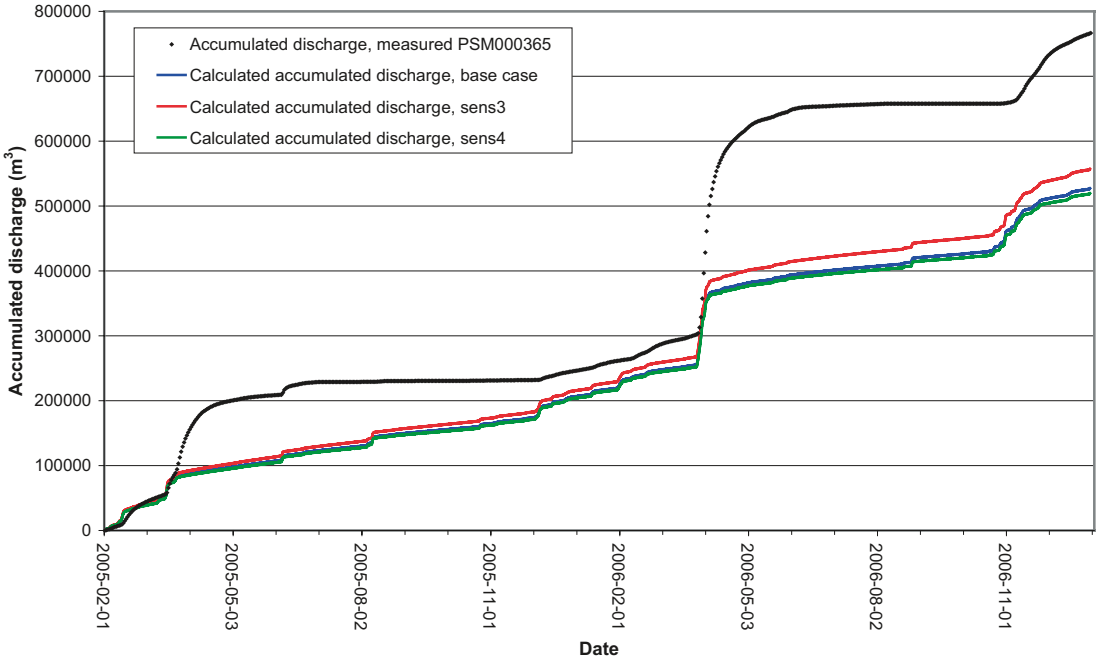

Figure 6-16. *Results for PSM000365 from sensitivity analysis of the root mass distribution parameter* A_{root}.

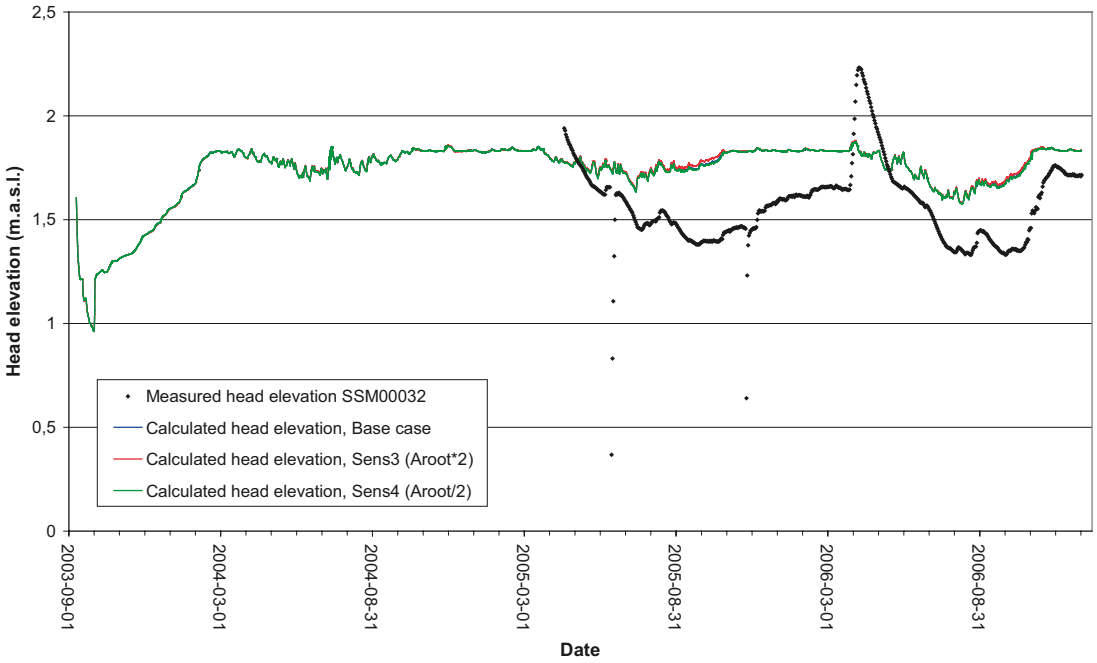

Figure 6-17. *Results for SSM000032 from sensitivity analysis of the root mass distribution parameter* A_{root}.

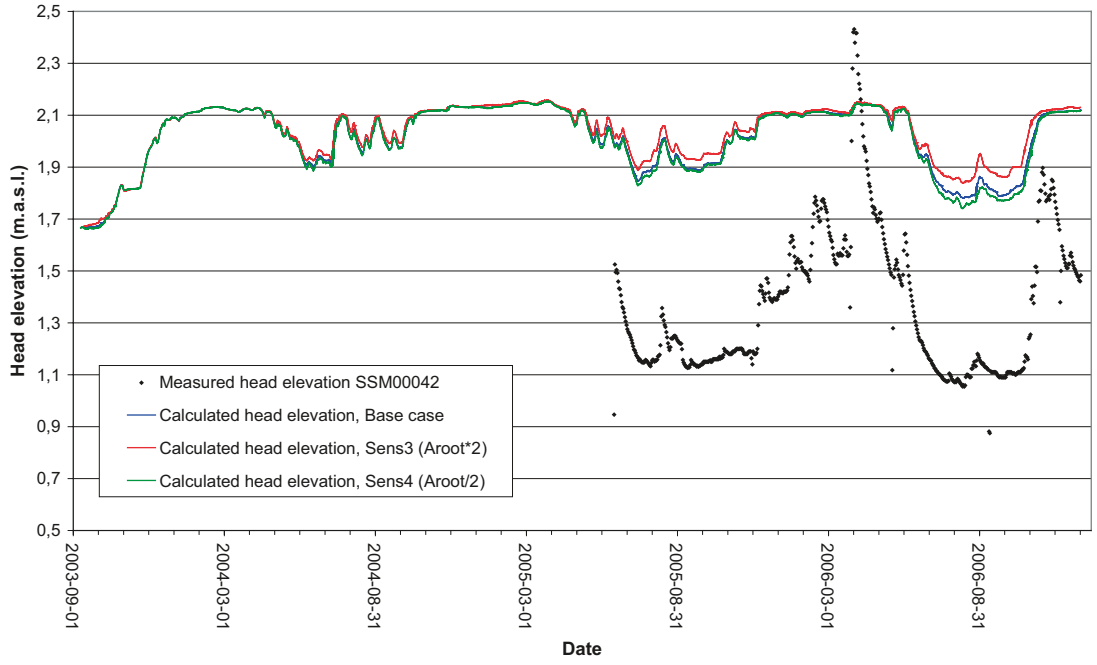

Figure 6-18. *Results for SSM000042 from sensitivity analysis of the root mass distribution parameter* $A_{root.}$

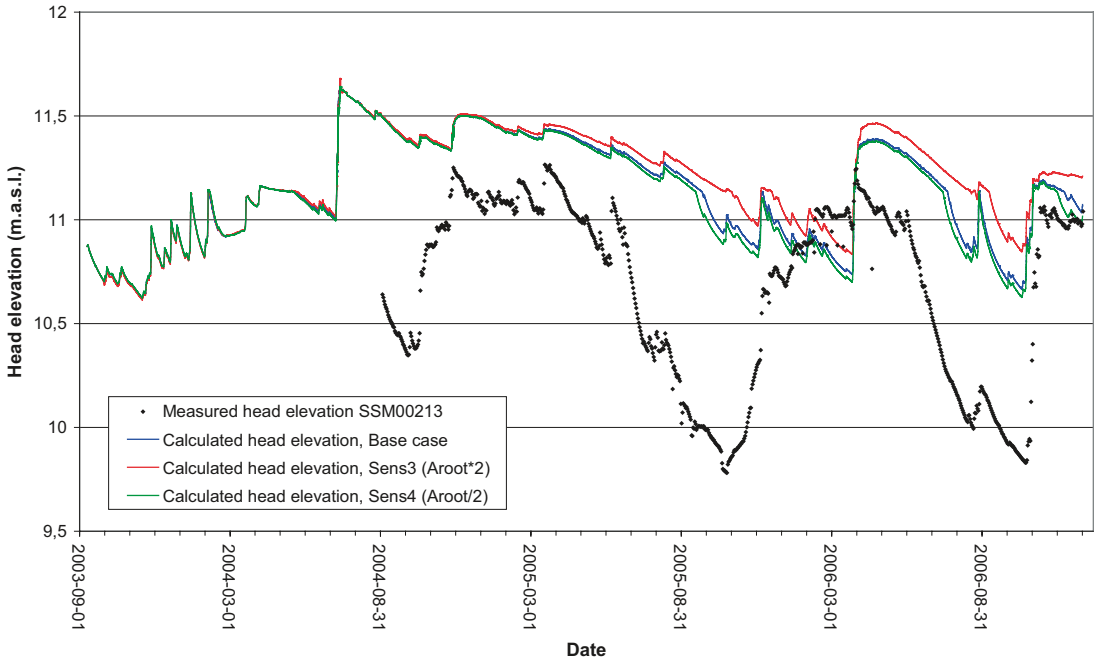

Figure 6-19. *Results for SSM000213 from sensitivity analysis of the root mass distribution parameter* A_{root}.

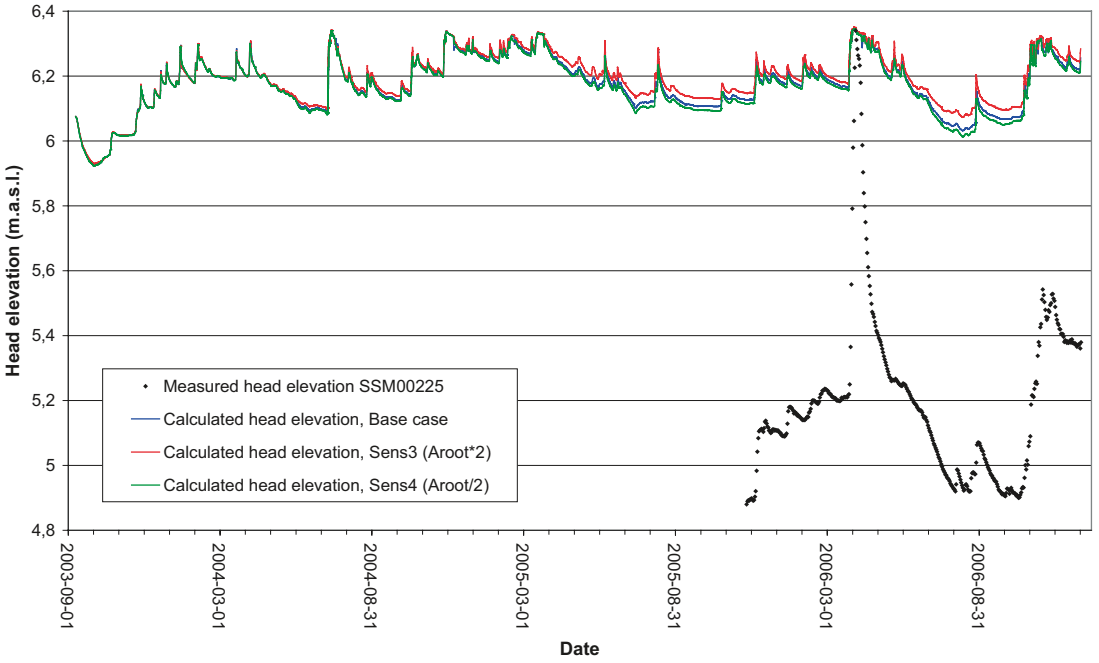

Figure 6-20. *Results for SSM000225 from sensitivity analysis of the root mass distribution parameter* A_{root}.

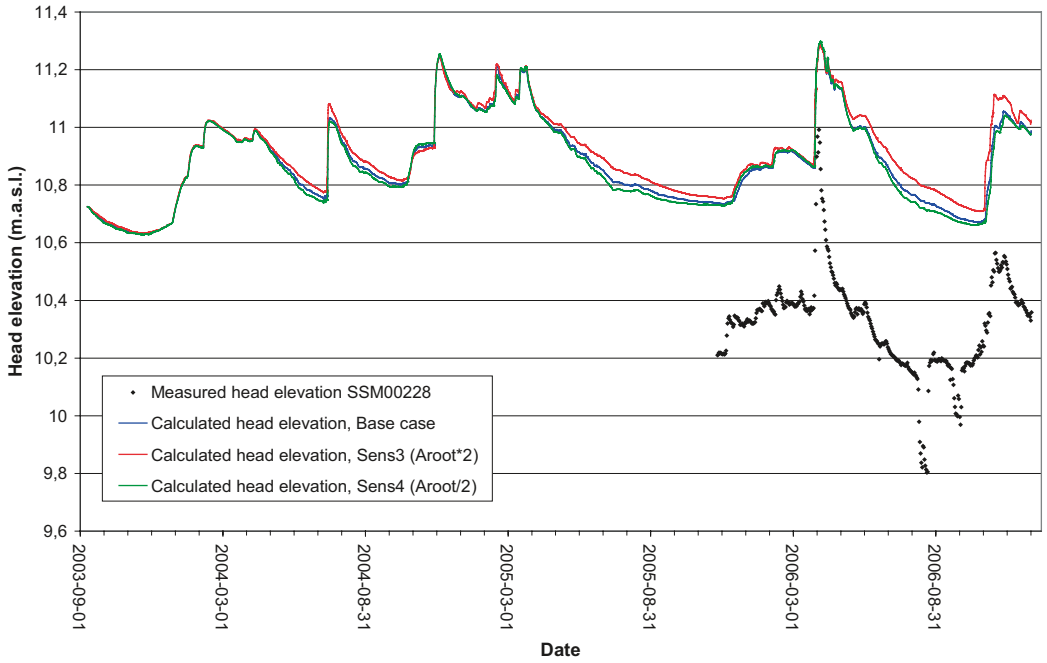

Figure 6-21. *Results for SSM000228 from sensitivity analysis of the root mass distribution parameter* A_{root}.

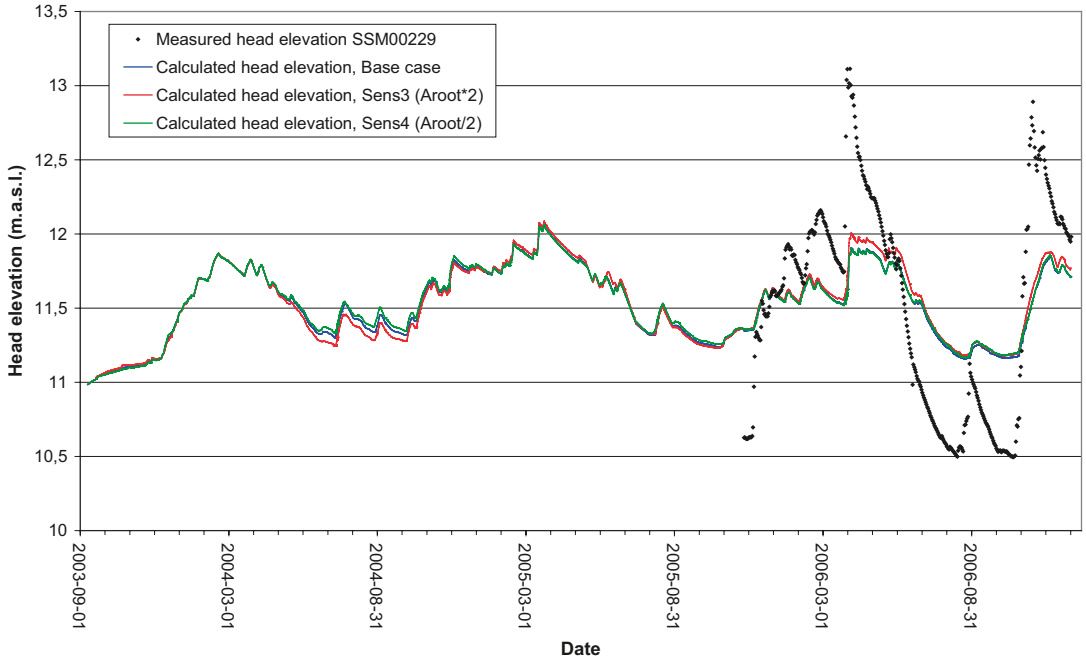

Figure 6-22. *Results for SSM000229 from sensitivity analysis of the root mass distribution parameter* A_{root}.

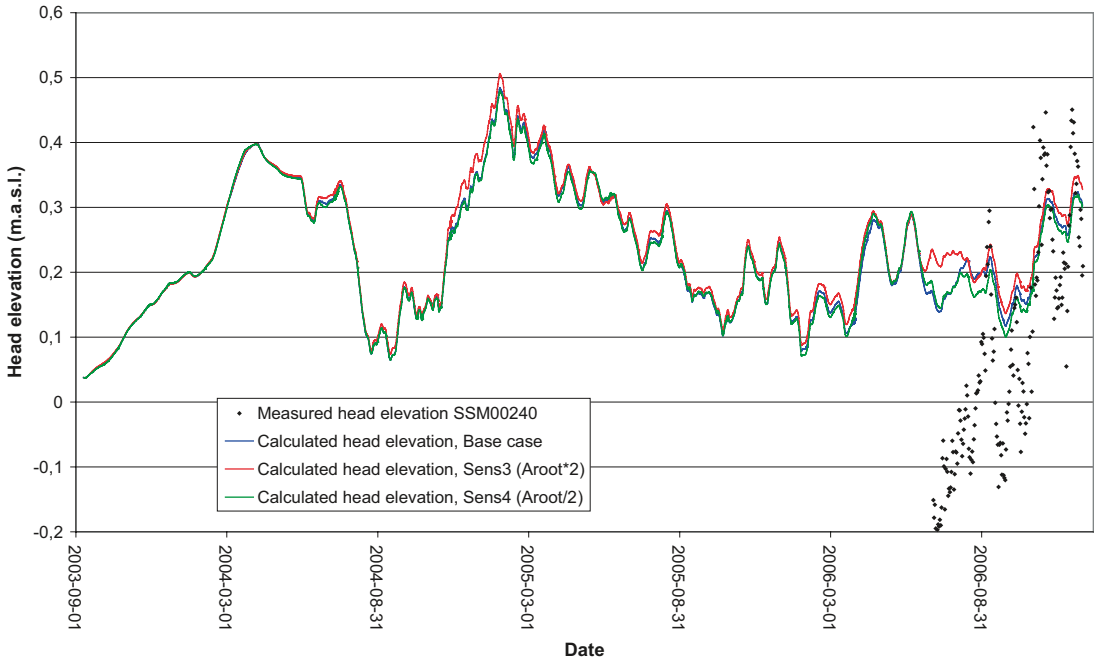

Figure 6-23. *Results for SSM000240 from sensitivity analysis of the root mass distribution parameter* A_{root}.

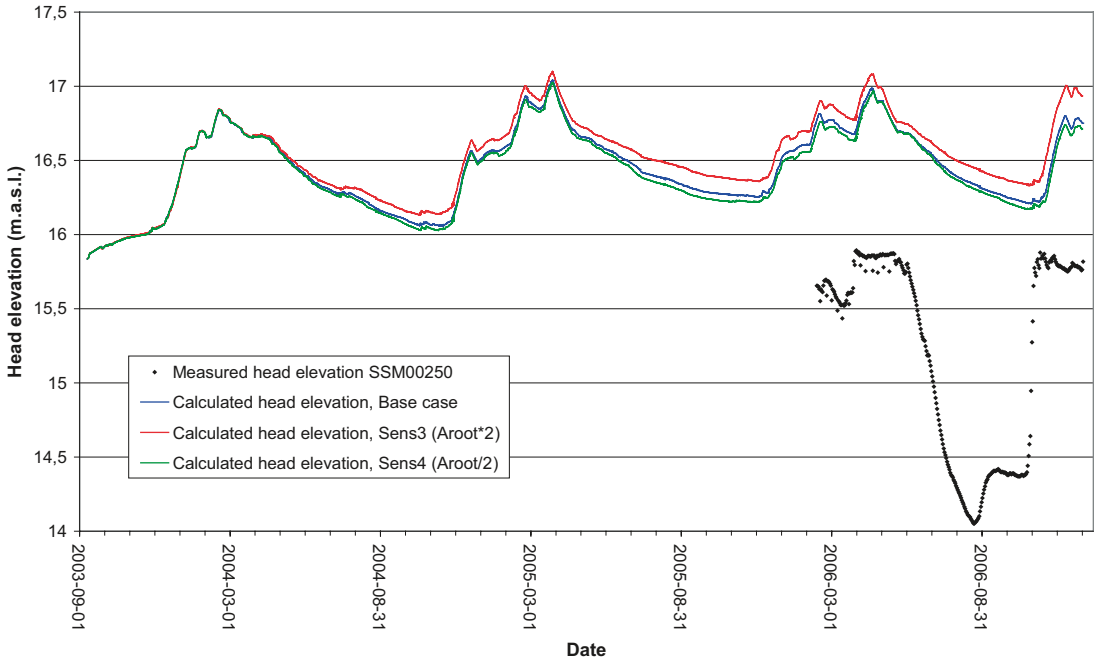

Figure 6-24. *Results for SSM000250 from sensitivity analysis of the root mass distribution parameter* A_{root}.

Table 6-4 shows a comparison of statistical mean absolute errors for the base case and the sensitivity cases Sens3 and Sens4. Sens4, with a decreased value of the root mass distribution, shows a generally improved agreement between observed and calculated data. However, the differences between the mean values for the different simulations are small.

Table 6-4. Comparison of mean absolute errors between the base case, Sens3 and Sens4 ("+" represents an improvement, "o" no change and "–" reduced agreement compared to the base case).

Borehole	Mean Absolute Error, Base case	Mean Absolute Error, Sens3 (A_{root}*2)	Mean Absolute Error, Sens4 (A_{root}/2)	Improved agreement with Sens3	Improved agreement with Sens4
SSM000009	0.21	0.23	0.20	–	+
SSM000011	1.17	1.19	1.16	–	+
SSM000017	0.70	0.79	0.69	–	+
SSM000019	1.35	1.41	1.34	–	+
SSM000021	1.63	1.68	1.60	–	+
SSM000030	1.03	1.07	1.01	–	+
SSM000031	0.77	0.82	0.76	–	+
SSM000032	0.23	0.23	0.23	o	o
SSM000033	1.15	1.17	1.15	–	o
SSM000037	2.09	2.16	2.07	–	+
SSM000039	1.62	1.69	1.58	–	+
SSM000041	2.06	2.16	2.03	–	+
SSM000042	0.63	0.66	0.62	–	+
SSM000210	2.35	2.36	2.35	–	o
SSM000213	0.53	0.60	0.52	–	+
SSM000215	1.63	1.64	1.63	–	o
SSM000218	0.77	0.72	0.79	+	–
SSM000219	2.02	2.12	1.98	–	+
SSM000220	1.31	1.32	1.32	–	–
SSM000221	0.51	0.51	0.51	o	o
SSM000222	1.74	1.81	1.71	–	+
SSM000223	1.29	1.36	1.27	–	+
SSM000224	0.72	0.74	0.71	–	+
SSM000225	0.98	1.00	0.97	–	+
SSM000226	1.41	1.50	1.37	–	+
SSM000227	1.54	1.63	1.50	–	+
SSM000228	0.56	0.60	0.55	–	+
SSM000229	0.44	0.43	0.45	+	–
SSM000230	1.57	1.64	1.55	–	+
SSM000237	1.97	1.98	1.97	–	o
SSM000239	0.14	0.15	0.14	–	o
SSM000240	0.16	0.17	0.15	–	+
SSM000242	1.18	1.22	1.17	–	+
SSM000249	0.76	0.76	0.76	o	o
SSM000250	1.34	1.46	1.31	–	+
SSM000252	5.42	5.45	5.41	–	+
SSM000253	1.96	2.01	1.95	–	+
SSM000255	1.66	1.70	1.65	–	+
SSM000256	1.67	1.69	1.66	–	+
SSM000257	1.68	1.72	1.67	–	+
Mean MAE	1.30	1.34	1.29		

Table 6-5 shows the total water balance for the base case compared to Sens3 and Sens4. The main differences between the cases are in the evapotranspiration parameter and in the subsurface storage change. Sens4 has a larger evapotranspiration and a smaller subsurface storage change than Sens3.

6.2 Unsaturated zone parameters

In the sensitivity analysis of the unsaturated zone parameters, three different parameters were changed: the specific yield (S_y), the Averjanov constant (n), and the saturated hydraulic conductivity (K_s). Sections 6.2.1–6.2.3 describe the parameters and the results from the sensitivity analysis of these unsaturated zone parameters.

6.2.1 Specific yield in the unsaturated zone

The specific yield of the unsaturated zone, i.e. the available pore volume in the pF curve between the porosity at field capacity and the total porosity, affects the groundwater head fluctuation. A higher value of the specific yield generates a smaller fluctuation of the groundwater elevation, while a smaller specific yield means a smaller storage capacity and larger fluctuations in the groundwater head elevation. Note that the value of the unsaturated specific yield is applied for the top layer of the saturated zone, whereas the fluctuations of the groundwater table are controlled by the specific yield value given in the saturated zone description.

In the sensitivity analysis, the specific yield in the unsaturated zone was increased by a factor of 1.5 in Sens5, and decreased by a factor of 2 in Sens6. The field capacity equals that of the base case. Figure 6-25 shows the pF-curves for coarse till used in the analysis and Figure 6-26 the corresponding curves for sand. Figures 6-27 to 6-30 show the effect of changing the unsaturated zone specific yield parameter on the surface water discharges. In all four measurement points, the simulation with a lower specific yield (Sens6) leads to an increased surface runoff.

Figures 6-31 to 6-38 show the effects on groundwater head elevations. For most of the monitoring wells, the simulation with the lower specific yield (Sens6) results in larger head elevation amplitudes, which better coincides with the observed amplitudes. However, the simulated heads are generally slightly higher using the lower specific yield in Sens6.

Table 6-5. Comparison of total water balances between the base case, Sens3 and Sens4.

Parameter	Base case	Sens3	Sens4
Precipitation	–1,774	–1,774	–1,774
Canopy storage change	0	0	0
Evapotranspiration	1,264	1,223	1,278
Overland storage change	55	56	54
Overland boundary inflow	–52	–54	–53
Overland boundary outflow	84	86	85
Overland to river	225	229	225
Subsurface storage change	43	65	33
Subsurface boundary inflow	14	13	14
Subsurface boundary outflow	83	87	82
Base flow to river	94	99	93
Base flow from river	0	0	0
Error	7	4	9

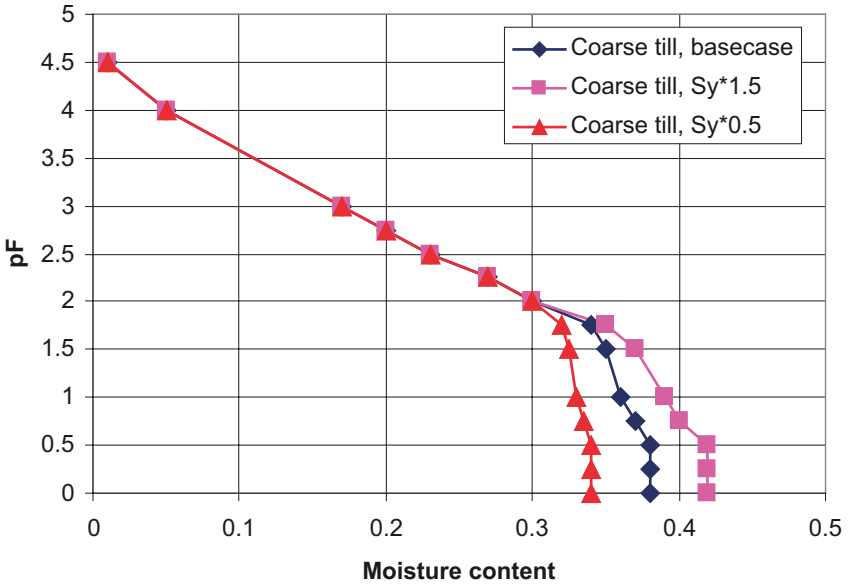

Figure 6-25. *Relation between moisture potential, pF, and moisture content for coarse till in the base case and in the two sensitivity cases Sens5 and Sens6.*

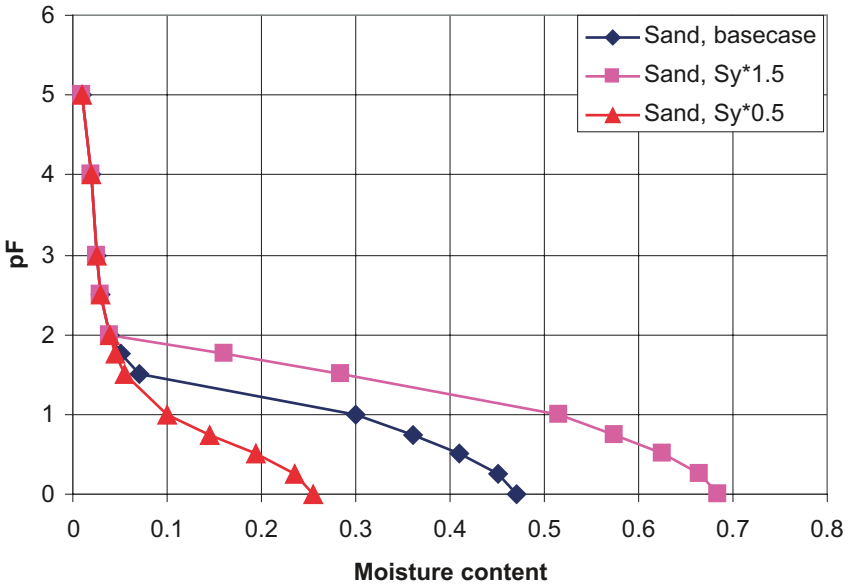

Figure 6-26. *Relation between moisture potential, pF, and moisture content for sand in the base case and in the two sensitivity cases Sens5 and Sens6.*

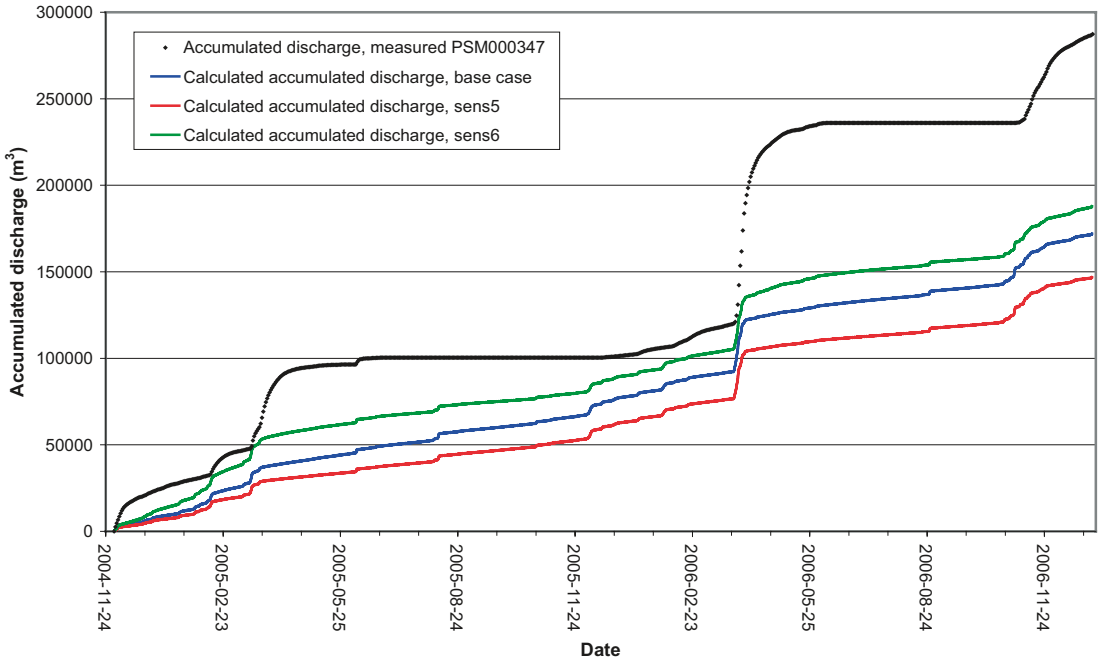

Figure 6-27. *Results for PSM000347 from sensitivity analysis of the unsaturated zone specific yield (S_y).*

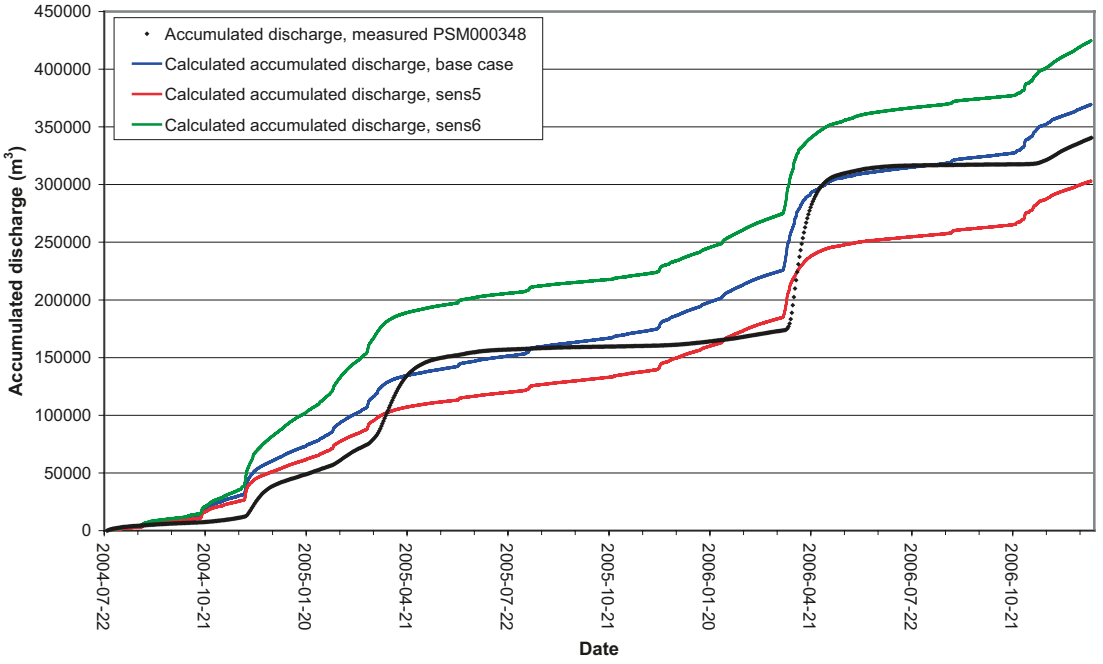

Figure 6-28. *Results for PSM000348 from sensitivity analysis of the unsaturated zone specific yield (S_y).*

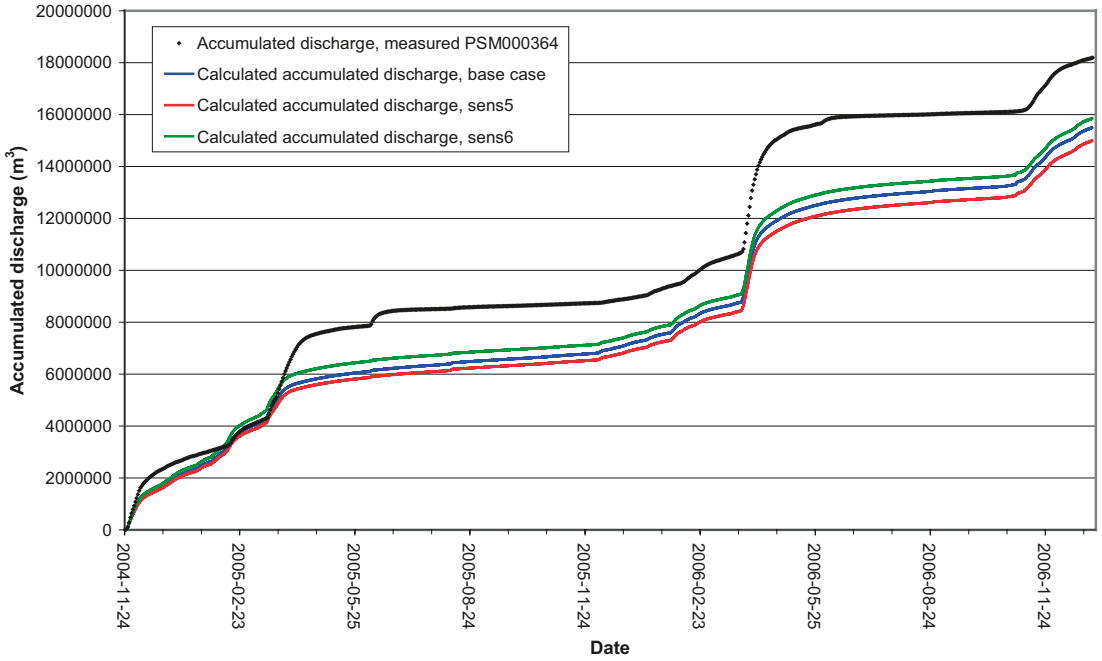

Figure 6-29. *Results for PSM000364 from sensitivity analysis of the unsaturated zone specific yield (S_y).*

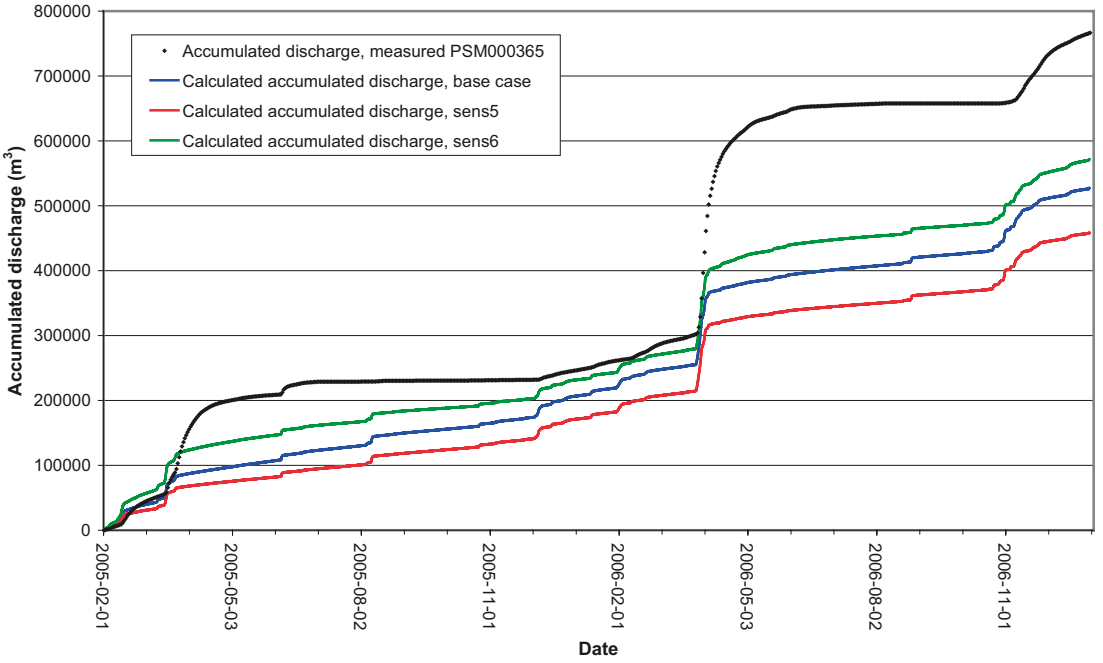

Figure 6-30. *Results for PSM000365 from sensitivity analysis of the unsaturated zone specific yield (S_y).*

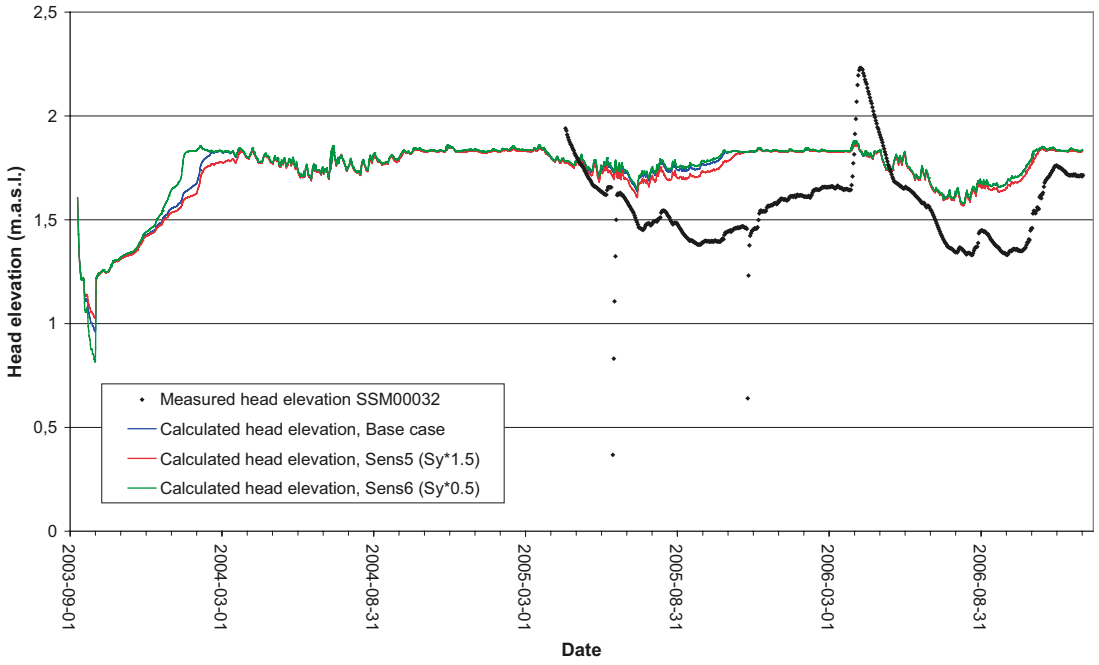

Figure 6-31. *Results for SSM000032 from sensitivity analysis of the unsaturated zone specific yield (S_y).*

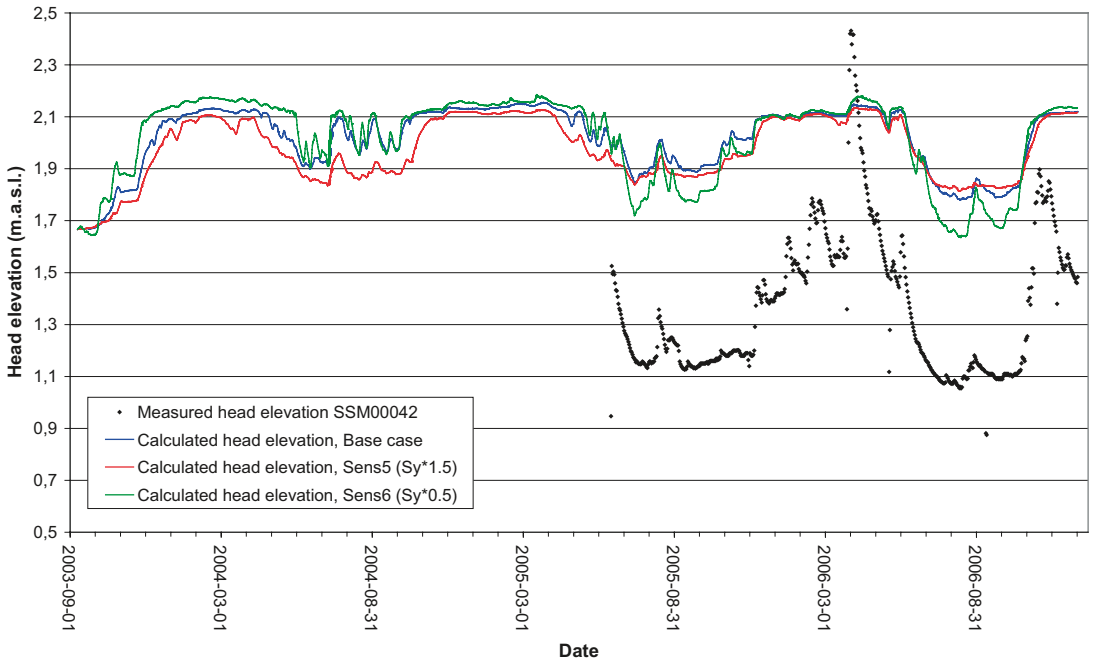

Figure 6-32. *Results for SSM000042 from sensitivity analysis of the unsaturated zone specific yield (S_y).*

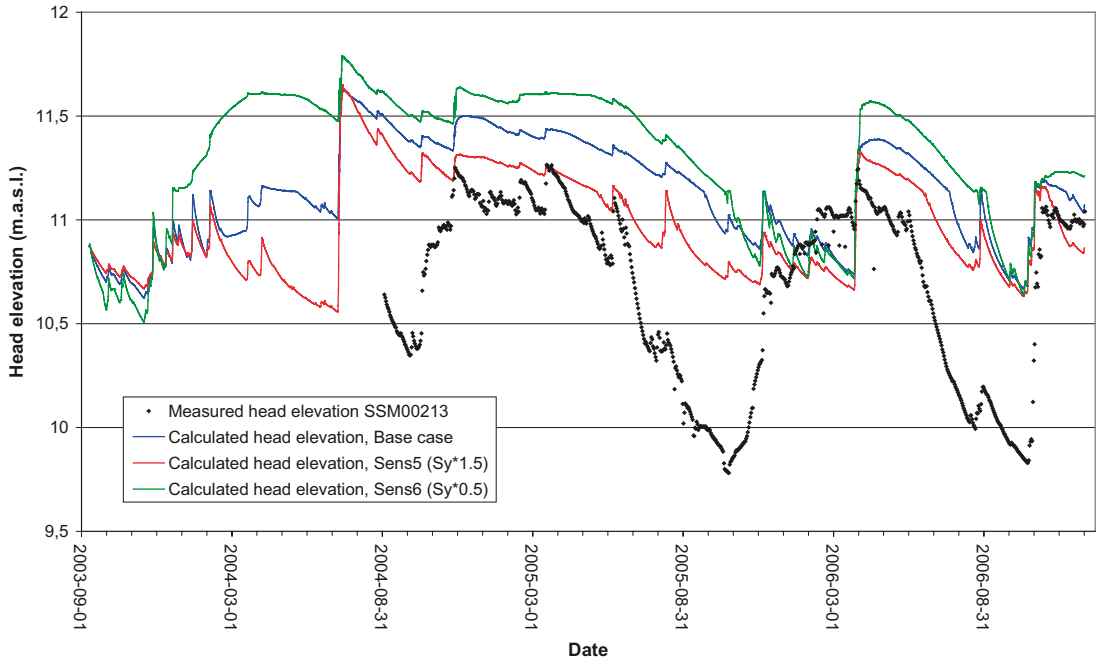

Figure 6-33. *Results for SSM000213 from sensitivity analysis of the unsaturated zone specific yield (S_y).*

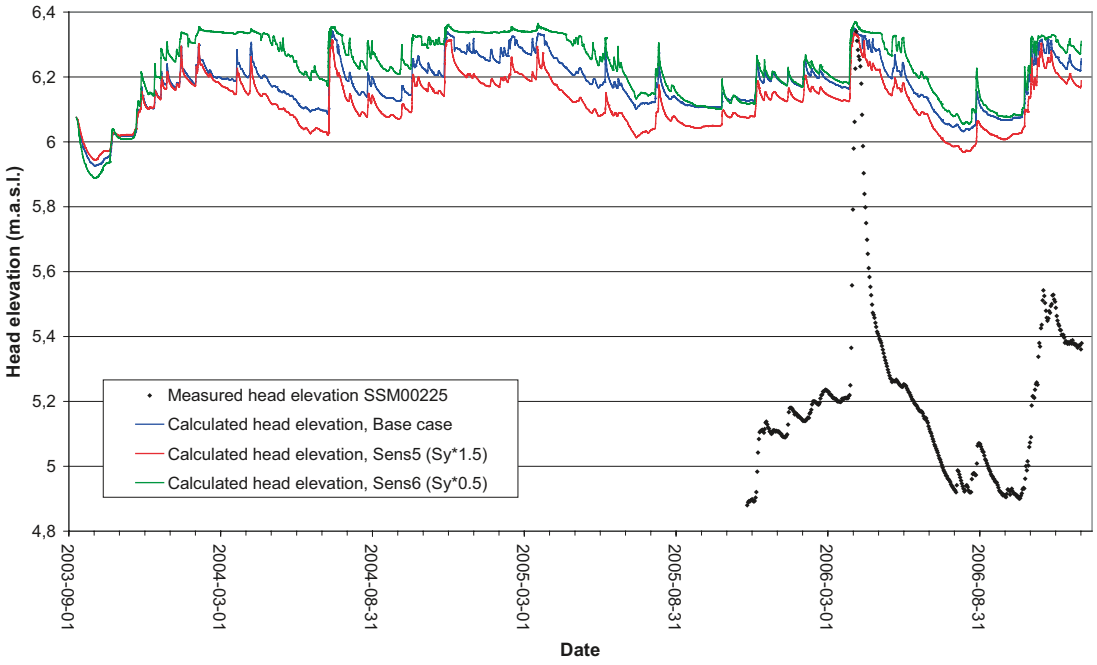

Figure 6-34. *Results for SSM000225 from sensitivity analysis of the unsaturated zone specific yield (S_y).*

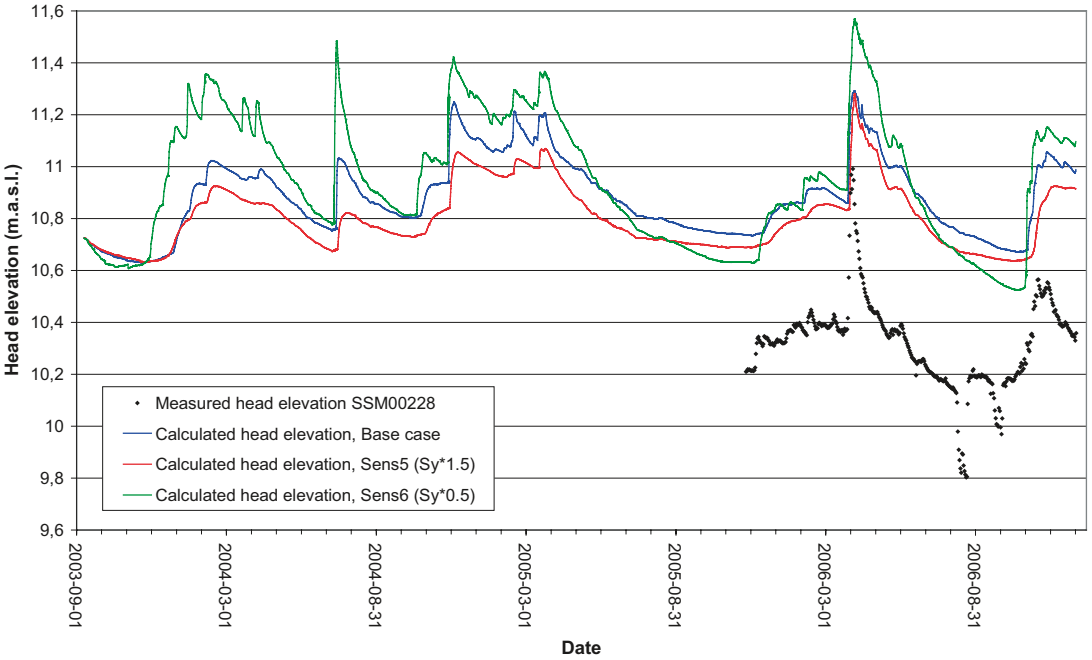

Figure 6-35. *Results for SSM000228 from sensitivity analysis of the unsaturated zone specific yield (S_y).*

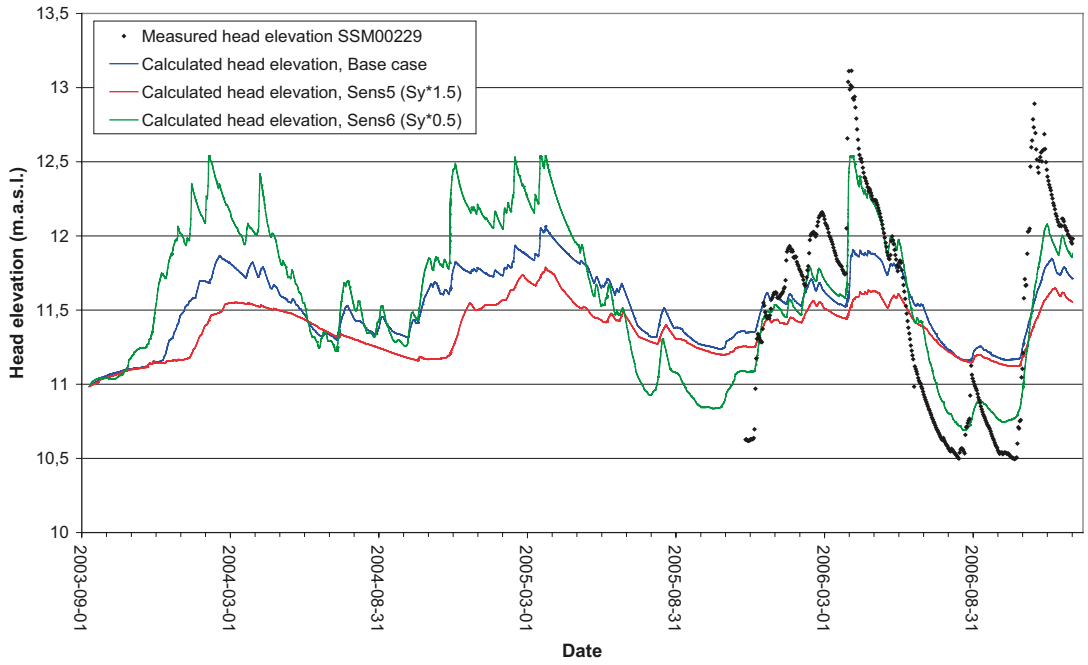

Figure 6-36. *Results for SSM000229 from sensitivity analysis of the unsaturated zone specific yield (S_y).*

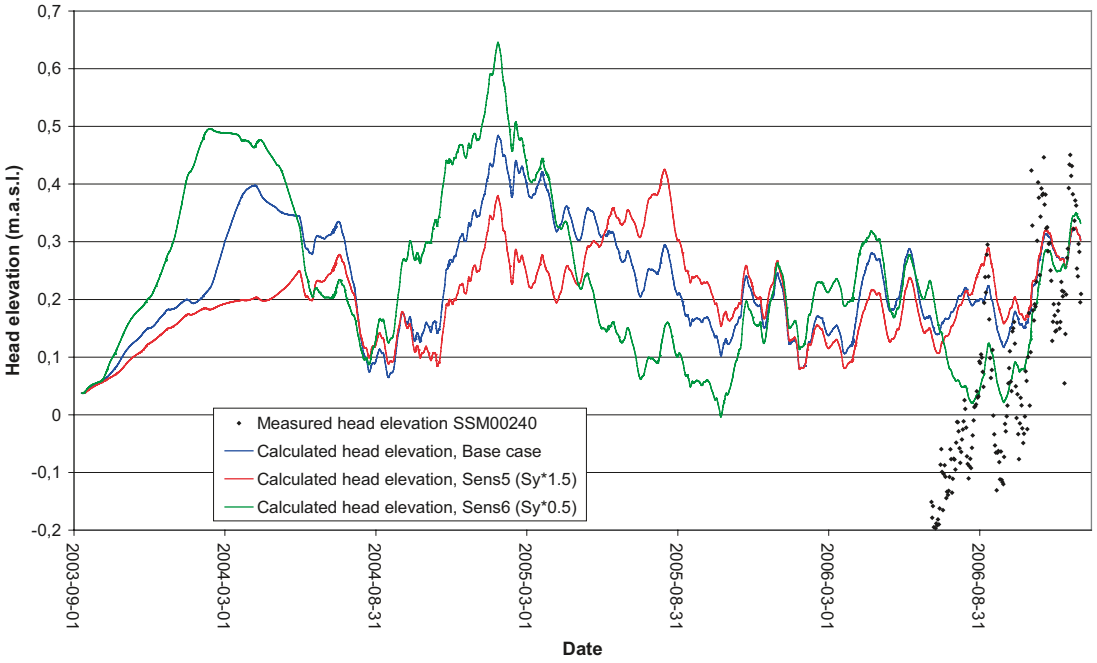

Figure 6-37. *Results for SSM000240 from sensitivity analysis of the unsaturated zone specific yield (S_y).*

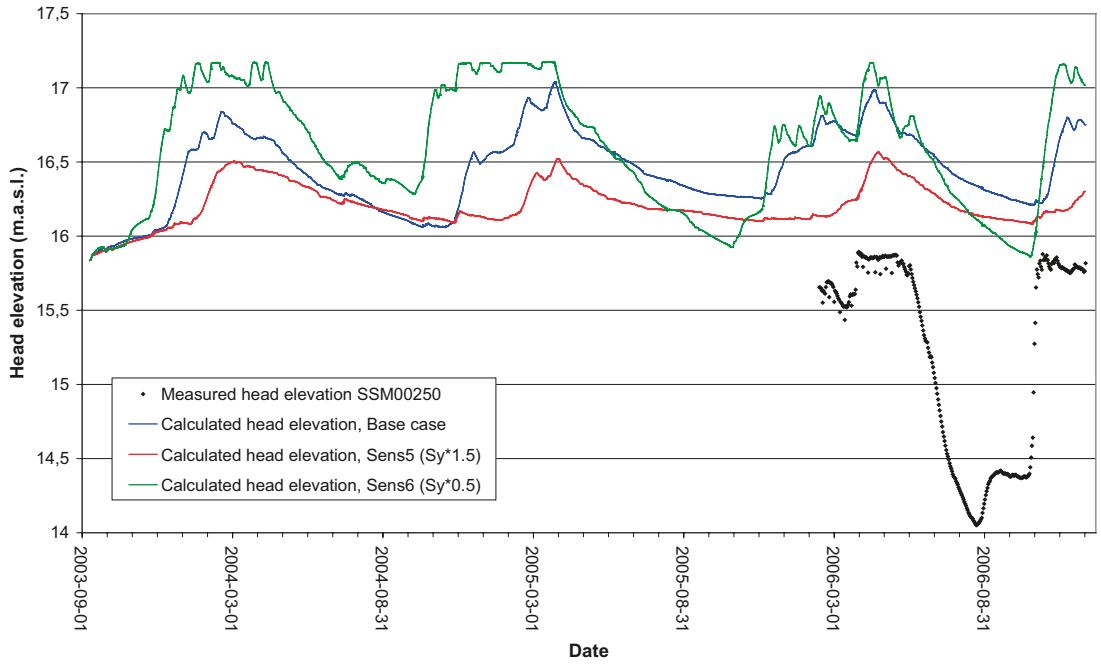

Figure 6-38. *Results for SSM000250 from sensitivity analysis of the unsaturated zone specific yield (S_y).*

Table 6-6 shows a comparison of statistical mean absolute errors for the base case, Sens5 and Sens6. For most monitoring wells, an increased specific yield (Sens5) results in smaller mean absolute errors. However, the differences in mean errors between the sensitivity cases are small. At the same time, many of the monitoring wells show better fits in terms of amplitudes when decreasing the unsaturated zone specific yield (Sens6).

Table 6-6. Comparison of mean absolute errors between base case, Sens5 and Sens6 ("+" represents an improvement, "o" no change and "–" reduced agreement compared to the base case).

Borehole	Mean Absolute Error, Base case	Mean Absolute Error, Sens5 (Sy*1.5)	Mean Absolute Error, Sens6 (Sy*0.5)	Improved agreement with Sens5	Improved agreement with Sens6
SSM000009	0.21	0.67	0.51	–	–
SSM000011	1.17	1.00	1.50	+	–
SSM000017	0.70	0.65	0.81	+	–
SSM000019	1.35	1.32	1.39	+	–
SSM000021	1.63	1.51	1.65	+	–
SSM000030	1.03	0.97	0.96	+	+
SSM000031	0.77	0.75	0.74	–	+
SSM000032	0.23	0.22	0.23	+	o
SSM000033	1.15	1.08	1.17	+	–
SSM000037	2.09	2.02	2.13	+	–
SSM000039	1.62	1.52	1.64	+	–
SSM000041	2.06	2.02	2.06	+	o
SSM000042	0.63	0.61	0.59	+	+
SSM000210	2.35	2.08	2.64	+	–
SSM000213	0.53	0.39	0.65	+	–
SSM000215	1.63	1.63	1.63	o	o
SSM000218	0.77	0.80	0.71	–	+
SSM000219	2.02	1.83	2.16	+	–
SSM000220	1.31	1.26	1.24	+	+
SSM000221	0.51	0.50	0.49	+	+
SSM000222	1.74	1.70	1.75	+	–
SSM000223	1.29	1.27	1.33	+	–
SSM000224	0.72	0.67	0.74	+	–
SSM000225	0.98	0.93	1.01	+	–
SSM000226	1.41	1.08	1.56	+	–
SSM000227	1.54	1.21	1.69	+	–
SSM000228	0.56	0.49	0.58	+	–
SSM000229	0.44	0.51	0.25	–	+
SSM000230	1.57	1.45	1.67	+	–
SSM000237	1.97	1.97	1.97	o	o
SSM000239	0.14	0.14	0.15	o	–
SSM000240	0.16	0.16	0.11	o	+
SSM000242	1.18	1.07	1.19	+	–
SSM000249	0.76	0.71	0.72	+	+
SSM000250	1.34	1.03	1.35	+	–
SSM000252	5.42	5.37	5.20	+	+
SSM000253	1.96	1.87	1.99	+	–
SSM000255	1.66	1.51	1.55	+	+
SSM000256	1.67	1.63	1.67	+	o
SSM000257	1.68	1.66	1.66	+	+
Mean MAE	1.30	1.23	1.33		

Table 6-7 shows the total water balance for the base case compared to Sens5 and Sens6. Most of the parameters show differences between the simulation cases. Parameters with notable changes are evapotranspiration, overland boundary outflow, overland flow to river, subsurface storage changes, subsurface boundary outflow, and base flow to river.

6.2.2 The Averjanov constant "n" for hydraulic conductivity

The empirical constant "n" is used in the Averjanov calculation of the hydraulic conductivity curve /DHI 2007/, and affects the relation between the hydraulic conductivity and the soil water content. The Averjanov equation for the hydraulic conductivity curve is given as:

$$K(\theta) = K_s \left(\frac{\theta - \theta_r}{\theta_s - \theta_r} \right)^n$$

where K_s is the saturated hydraulic conductivity

θ_s is the saturated moisture content

θ_r is the residual moisture content

n is an empirical constant (the Averjanov constant)

An increased n leads to lower conductivities at low soil water contents. Two simulations with changed n were performed. In Sens7, all n-values were increased by a factor of 1.5, whereas in Sens8 all n-values were reduced by a factor of 0.5. Figures 6-39 to 6-42 show how changes in the constant n affect the surface water runoff at the four discharge measurement points. The effects are rather small. At all four stations, the discharge in Sens8 is greater than the discharge for the base case during the early part of the simulation period, then decreases with time to give a very small difference over the whole period.

Figures 6-43 to 6-50 show the effect of changing the coefficient n on the heads in the groundwater monitoring points. The effects on the groundwater head elevations differ between the different wells. Some wells show the same type of pattern as the surface discharge, i.e. during the early part of the simulation the calculated head elevations are higher for Sens8 and then decrease with time. The difference is rather small. However, in most wells, a decreased value of the parameter n (Sens8) gives larger amplitudes, which implies improved fits to the measurements.

Table 6-7. Comparison of total water balances between the base case, Sens5 and Sens6.

Parameter	Base case	Sens5	Sens6
Precipitation	–1,774	–1,774	–1,774
Canopy storage change	0	0	0
Evapotranspiration	1,264	1,320	1,227
Overland storage change	55	52	54
Overland boundary inflow	–52	–55	–55
Overland boundary outflow	84	81	93
Overland to river	225	192	265
Subsurface storage change	43	60	3
Subsurface boundary inflow	14	16	13
Subsurface boundary outflow	83	68	97
Base flow to river	94	81	106
Base flow from river	0	0	0
Error	7	9	4

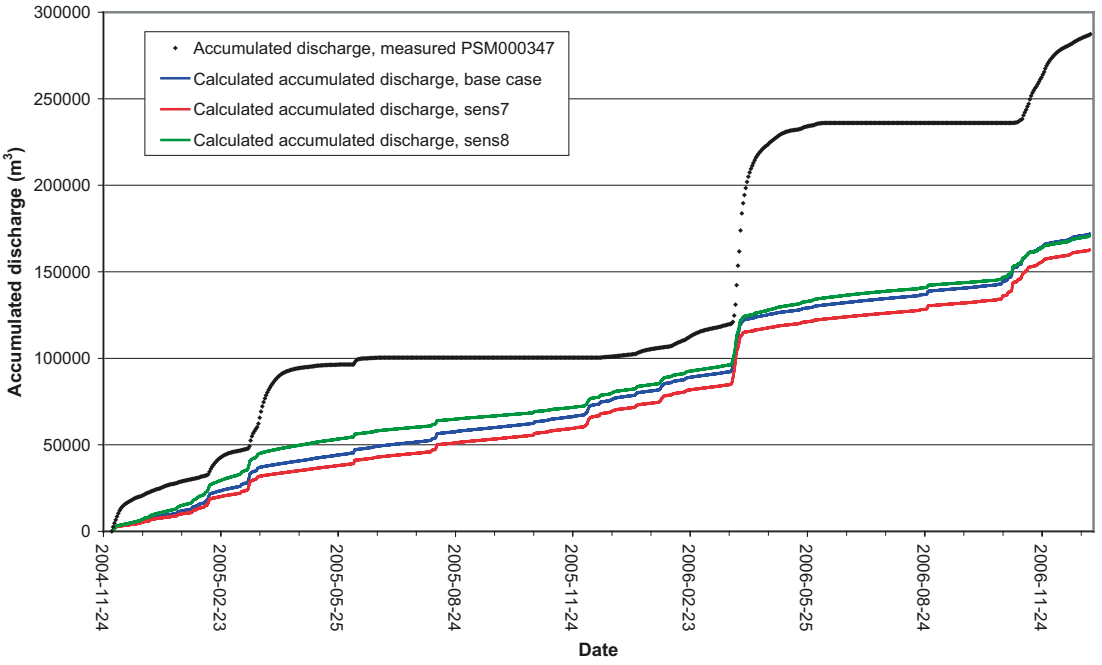

Figure 6-39. *Results for PSM000347 from sensitivity analysis of the empirical Averjanov constant n.*

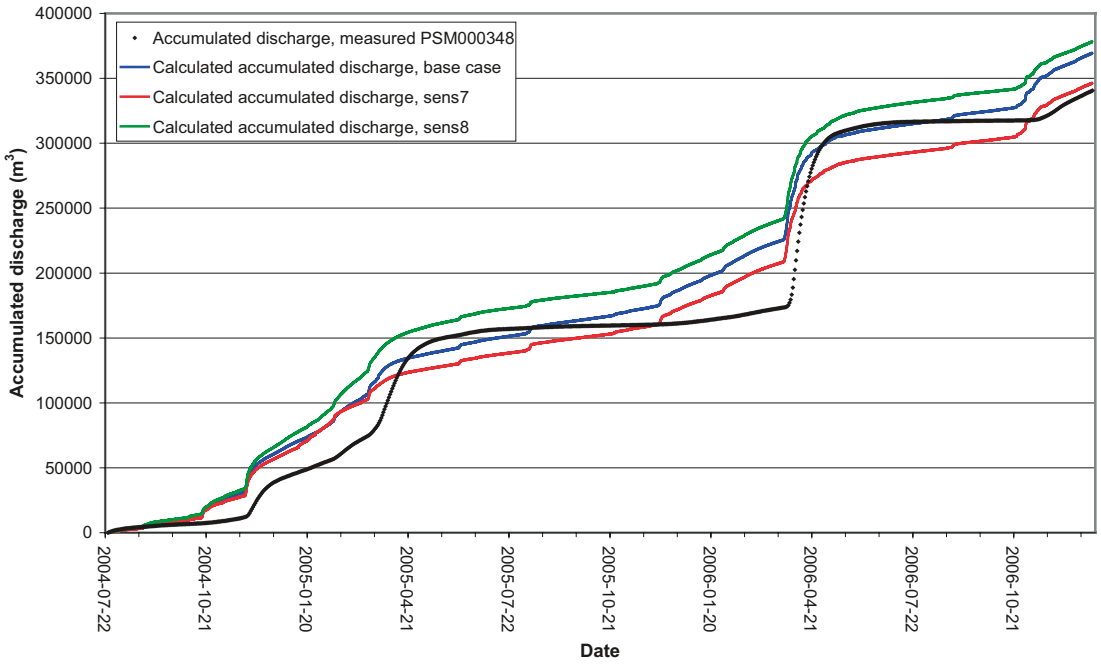

Figure 6-40. *Results for PSM000348 from sensitivity analysis of the empirical Averjanov constant n.*

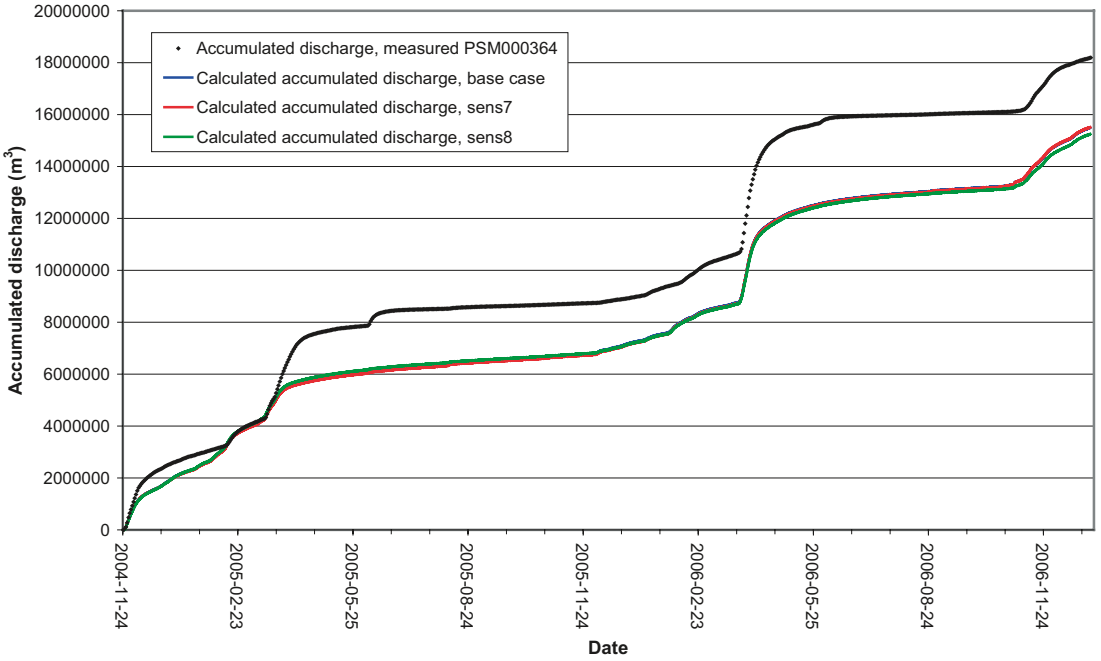

Figure 6-41. *Results for PSM000364 from sensitivity analysis of the empirical Averjanov constant n.*

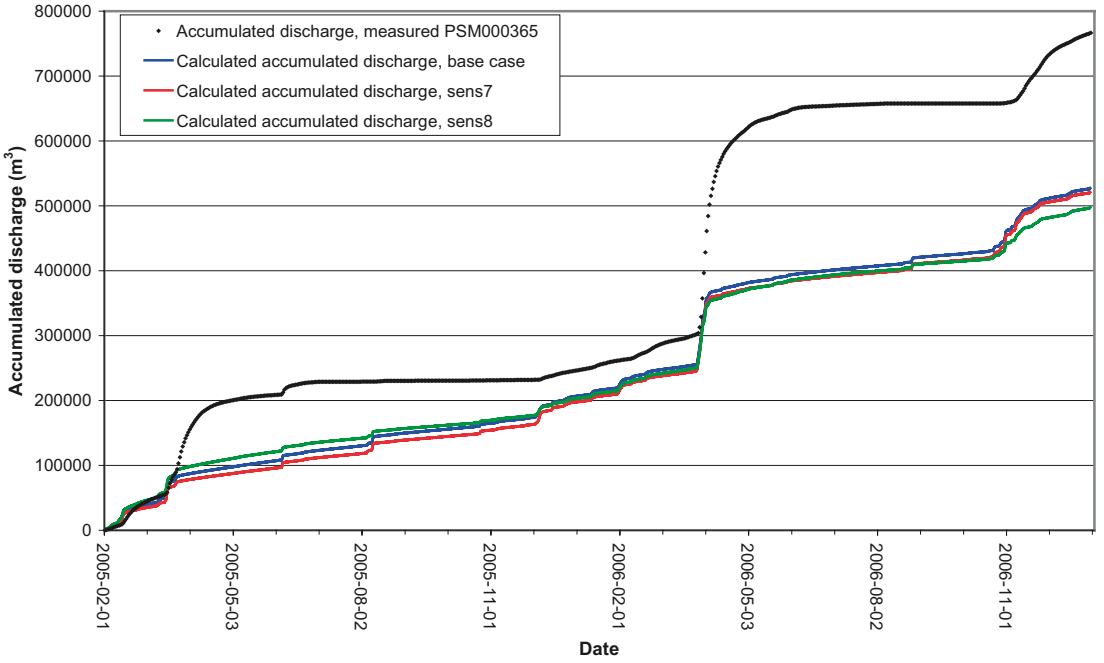

Figure 6-42. *Results for PSM000365 from sensitivity analysis of the empirical Averjanov constant n.*

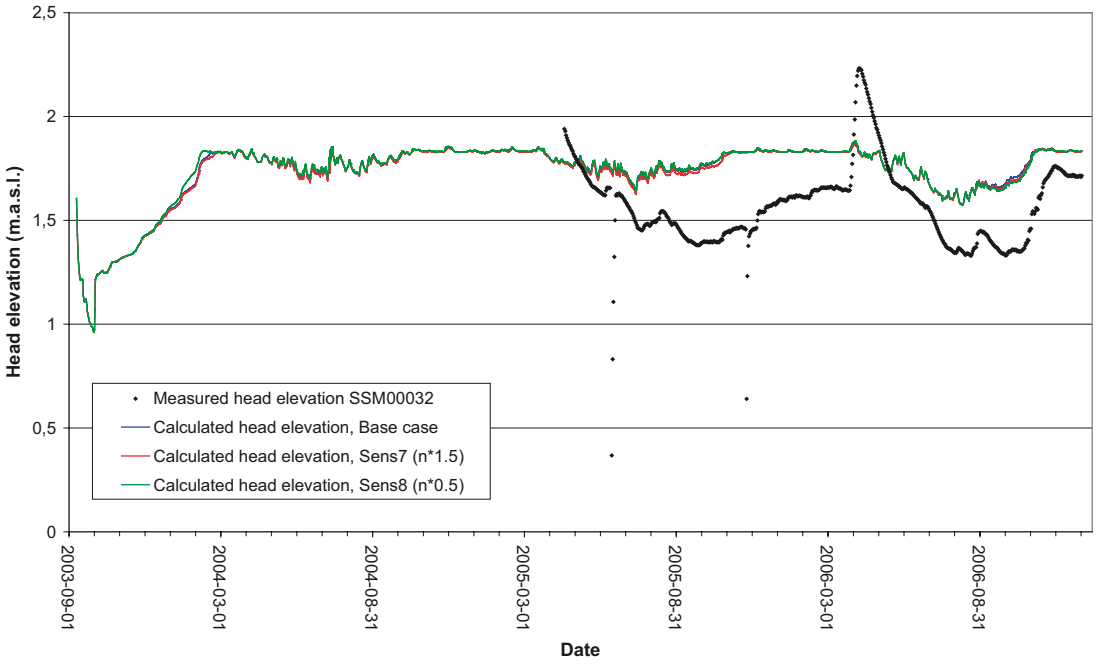

Figure 6-43. *Results for SSM000032 from sensitivity analysis of the empirical Averjanov constant n.*

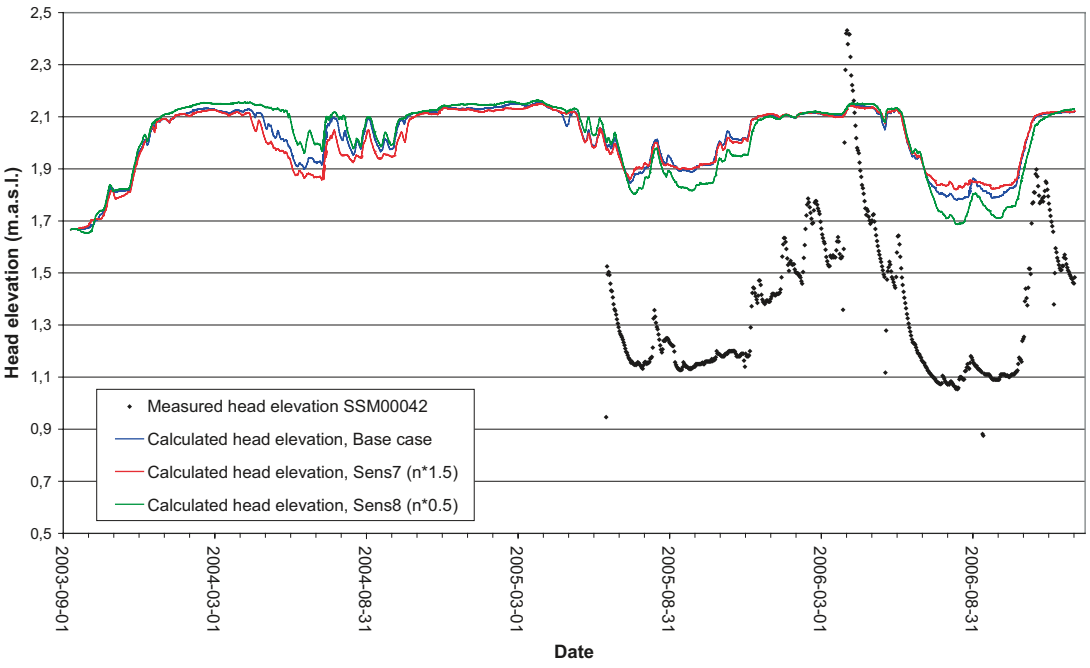

Figure 6-44. *Results for SSM000042 from sensitivity analysis of the empirical Averjanov constant n.*

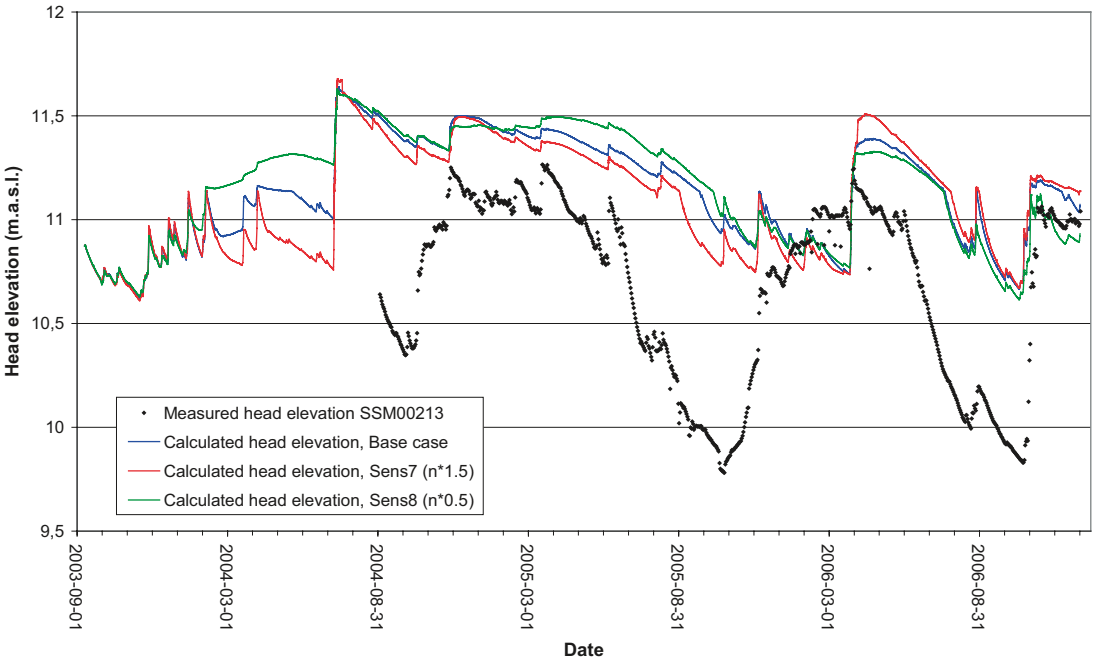

Figure 6-45. *Results for SSM000213 from sensitivity analysis of the empirical Averjanov constant n.*

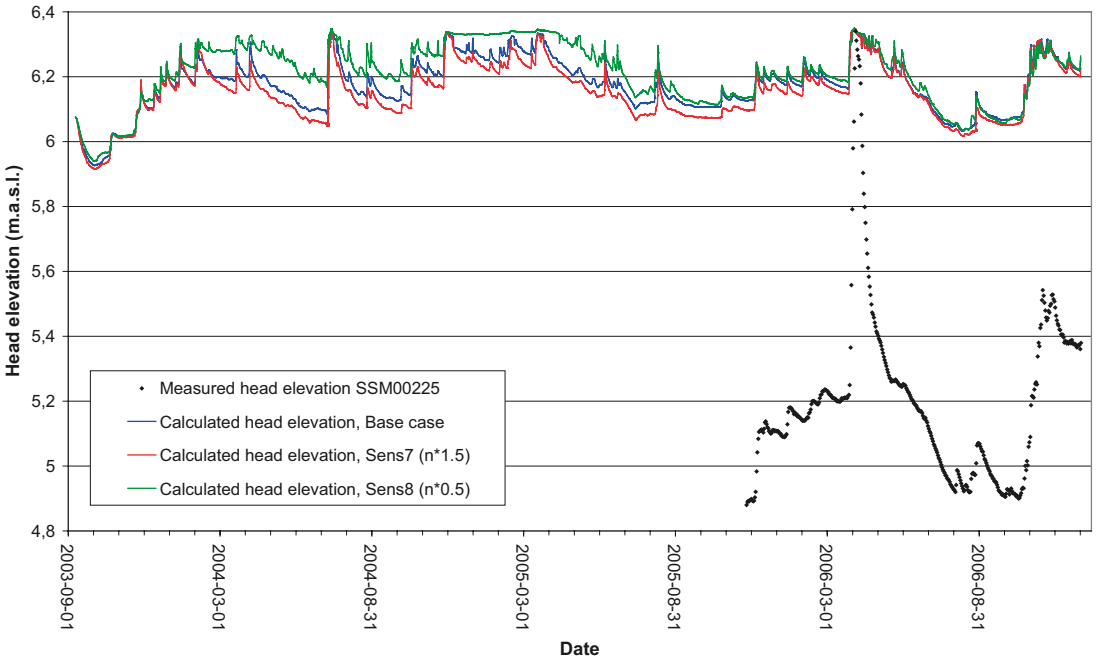

Figure 6-46. *Results for SSM000225 from sensitivity analysis of the empirical Averjanov constant n.*

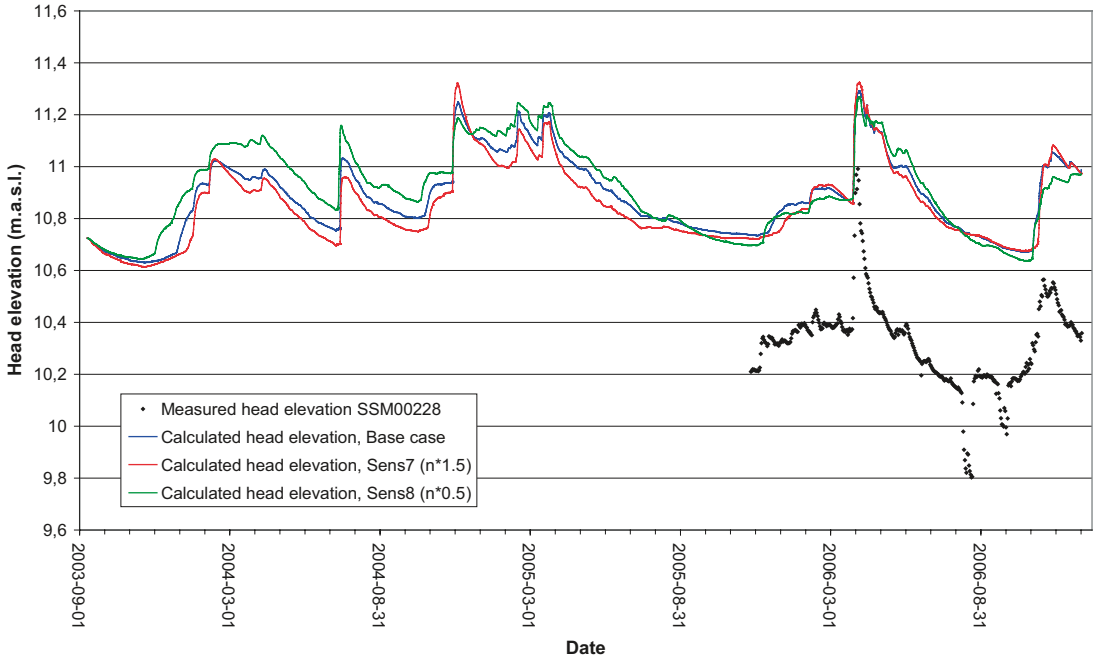

Figure 6-47. *Results for SSM000228 from sensitivity analysis of the empirical Averjanov constant n.*

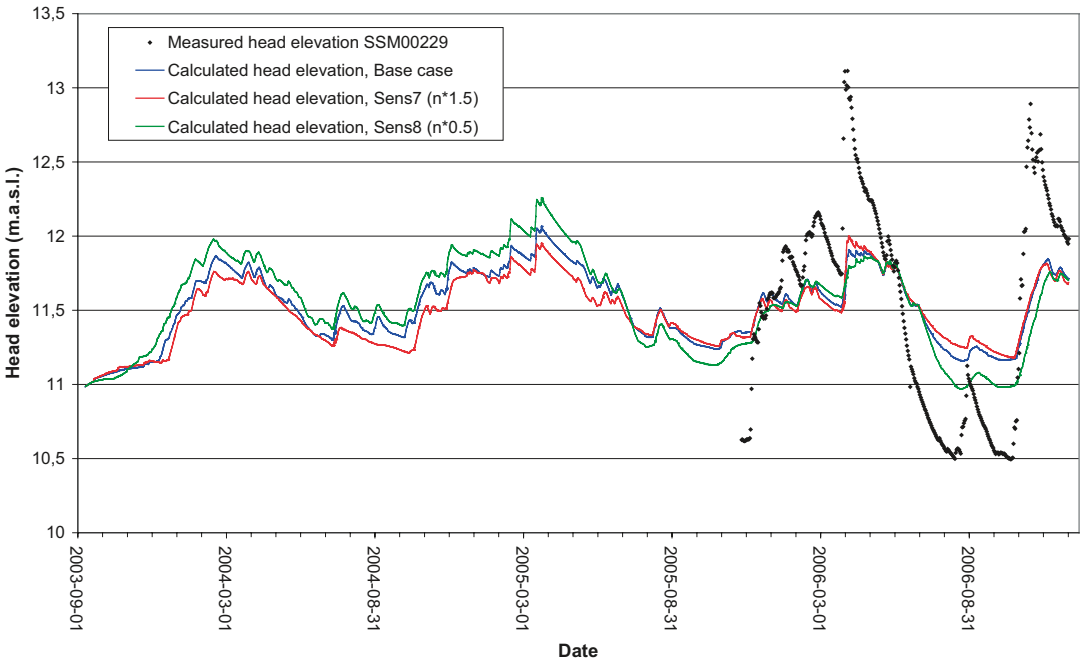

Figure 6-48. *Results for SSM000229 from sensitivity analysis of the empirical Averjanov constant n.*

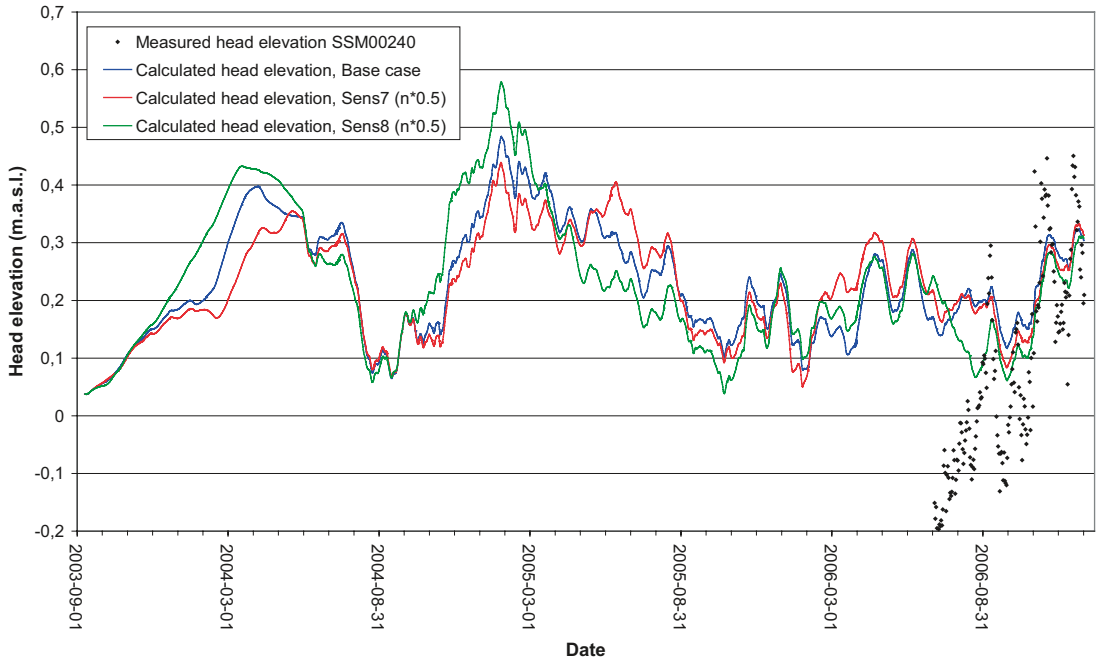

Figure 6-49. *Results for SSM000240 from sensitivity analysis of the empirical Averjanov constant n.*

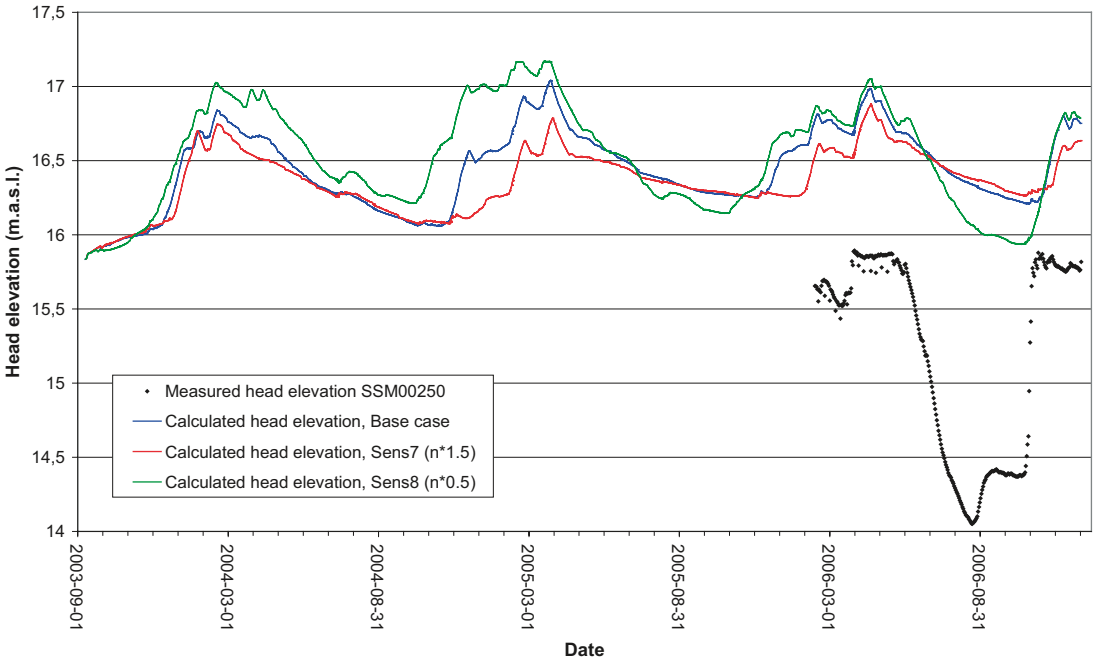

Figure 6-50. *Results for SSM000250 from sensitivity analysis of the empirical Averjanov constant n.*

Table 6-8 shows a comparison of statistical mean absolute errors for the base case, Sens7 and Sens8. Looking at the individual monitoring wells, it is not obvious which sensitivity case (Sens7 or Sens8) that gives the best fit to the measurements. With regard to the mean error for all wells, Sens7 shows an improved agreement in comparison to the base case, while Sens8 does not. However, it should be noted that the difference is rather small.

Table 6-8. Comparison of mean absolute errors between the base case, Sens7 and Sens8 ("+" represents an improvement, "o" no change and "–" a reduced agreement compared to the base case).

Borehole	Mean Absolute Error, Base case	Mean Absolute Error, Sens7 (n*1.5)	Mean Absolute Error, Sens8 (n*0.5)	Improved agreement with Sens7	Improved agreement with Sens8
SSM000009	0.21	0.35	0.71	–	–
SSM000011	1.17	1.16	1.43	+	–
SSM000017	0.70	0.71	0.66	–	+
SSM000019	1.35	1.41	1.37	–	–
SSM000021	1.63	1.57	1.66	+	–
SSM000030	1.03	1.02	0.97	+	+
SSM000031	0.77	0.77	0.75	o	+
SSM000032	0.23	0.22	0.23	+	o
SSM000033	1.15	1.13	1.16	+	–
SSM000037	2.09	2.07	2.09	+	o
SSM000039	1.62	1.57	1.64	+	–
SSM000041	2.06	2.05	2.06	+	o
SSM000042	0.63	0.64	0.60	–	+
SSM000210	2.35	2.19	2.43	+	–
SSM000213	0.53	0.51	0.54	+	–
SSM000215	1.63	1.63	1.63	o	o
SSM000218	0.77	0.84	0.71	–	+
SSM000219	2.02	1.80	2.20	+	–
SSM000220	1.31	1.30	1.29	+	+
SSM000221	0.51	0.51	0.49	o	+
SSM000222	1.74	1.17	1.73	+	+
SSM000223	1.29	1.29	1.28	o	+
SSM000224	0.72	0.70	0.72	+	o
SSM000225	0.98	0.96	0.99	+	–
SSM000226	1.41	1.23	1.45	+	–
SSM000227	1.54	1.36	1.58	+	–
SSM000228	0.56	0.55	0.55	+	+
SSM000229	0.44	0.46	0.41	–	+
SSM000230	1.57	1.51	1.60	+	–
SSM000237	1.97	1.97	1.97	o	o
SSM000239	0.14	0.14	0.15	o	–
SSM000240	0.16	0.15	0.13	+	+
SSM000242	1.18	1.13	1.14	+	+
SSM000249	0.76	0.73	0.72	+	+
SSM000250	1.34	1.29	1.28	+	+
SSM000252	5.42	5.44	5.20	–	+
SSM000253	1.96	1.95	1.95	+	+
SSM000255	1.66	1.65	1.62	+	+
SSM000256	1.67	1.67	1.66	o	+
SSM000257	1.68	1.69	1.64	–	+
Mean MAE	1.30	1.26	1.31		

Table 6-9 shows the total water balance for the base case compared to Sens7 and Sens8. A decreased value of the n parameter (Sens8) gives a larger conductivity at low soil water contents, which, in turn, gives an increased recharge and base flow (and less overland flow) during wet periods and increased evapotranspiration during dry periods.

6.2.3 Hydraulic conductivity in the unsaturated zone

The hydraulic conductivity in the unsaturated zone is active only in the vertical direction, since MIKE SHE has a one-dimensional modelling approach for the unsaturated zone. The hydraulic conductivity directly affects the infiltration capacity of the soil. An increase in the saturated hydraulic conductivity, K_s, allows for more infiltration to the saturated zone. The adopted relation between actual (unsaturated) hydraulic conductivity and saturated hydraulic conductivity is given in Section 6.2.2.

In the sensitivity analysis for Laxemar, all saturated hydraulic conductivities in the unsaturated zone, K_s, were reduced by a factor of 5 (Sens12). Figures 6-51 to 6-54 show the effect of reducing K_s on the surface water discharges. For all four discharge stations, the accumulated discharge is higher for Sens12, i.e. with decreased K_s-values. Since a lower K_s leads to a reduced infiltration, the surface runoff is larger in this case.

Figures 6-55 to 5-62 show the effect of reducing K_s on the heads in the groundwater monitoring wells. Most of them show lower head elevations for the simulations with reduced K_s-values. The lower head elevations are an effect of the smaller amount of water available for infiltration. However, SSM000213, which is situated in a slope close to Lake Frisksjön, shows the opposite pattern, with higher head elevations for the lower K_s-values.

Table 6-9. Comparison of total water balances between the base case, Sens7 and Sens8.

Parameter	Base case	Sens7	Sens8
Precipitation	–1,774	–1,774	–1,774
Canopy storage change	0	0	0
Evapotranspiration	1,264	1,265	1,303
Overland storage change	55	54	52
Overland boundary inflow	–52	–53	–50
Overland boundary outflow	84	85	79
Overland to river	225	228	209
Subsurface storage change	43	53	11
Subsurface boundary inflow	14	15	13
Subsurface boundary outflow	83	74	93
Base flow to river	94	89	100
Base flow from river	0	0	0
Error	7	6	10

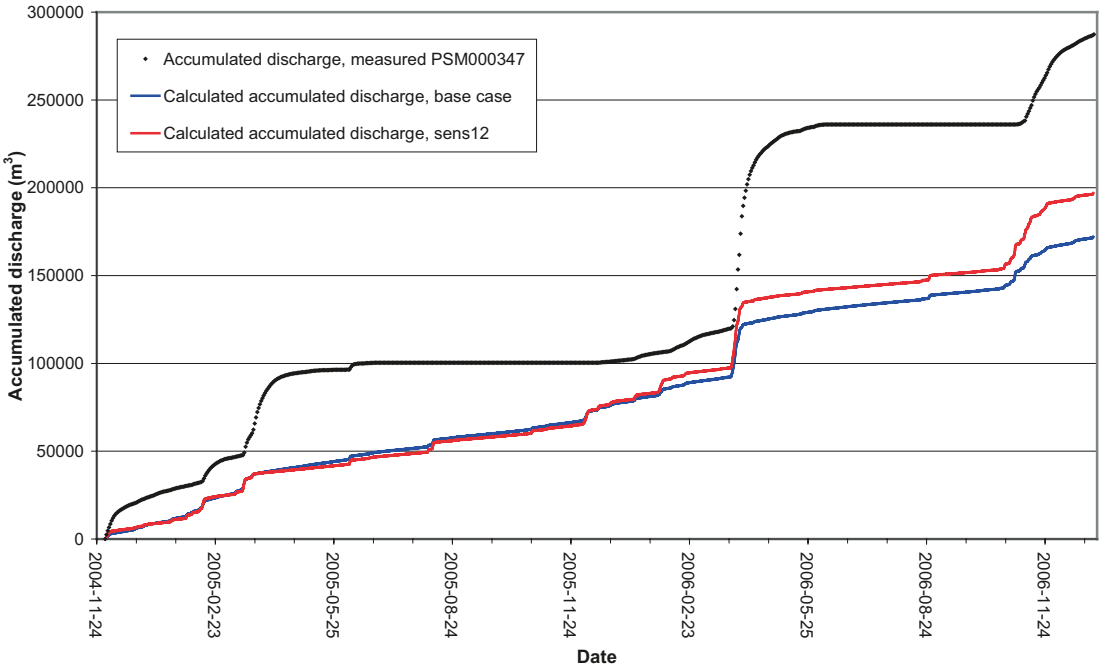

Figure 6-51. *Results for PSM000347 from sensitivity analysis of the hydraulic conductivity in the unsaturated zone.*

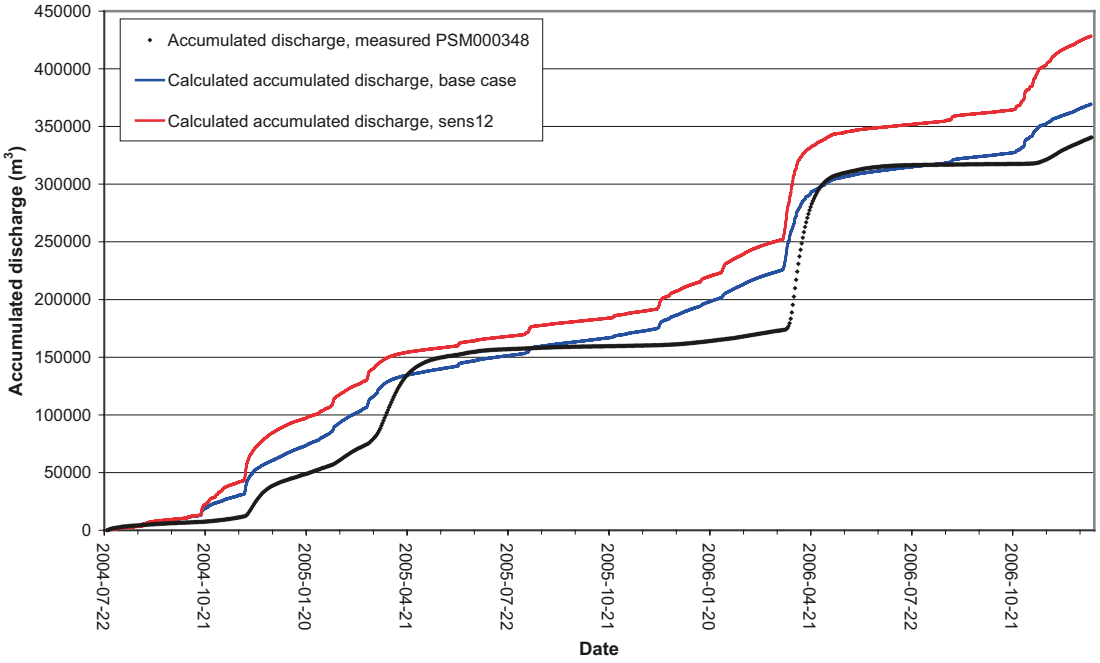

Figure 6-52. *Results for PSM000348 from sensitivity analysis of the hydraulic conductivity in the unsaturated zone.*

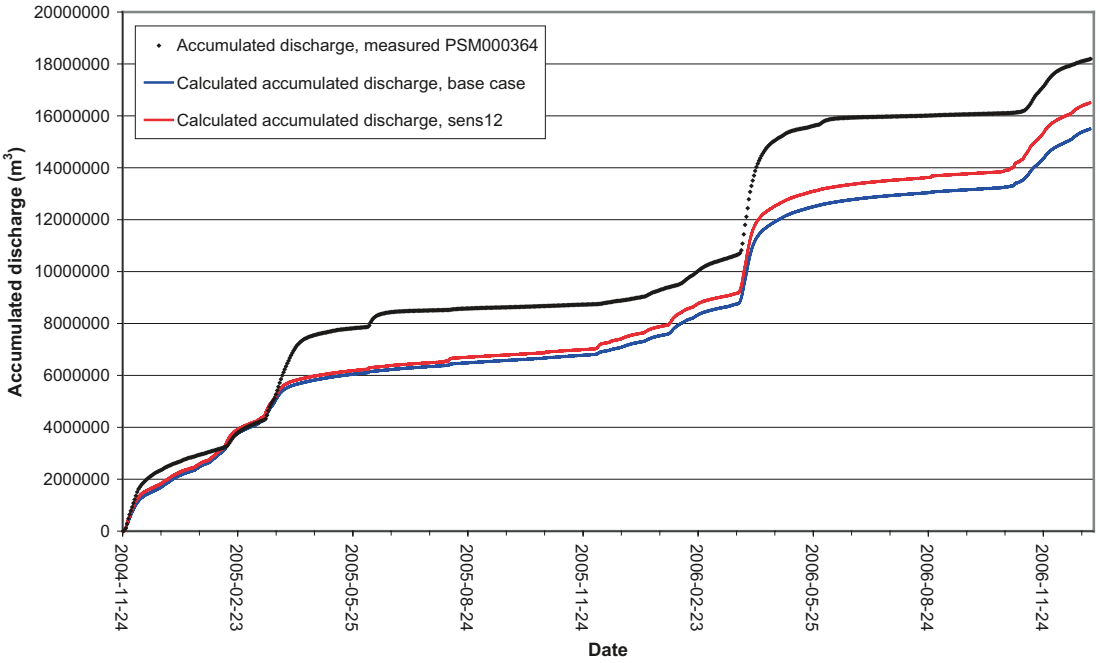

Figure 6-53. *Results for PSM000364 from sensitivity analysis of the hydraulic conductivity in the unsaturated zone.*

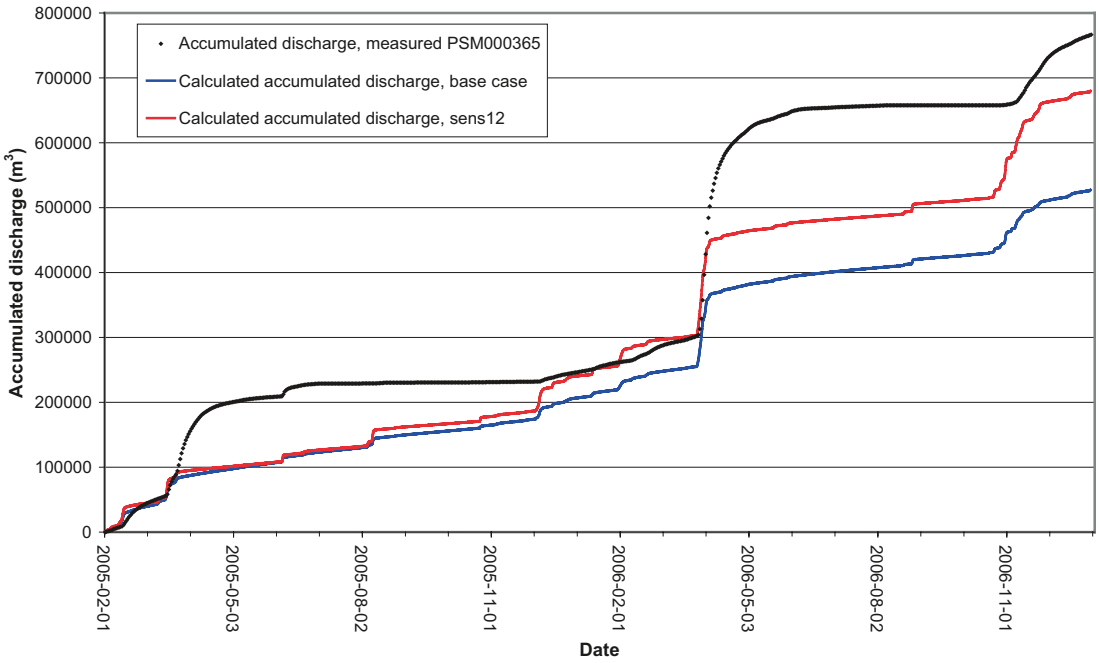

Figure 6-54. *Results for PSM000365 from sensitivity analysis of the hydraulic conductivity in the unsaturated zone.*

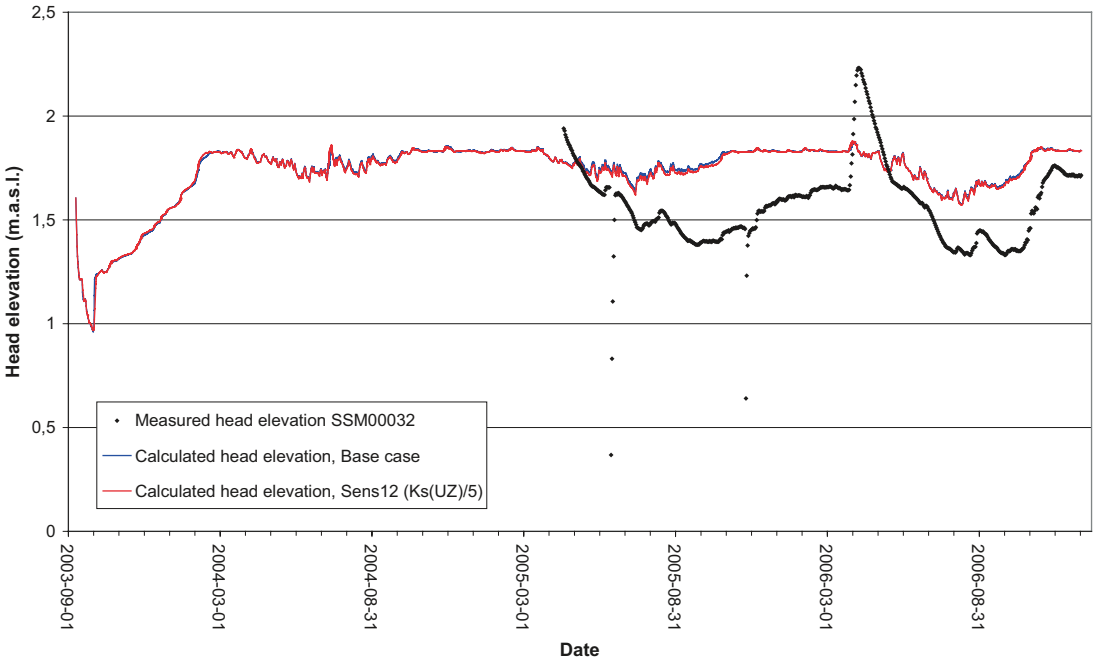

Figure 6-55. *Results for SSM000032 from sensitivity analysis of the hydraulic conductivity in the unsaturated zone.*

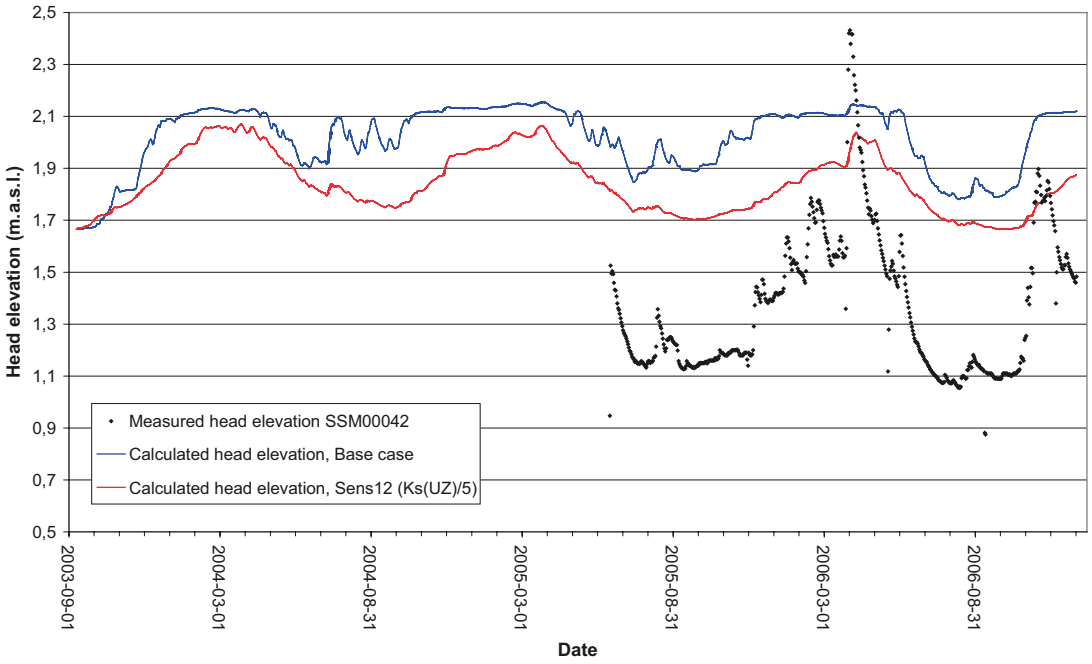

Figure 6-56. *Results for SSM000042 from sensitivity analysis of the hydraulic conductivity in the unsaturated zone.*

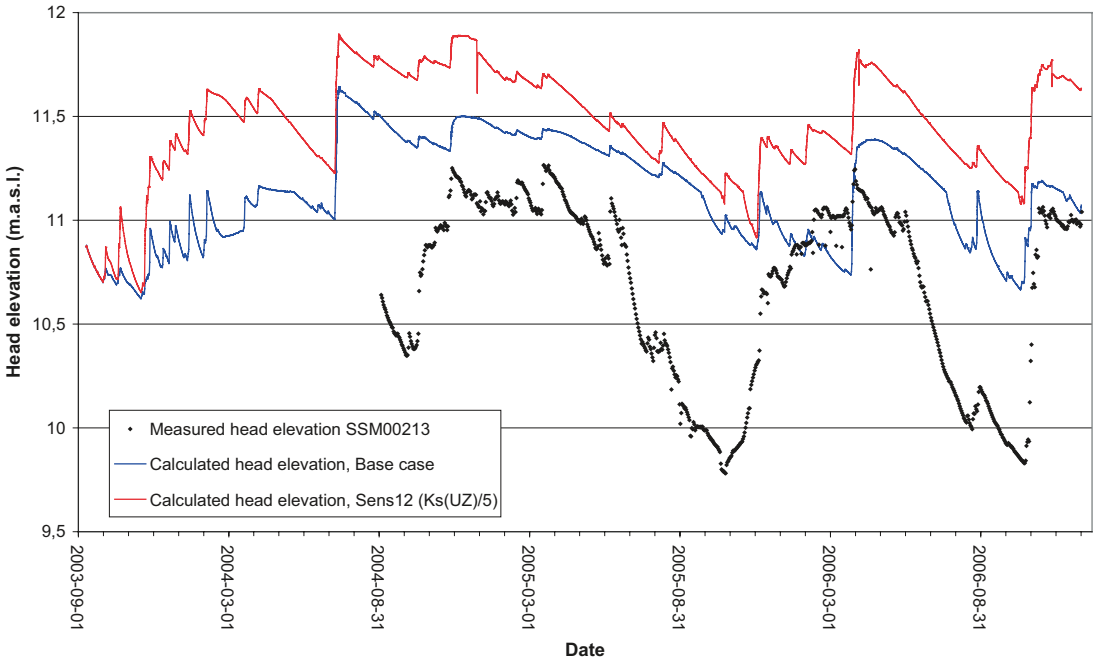

Figure 6-57. *Results for SSM000213 from sensitivity analysis of the hydraulic conductivity in the unsaturated zone.*

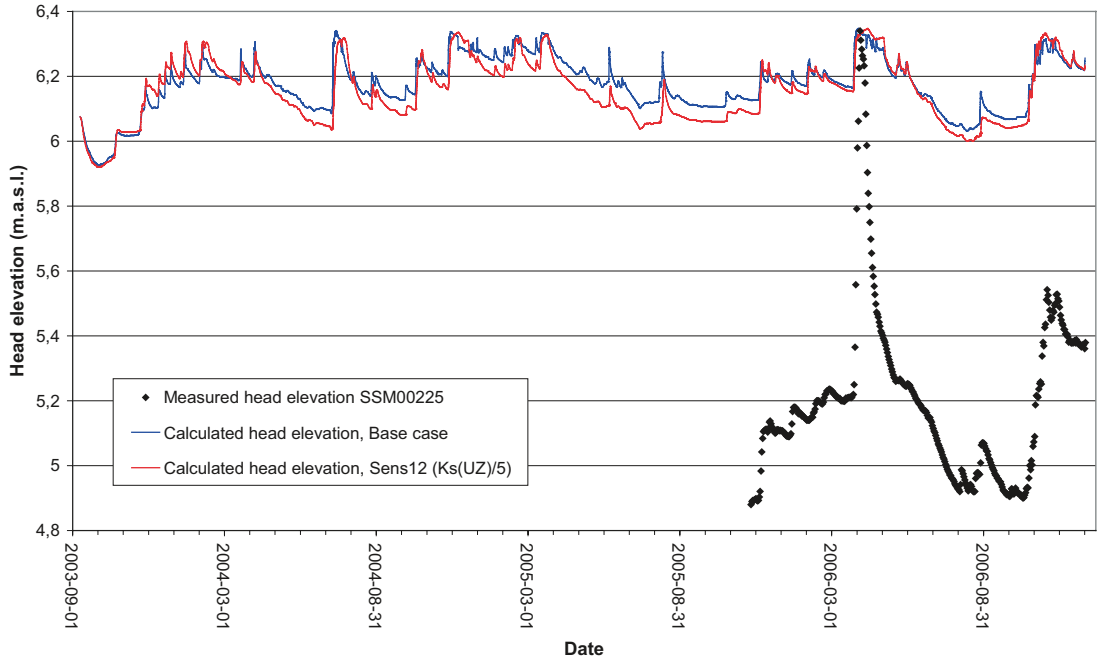

Figure 6-58. *Results for SSM000225 from sensitivity analysis of the hydraulic conductivity in the unsaturated zone.*

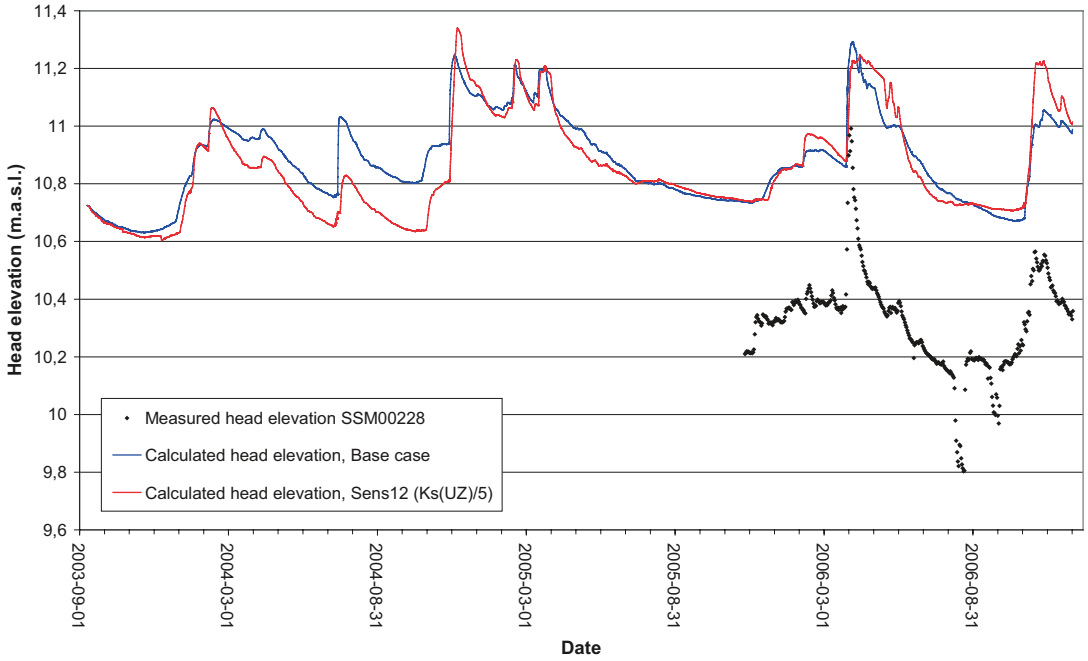

Figure 6-59. *Results for SSM000228 from sensitivity analysis of the hydraulic conductivity in the unsaturated zone.*

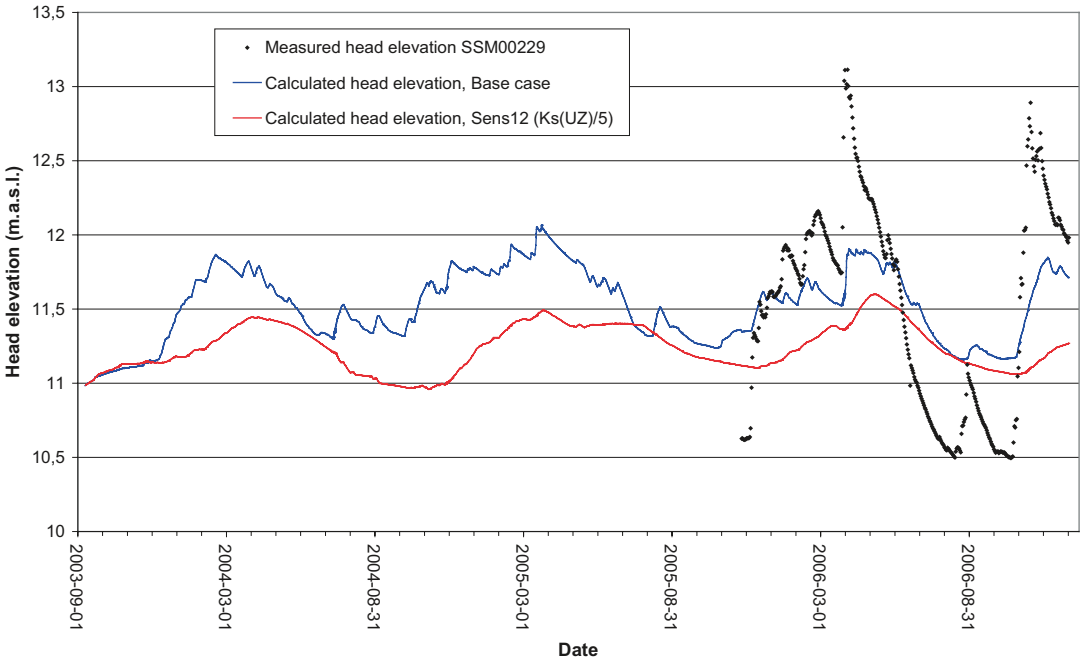

Figure 6-60. *Results for SSM000229 from sensitivity analysis of the hydraulic conductivity in the unsaturated zone.*

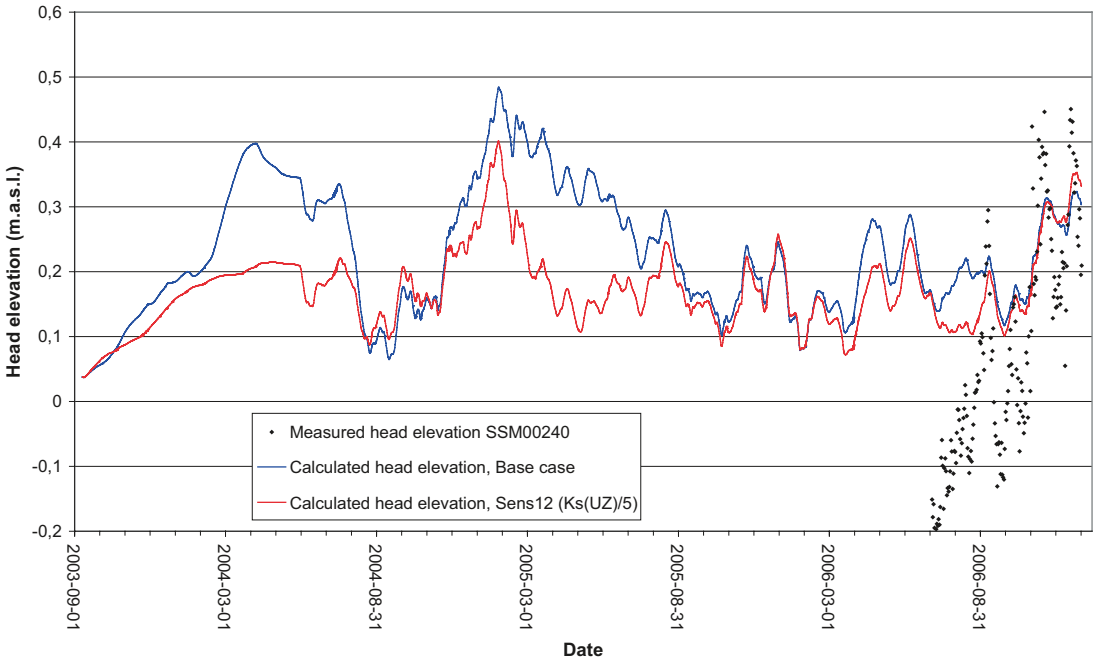

Figure 6-61. *Results for SSM000240 from sensitivity analysis of the hydraulic conductivity in the unsaturated zone.*

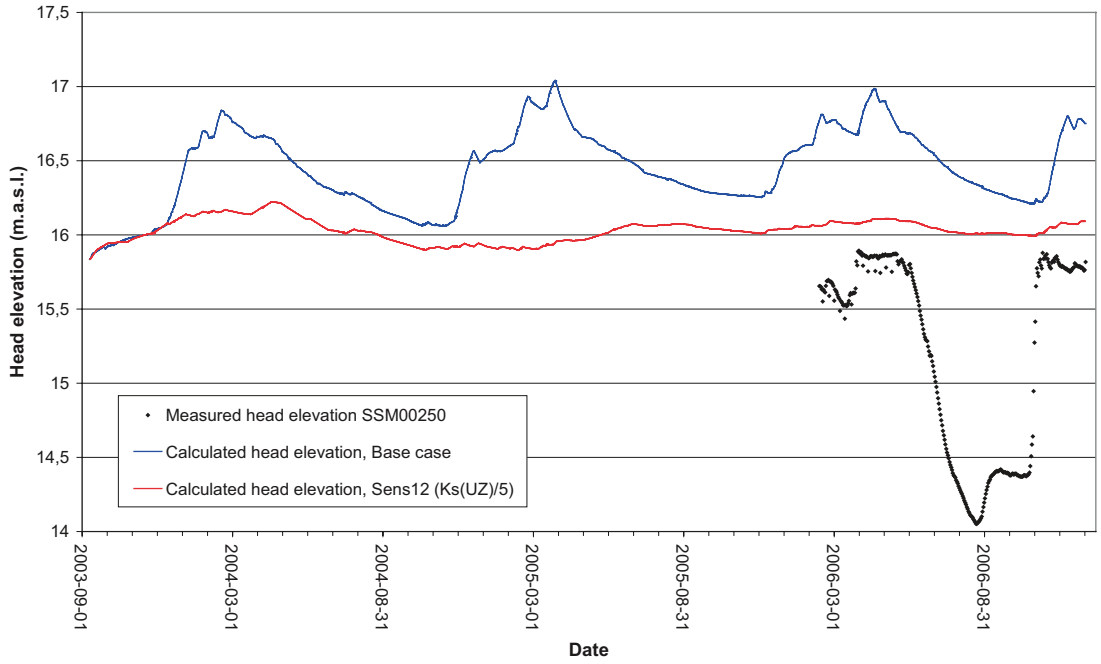

Figure 6-62. *Results for SSM000250 from sensitivity analysis of the hydraulic conductivity in the unsaturated zone.*

Table 6-10 shows a comparison of mean absolute errors for the base case and Sens12. Most of the wells show an improved agreement, although for most wells the effects are small.

Table 6-10. Comparison of mean absolute errors between the base case and Sens12 ("+" represents an improvement, "o" no change and "–" reduced agreement compared to the base case).

Borehole	Mean Absolute Error, Base case	Mean Absolute Error Sens12 (K_s / 5)	Improved agreement with Sens12
SSM000009	0.21	0.89	–
SSM000011	1.17	1.24	–
SSM000017	0.70	0.65	+
SSM000019	1.35	1.33	+
SSM000021	1.63	1.42	+
SSM000030	1.03	0.89	+
SSM000031	0.77	0.63	+
SSM000032	0.23	0.22	+
SSM000033	1.15	1.15	o
SSM000037	2.09	1.98	+
SSM000039	1.62	1.49	+
SSM000041	2.06	1.88	+
SSM000042	0.63	0.44	+
SSM000210	2.35	2.19	+
SSM000213	0.53	0.82	–
SSM000215	1.63	1.62	+
SSM000218	0.77	0.90	–
SSM000219	2.02	1.65	+
SSM000220	1.31	1.23	+
SSM000221	0.51	0.51	o
SSM000222	1.74	1.63	+
SSM000223	1.29	2.00	–
SSM000224	0.72	0.68	+
SSM000225	0.98	0.97	+
SSM000226	1.41	1.24	+
SSM000227	1.54	1.36	+
SSM000228	0.56	0.58	–
SSM000229	0.44	0.62	–
SSM000230	1.57	1.39	+
SSM000237	1.97	1.97	o
SSM000239	0.14	0.13	+
SSM000240	0.16	0.13	+
SSM000242	1.18	1.10	+
SSM000249	0.76	0.74	+
SSM000250	1.34	0.84	+
SSM000252	5.42	5.46	–
SSM000253	1.96	1.89	+
SSM000255	1.66	1.54	+
SSM000256	1.67	1.66	+
SSM000257	1.68	1.67	+
Mean MAE	1.30	1.27	

Table 6-11 shows the total water balance for the base case compared to that for Sens12. The results show differences for several water balance components. The largest difference is in the overland flow to the water courses ("river" in Table 6-11) component. The increase in Sens12 compared to the base case is about 50%. The saturated hydraulic conductivities used in the calculations of unsaturated zone conductivities are apparently important for a correct description of the surface runoff dynamics.

6.3 Hydraulic conductivities of Quaternary deposits and upper bedrock

In the sensitivity analysis of the saturated zone hydraulic parameters, only the conductivities were varied. The changes were made in the same way for both the horizontal and vertical conductivity, at the same time in one simulation. These parameters were varied for all the geological Quaternary deposit layers, as well as for the two top bedrock layers. In the sensitivity simulation case Sens9, both the horizontal and vertical hydraulic conductivities were increased by a factor of 5. In simulation case Sens10, the horizontal and vertical hydraulic conductivities were decreased by a factor 5.

Figures 6-63 to 6-66 show the accumulated surface discharges for the base case, Sens9 and Sens10. Sens9, with the increased hydraulic conductivities, increases the accumulated river discharge, and vice versa when decreasing the hydraulic conductivities (Sens10). Conversely, a decrease in the hydraulic conductivities increases the surface runoff and the peak discharges in the water courses (e.g. the peak in March 2006). At the same time, the base flow in the water courses decreases (e.g. during May–November 2005). Thus, both changes give a better match between simulated and observed discharges; they improve the agreement between measured and calculated discharges in different ways.

Figures 6-67 to 6-74 show a comparison between measured and calculated head elevations from the base case and the sensitivity cases Sens9 and Sens10. The increased conductivity case (Sens9) results for most monitoring wells in a lower groundwater table, whereas the decreased conductivity case (Sens10) results in a higher groundwater table. However, in SSM000032, which is located in a local depression, the result is the opposite. At the same time, a decreased conductivity (Sens10) increases the head amplitudes in many of the wells. The picture is somewhat scattered, since different wells give different responses to the parameter variations. Thus, it is hard to find a consistent pattern in the results when comparing modelled and observed head elevations. The reason for this could be that the inflows from the boundaries and/or the recharge are too large.

Table 6-11. Comparison of total water balances between the base case and Sens12.

Parameter	Base case	Sens12
Precipitation	–1,774	–1,774
Canopy storage change	0	0
Evapotranspiration	1,264	1,225
Overland storage change	55	51
Overland boundary inflow	–52	–55
Overland boundary outflow	84	100
Overland to river	225	344
Subsurface storage change	43	5
Subsurface boundary inflow	14	18
Subsurface boundary outflow	83	63
Base flow to river	94	73
Base flow from river	0	0
Error	7	14

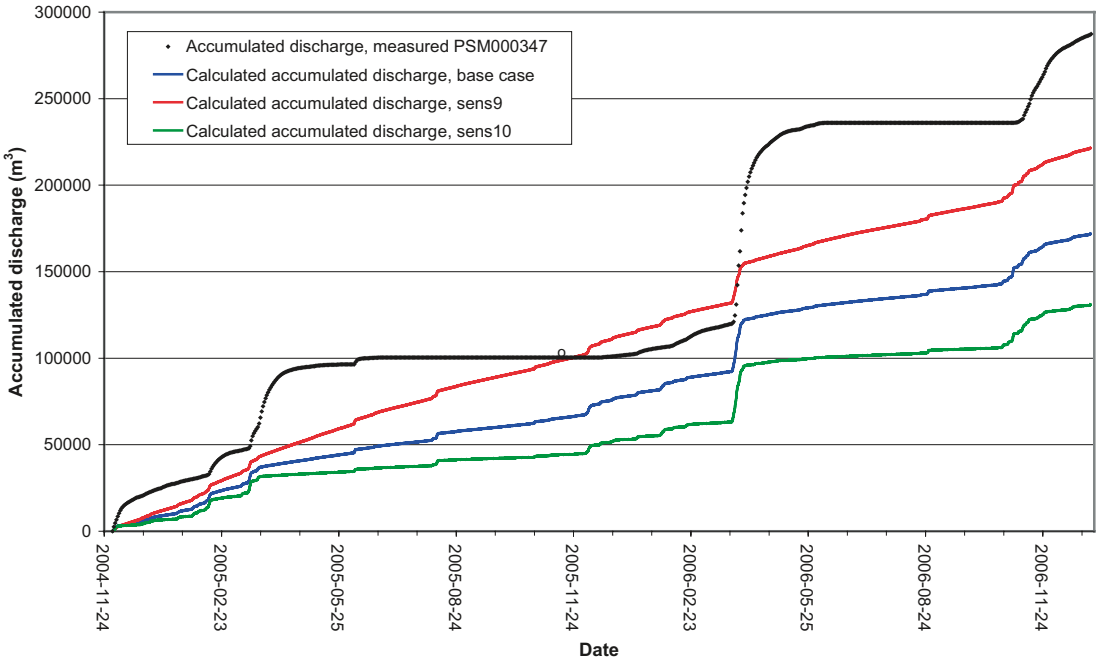

Figure 6-63. *Results for PSM000347 from sensitivity analysis of the hydraulic conductivities in the saturated zone.*

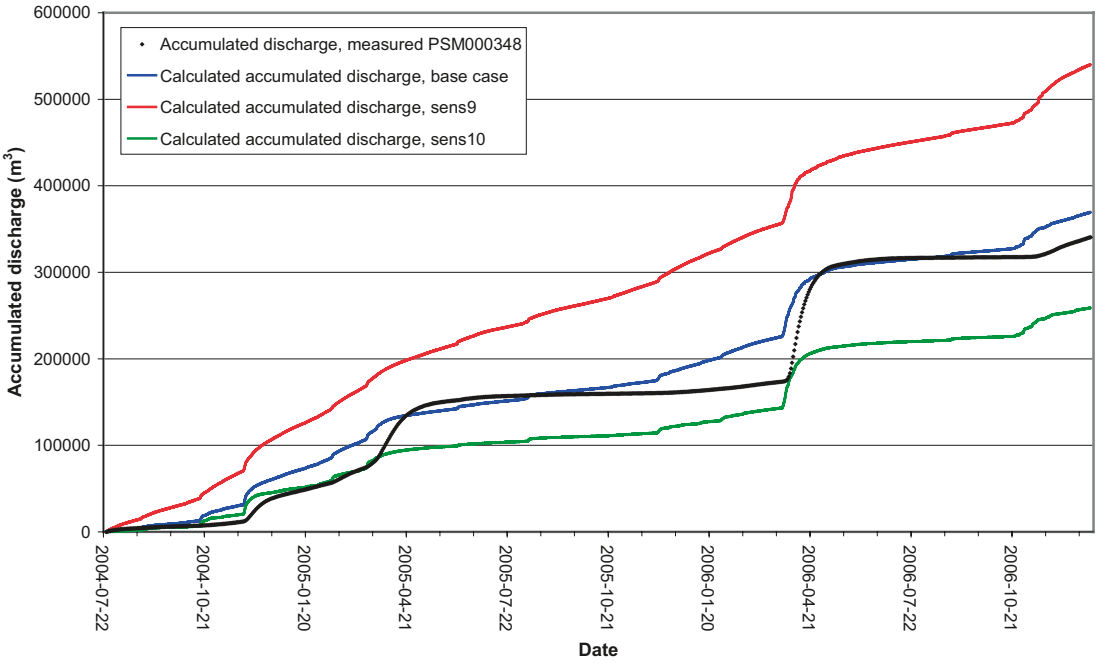

Figure 6-64. *Results for PSM000348 from sensitivity analysis of the hydraulic conductivities in the saturated zone.*

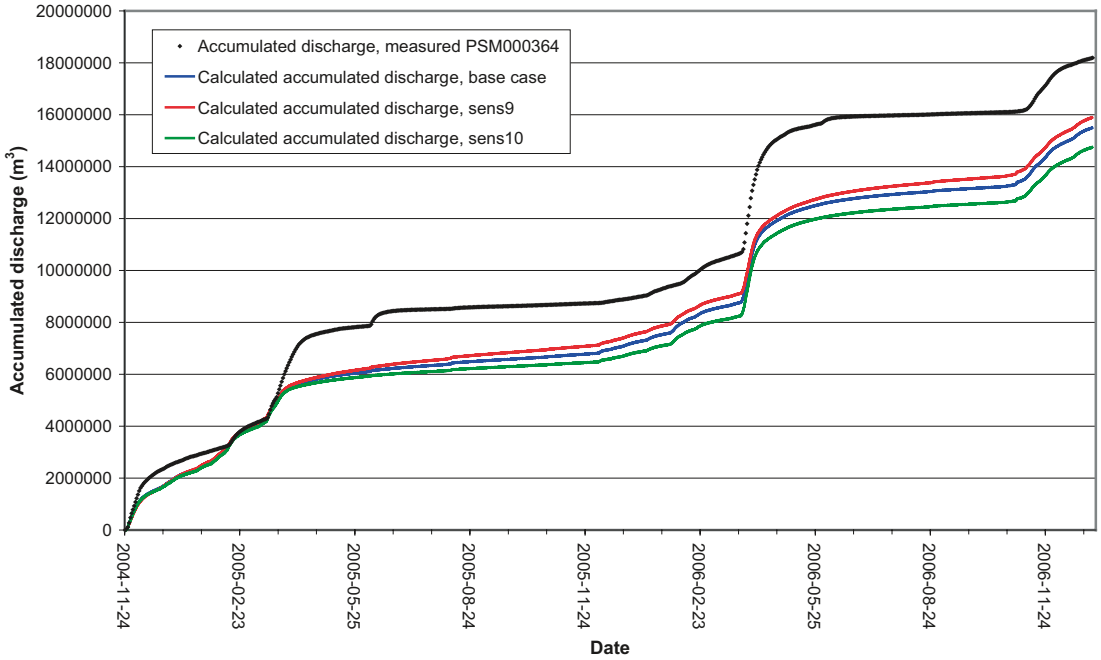

Figure 6-65. *Results for PSM000364 from sensitivity analysis of the hydraulic conductivities in the saturated zone.*

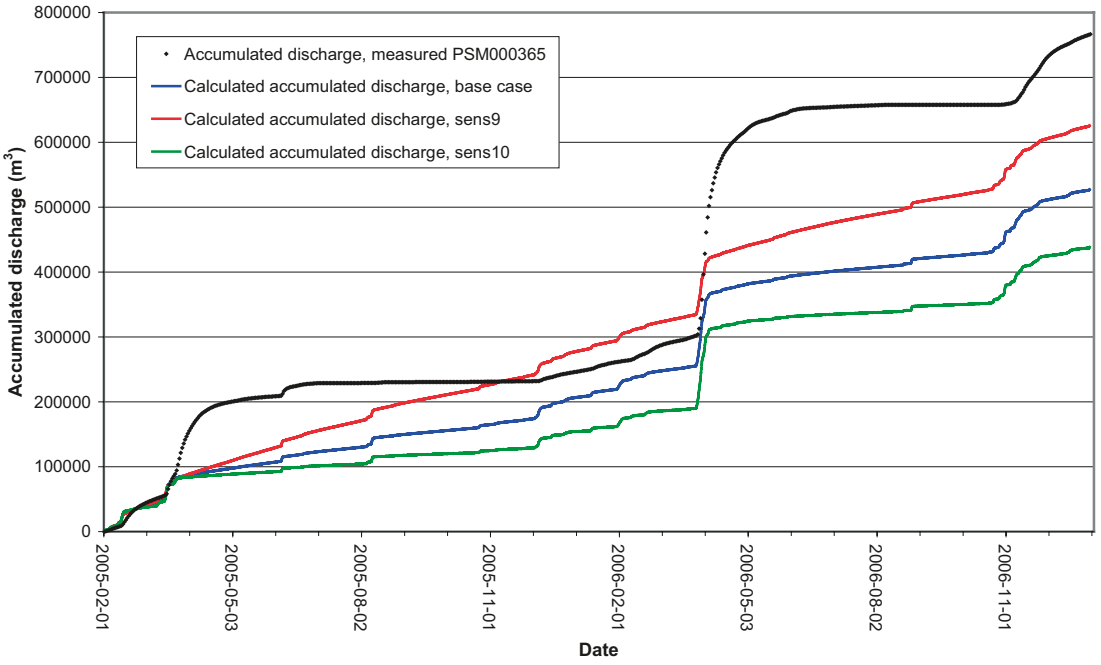

Figure 6-66. *Results for PSM000365 from sensitivity analysis of the hydraulic conductivities in the saturated zone.*

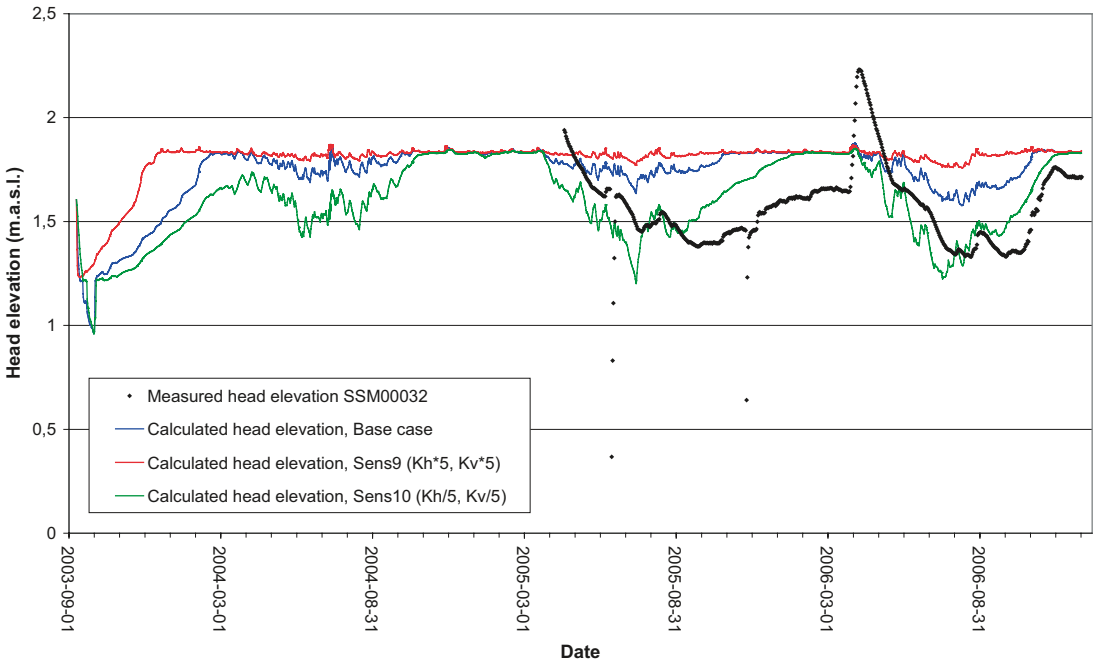

Figure 6-67. *Results for SSM000032 from sensitivity analysis of the hydraulic conductivities in the saturated zone.*

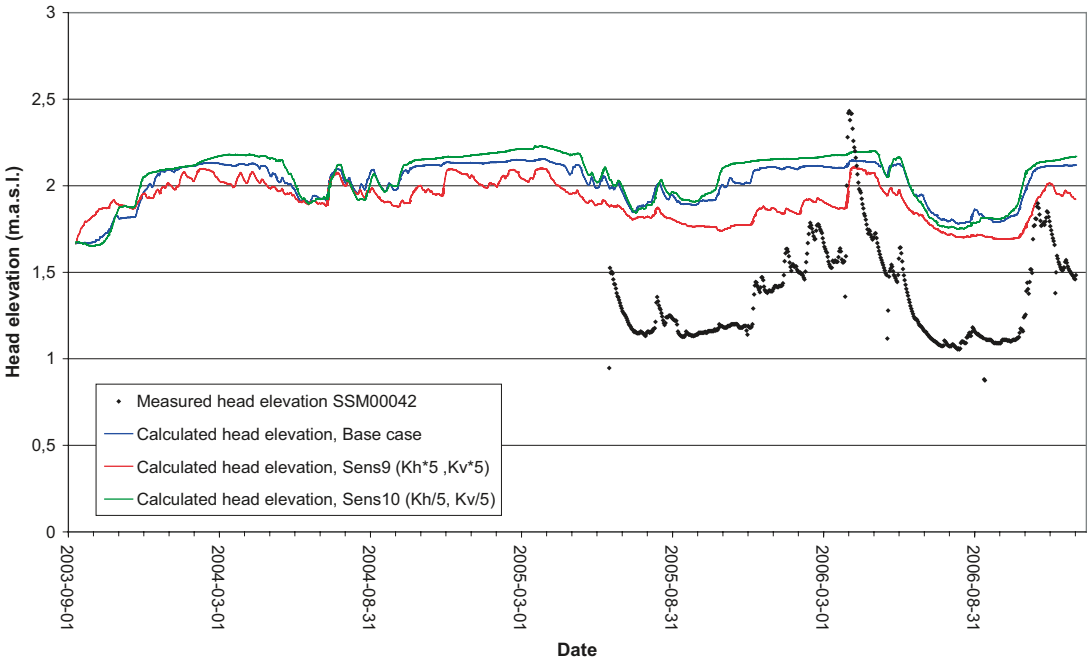

Figure 6-68. *Results for SSM000042 from sensitivity analysis of the hydraulic conductivities in the saturated zone.*

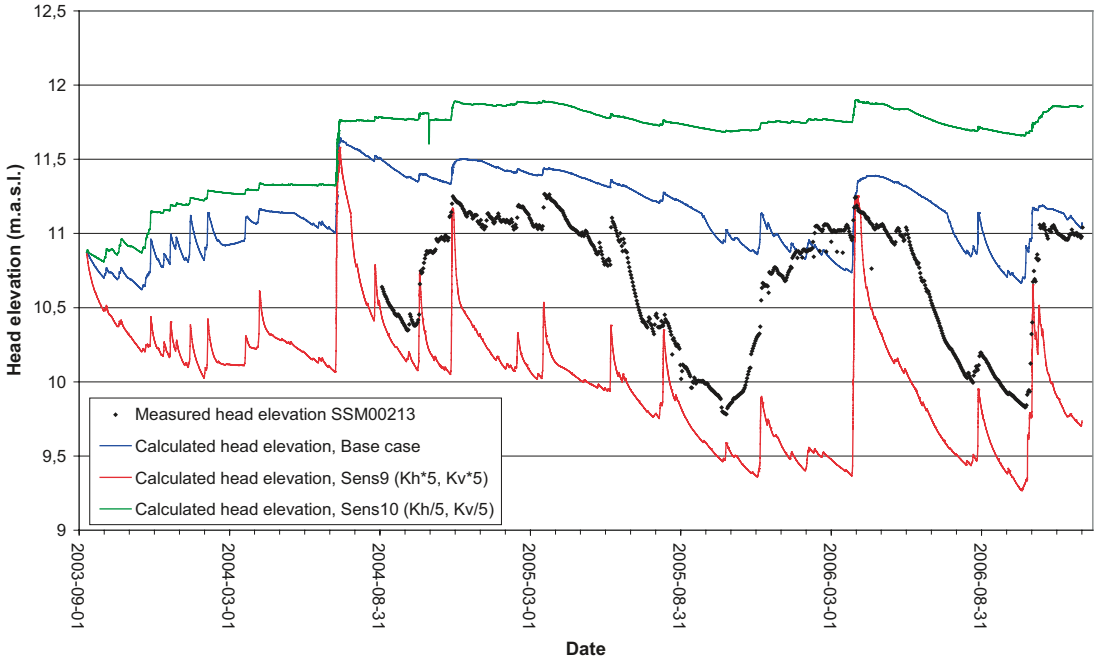

Figure 6-69. *Results for SSM000213 from sensitivity analysis of the hydraulic conductivities in the saturated zone.*

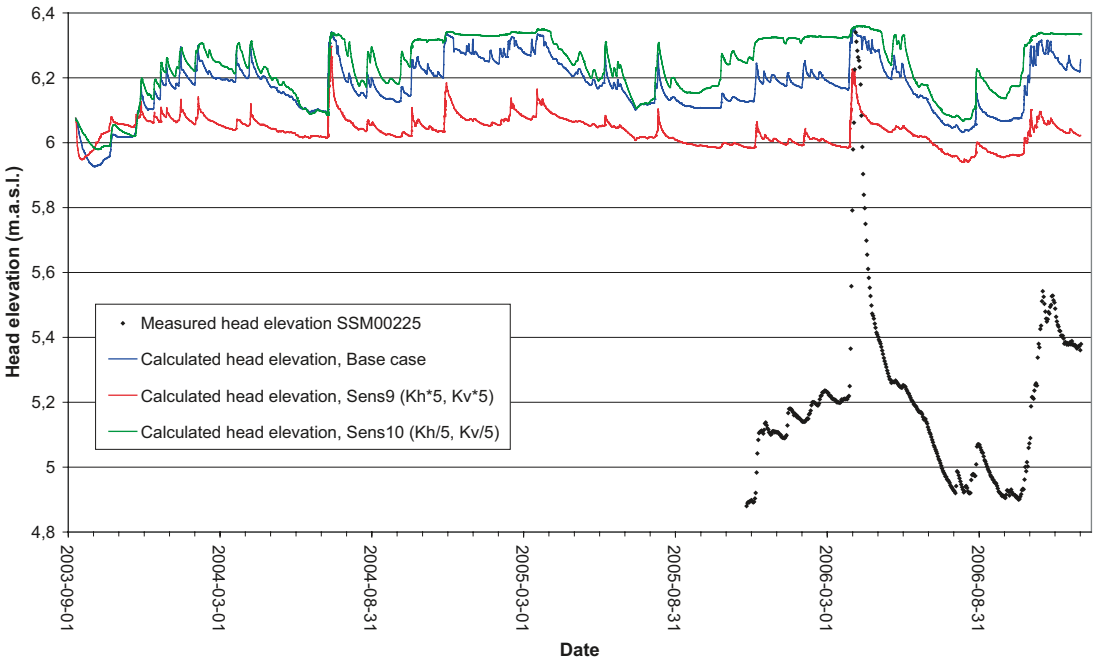

Figure 6-70. *Results for SSM000225 from sensitivity analysis of the hydraulic conductivities in the saturated zone.*

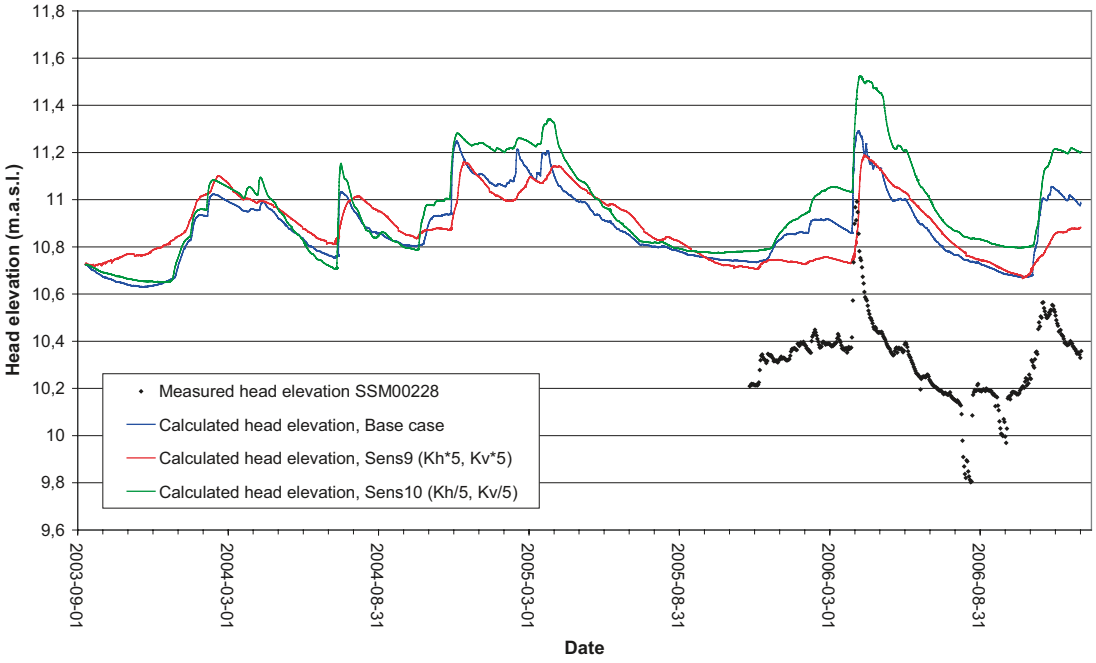

Figure 6-71. *Results for SSM000228 from sensitivity analysis of the hydraulic conductivities in the saturated zone.*

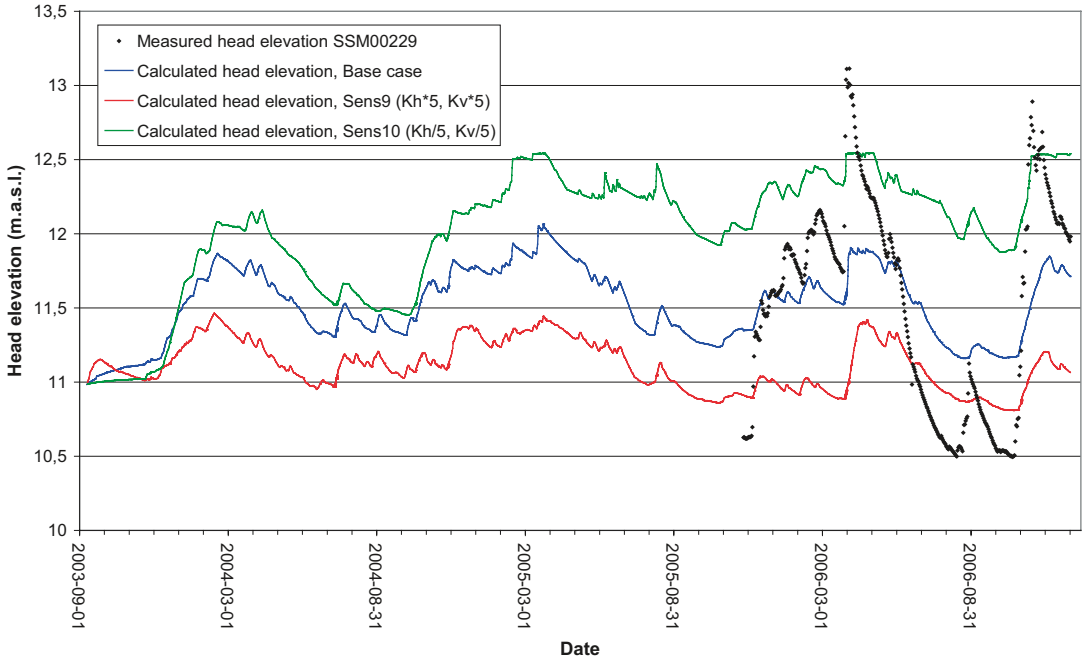

Figure 6-72. *Results for SSM000229 from sensitivity analysis of the hydraulic conductivities in the saturated zone.*

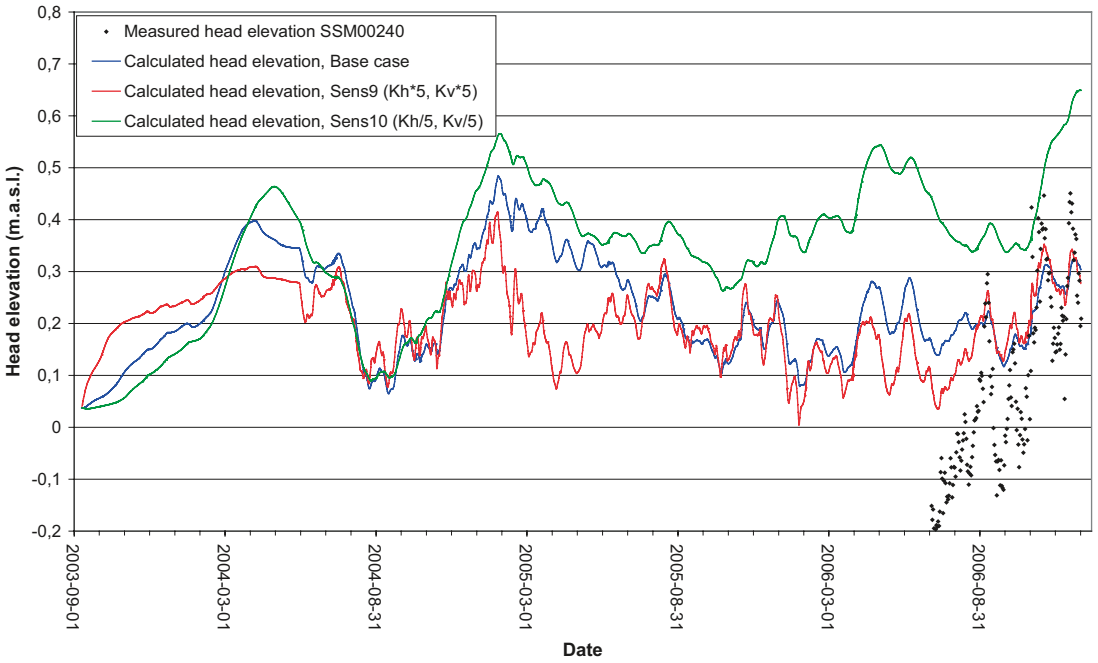

Figure 6-73. *Results for SSM000240 from sensitivity analysis of the hydraulic conductivities in the saturated zone.*

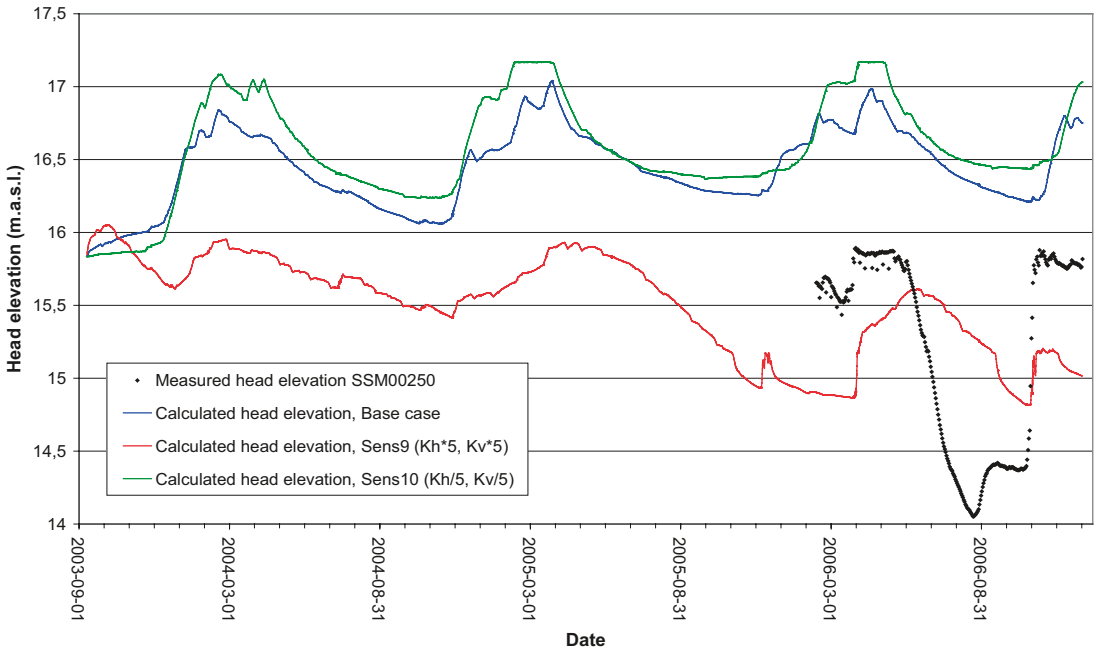

Figure 6-74. *Results for SSM000250 from sensitivity analysis of the hydraulic conductivities in the saturated zone.*

Table 6-12 shows a comparison of the mean absolute errors for the base case and the sensitivity cases. Sens9, with increased hydraulic conductivities, shows a generally improved agreement between observed and calculated heads when comparing the mean absolute errors. However, for some wells a decreased conductivity (Sens10) results in an improved pattern of the temporal head variations, including the amplitudes, although the mean absolute error is larger.

Table 6-12. Comparison of mean absolute errors between the base case, Sens9 and Sens10 ("+" represents an improvement, "o" no change and "–" reduced agreement compared to the base case).

Borehole	Mean Absolute Error, Base case	Mean Absolute Error, Sens9 (K soil * 5)	Mean Absolute Error, Sens10 (K soil/5)	Improved agreement with Sens9	Improved agreement with Sens10
SSM000009	0.21	1.17	1.41	–	–
SSM000011	1.17	1.55	2.05	–	–
SSM000017	0.70	0.44	0.77	+	–
SSM000019	1.35	1.29	1.02	+	+
SSM000021	1.63	1.44	1.88	+	–
SSM000030	1.03	0.90	1.21	+	–
SSM000031	0.77	0.75	0.71	+	+
SSM000032	0.23	0.28	0.16	–	+
SSM000033	1.15	0.43	1.14	+	+
SSM000037	2.09	1.98	2.38	+	–
SSM000039	1.62	1.38	1.82	+	–
SSM000041	2.06	1.75	2.44	+	–
SSM000042	0.63	0.48	0.66	+	–
SSM000210	2.35	1.30	2.65	+	–
SSM000213	0.53	0.77	1.11	–	–
SSM000215	1.63	1.49	1.67	+	–
SSM000218	0.77	1.85	0.82	–	–
SSM000219	2.02	0.87	2.08	+	–
SSM000220	1.31	0.72	1.63	+	–
SSM000221	0.51	0.40	0.48	+	+
SSM000222	1.74	1.42	2.18	+	–
SSM000223	1.29	1.17	1.83	+	–
SSM000224	0.72	0.56	0.90	+	–
SSM000225	0.98	0.82	1.06	+	–
SSM000226	1.41	0.63	2.46	+	–
SSM000227	1.54	0.73	2.60	+	–
SSM000228	0.56	0.51	0.70	+	–
SSM000229	0.44	0.66	0.78	–	–
SSM000230	1.57	1.34	2.20	+	–
SSM000237	1.97	1.88	1.95	+	+
SSM000239	0.14	0.10	0.22	+	–
SSM000240	0.16	0.13	0.34	+	–
SSM000242	1.18	0.85	1.51	+	–
SSM000249	0.76	0.28	0.60	+	+
SSM000250	1.34	0.65	1.52	+	–
SSM000252	5.42	6.04	4.88	–	+
SSM000253	1.96	1.91	1.65	+	+
SSM000255	1.66	1.05	1.69	+	–
SSM000256	1.67	1.36	1.66	+	+
SSM000257	1.68	1.43	1.76	+	–
Mean MAE	1.30	1.12	1.51		

Table 6-13 shows the total water balance for the base case compared to Sens9 and Sens10. The largest differences are in the components “Subsurface storage change” and “Base flow to river”, which is consistent with the results shown in Figures 6-63 to 6-74.

6.4 Influence of boundary conditions

According to Table 5-2, the applied bottom boundary head elevation is higher than both observed and simulated mean head elevations in a large number of observation points. This indicates that either the boundary head or the applied hydraulic conductivities in the bedrock may need to be adjusted in order to reach a better agreement between observed and simulated heads. A sensitivity simulation was therefore conducted (Sens11), using adjusted groundwater heads in the rock. The heads obtained from the DarcyTools model were lowered by 3 metres in all bedrock layers including the vertical and bottom boundaries where a constant-head boundary condition was applied in the MIKE SHE model. Thus, both the initial head values for the whole rock part of the model and the constant-head boundary conditions were changed in the Sens11 case.

Figures 6-75 to 6-78 compare the Sens11 and base case results in terms of surface water discharges. For all four hydrological stations, the discharges are smaller for Sens11 than for the base case. In particular, there is a large effect on the base flow, with lower base flow when the head boundary is lowered. Figures 6-79 to 6-86 show the results for head elevations in the selected groundwater monitoring wells. In all wells, the head elevation is lower for the Sens11 case compared to the base case, which is logical given the reduced heads in the rock. For some of the wells, the differences between Sens11 and the base case are very small, indicating a limited hydraulic contact between rock and Quaternary deposits.

Table 6-13. Comparison of total water balances between the base case, Sens9 and Sens10.

Parameter	Base case	Sens9	Sens10
Precipitation	–1,774	–1,774	–1,774
Canopy storage change	0	0	0
Evapotranspiration	1,264	1,264	1,278
Overland storage change	55	38	58
Overland boundary inflow	–52	–68	–46
Overland boundary outflow	84	108	70
Overland to river	225	217	209
Subsurface storage change	43	7	91
Subsurface boundary inflow	14	27	9
Subsurface boundary outflow	83	72	81
Base flow to river	94	175	39
Base flow from river	0	0	0
Error	7	12	–2

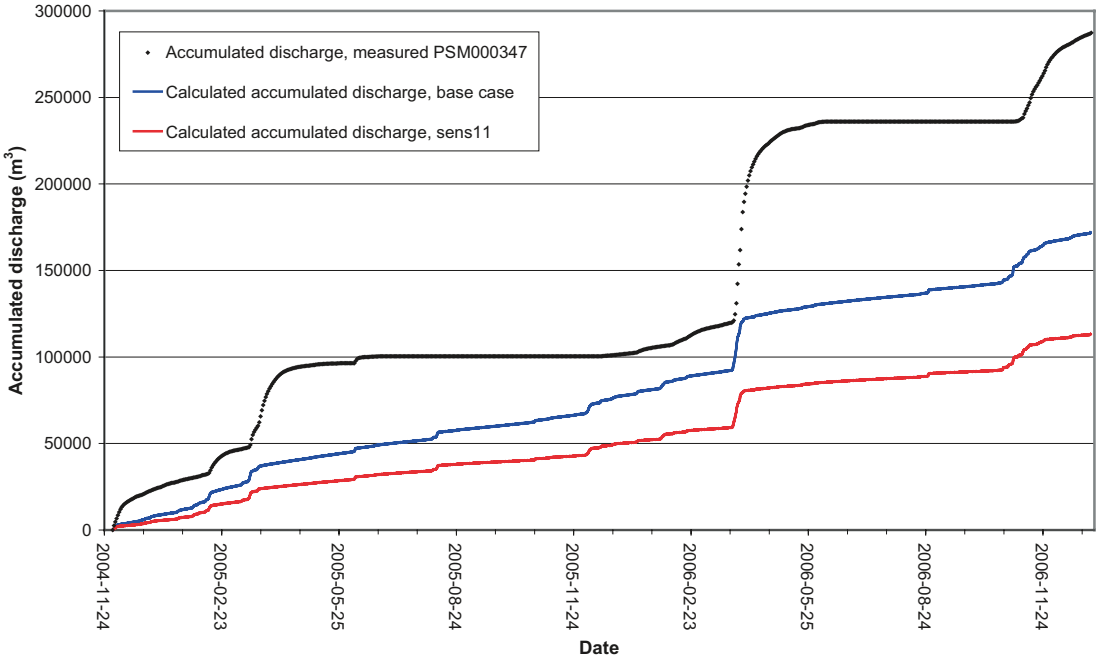

Figure 6-75. *Sensitivity of the accumulated discharge in PSM000347 to lowered initial and boundary heads in the rock.*

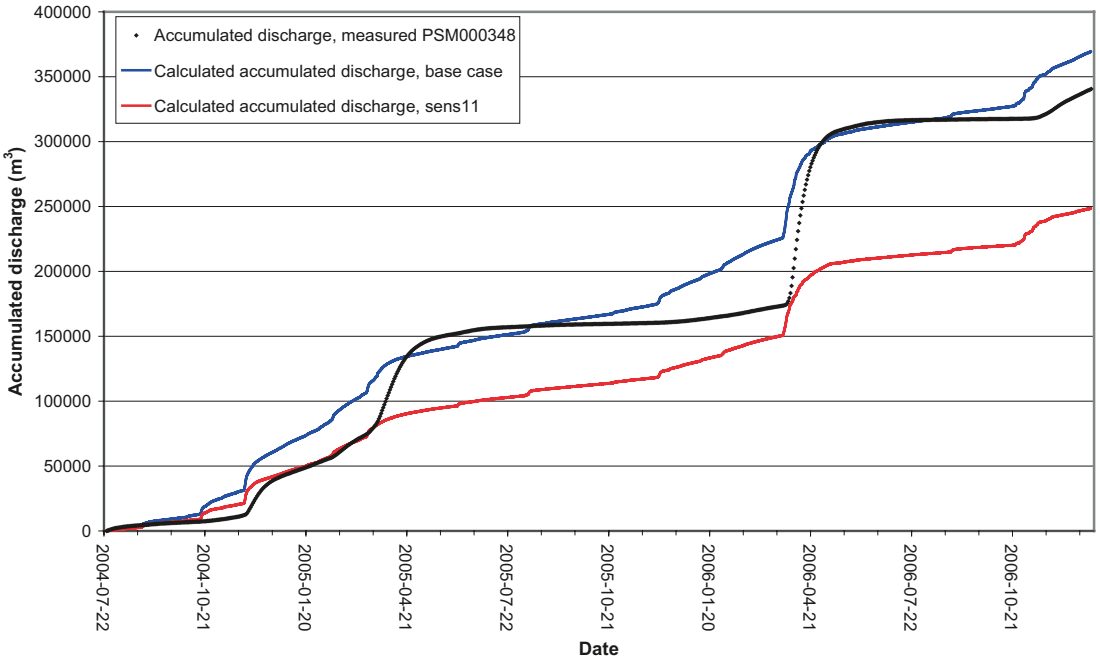

Figure 6-76. *Sensitivity of the accumulated discharge in PSM000348 to lowered initial and boundary heads in the rock.*

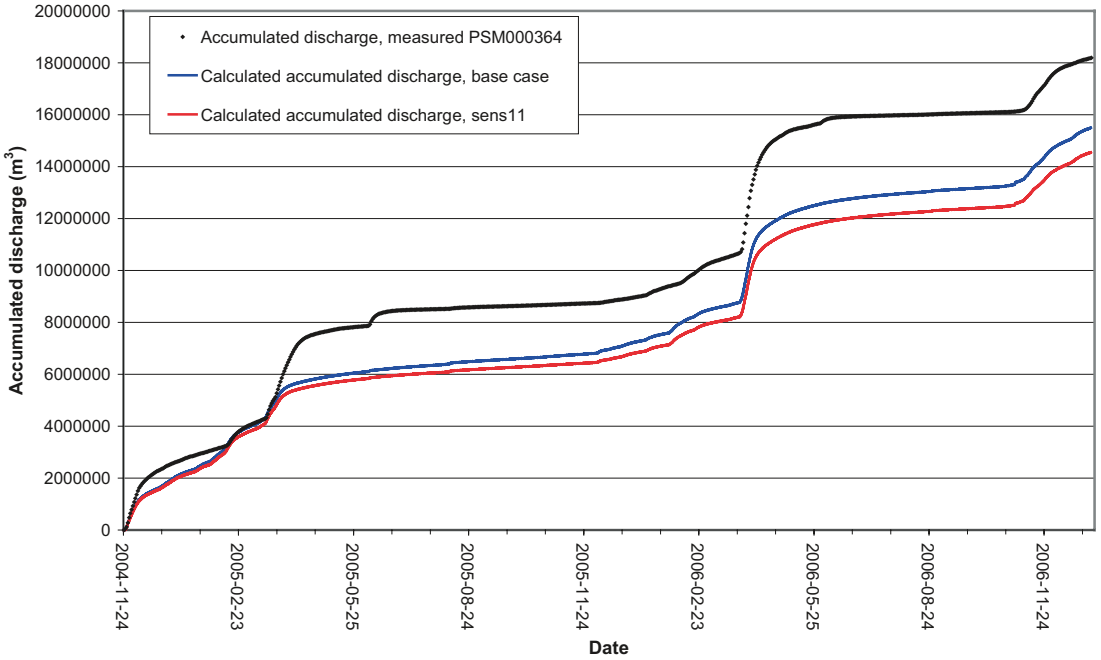

Figure 6-77. *Sensitivity of the accumulated discharge in PSM000364 to lowered initial and boundary heads in the rock.*

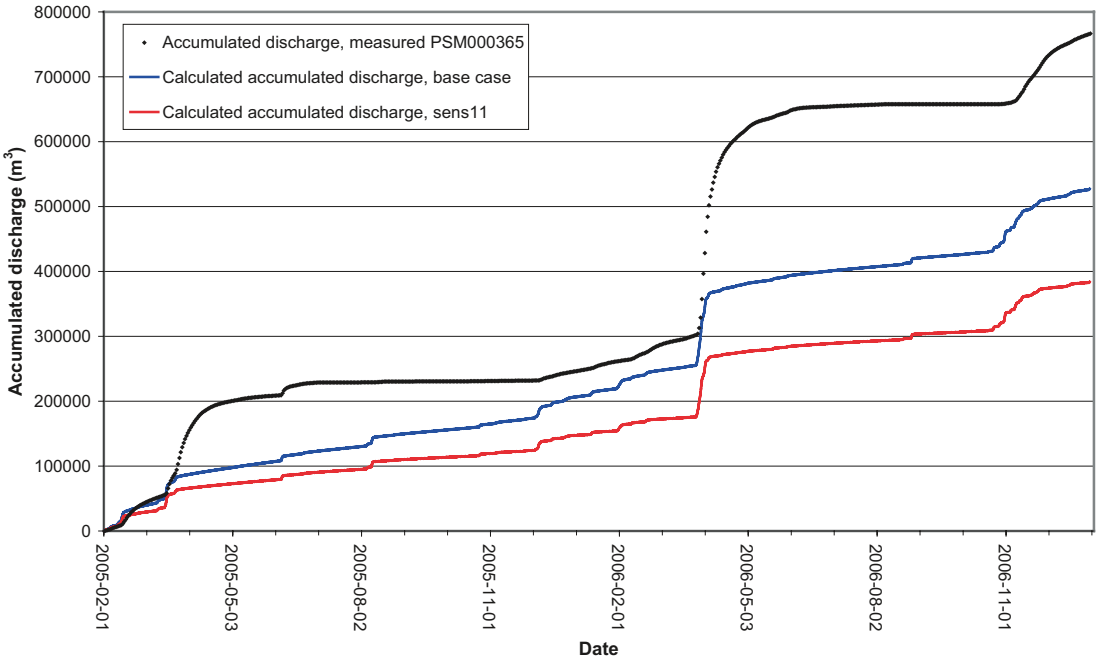

Figure 6-78. *Sensitivity of the accumulated discharge in PSM000365 to lowered initial and boundary heads in the rock.*

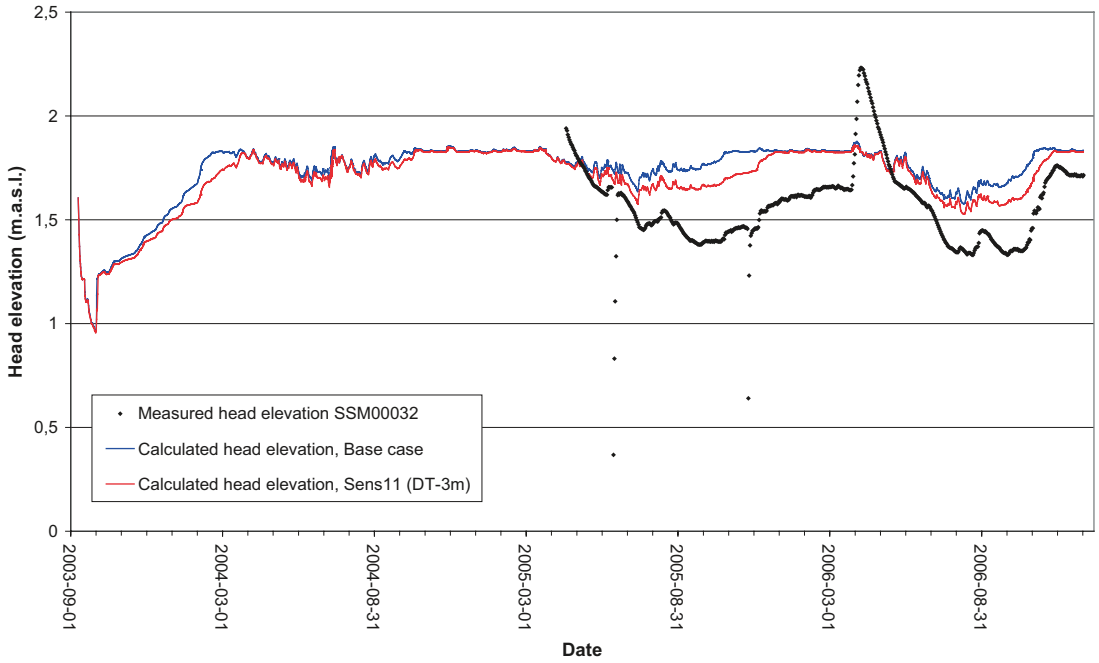

Figure 6-79. *Sensitivity of the groundwater level in SSM000032 to lowered initial and boundary heads in the rock.*

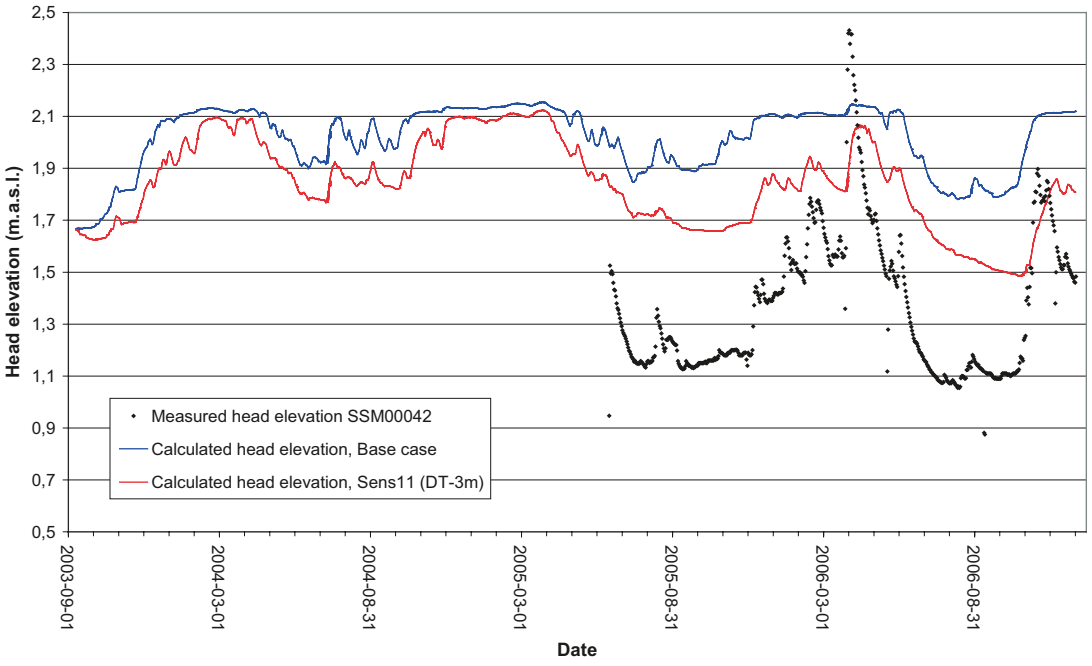

Figure 6-80. *Sensitivity of the groundwater level in SSM000042 to lowered initial and boundary heads in the rock.*

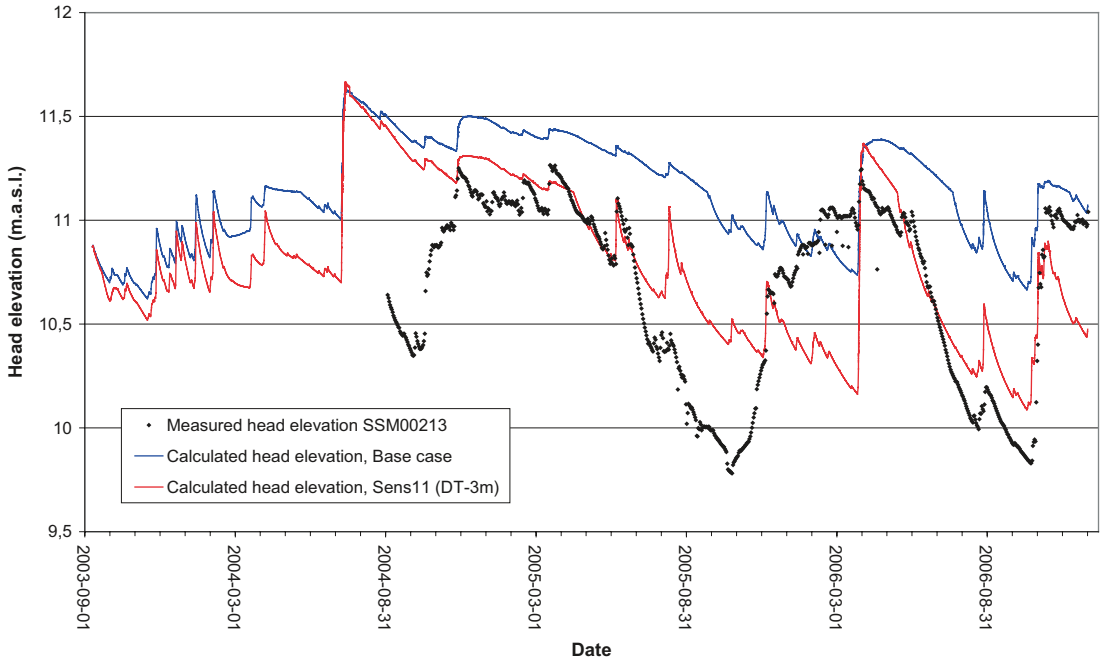

Figure 6-81. *Sensitivity of the groundwater level in SSM000213 to lowered initial and boundary heads in the rock.*

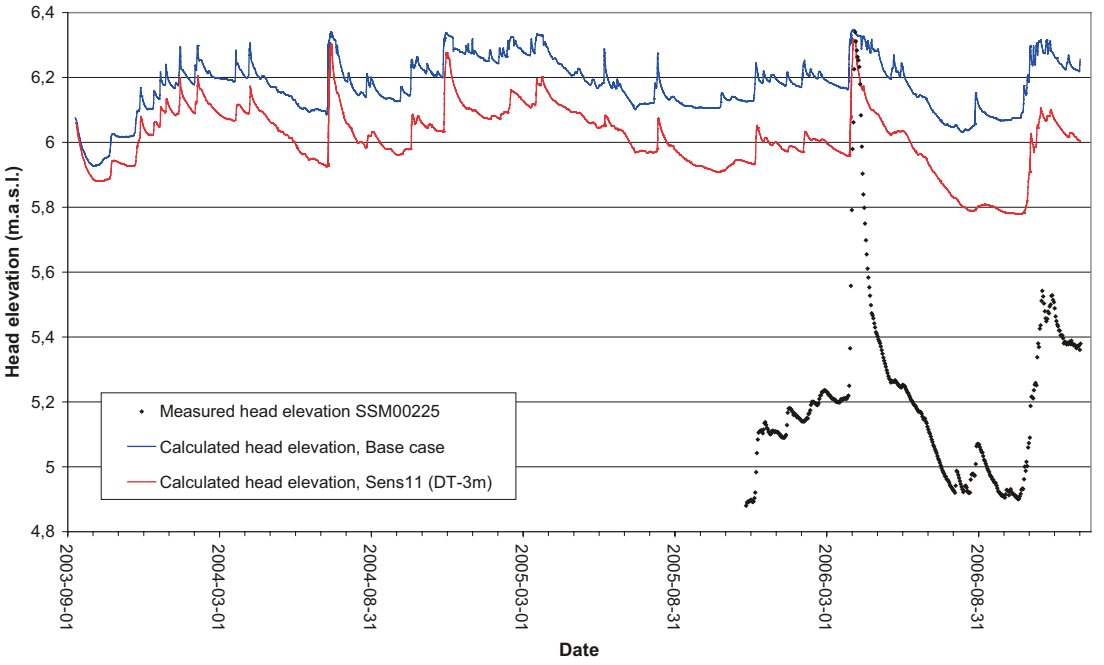

Figure 6-82. *Sensitivity of the groundwater level in SSM000225 to lowered initial and boundary heads in the rock.*

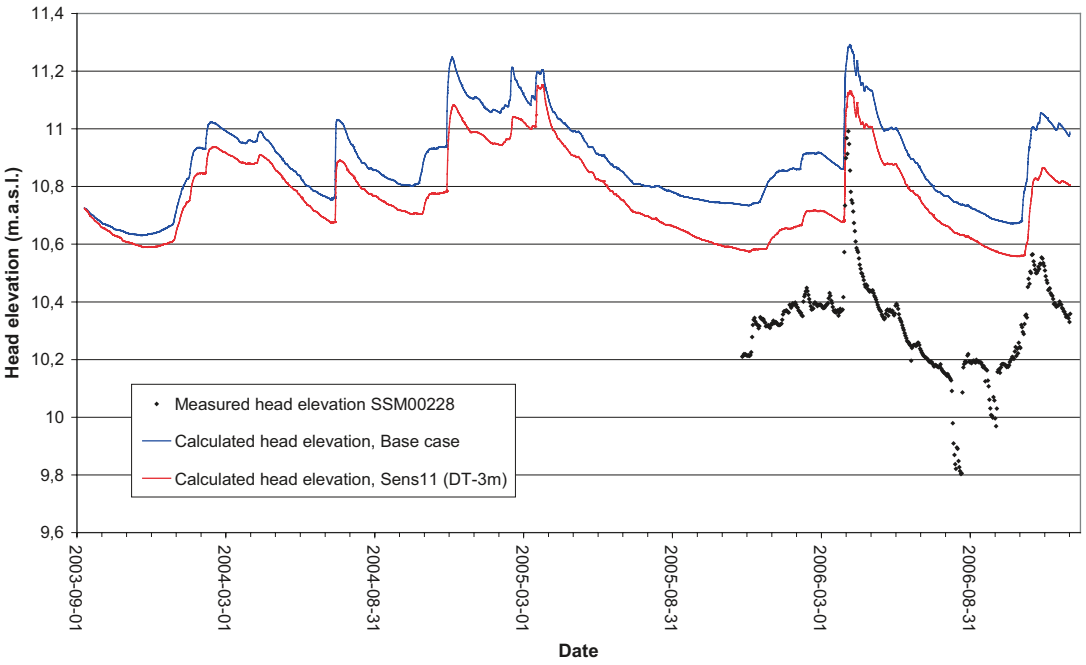

Figure 6-83. *Sensitivity of the groundwater level in SSM000228 to lowered initial and boundary heads in the rock.*

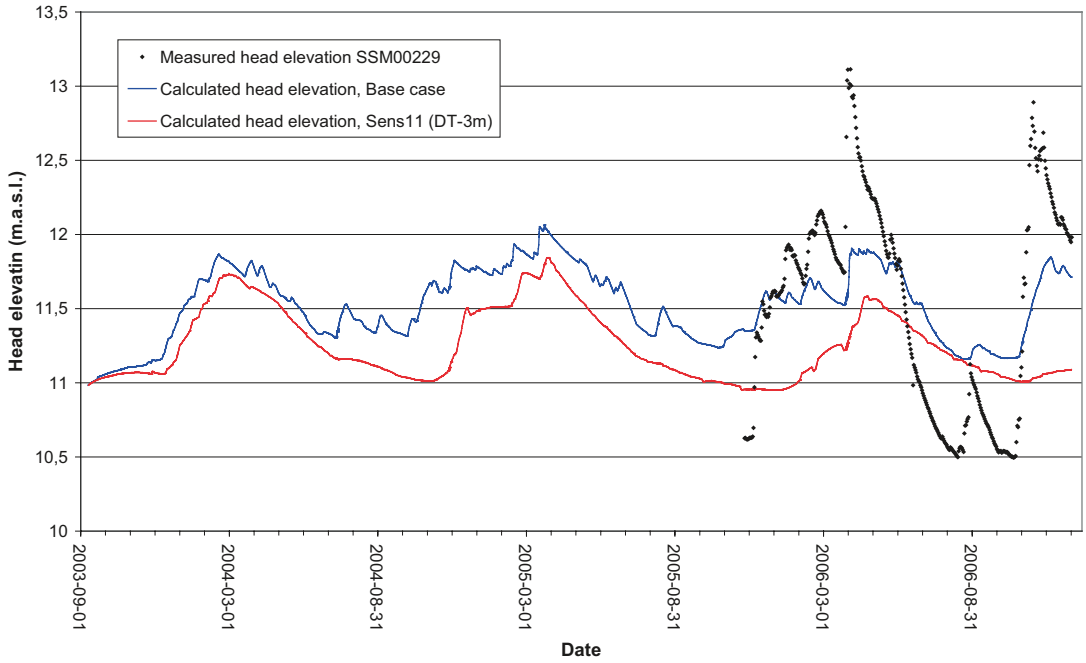

Figure 6-84. *Sensitivity of the groundwater level in SSM000229 to lowered initial and boundary heads in the rock.*

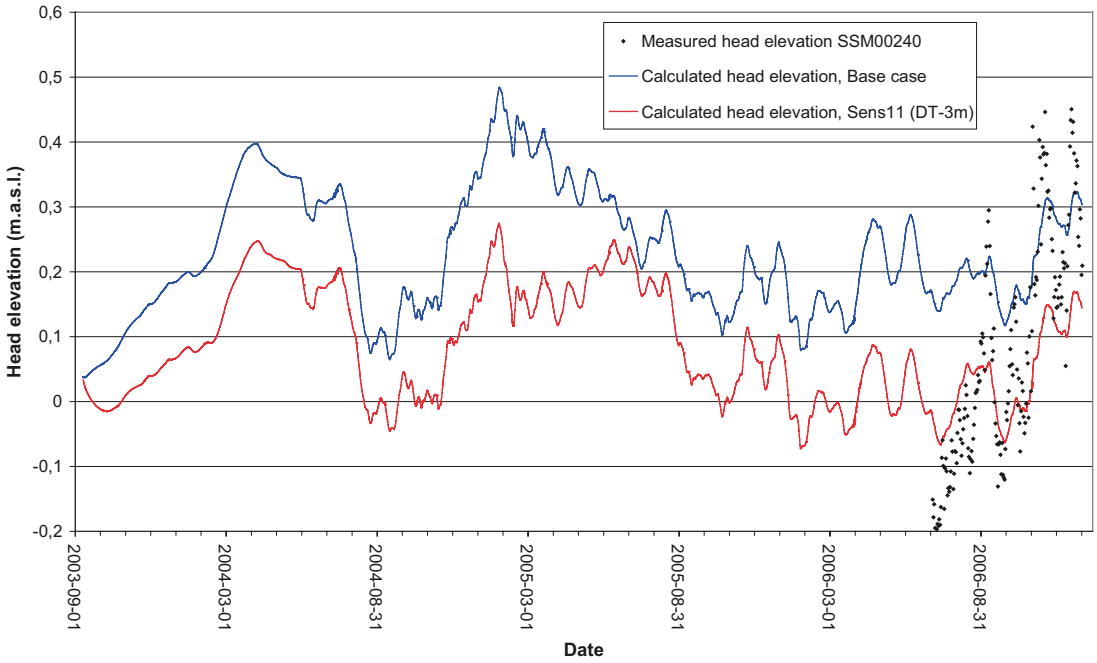

Figure 6-85. *Sensitivity of the groundwater level in SSM000240 to lowered initial and boundary heads in the rock.*

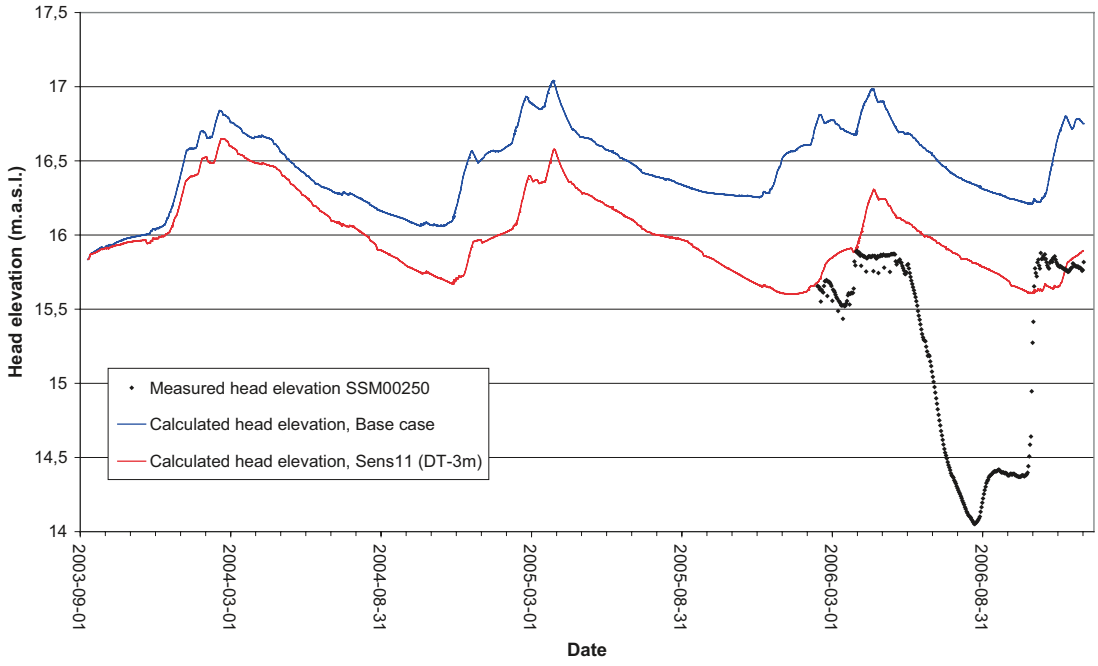

Figure 6-86. *Sensitivity of the groundwater level in SSM000250 to lowered initial and boundary heads in the rock.*

Table 6-14 compares the mean absolute errors in the Sens11 case and in the base case. In almost all monitoring wells, the mean error is reduced in the Sens11 case compared to the base case. In some of the wells, there is a small or no effect, whereas the absolute error is reduced to less than half of that in the base case for many wells. In approximately one third of the wells, there is a considerable improvement. The mean MAE for all wells is reduced by approximately 25%.

Table 6-14. Comparison of mean absolute errors between the base case and Sens11 ("+" represents an improvement, "o" no change and "–" reduced agreement compared to the base case).

Borehole	Mean Absolute Error, Base case	Mean Absolute Error, Sens11 (DT–3m)	Improved agreement with Sens11
SSM000009	0.21	0.15	+
SSM000011	1.17	1.17	o
SSM000017	0.70	0.58	+
SSM000019	1.35	1.36	–
SSM000021	1.63	0.97	+
SSM000030	1.03	0.78	+
SSM000031	0.77	0.58	+
SSM000032	0.23	0.18	+
SSM000033	1.15	1.10	+
SSM000037	2.09	1.56	+
SSM000039	1.62	1.02	+
SSM000041	2.06	1.87	+
SSM000042	0.63	0.39	+
SSM000210	2.35	1.79	+
SSM000213	0.53	0.30	+
SSM000215	1.63	1.50	+
SSM000218	0.77	0.82	–
SSM000219	2.02	1.75	+
SSM000220	1.31	1.07	+
SSM000221	0.51	0.49	+
SSM000222	1.74	1.04	+
SSM000223	1.29	0.61	+
SSM000224	0.72	0.69	+
SSM000225	0.98	0.77	+
SSM000226	1.41	0.92	+
SSM000227	1.54	1.03	+
SSM000228	0.56	0.41	+
SSM000229	0.44	0.67	–
SSM000230	1.57	1.03	+
SSM000237	1.97	1.94	+
SSM000239	0.14	0.12	+
SSM000240	0.16	0.10	+
SSM000242	1.18	0.43	+
SSM000249	0.76	0.71	+
SSM000250	1.34	0.70	+
SSM000252	5.42	5.16	+
SSM000253	1.96	0.83	+
SSM000255	1.66	1.45	+
SSM000256	1.67	1.18	+
SSM000257	1.68	1.11	+
Mean MAE	1.30	1.01	

Table 6-15 compares the total water balance for the base case and the Sens11 case. A large difference is found in the "Overland to river" and "Base flow to river" components, which is also indicated by the results in Figures 6-75 to 6-78. However, the main difference is found in the "Subsurface boundary outflow" component, which is a logical result of the changed head conditions in the model.

6.5 Influence of the surface stream network

As described in Section 3.3, the MIKE 11 stream network has been extended to include more branches in order to allow for more surface water flow within and from the model area. However, it was noted that some areas where there are no lakes in reality still had ponding of water in the model during the simulation.

In order to reduce the amount of water ponding on the surface, a sensitivity simulation with drainage included was conducted, Sens13. This drainage description should be seen as a fictitious description of a complex, small-scale surface stream network not mapped and therefore not included in the model. Drainage was introduced in all areas with ponding water, except for Lake Frisksjön. In the Sens13 case, a drainage depth was set to 0.05 m below ground surface and a time constant of $2 \cdot 10^{-6}$ s^{-1} was applied. This means that when the groundwater table reaches above 0.05 m below ground surface, the groundwater is extracted at a rate determined by the applied time constant and transported towards the closest water course in the model.

Figures 6-87 to 6-90 show the results for Sens13 in terms of surface water discharges in comparison to the base case discharges. At all four discharge stations the discharge is higher in the Sens13 case than in the base case. The increase of the accumulated discharge is approximately linear over time, although with a slightly dampened peak response, which gives a better match with the observed values.

Figures 6-91 to 6-98 show the results in terms of head elevations at the groundwater monitoring wells. For all wells, the head elevation is lower in the Sens13 case than in the base case. In most of the wells, the head elevations in Sens13 are lowered the most during summer periods, giving higher head amplitudes. This gives a better fit to the measured heads.

Table 6-15. Comparison of total water balances between the base case and Sens11.

Parameter	Base case	Sens11
Precipitation	–1,774	–1,774
Canopy storage change	0	0
Evapotranspiration	1,264	1,273
Overland storage change	55	48
Overland boundary inflow	–52	–54
Overland boundary outflow	84	74
Overland to river	225	172
Subsurface storage change	43	17
Subsurface boundary inflow	14	4
Subsurface boundary outflow	83	196
Base flow to river	94	66
Base flow from river	0	–1
Error	7	12

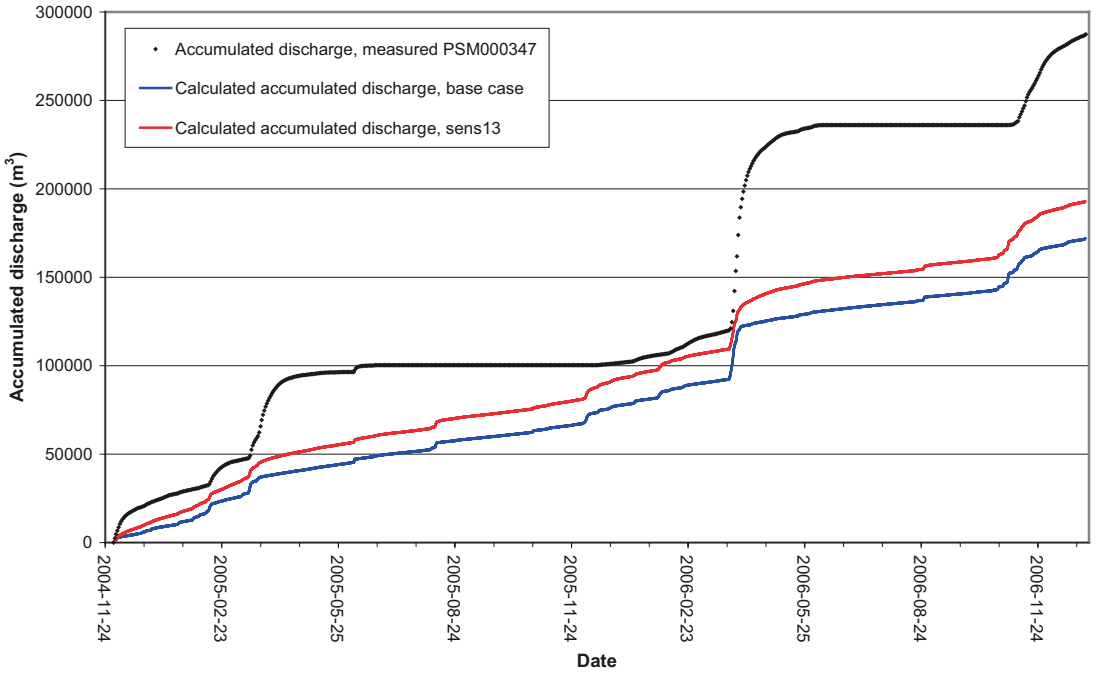

Figure 6-87. *Results for PSM000347 (discharge) showing the sensitivity to including near-surface drainage in the model.*

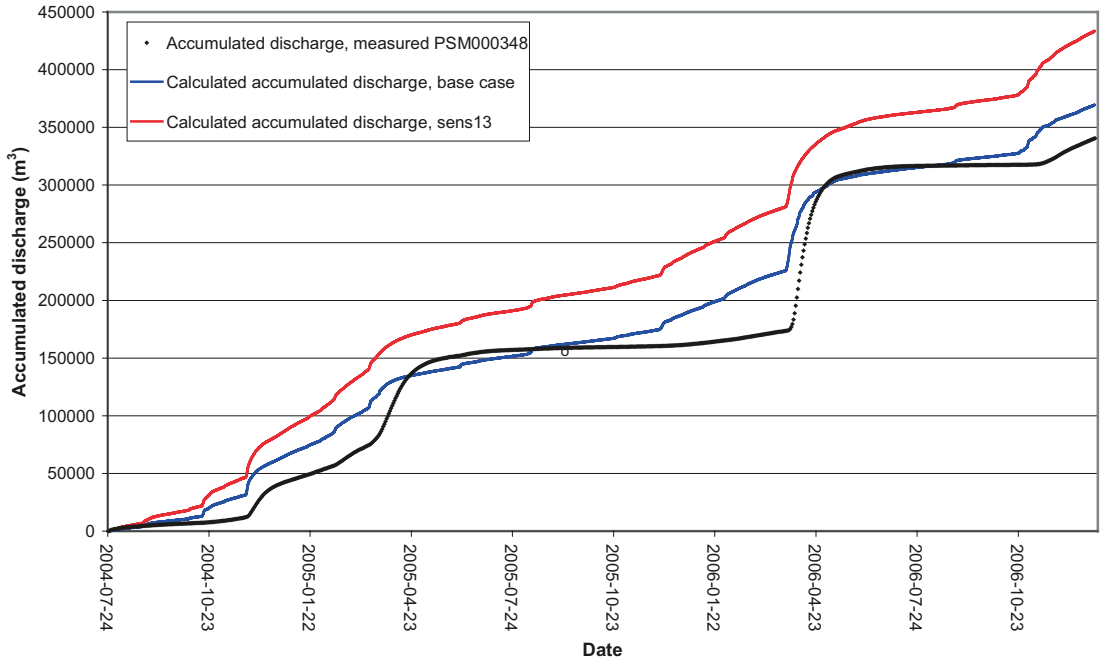

Figure 6-88. *Results for PSM000348 (discharge) showing the sensitivity to including near-surface drainage in the model.*

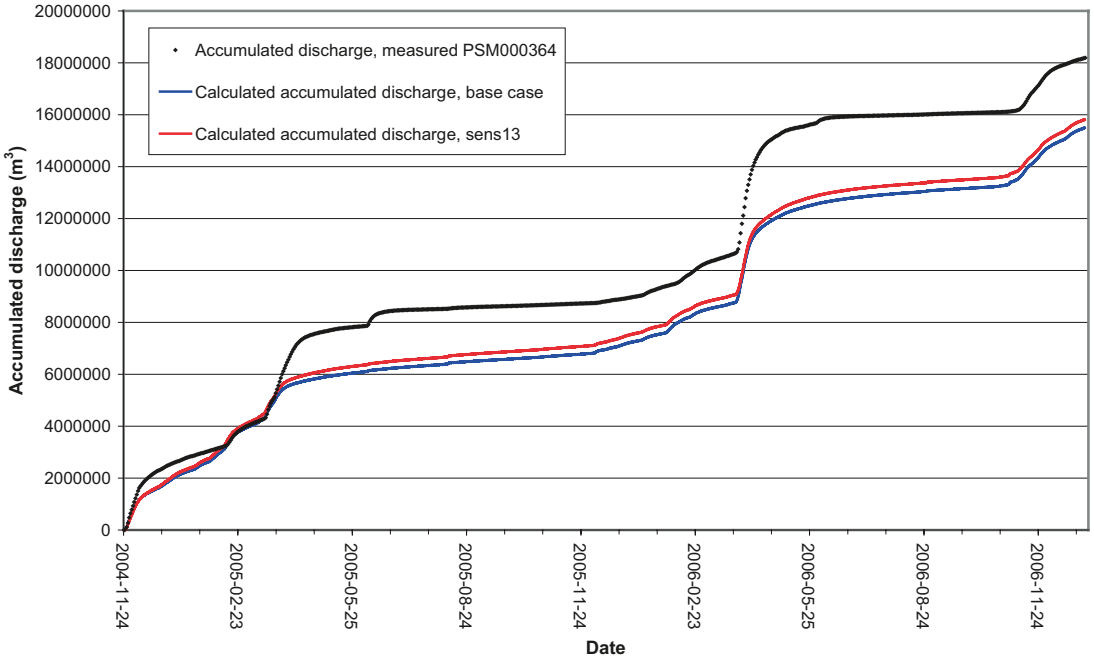

Figure 6-89. *Results for PSM000364 (discharge) showing the sensitivity to including near-surface drainage in the model.*

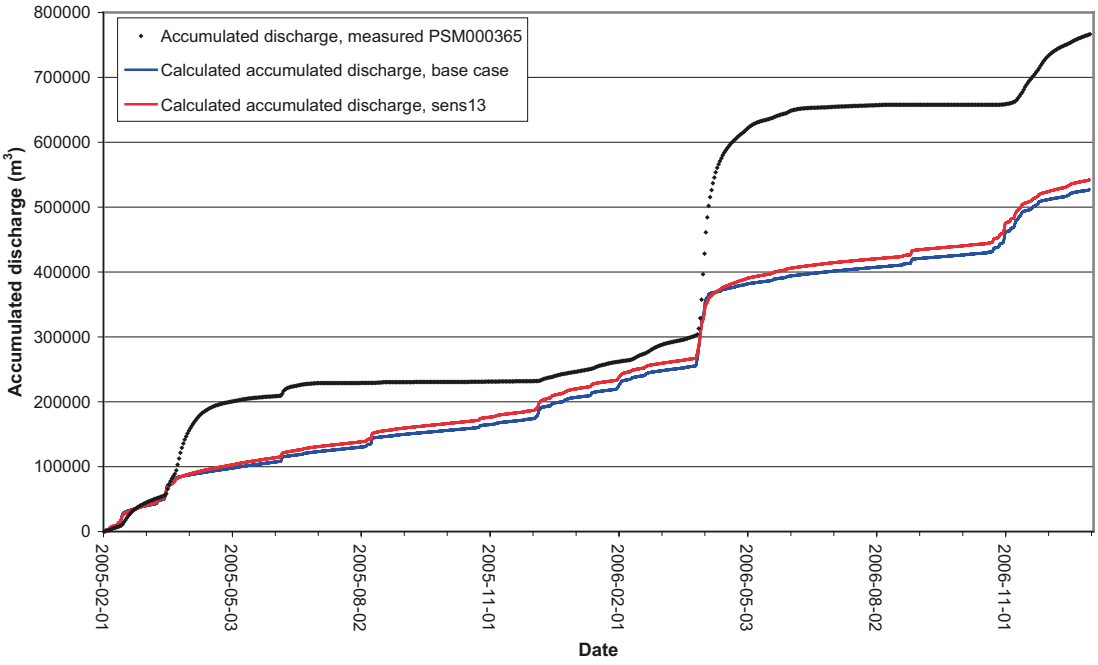

Figure 6-90. *Results for PSM000365 (discharge) showing the sensitivity to including near-surface drainage in the model.*

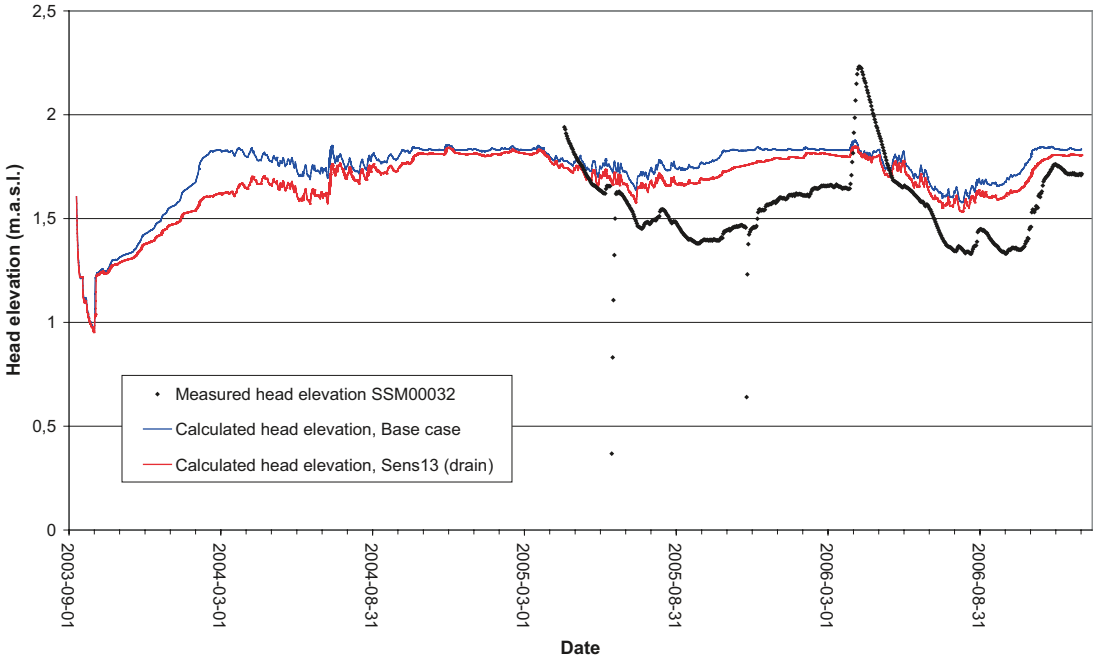

Figure 6-91. *Results for SSM000032 (groundwater head) showing the sensitivity to including near-surface drainage in the model.*

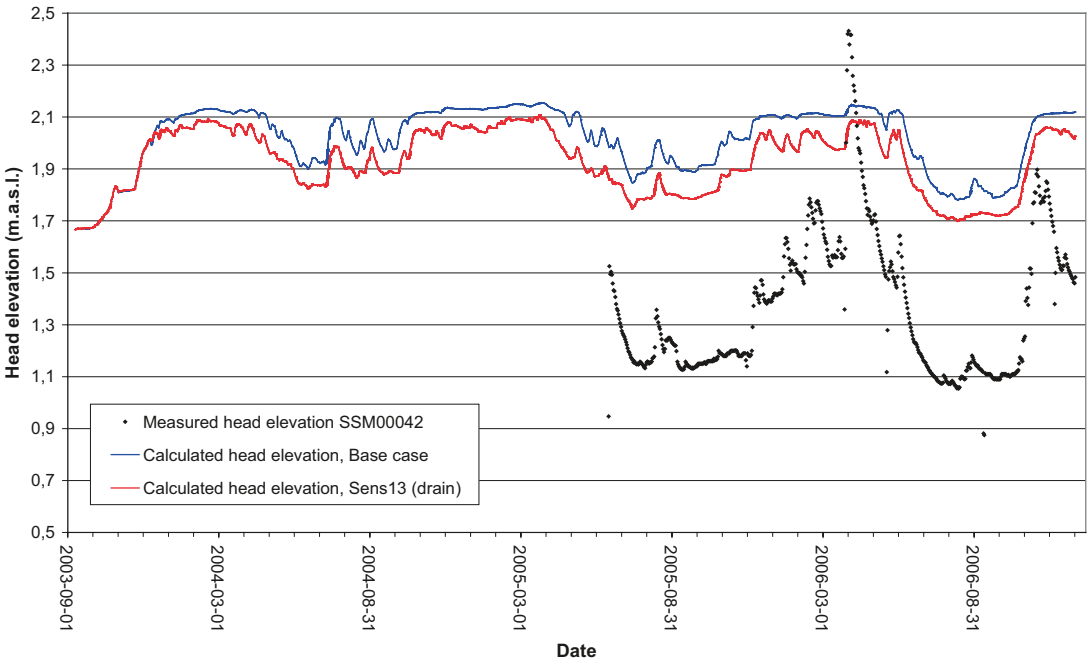

Figure 6-92. *Results for SSM000042 (groundwater head) showing the sensitivity to including near-surface drainage in the model.*

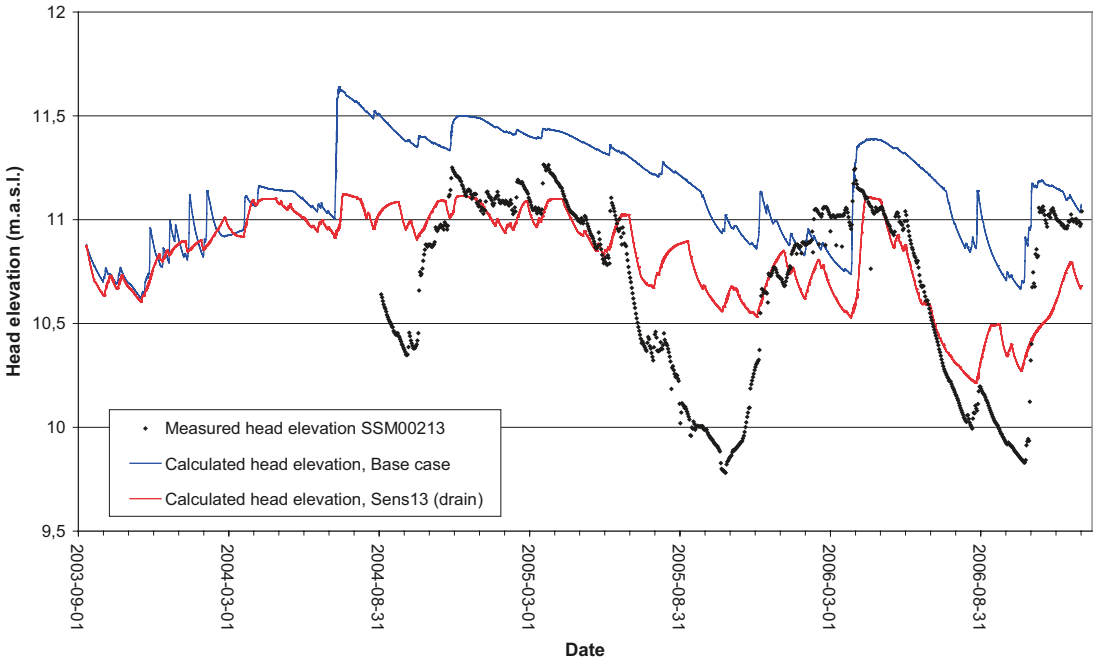

Figure 6-93. *Results for SSM000213 (groundwater head) showing the sensitivity to including near-surface drainage in the model.*

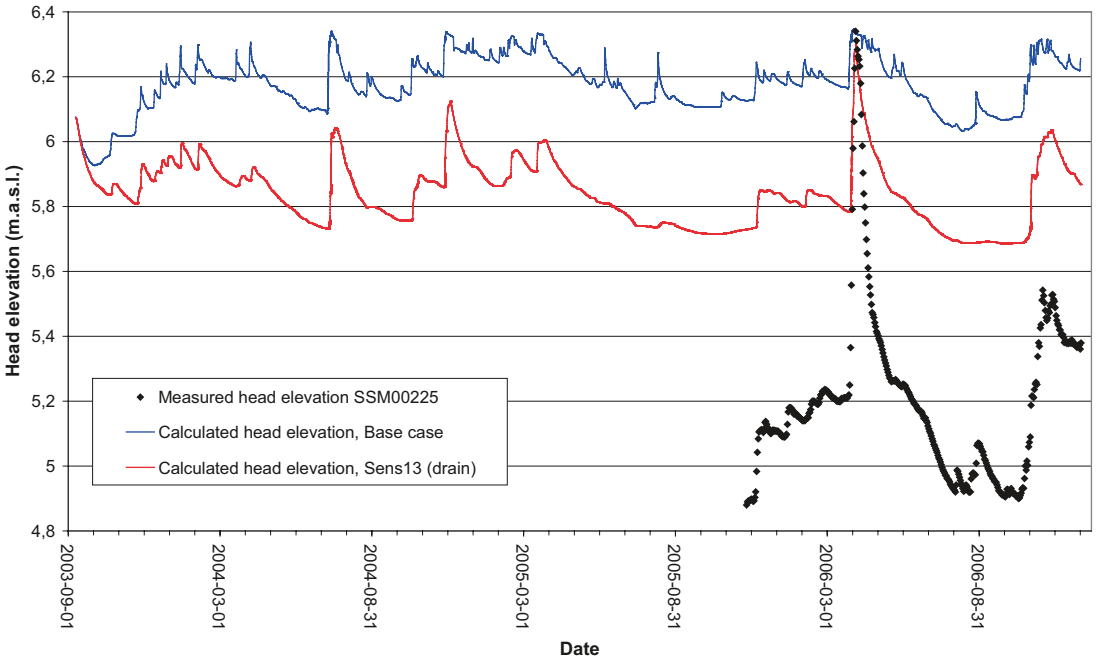

Figure 6-94. *Results for SSM000225 (groundwater head) showing the sensitivity to including near-surface drainage in the model.*

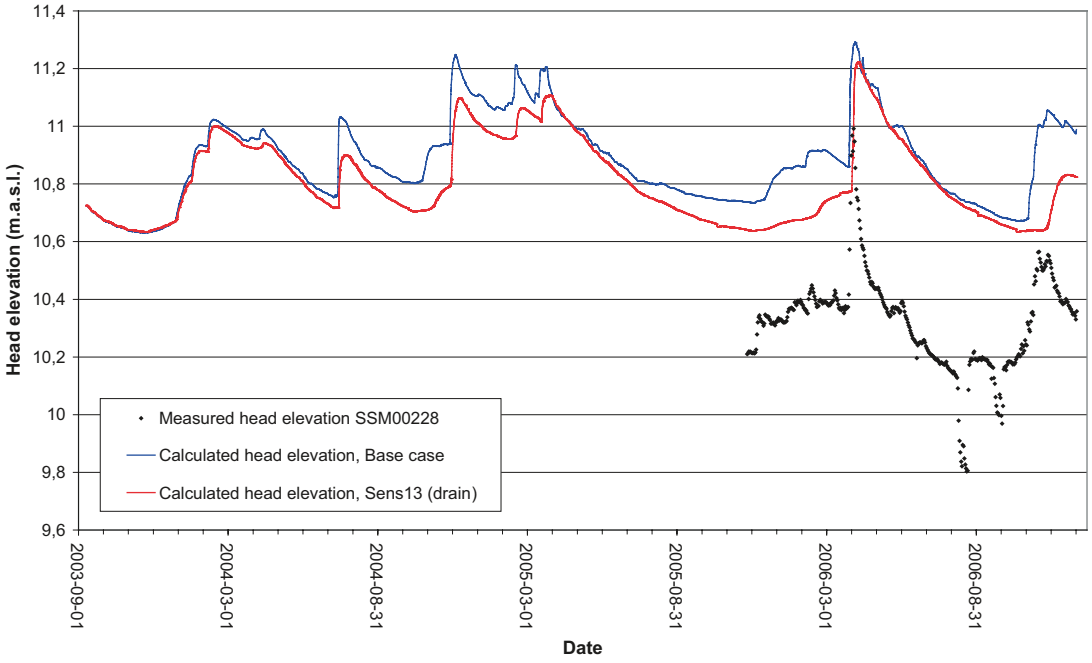

Figure 6-95. *Results for SSM000228 (groundwater head) showing the sensitivity to including near-surface drainage in the model.*

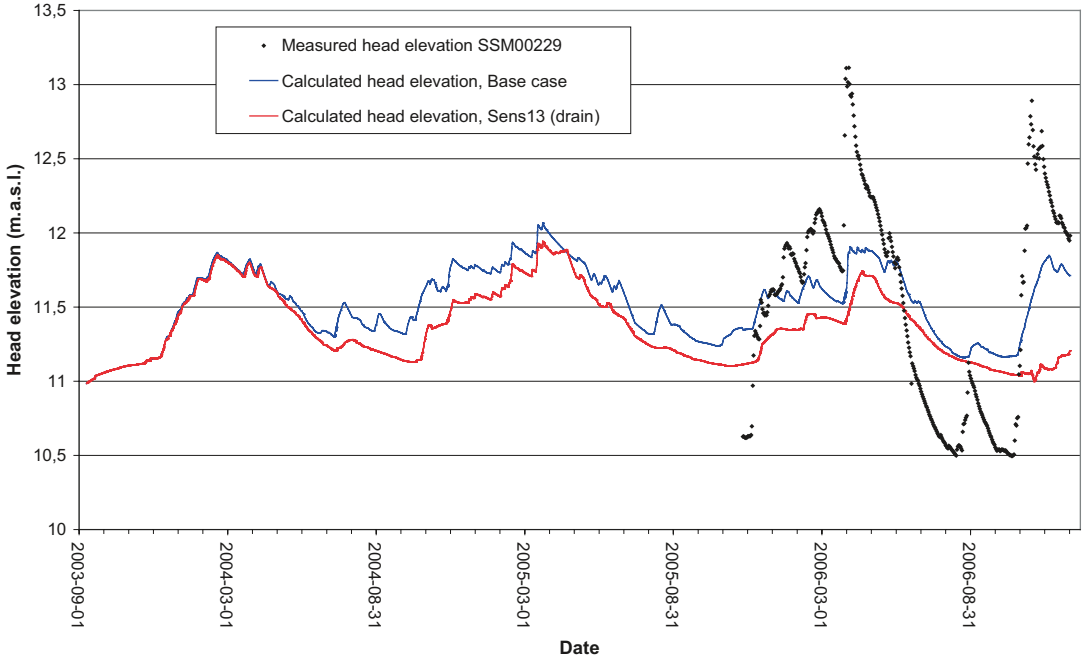

Figure 6-96. *Results for SSM000229 (groundwater head) showing the sensitivity to including near-surface drainage in the model.*

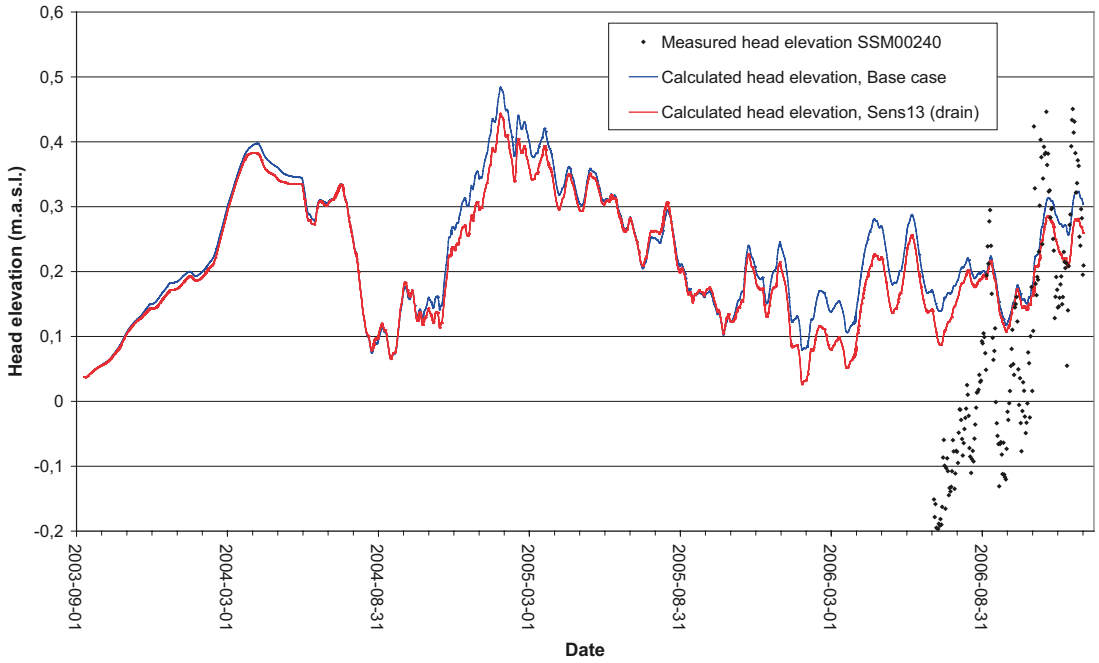

Figure 6-97. *Results for SSM000240 (groundwater head) showing the sensitivity to including near-surface drainage in the model.*

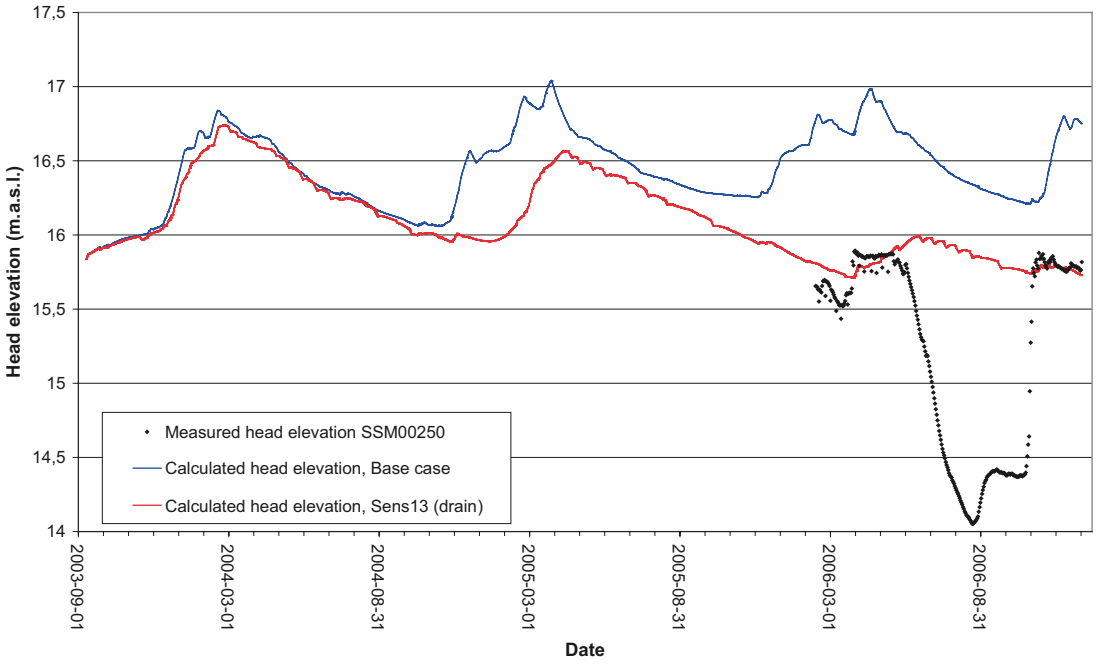

Figure 6-98. *Results for SSM000250 (groundwater head) showing the sensitivity to including near-surface drainage in the model.*

Table 6-16 compares the mean absolute errors in the Sens13 case and in the base case. In almost all monitoring wells, the mean errors are smaller in the Sens13 case than in the base case. In some of the wells the improvement is greater than 50%. For approximately half of the wells, there is a considerable improvement. The mean error for all wells is reduced with approximately 25%.

Table 6-16. Comparison of mean absolute errors between the base case and Sens13 ("+" represents an improvement, "o" no change and "–" reduced agreement compared to the base case).

Borehole	Mean Absolute Error, Base case	Mean Absolute Error, Sens13 (drainage)	Improved agreement with Sens13
SSM000009	0.21	0.21	o
SSM000011	1.17	1.17	o
SSM000017	0.70	0.16	+
SSM000019	1.35	1.06	+
SSM000021	1.63	1.59	+
SSM000030	1.03	1.00	+
SSM000031	0.77	0.49	+
SSM000032	0.23	0.18	+
SSM000033	1.15	0.26	+
SSM000037	2.09	2.08	+
SSM000039	1.62	1.59	+
SSM000041	2.06	1.78	+
SSM000042	0.63	0.53	+
SSM000210	2.35	1.82	+
SSM000213	0.53	0.27	+
SSM000215	1.63	1.60	+
SSM000218	0.77	0.78	–
SSM000219	2.02	1.95	+
SSM000220	1.31	0.93	+
SSM000221	0.51	0.19	+
SSM000222	1.74	1.72	+
SSM000223	1.29	1.29	o
SSM000224	0.72	0.54	+
SSM000225	0.98	0.63	+
SSM000226	1.41	1.31	+
SSM000227	1.54	1.43	+
SSM000228	0.56	0.46	+
SSM000229	0.44	0.57	–
SSM000230	1.57	1.26	+
SSM000237	1.97	1.01	+
SSM000239	0.14	0.14	o
SSM000240	0.16	0.14	+
SSM000242	1.18	1.13	+
SSM000249	0.76	0.58	+
SSM000250	1.34	0.65	+
SSM000252	5.42	5.36	+
SSM000253	1.96	1.59	+
SSM000255	1.66	1.39	+
SSM000256	1.67	0.76	+
SSM000257	1.68	1.02	+
Mean MAE	1.30	1.07	

Table 6-17 shows the total water balance for the base case compared to Sens13. The largest differences are in the overland components. It is noted that there is a new subsurface component, “Subsurface drain flow to river”.

6.6 Model resolution

In order to reduce the computational times, the number of computational layers in the bedrock was reduced, from the original eight layers in the base case to four (see description in Section 4.1). In this section, the effect of reducing the number of computational bedrock layers is illustrated by comparing the base case results to the results from the simulation case Sens14 where the bedrock description is changed.

Figures 6-99 to 6-102 show the effect of reducing the number of computational bedrock layers on the surface water discharge. For all discharge stations, the results indicate that the discharge is somewhat larger when all layers are included. The difference is rather small, but notable in PSM000348.

Figures 6-103 to 6-110 show the effect of reducing the number of computational layers on the groundwater head elevations. Different monitoring wells demonstrate different results with regard to changes in head elevations. In some wells, there is almost no change, in some the head elevations are higher, whereas in others the head elevations are lower in the sensitivity case. In the wells with lower head elevations, the largest difference compared to the base case is c. 0.25 m.

Table 6-17. Comparison of total water balances between the base case and Sens13.

Parameter	Base case	Sens13
Precipitation	–1,774	–1,774
Canopy storage change	0	0
Evapotranspiration	1,264	1,293
Overland storage change	55	17
Overland boundary inflow	–52	–121
Overland boundary outflow	84	124
Overland to river	225	107
Subsurface drain flow to river	0	194
Subsurface storage change	43	19
Subsurface boundary inflow	14	16
Subsurface boundary outflow	83	74
Base flow to river	94	75
Base flow from river	0	–1
Error	7	9

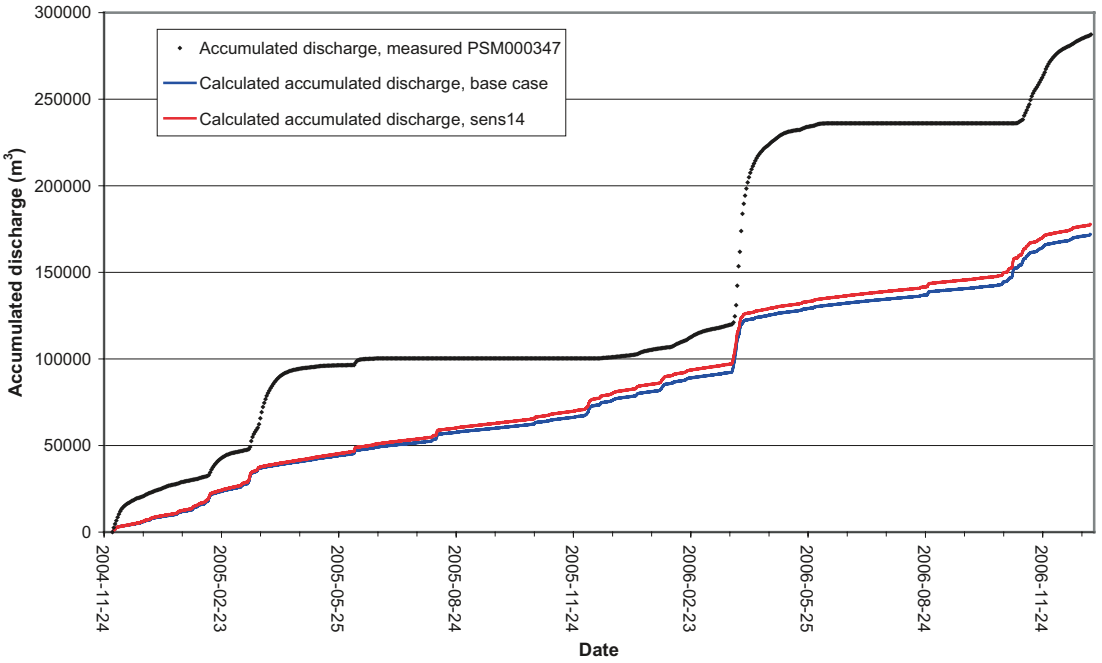

Figure 6-99. *Results for PSM000347 (discharge) from sensitivity analysis of the vertical model resolution in the bedrock.*

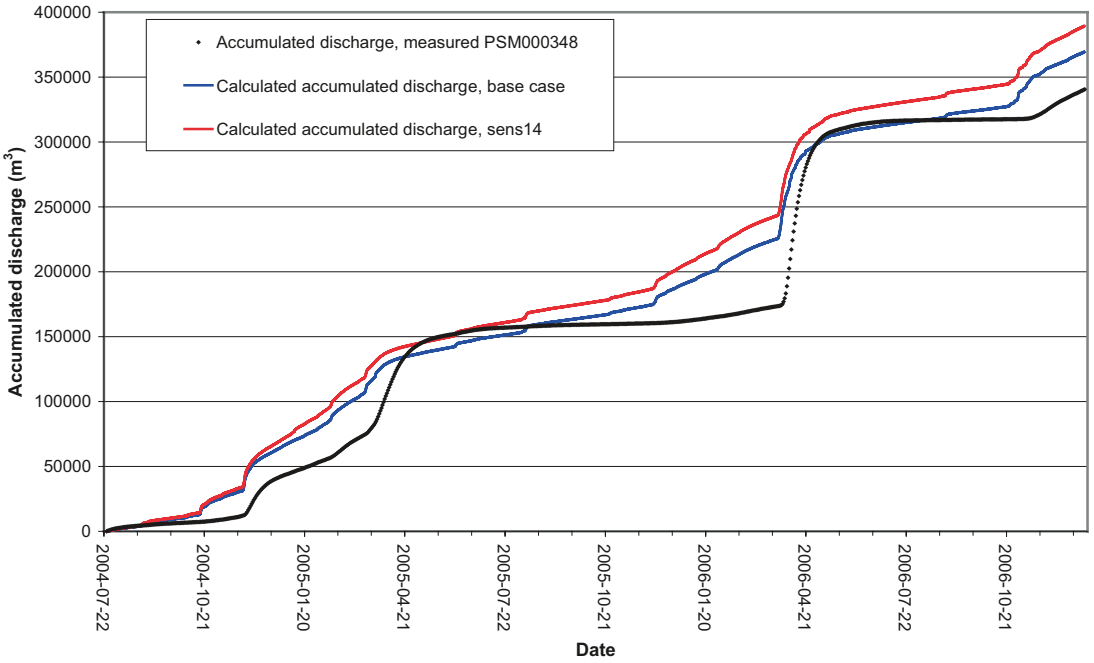

Figure 6-100. *Results for PSM000348 (discharge) from sensitivity analysis of the vertical model resolution in the bedrock.*

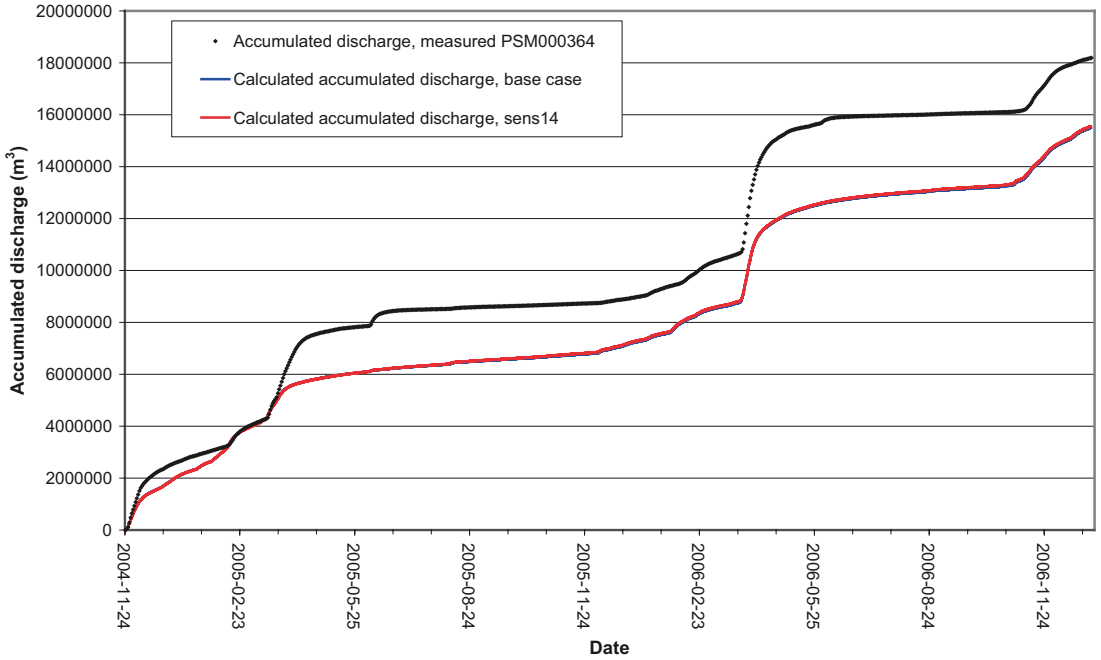

Figure 6-101. *Results for PSM000364 (discharge) from sensitivity analysis of the vertical model resolution in the bedrock.*

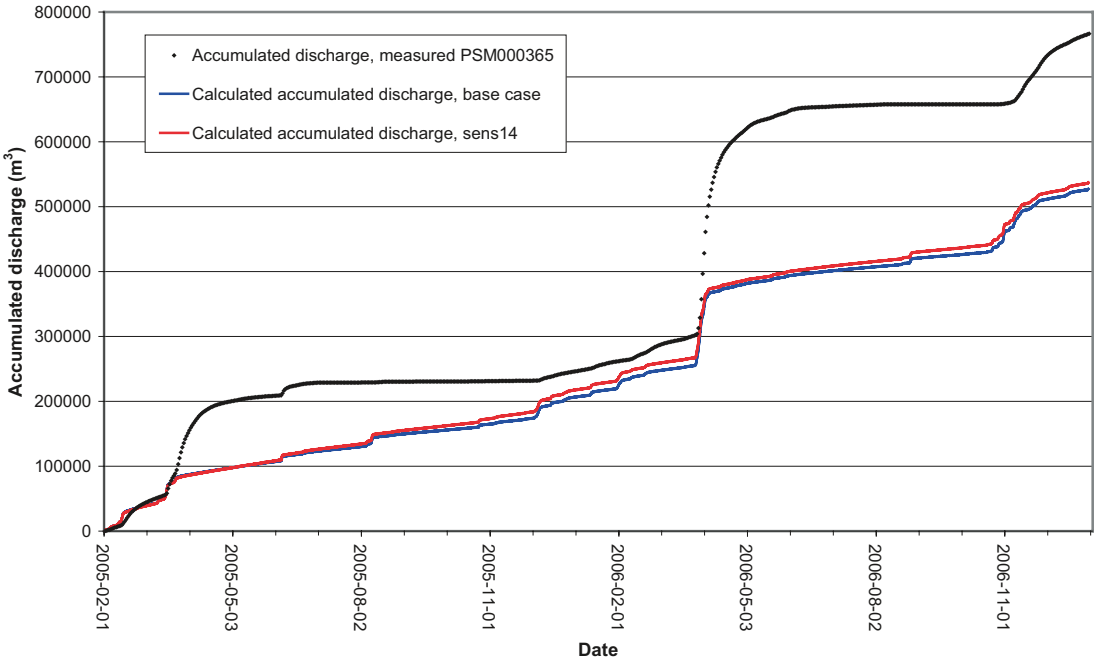

Figure 6-102. *Results for PSM000365 (discharge) from sensitivity analysis of the vertical model resolution in the bedrock.*

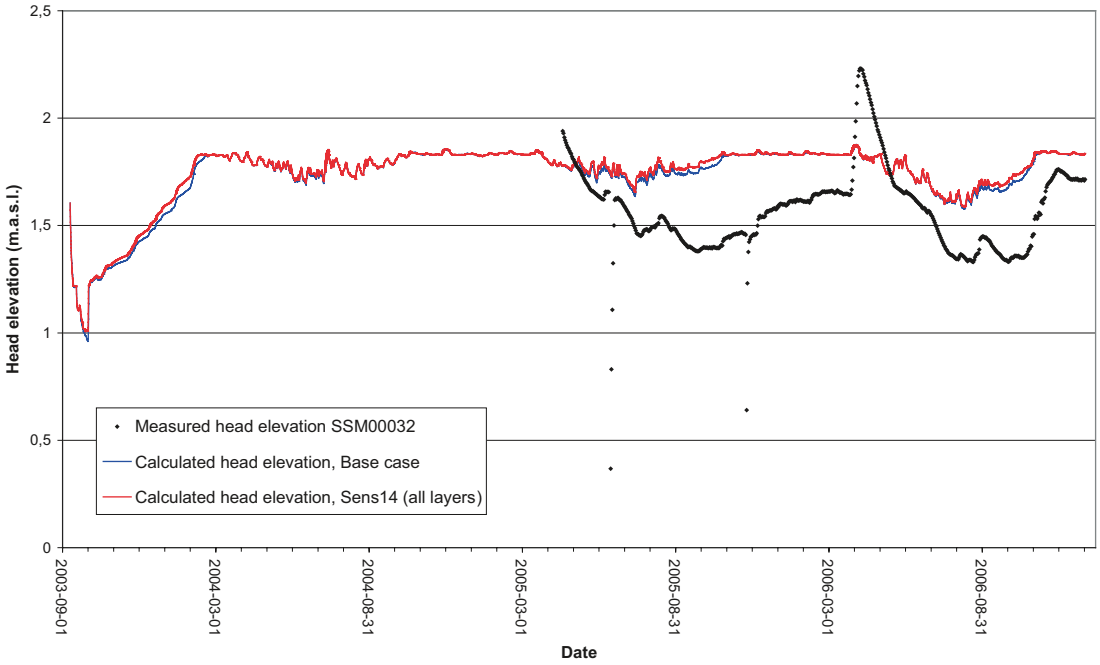

Figure 6-103. *Results for SSM000032 (groundwater head) from sensitivity analysis of the vertical model resolution in the bedrock.*

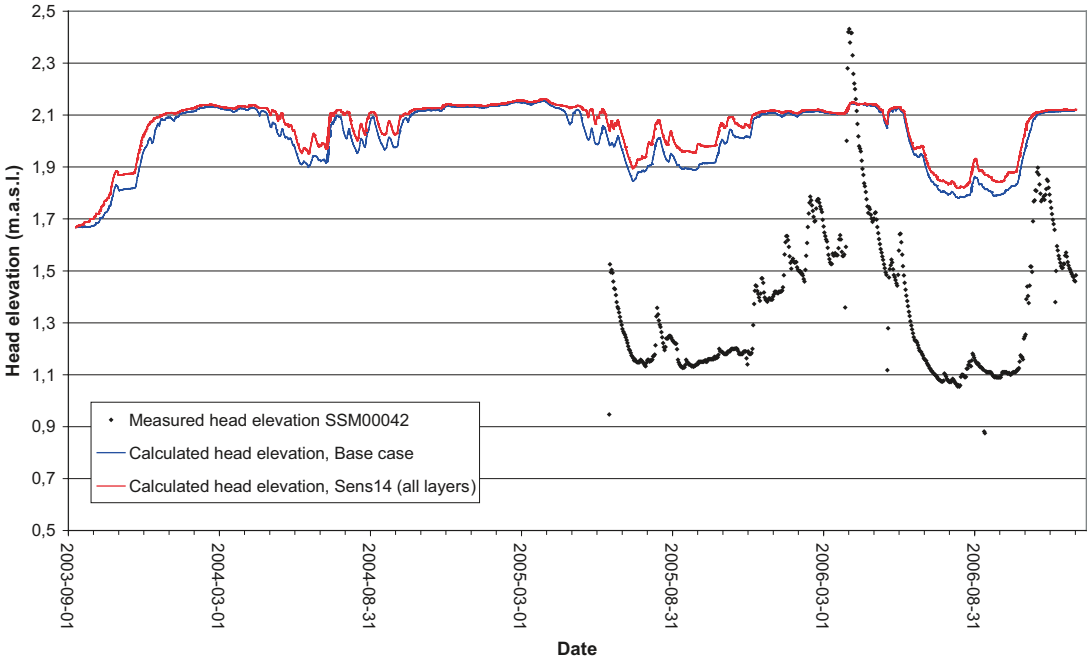

Figure 6-104. *Results for SSM000042 (groundwater head) from sensitivity analysis of the vertical model resolution in the bedrock.*

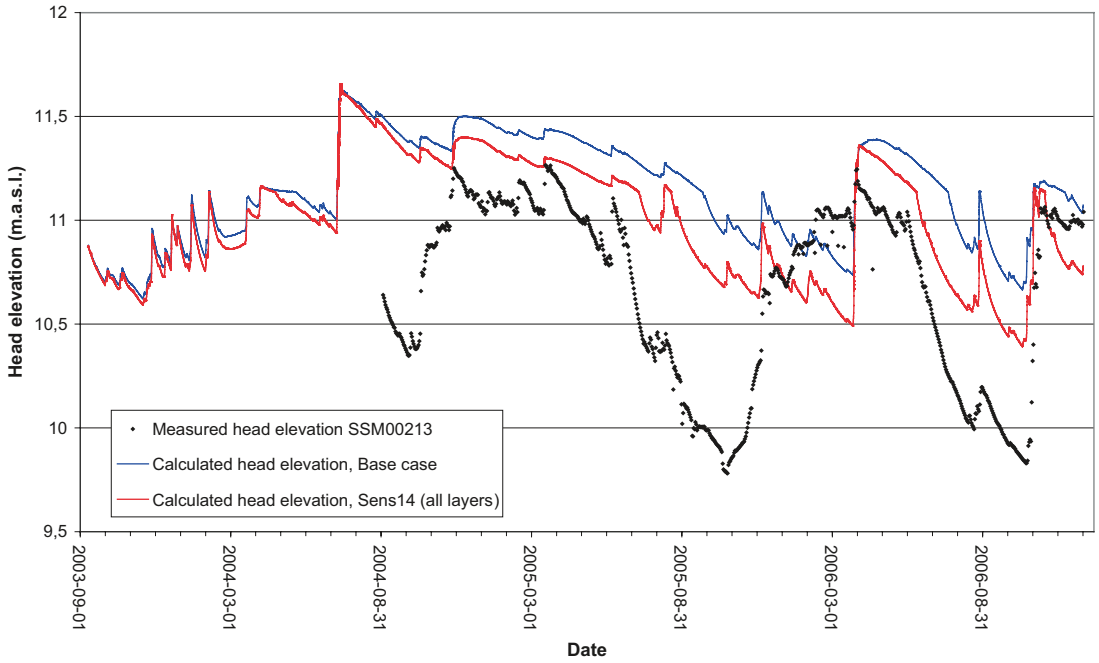

Figure 6-105. *Results for SSM000213 (groundwater head) from sensitivity analysis of the vertical model resolution in the bedrock.*

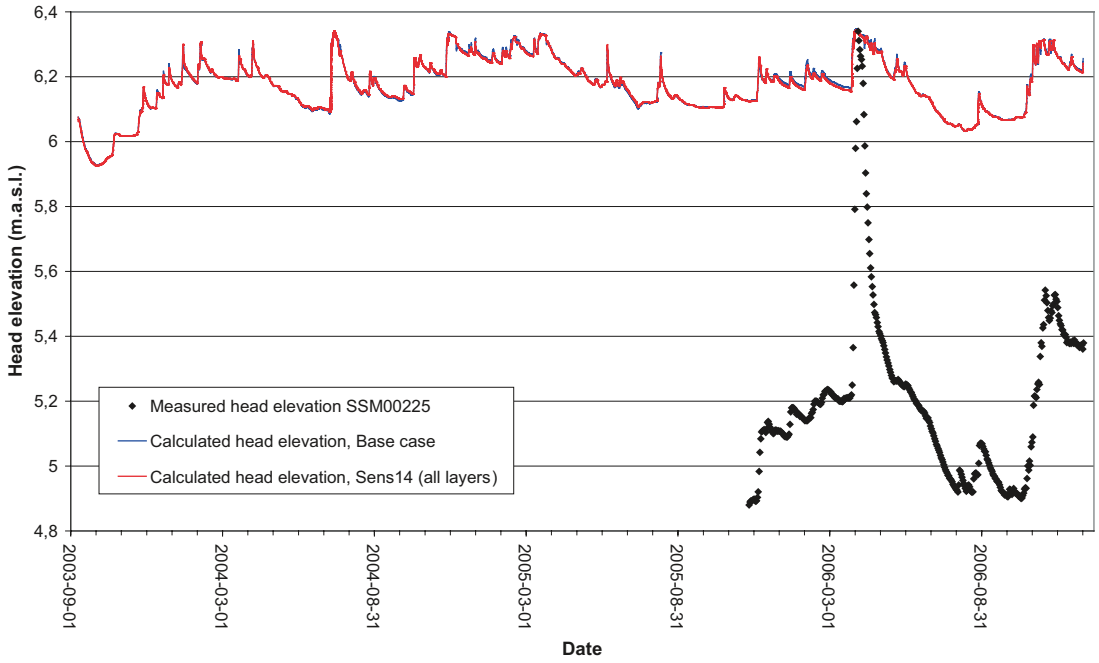

Figure 6-106. *Results for SSM000225 (groundwater head) from sensitivity analysis of the vertical model resolution in the bedrock.*

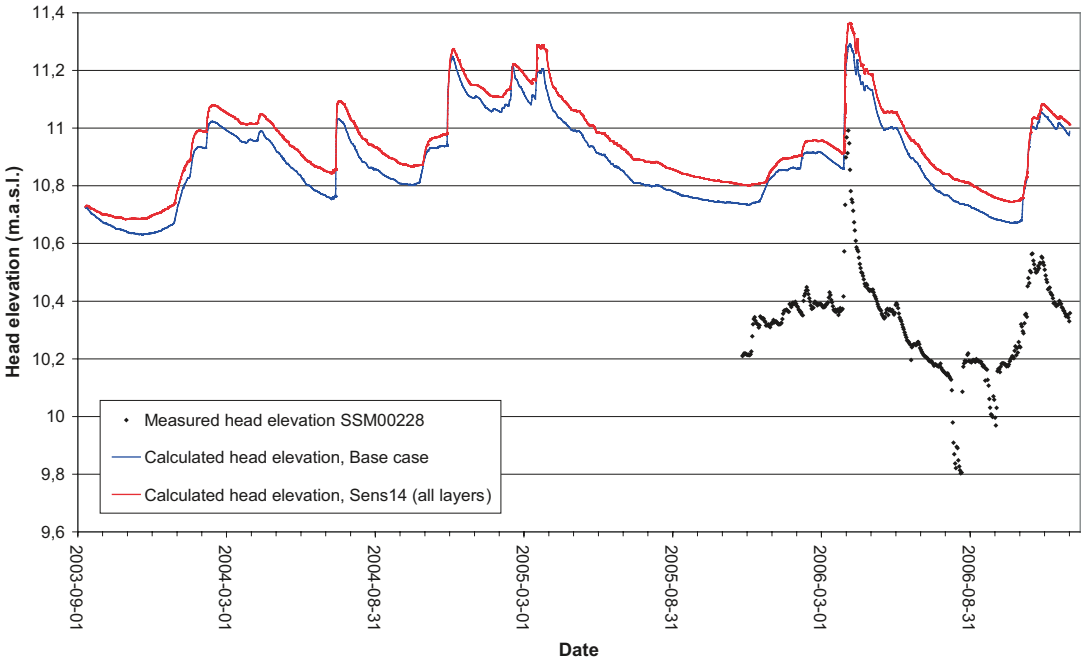

Figure 6-107. *Results for SSM000228 (groundwater head) from sensitivity analysis of the vertical model resolution in the bedrock.*

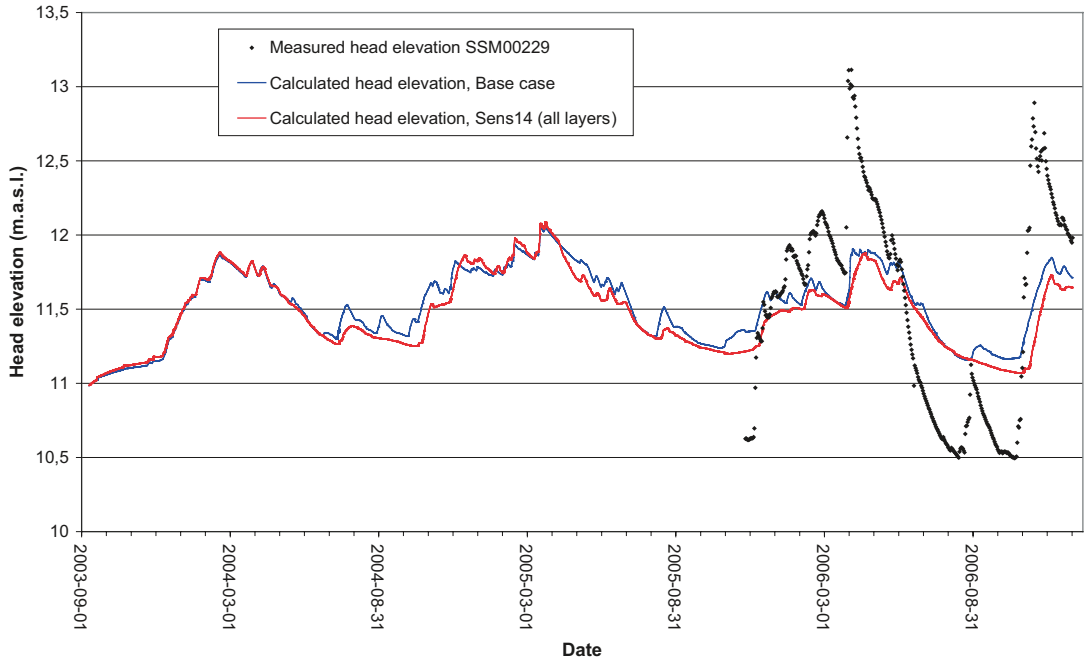

Figure 6-108. *Results for SSM000229 (groundwater head) from sensitivity analysis of the vertical model resolution in the bedrock.*

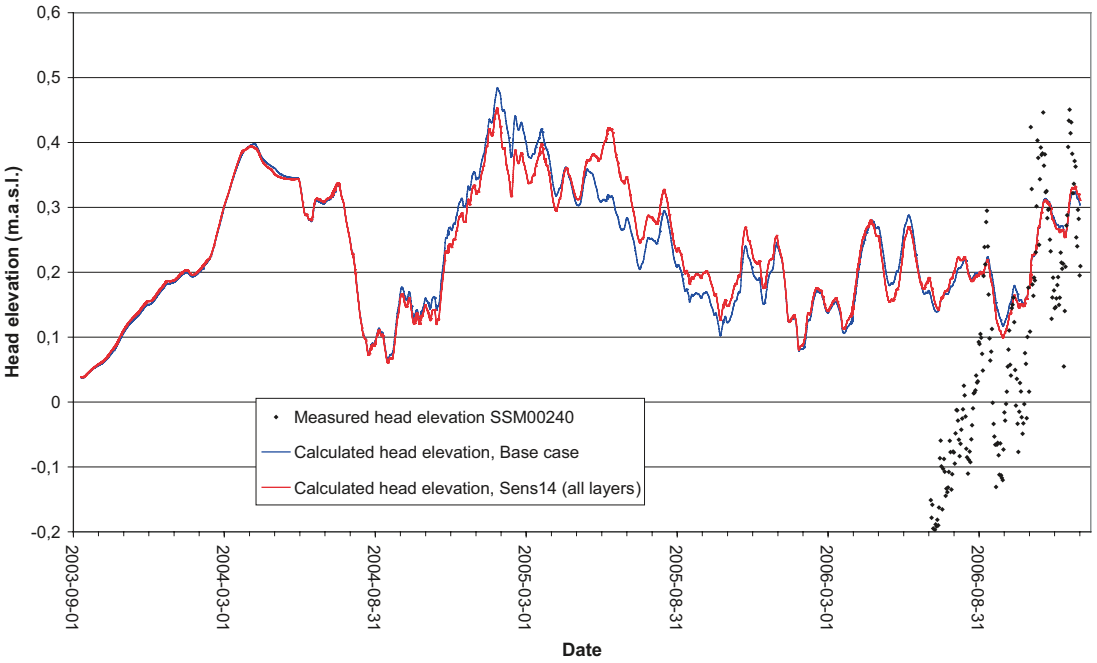

Figure 6-109. *Results for SSM000240 (groundwater head) from sensitivity analysis of the vertical model resolution in the bedrock.*

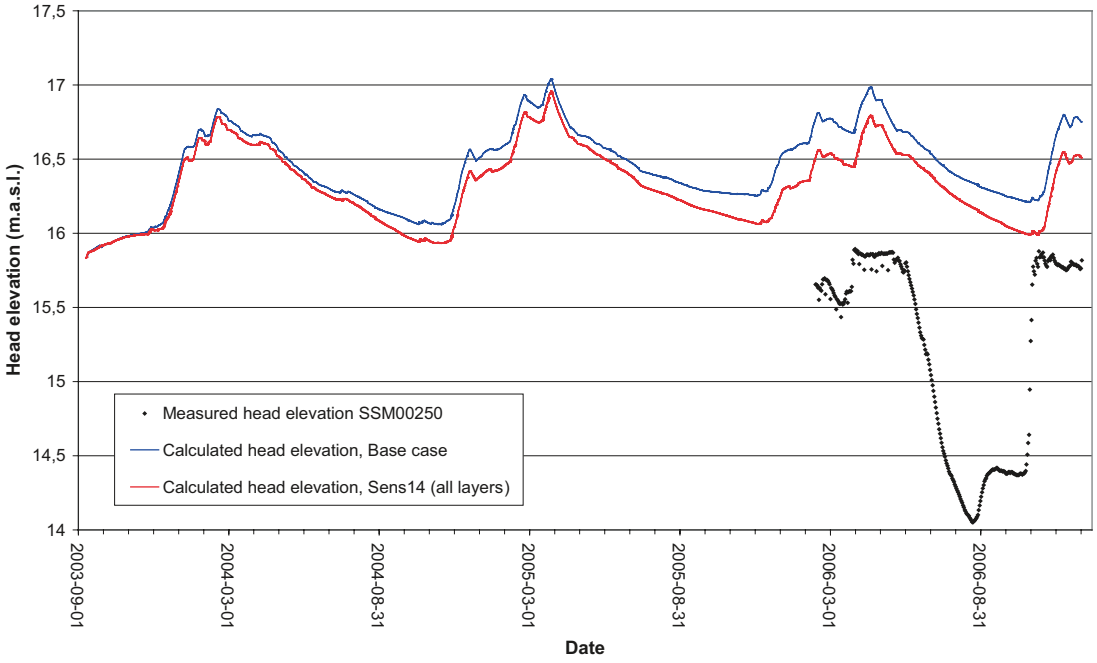

Figure 6-110. *Results for SSM000250 (groundwater head) from sensitivity analysis of the vertical model resolution in the bedrock.*

Table 6-18 compares the mean absolute errors in the base case and in the Sens14 case. The results indicate that the effect of reducing the number of computational layers in the bedrock is not significant, but also that the largest changes are improvements. The largest difference is an approximately 0.35 m improvement of the mean error.

Table 6-18. Comparison of mean absolute errors between the base case and Sens14 ("+" represents an improvement, "o" no change and "–" reduced agreement compared to the base case).

Borehole	Mean Absolute Error, Base case	Mean Absolute Error, Sens14 (resolution)	Improved agreement with Sens14
SSM000009	0.21	0.14	+
SSM000011	1.17	0.99	+
SSM000017	0.70	0.65	+
SSM000019	1.35	1.40	–
SSM000021	1.63	1.72	–
SSM000030	1.03	1.12	–
SSM000031	0.77	0.79	–
SSM000032	0.23	0.24	–
SSM000033	1.15	1.14	+
SSM000037	2.09	2.14	–
SSM000039	1.62	1.67	–
SSM000041	2.06	2.12	–
SSM000042	0.63	0.67	–
SSM000210	2.35	2.28	+
SSM000213	0.53	0.40	+
SSM000215	1.63	1.63	o
SSM000218	0.77	0.88	–
SSM000219	2.02	1.68	+
SSM000220	1.31	1.21	+
SSM000221	0.51	0.52	–
SSM000222	1.74	1.79	–
SSM000223	1.29	1.33	–
SSM000224	0.72	0.98	–
SSM000225	0.98	0.98	o
SSM000226	1.41	1.46	–
SSM000227	1.54	1.58	–
SSM000228	0.56	0.61	–
SSM000229	0.44	0.47	–
SSM000230	1.57	1.50	+
SSM000237	1.97	1.97	o
SSM000239	0.14	0.14	o
SSM000240	0.16	0.15	+
SSM000242	1.18	1.29	–
SSM000249	0.76	0.62	+
SSM000250	1.34	1.15	+
SSM000252	5.42	5.47	–
SSM000253	1.96	1.82	+
SSM000255	1.66	1.65	+
SSM000256	1.67	1.67	o
SSM000257	1.68	1.68	o
Mean MAE	1.30	1.29	

Table 6-19 compares the total water balance for the base case and the Sens14 case. The largest differences are found in the components “Overland boundary inflow” and “Overland boundary outflow”.

Table 6-19. Comparison of total water balances between the base case and Sens14.

Parameter	Base case	Sens14
Precipitation	–1,774	–1,774
Canopy storage change	0	0
Evapotranspiration	1,264	1,267
Overland storage change	55	53
Overland boundary inflow	–52	–114
Overland boundary outflow	84	145
Overland to river	225	228
Subsurface storage change	43	31
Subsurface boundary inflow	14	17
Subsurface boundary outflow	83	89
Base flow to river	94	101
Base flow from river	0	0
Error	7	9

7 Conclusions from the base case and sensitivity analyses

Along the whole calibration process, the model-calculated surface water flow was smaller than the measured flow. However, a reasonable water balance was achieved after the initial calibration that resulted in the base case. Still, the model underestimates the peak flow during the snow melt event in the spring of 2006. One explanation for this might be that the model simulates snow melt also during the preceding winter months, leaving less available snow to melt during the actual snow melt peak. The reason is that the model generates snow melt runoff as soon as the melting process starts (air temperatures above zero), whereas in reality the snow pack has a certain water storage capacity that can refreeze to snow/ice when the air temperature drops below zero. A possible solution of this problem could be to adjust the temperature threshold for snow melt in the model. However, this was not tested in this project.

Another and likely more important reason for the calculated surface water flow being too small, is that the present description of the surface stream network is incomplete and not detailed enough. The effect is that parts of the surface water in the model will not be transported to the (monitored) larger streams, creating ponded areas from where water instead can evaporate or infiltrate. A more complete surface stream network would increase the stream discharges, decrease the infiltration and lower the groundwater table, which would give a better match to both observed discharges and groundwater levels.

In order to attain a more reasonable surface water balance, the evapotranspiration was adjusted in the model to reduce the effect of these processes through a less active vegetation. Possibly, this was driven to far, creating too small evaporative losses from the groundwater during summer, and consequently too small variations in the groundwater head elevations. A more effective (in terms of its drainage capacity) and complete surface stream network description would possibly allow somewhat higher evapotranspiration, increasing the head elevation amplitudes.

In general, the infiltration across the ground surface in the model (and hence the groundwater recharge) appears to be too high, as inferred from the fact that the simulated groundwater head elevations are high compared to the measured ones. In the base case, the absolute mean error of all evaluated monitoring wells is 1.3 m, which is not a good result. The simulated groundwater table is too high in more or less all of the boreholes. A larger surface runoff, resulting in less ponding on the surface, would decrease the infiltration and groundwater recharge and therefore improve the fit. A larger transpiration and evaporation from the groundwater would also decrease the groundwater recharge.

Another possible reason for the too high groundwater head elevations in the Quaternary deposits is that the groundwater flow from the deeper bedrock layers is too large. This may either be due to the applied head boundary condition in the bottom bedrock layer, which is associated with some uncertainty, or to errors in the applied hydraulic conductivities in the bedrock. The model proved to be relatively sensitive to the head boundary condition at the bottom boundary in the rock (located at 150 m.b.s.l.). The mean error was reduced by as much as approximately 25%, when lowering the bottom head boundary by 3 metres, which on the other hand is a rather large change in the head boundary. Reducing the vertical hydraulic conductivity in the bedrock (and maybe increasing the horizontal) would also be interesting, but was not done in this study. A reduction of vertical bedrock conductivities will most likely raise the groundwater table in higher-altitude recharge areas, but on the other hand lower the groundwater table in lower-lying discharge areas.

An increase of the horizontal bedrock conductivities will even out the head variations in the bedrock over the area, but also increase the flow towards the sea boundary. Whether these changes give a better fit to observed levels or not cannot be concluded without running model tests. Therefore, it is strongly recommended that the correctness of the boundary condition, as well as the sensitivity to the bedrock conductivities, is evaluated in the next modelling phase for Laxemar. A deeper model, down to less fractured bedrock, with a no-flow bottom boundary instead of the present head boundary, may solve some of the problems and should therefore be evaluated in the next modelling stage.

The sensitivities of five vegetation and unsaturated zone parameters were tested. The specific yield (S_y) and saturated hydraulic conductivity (K_s) showed the highest sensitivity in terms of effects on both surface water discharges and groundwater tables. The root mass distribution parameter (A_{root}) also showed some sensitivity, although much less, while the interception coefficient (C_{int}) and the Averjanov constant (n) showed very little sensitivity when changing them within estimated reasonable intervals of variability. However, the hydraulic conductivity in the saturated zone proved to be more important then all of the tested vegetation and unsaturated zone parameters.

The effects on the results when changing the more important parameters are summarized as follows:

- A more effective (in terms of its drainage capacity) and complete stream network increases the surface water flow, decreases the groundwater head elevations, and increases the groundwater head amplitudes.
- A lower conductivity in the unsaturated zone (K_s) increases the surface water flow, and, to some extent, decreases the groundwater head elevations.
- A lower specific yield (S_y) in the unsaturated zone increases the surface water flow (although less than K_s), increases the groundwater head amplitudes, and, to some extent, increases the groundwater head elevations.
- A lower hydraulic conductivity in the saturated zone increases the peak surface water flows, decreases the base flows, and increases the groundwater head amplitudes and the overall groundwater head elevations. However, at some locations decreased groundwater head elevations are observed when lowering the hydraulic conductivities.
- A lower head at the bottom boundary decreases the surface water flow, decreases the groundwater head elevations, and increases the groundwater head amplitudes.

In order to reduce computer simulation times, the simulations in this study were done with a reduced number of bedrock calculation layers. However, it can be doubted whether a reduction of the number of bedrock calculation layers is justifiable, taking into account the effects on the results, when compared with the benefits of the reduced simulation times. For some of the groundwater monitoring wells, the deviations were not negligible.

8 Proposed calibration methodology

Based on experiences from the initial calibration, the definition of the base case and the sensitivity analyses, the following steps in a proposed calibration procedure have been identified.

1. Include all available field data and local knowledge of the area when evaluating model parameters and input data used in the model setup.
2. Inspect all measured calibration data carefully with respect to accuracy, validity and disturbances. For instance, seek information about how reference levels from groundwater level data are obtained and evaluate other sources to uncertainty. Finally, divide the calibration data into subsets of data associated with different degrees of uncertainty.
3. Make a first evaluation of initial results with respect to possible errors in physical input data (such as lake thresholds and river cross-section elevations) and boundary conditions (such as precipitation, temperature and potential evapotranspiration).
4. Evaluate the surface runoff to the stream network to make a rough calibration of the runoff processes. Check the general water balance for the area
   (Precipitation – Evaporation = Runoff + Groundwater recharge – Groundwater discharge).

   Governing parameters are, in order of importance:
   - Meteorological data (precipitation, temperature, potential evapotranspiration and snow melt).
   - Hydraulic conductivity in the saturated zone for the uppermost layers.
   - Unsaturated zone parameters, where the hydraulic conductivity (K_s) and the specific yield (S_y) are the most important.
   - Manning's numbers in both MIKE 11 and in the overland flow component of MIKE SHE.
   - Drainage parameters, if the drainage option is activated for the saturated zone.
   - Vegetation parameters, where the root mass distribution parameters (root depth and A_{root}) are the most important.
   - Leakage coefficient between the stream network and the saturated zone, if streambed sediments are present.
5. Characterize deviations between measured and calculated groundwater head elevations, both in Quaternary deposits and bedrock, to point out and locate systematic errors in input data and parameters, such as:
   - Deviations in topographic model (the DEM).
   - Communication between different model components.
   - Influence of boundaries (e.g. the bottom boundary) of the saturated zone.
   - Limitations of the model code (such as evapotranspiration only being calculated in the uppermost calculation layer of the model).

   It should be noted that step 4 may need a second evaluation after modifications have been made in step 5.
6. Characterize deviations between measured and calculated groundwater head elevations to locate areas and parameters that need to be systematically adjusted:
   - Communication between different model components and layers.
   - Influence of evapotranspiration.

7. Divide the model catchment into sub-areas based on the characterization above and make a general classification of the local topographical conditions at each monitoring well location.

8. Make a parameter analysis of the governing parameters for each area to minimize the deviations, both in groundwater head elevations, surface water elevations and surface water discharges. Based on results from chapters 6 and 7 in the present report, the parameter analysis should focus on the following parameters within each area, preferably in the order they are listed:
   - Horizontal hydraulic conductivity in the saturated zone of the Quaternary deposits.
   - Vertical hydraulic conductivity in the saturated zone of soil layers. Results from previous model studies indicate that the vertical conductivity for Quaternary deposits typically should be 5–10 times less then the horizontal.
   - Vertical and horizontal hydraulic conductivities of the bedrock layers.
   - Communication between surface water and groundwater, e.g. the vertical hydraulic conductivity of lake sediments.
   - Unsaturated zone parameters, where the hydraulic conductivity (K_s) and the specific yield (S_y) are the most important.
   - Vegetation parameters, where the root mass distribution (root depth and A_{root}) and the crop coefficient (K_c) are the most important.

9 References

Alexandersson H, 2003. Korrektion av nederbörd enligt enkel klimatologisk metodik. SMHI Meteorologi 111. Swedish Meteorological and Hydrological Institute, Norrköping (in Swedish).

Aneljung M, Gustafsson L G, 2007. Sensitivity analysis and development of calibration methodology for near-surface hydrogeology model of Forsmark. SKB R-07-27, Svensk Kärnbränslehantering AB.

Bosson E, 2006. Near-surface hydrogeological model of Laxemar. Open repository – Laxemar 1.2. SKB R-06-66, Svensk Kärnbränslehantering AB.

DHI Water & Environment, 2007. MIKE SHE – User Manual. DHI Water & Environment, Hörsholm, Denmark.

Eriksson B, 1981. Den potentiella evapotranspirationen i Sverige. SMHI, Rapport RMK 28 (in Swedish).

Kristensen K J, Jensen S E, 1975. A model for estimating actual evapotranspiration from potential evapotranspiration. Nordic Hydrology, 6, pp. 170–188.

SKB, 2004. Preliminary site description. Forsmark area – version 1.1. SKB R-04-15, Svensk Kärnbränslehantering AB.

Svensson U, Kuylenstierna H O, Ferry M, 2004. Darcy Tools, Version 2.1. Concepts, methods, equations and demo simulations. SKB R-04-19, Svensk Kärnbränslehantering AB.

Svensson U, 2006. The Laxemar repository – Modelling changes in the flow, pressure and salinity fields, due to a repository for spent nuclear fuel. SKB R-06-57, Svensk Kärnbränslehantering AB.

Werner K, Bosson E, Berglund S, 2005. Description of climate, surface hydrology, and near-surface hydrogeology. Preliminary site description Laxemar subarea – version 1.2. SKB R-05-61, Svensk Kärnbränslehantering AB.